

For Reference

NOT TO BE TAKEN FROM THIS ROOM

Ex LIBRIS
UNIVERSITATIS
ALBERTAEASIS



For Reference

NOT TO BE TAKEN FROM THIS ROOM



Digitized by the Internet Archive
in 2020 with funding from
University of Alberta Libraries

<https://archive.org/details/LTChen1968>

THE UNIVERSITY OF ALBERTA

PRIMORDIA OF THE LYMPHOID ORGANS OF THE CHICKEN

by



LI-TSUN CHEN

A THESIS

SUBMITTED TO THE FACULTY OF GRADUATE STUDIES IN
PARTIAL FULFILMENT OF THE REQUIREMENTS FOR THE
DEGREE OF

DOCTOR OF PHILOSOPHY

DEPARTMENT OF ZOOLOGY

EDMONTON, ALBERTA

Date *Oct. 25, 1968.*

1968 (F)
18 D

UNIVERSITY OF ALBERTA

FACULTY OF GRADUATE STUDIES

The undersigned certify that they have read, and recommend to the Faculty of Graduate Studies for acceptance, a thesis entitled Primordia of the Lymphoid Organs of the Chicken submitted by Li-tsun Chen in partial fulfilment of the requirements for the degree of Doctor of Philosophy.

ABSTRACT

The thymus and the bursa of Fabricius are the first lymphoid organs of the chicken. They appear on the fifth day of incubation as proliferations of endodermal epithelia. The bursa appears in the caudal half of the urodeal membrane. The bursa appears as a median chain of intercellular vesicles subjacent to the ectoderm and just within the endoderm. These vesicles enlarge and fuse to become the lumen of the bursa. The surrounding endodermal cells proliferate to form the lining of the bursa. The electron micrographs suggest that the urodeal ectoderm ingests extracorporeal fluid by pinocytosis and transfers it to the endoderm which releases it into the intercellular space to form the vesicles.

The thymus appears as four separate proliferations. These arise from the dorsal, lateral extremes of Pharyngeal Pouches III and IV. Each of these proliferations lies just dorsad and mediad to the medial end of a small, transverse membrane connecting the pharyngeal pouch to the corresponding branchial groove. The dorsal part of Membrane III is a tube of ectoderm which intrudes mediad from Groove III and the ventral part is a tube of endoderm which protrudes laterad from the ventral part of Pouch III. The contact of ectoderm with endoderm is continuous from just beneath the body surface to a point just ventral and lateral to Thymus III. Membrane IV does not have a ventral, endodermal part. The contact of ectoderm with endoderm is restricted to the area just ventral and lateral to Thymus IV. There is no chain

of vesicles and no indication of extracorporeal pinocytosis and internal secretion in Membranes III and IV.

The urodeal membrane, and Membranes III and IV, contain the debris of many dead cells. The acid phosphatase activity of these membranes is high, which supports the morphological evidence for cell deterioration and cell death. The activity is high in (a) the urodeal ectoderm, the urodeal endoderm, and the lymphoid follicles of the bursa, and in (b) the ectoderm of Membranes III and IV, the endoderm of Membranes III and IV, and the endodermal epithelium of the developing thymus. The significance of this activity is unknown excepting its frequent association with cell deterioration and cell death, whether in the epithelia or at sites of active lymphopoiesis.

The morphological indications of cell deterioration and cell death are particularly noticeable in the urodeal ectoderm and the branchial extoderm, and are remarkable in the ectoderm of the branchial grooves. Here, as in the thymus, the debris of epithelial cells is discharged into the surrounding mesenchyme where it is phagocytized. There is no indication that mesenchymal cells invade the epithelia. The extreme deterioration of the ectoderm is followed by rapid proliferation of the bursa and the thymus. Despite the intimate contact of ectoderm with endoderm it has not been possible to trace ectodermal cells into either organs.

ACKNOWLEDGMENTS

I am greatly indebted to Dr. R. F. Ruth for his guidance and encouragement throughout the work. I am also grateful to Dr. T. A. Shnitka for his helpful discussions and interpretations of the electron micrographs. I wish to thank Mr. Vincent Lao for his assistance in tissue sectioning, Dr. Sylvia Sheridan for her useful discussions, and Mr. George Menges for his photographic assistance. The Photo Service staff was very cooperative. Facilities for electron microscopy were provided by the Electron Microscope Laboratory.

Financial support was provided by a University of Alberta Dissertation Fellowship and National Research Council and Medical Research Council of Canada research grants to Dr. R. F. Ruth.

TABLE OF CONTENTS

| | <u>Page</u> |
|--|-------------|
| I. INTRODUCTION | 1 |
| II. MATERIALS AND METHODS | 3 |
| Light and Electron Microscopy | 3 |
| Acid Phosphatase Localization | 4 |
| Feulgen Reaction for DNA Demonstration | 6 |
| Colcemid Treatment | 6 |
| III. OBSERVATIONS | 7 |
| The Bursa of Fabricius | 7 |
| The Thymus | 19 |
| IV. DISCUSSION | 29 |
| The Bursa of Fabricius | 30 |
| The Thymus | 35 |
| V. SUMMARY | 49 |
| VI. BIBLIOGRAPHY | 53 |
| VII. EXPLANATION OF FIGURES | 63 |

I. INTRODUCTION

Although the lymphoid tissue of adult amniotes is distributed throughout the body it appears in the avian embryo in two small organs, the thymus and the bursa of Fabricius, before it can be detected elsewhere. This has been interpreted to mean: (1) all vertebrate leukocytes are descendants of the epithelial cells of the thymus (Beard, 1900), (2) the leukocytes are descendants of mesenchymal cells which invade the thymus and proliferate there (Maximow, 1909), (3) some of the lymphocytes are descendants of the epithelial cells of the bursa (Ackerman and Knouff, 1959), (4) the antibody-producing cells are probably derived from the endodermal epithelia of the thymus and the bursa (Ruth, 1960), (5) the first lymphocytes of the thymus are descendants of the epithelial cells of the thymus (Auerbach, 1961), and (6) the lymphocytes of the thymus and the bursa and all other lymphocytes are descendants of blood cells which invade the bursa and the thymus (Moore and Owen, 1966 and 1967). All of these arguments suffer from a lack of detailed information about the origins of the bursa and the thymus. Even if the arguments about the origins of the lymphocytes are set aside, a detailed examination of the primordial epithelia may go some distance toward the redefinition of questions relevant to the differentiation of lymphocytes and the acquisition of immunological competence. One of the principal questions

is "What do the epithelia of the bursa and the thymus have in common which sets them apart from other derivatives of the gut?"

Grossly, the bursa and the thymus are unusual by their locations near the opposite ends of the gut. The epithelial parts arise from endoderm which connects with ectodermal epithelium of the body surface. This raises the possibility that the epithelial primordia of the bursa and the thymus may arise from the contact of ectoderm with endoderm. Because the anatomical relationship of the ectoderm and the endoderm have been disputed this has been re-investigated. The relationship is intimate.

The intimate contact of ectoderm with endoderm raises the possibility that ectodermal cells may be included in the thymus and the bursa. This is not a new question. The older literature includes many references to this possibility although the more recent literature tends to ignore or dismiss it. Ultrastructural studies were undertaken in the hope of providing some basis for resolving this question. These studies place the question in a different context. The primordia and the adjacent epithelia undergo extensive degeneration. This circumstance changed the immediate question from one of cell lineage to one of establishing the extent of autolysis and the relationship of autolysis to the formation of the bursa and the thymus.

II. MATERIALS AND METHODS

All tissues were taken from F1 hybrids of two highly inbred lines of White Leghorns maintained by the Hy-Line Poultry Farms, Johnston, Iowa. The anatomical and ultrastructural studies are based on many four to six day embryos and a few embryos of other ages. The histochemical studies include a wide range of ages.

Light and Electron Microscopy

Whole embryos are shown in Figs. 1 to 3. Figures 4 to 6 indicate the locations of the lymphoid anlagen. For anatomical and ultrastructural studies, the embryos were cut in half (Fig. 7) and hardened in fixative for 10 to 20 minutes. Two fixatives were used. These were Palade's (1952) and that of Sabatini et al. (1962). The tissues were dehydrated in ethanol and embedded in Araldite 502 or Epon modified from Luft (1961). The tissues were oriented in gelatine capsules by placing the tissues on two drops of polymerizing resin. The branchial region was oriented for frontal sectioning and the urodeal region was oriented for sagittal sectioning. For anatomical studies by light microscopy, 7 to 10 μ sections were cut with a steel knife and mounted in resin. Phase contrast photographs were taken on Agepe FF film (Agfa).

For ultrastructural studies it was necessary to orient the tissue more precisely. This was done by examining 7 to

10 μ sections with the phase microscope, identifying the exact position and plane of the pharyngeal and cloacal complexes, and further trimming and positioning of the block. Sections were cut at 600 to 1000 \AA ⁰ with glass or diamond knives, floated on a 15% solution of acetone in water.

The sections were picked up on 150 or 200 mesh coated or uncoated copper grids and stained by floating the grids face down on a drop of saturated uranyl acetate (Watson, 1958) at room temperature. The sections were washed briefly and blotted dry. The sections were examined in a Phillips EM 100 B operated at 60 KV with a 25 micra aperture. The photographs were taken on 35 mm Kodak film (P 426) at magnifications of 1000 to 5000.

Acid Phosphatase Localization

For light microscopic localization of acid phosphatase activity, the whole embryo or part of the embryo was fixed in ice cold formaldehyde-calcium fixative for 24 hours, and infiltrated with cold gum-sucrose (Holt, 1958), and frozen in isopentane at a temperature below -100°C . The whole 5 day embryo, the anterior and posterior halves of the 6 day embryo, and the neck and tail of the 7 to 14 day embryos were frozen and embedded in O.C.T. compound (Lab-Tek, Westmount, Illinois). Sections (8 μ) were cut at -15°C , frontal sections for the thymus and sagittal sections for the bursa (Figs. 8 and 9).

The sections were mounted on gelatin coated slides and dried in air at room temperature. Within one week of sectioning, slides were washed in distilled water and incubated in fresh Barka's medium (1960). After incubation for 10 to 30 minutes at room temperature, the slides were cleared and mounted in Permunt. The counterstain was 1% methyl green at pH 4.0.

For electron microscopic localization of acid phosphatase activity, the bursa of Fabricius was removed from the 20 day embryo and cut into halves. The tissue was spread on filter paper, luminal side up and placed in cold 3% glutaraldehyde in 0.05M sodium cacodylate buffer at pH 7.2 for 80 minutes. Fixed tissues were washed in cold (sodium cacodylate) buffered 10% sucrose for 4 hours and cut into small pieces. These were incubated at 37°C in Gomori's (1952) medium for 90 minutes.

The incubation medium was prepared immediately before use by dissolving 0.24 gm lead nitrate in 200 ml 0.05M sodium acetate buffer at pH 5.0 containing 7.5% sucrose and then slowly adding 20 ml of a 3% solution of sodium-glycero-phosphate. Then the mixture was warmed at 60°C for one hour cooled to room temperature, and filtered before incubation (Miller and Palade, 1964).

The tissue blocks were washed twice (10 minutes each) in a cold solution of 0.05M sodium acetate buffer (pH 5.0), 7.5% sucrose, and 4% formaldehyde (Holt and Hicks, 1961), with a 10 minute rinse in 2% acetic acid between the washes

of acetate-buffered formaldehyde.

The tissue blocks were post fixed in 1% OsO_4 veronal-acetate buffer (pH 7.3) at $0-4^\circ\text{C}$ for 60 minutes, dehydrated in ethanol, and embedded in Epon 812 (Luft, 1961).

For both Barka and Gomori methods, the controls were the omission of substrate and the inclusion of 0.01M NaF in the incubation medium.

Feulgen Reaction for DNA Demonstration

Frozen sections, prepared as mentioned before, were used for demonstrating Feulgen-positive pyknotic nuclei. The preparation of Schiff reagent was after Barger and de Lamater (1948). The stained sections were counterstained with luxol fast blue (Margolis and Pickett, 1956). Both normal nuclei and pyknotic nuclei stain red in the Feulgen reaction preparation. The Feulgen-positive pyknotic nuclei are readily distinguishable from the normal nuclei by their deeper color.

Colcemid Treatment

Colcemid (CIBA Co. Ltd., Dorval, Quebec) was given to 5 day embryos. The optimal dose, 0.2 μg , was high enough to arrest all dividing cells at metaphase and low enough to allow embryos to survive until hatching. The addition of Colcemid to the embryos was carried out as follows: The 5 day embryos were candled with ultraviolet light. Only embryos having yolk sacs close to the air chamber of the egg were chosen for this experiment. A 5 mm² shell win-

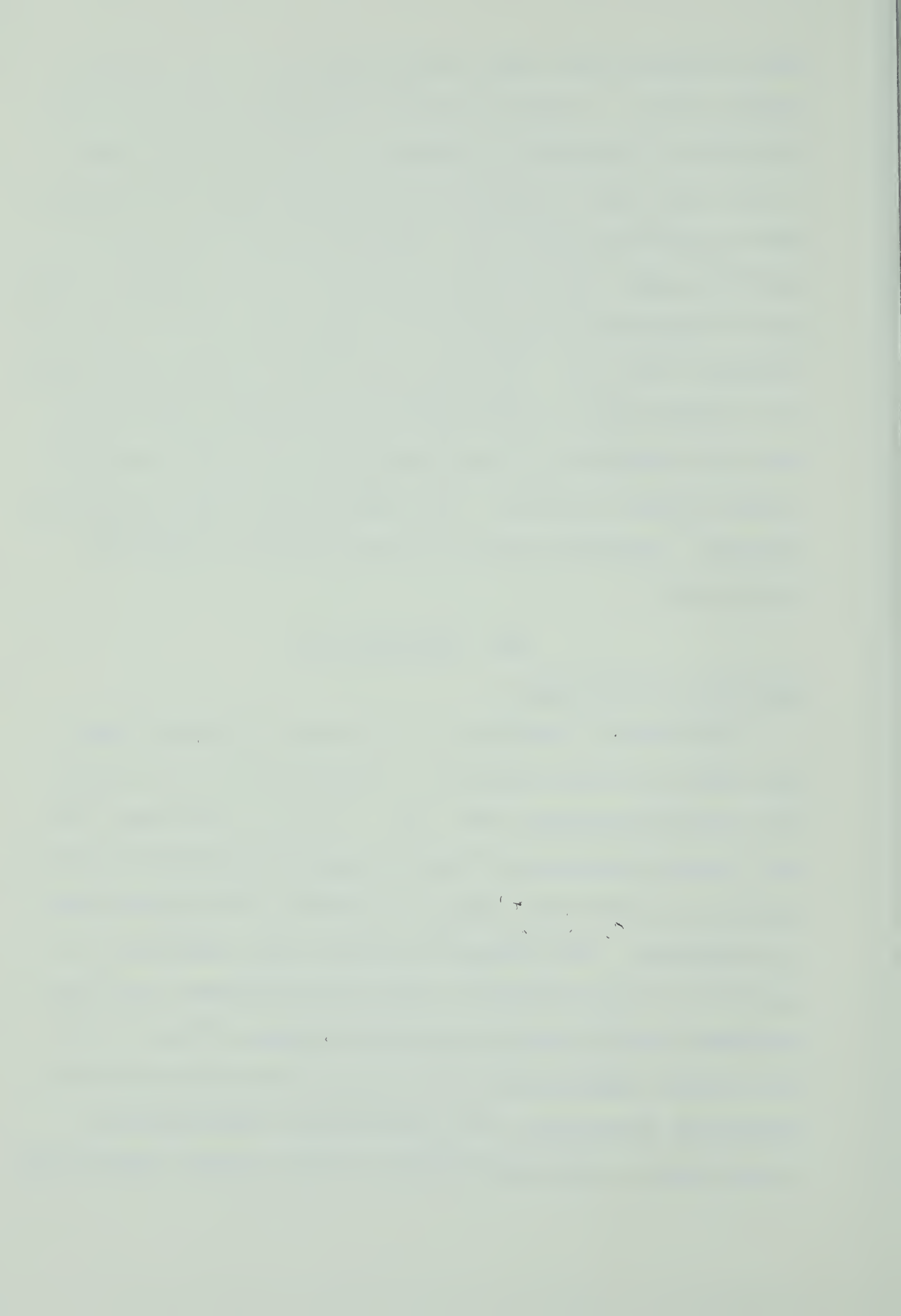


dow was made on the blunt end of the egg, i. e., the air chamber side. In order to avoid hemorrhage during the application of Colcemid to embryos, a small slit was made in the inner shell membrane lying on the chorionic membrane and the primitive yolk sac. Colcemid solution of 0.1 ml was then added drop by drop to the slit of the shell membrane and it immediately spread to the chorionic membrane and the primitive yolk sac. After this the shell window was sealed with masking tape. The embryos were returned to the incubator for another six hours incubation, and then fixed in formol calcium fixative. The fixed embryos were embedded in paraffin. Sections cut at 7 μ were stained with Ehrlich haematoxylin.

III. OBSERVATIONS

The Bursa of Fabricius

The bursa of Fabricius is an unusual lymphoid organ. The medulla of each follicle is separated from its cortex by a basement membrane (Fig. 10). This is continuous with the basement membrane of the non-lymphoid epithelium which connects the follicles (Figs. 11 and 12). The epithelium is endodermal. The basement membrane can, therefore, be regarded as the fundamental demarcation between a modified endodermal medulla and a mesenchymal cortex (Figs. 11 and 12) without implying that all the cells of the medulla are endodermal derivatives. The histological distinction is recognizable in the distribution of the vascular capillaries.



These surround the medulla closely, but do not penetrate it. In consequence, erythrocytes may be found close to the medulla, but not in it (Fig. 13).

Cell degeneration and cell death are common in the medulla (Fig. 14 to 16). Since degeneration is associated with the activity of lysosomal enzymes, the activity of the most definitive of these was examined. The acid phosphatase activity of the 12 day, pre-lymphoid, bursa is concentrated in small groups of cells scattered through the tunica propria (Fig. 17). The appearance of follicles at 13 days is accompanied by the appearance of high, punctate activity in the epithelium, particularly at the follicles (Fig. 18). The punctate distribution is more evident in the epithelium and the follicles at 14 days (Fig. 19). At 19 days, the tunica propria and the epithelium are not very reactive, but the medullae of the follicles contain many punctate centers of activity (Fig. 20). At all ages the punctate centers of the epithelium and the follicles are not as large as the largest punctate centers of the tunica propria and this difference has a fundamental basis.

The punctate activity of the 12, 13, and 14 day tunica propria (Figs. 17 to 19) corresponds in size and distribution to groups of immature heterophils (Figs. 21 and 22). At 19 days, there are fewer punctate centers in the tunica propria (compare Fig. 20 with 23 and 24) and fewer groups of immature heterophils. Two kinds of granulocytes, eosinophils



and heterophils, may contribute to the activity of the 19 day tunica propria (Figs. 25 and 26), but only heterophils are present at 12, 13 and 14 days. Neither eosinophils nor heterophils are present in the epithelium and the follicles. The punctate activity of these two structures must be due to other cells. It is presumed that the activity is indigenous to the endodermal cells of the epithelium and the agranulocytes of the follicles for lack of evidence to the contrary.

The acquisition of acid phosphatase activity by the 13 day epithelium does not mean that activity is negligible throughout earlier development. The epithelium is very active at 14 days (Fig. 27) and 13 days (Fig. 28), inactive at 12, 11, 10 and 9 days (Figs. 29 to 32), and very active at 7 days. (Fig. 34). The 7 day epithelium is the urodeal membrane. The epithelium of the bursa develops in this membrane and as it develops it separates (Figs. 34 and 33, in that order) and loses activity (Fig. 32). The urodeal membrane retains activity (Figs. 35, 37 and 38). The times at which the epithelium of the bursa has high activity are the times of active differentiation: the formation of the definitive epithelium, and its transformation into follicles.

The anatomy of the urodeal membrane is quite complex, but the principal features can be learned from serial sections. It is easiest to do this with para-sagittal sections



(Figs. 39 to 44). These show the 4 day proctodaeum on the right, the urodeal membrane in the center, and the cloaca on the left. The proctodaeum is lined with ectoderm which is fused through the urodeal membrane to the endoderm which lines the cloaca.

The ectoderm and endoderm are not demarcated. This continuity of ectoderm with endoderm represents a persistence of the median, sagittal continuity of the epiblast and hypoblast formed during gastrulation. The continuity persists as the 'anal plate' which is displaced to the ventral side of the embryo during the formation of the tail or caudal body fold and the elongation of the dorsal, axial skeleton. By the fourth day the anal plate has thickened to become the urodeal membrane.

The proctodaeum points toward the head which lies far outside the right margin of the figures (Figs. 39 to 44). The most caudal part of the urodeal membrane is seen in Fig. 39 and the successive, para-sagittal sections show more of the anterior membrane. It is difficult to align the sections so that they are perfectly sagittal or para-sagittal and these figures may represent sections which are tilted and twisted. For instance, the cloacal fenestra (Fig. 40) marks the midline of the posterior cloaca and the tip of the proctodaeum (Fig. 44) marks the midline of the anterior cloaca. The location of these two structures in different sections suggests that the sections are twisted

or rotated on the dorsal-ventral axis. The fact that the urodeal membrane is defined less sharply and the ventral wall of the cloaca is thicker in Figs. 42 and 43 suggests that these structures are cut tangentially which might suggest that the sections are tilted or rotated on the anterior-posterior axis. It is apparent, however, that part of the asymmetry is contributed by the embryo. This is recognized more easily in the 5 day embryos.

Sections which cut the neural tube, the notochord, the aorta, and the tip of the proctodaeum (Fig. 45) show that the tail of the embryo curves laterad, away from the plane of the section. This is most easily recognized by the presence of somites in the figure just above the amnion. The sections are twisted on the dorsal-ventral axis with respect to the cloaca, but the sections are not twisted with respect to the torso. In reality, the urodeal membrane extends from the tip of the proctodaeum to a point just beyond the left margin of the small rectangle (Fig. 45). The cavity of the cloaca appears at two points: inside the rectangle just above the tip of the proctodaeum, and above the left margin of the rectangle. The cloacal cavity is really continuous from right to left and so is the urodeal membrane which separates it from the proctodeal ectoderm. Frequently, the curve of the urodeal membrane and the cloacal cavity is exaggerated in that sections may cut through the front and rear of the urodeal membrane, but not through its center.

The posterior part of the urodeal membrane probably represents the eventual opening of the bursa into the proctodaeum and the anterior part represents the eventual opening of the embryonic cloaca. The early, incidental and temporary convolutions make the anatomical study more tedious, but are not fundamental to the contact of the ectoderm with the endoderm. There are morphological characteristics of greater relevance.

Much cell debris is present in the tip of the proctodeal ectoderm (Figs. 41 to 44) and in the anterior part of the urodeal membrane (Fig. 44). Cell debris is found, however, throughout the adjacent ectoderm, including the ectoderm in contact with the posterior part of the urodeal membrane (Fig. 41). The extent and intensity of cell degeneration may reach a peak during the fourth day (Figs. 46 to 51). At this time a mass of cells and debris protrudes into the cloacal cavity. The protrusion resembles ectoderm, but it may not be ectoderm. The protrusion is not obvious in 5 day embryos (Figs. 52 to 57), but this may be due to the great growth of the urodeal membrane which expands over the region in which the protrusion was formed (Figs. 56 and 57). Numerous vesicles appear in the urodeal membrane subjacent to the ectoderm. They form a rough arc from the rear (Fig. 53) to the front (Fig. 57) of the membrane. Some are deep within the membrane. The fate of these vesicles is more evident in 6 day embryos.

The vesicles seem to fuse. This is suggested by the bulges of some (Figs. 59, 61 and 63), the close contact of others (Figs. 58, 60 and 62), and the constriction of a few large vesicles (Figs. 61 and 62). The number and size of the vesicles suggests that active secretion of fluid occurs throughout the urodeal membrane. Their clarity indicates that they are not deposits of cell debris. These vesicles fuse to form the lumen of the bursa. The vesicles at the anterior of the urodeal membrane may not contribute to the lumen of the bursa (Figs. 33 to 31, in that order).

The anatomical study suggests that the ectoderm plays an important role in the formation and development of the urodeal membrane. The ectoderm in and near the membrane is peculiar in at least two ways: it produces much debris and this is followed by the formation of extracellular vesicles. Electron micrographs show that the production of debris is accompanied by the formation of intercellular spaces which may be the forerunners of the extracellular vesicles. The most superficial of the intercellular spaces are separated from the proctodeal cavity by just one layer of cells (Fig. 64). The proctodeal surface of these cells has many indentations and small vesicles suggestive of active pinocytosis. Small and large vesicles are scattered throughout the cytoplasm. The cells are linked by tight junctions, desmosomes (Fig. 65), and interdigitations. The cells may look healthy, but they contain masses of lipid and membrane-bound debris,



which may resemble organelles. The free mitochondria contain the distinctive cristae, but these may be incomplete and irregularly spaced. There are many irregular, osmophilic bodies, presumably lipid, throughout the cytoplasm. Golgi-like vesicles are present, but few if any multivesicular bodies are found in the superficial cells.

Cells beneath the superficial cells may contain long, clear membrane-bound spaces which resemble tubular endoplasmic reticulum (Fig. 65). The diameters of these are comparable to the diameters of the larger, rounded vesicles of the superficial cells. It is conceivable, therefore, that the rounded vesicles of the superficial cells may represent cross-sections of tubular reticulum. If so, the arrangement of the tubular reticulum is highly ordered in a manner not reflected in the arrangement of the tubular mitochondria. Tubular reticulum is common in the internal cells, but has not been recognized in the superficial cells.

The boundaries of internal cells may lead into areas of unusual opacity. These may be diffuse near the proctodeal cavity (Fig. 65), but the deeper ones have distinct interdigitations, condensations near the cell surfaces, and thickenings of the cell surfaces (Fig. 73). The diffuse areas are presumed to be early stages in the formation of the more distinct areas.

The nuclei of urodeal cells have typical nuclear envelopes; the space between the membranes is slightly irregular,



but the two membranes join at the pores (Fig. 66). There are small groups of Golgi-like vesicles near the nucleus. Multivesicular bodies are found near the nucleus. These are more common in the deeper cells. A few ribosomes are attached to the intracytoplasmic membranes, but this is not the usual location in young embryos. Most occur in groups of four or more scattered through the cytoplasm (Fig. 66); nuclear granules are not grouped this way.

The cell surfaces which border the intercellular spaces may show interruptions. Sharp, dark cell membrane may be interrupted by streams of cytoplasm which enter the intercellular space (Fig. 66). This is not necessarily an artifact of fixation. Spaces, so close to each other that they must have experienced similar changes during preparation, may differ; one may have the interrupted, dark boundary and the other may have a continuous, light boundary (Fig. 66). The latter resembles the cell membranes at the proctodeal and cloacal surfaces and the former resembles the cell membranes around the extracellular vesicles (Figs. 64, 72 and 73). If the granular contents of the cytoplasm do enter the intercellular spaces and these fuse to form the extracellular vesicles, this would account for the presence of granular material in the extracellular vesicles (Figs. 71 to 73).

Deeper within the urodeal membrane, the Golgi vesicles are more numerous (Fig. 67). The nucleoli may contain dense linear segments suggestive of the nucleolemma. Intercellular

spaces are frequent. Large clumps of debris occur (Figs. 67 and 68). These may represent dead cells. The debris is found next to apparently healthy cells which may or may not have a vesicular cytoplasm. The debris seems therefore to represent real degeneration in normal development rather than some artifact of fixation. The same interpretation should apply to the membranes which enclose the debris or delimit cytoplasmic vesicles.

The urodeal membrane is heterogeneous. The foci of degeneration are not large and are not far from cells of very different composition (Fig. 69). In some of these the tubular endoplasmic reticulum may be prominent and may possess many attached and proximate ribosomes. The outer nuclear membrane may be raised in numerous blebs, and there is some indication that ribosomes may attach to it. The cytoplasmic membranes to which ribosomes are not attached are those of the Golgi, the multivesicular bodies, and the cell surface. A few ribosomes lie at the cell membrane, but there are no groups of ribosomes aligned on this membrane.

The Golgi of the deeper cells differs from the Golgi of superficial cells by the presence of cisternae and more vesicles (Fig. 70). These may be close to multivesicular bodies. The cisternae have terminal blebs suggestive of the formation of Golgi vesicles and the multivesicular bodies may have appended vesicles suggestive of fusion with Golgi vesicles. There is no indication of the attachment



of ribosomes to these three membranous structures which would seem to set them apart from the general reticulum. The location of elaborate Golgi in cells close to degenerating cells (Figs. 67, 70 and 71) prompts the possibility that there may be some meaning to this proximity. For instance, in Fig. 70 the Golgi and the multivesicular bodies are found in a cell which is firmly attached to another cell, the proximate region of which shows signs of dissolution. Instead of the distinct groups of ribosomes found elsewhere in the cell there is an arc of rather amorphous material. The nearest multivesicular body is perforated and a series of small vesicular bodies extends through this and along the outside wall of the multivesicular body. The coincidence of the various structures may be nothing more than coincidence or artifact, but it raises the possibility that an adjacent cell may play a role in the degeneration of another cell by means other than direct phagocytosis. This may involve the Golgi and multivesicular bodies of the viable cells. Figure 70 is reproduced as part of Fig. 71.

The borders of the extracellular or bursa vesicles may be lined by long extensions of cytoplasm bearing long or numerous tight junctions (Fig. 71). These are common and are similar to extensions which border the cavity of the cloaca (Fig. 73). The tight coupling of these cells and the symmetry of the vesicles (Fig. 73) suggest that the fluid of



the vesicles is under pressure. The flattening of the cells reduces the distance between cell membrane and nuclear envelope. The nuclear blebs may come close to the cell membrane and may be difficult to distinguish from it and from intracytoplasmic membranes (Fig. 72). The cell membrane bordering the extracellular vesicles may show the dark-light alteration described previously. Again, there is the hint that the light segments may be portals through which amorphous and granular cytoplasm enters the vesicles (Fig. 72). The dark segments seem to be darker than the nuclear and intracytoplasmic membranes.

Extracellular vesicles are found close to the cloaca, but no indication of fusion with the cavity of the cloaca has been seen. If fusion occurs it might be difficult to detect. The contrast between the contents of the extracellular vesicles and the cavity of the cloaca, as shown in Fig. 73, is practically invariant. The former always contains visible material and the latter never does. Complex arrays of tight junctions are more common near the cloaca (Fig. 73). The complex tight junctions are less common in areas which lack extracellular vesicles, but interdigitations and desmosomes are common throughout the urodeal membrane (Fig. 74).

Another feature of the membrane is the widespread occurrence of cytolysosomes (Fig. 75). These are largest near

the proctodaeum (Figs. 67 and 68). Perhaps these represent phagocytosis, but typical phagocytes were not seen. Degeneration is remarkably discrete away from the proctodaeum. Death seems to come to the urodeal cells individually by mechanisms which are either internal or involve only the dying cell and those adhering to it.

The urodeal membrane is demarcated from mesenchyme by a basement membrane (Fig. 76). No cells were seen to broach this. The cells along the basement membrane are healthy, and contain multivesicular bodies, nuclear blebs, and many cytoplasmic vesicles, but little debris. These are the most uniform of the urodeal cells. Most are polarized with the nucleus located toward the basement membrane and the bulk of the cytoplasm and its organelles located away from the basement membrane. As in the follicles of the lymphoid bursa (Figs. 10, 13, and 14), the basement membrane of the urodeal membrane is simple and continuous and serves as a useful histological marker. This contrasts with the basement membrane of the thymus.

The Thymus

Unlike the follicles of the bursa, the cortex and medulla of a thymus follicle are not separated by a basement membrane. The original basement membrane of the thymus corresponds in position to the outer surface of the cortex, i.e. to its demarcation from free mesenchyme (Chan and Sainte-Marie, 1968). Even this original demarcation doesn't mean much because the vascular capillaries penetrate deeply

into the cortex and the medulla in company with mesenchyme. To its center, the mature thymus must be regarded as an organ of mixed origin, a mesenchymal-endodermal organ. The epithelium is demonstrable in mammals, after treatments which deplete the organ of its lymphocytes, as a complex, convoluted, and tenous tissue (R. N. Baillif, 1948). The basement membrane may persist around the epithelial cells, but its demonstration in the normal thymus as a continuous, histological boundary is formidable for topological reasons if it is, in fact, continuous.

Unlike that of mammals, the thymus of birds does not fuse into one median organ. It persists as two unconnected bilateral organs. Each is formed of many lobes arranged on either side of the esophagus and trachea. The lobes take cervical positions very early and can be seen under the surface of the neck on the 13th day (Fig. 77). At this age the thymus contains a little punctate acid phosphatase activity (Fig. 78) which is less abundant than that of the bursa.

The positions of the lobes at 12 days are not much different (Figs. 78 and 79). At 11 days the lobes are thinner, but still lymphoid (Figs. 81 and 82). At 10 days the thymus is in transition from the pre-lymphoid, epithelial condition (Figs. 83 and 84). At 8 days some lobules are epithelial and some are beginning the histological transition (Figs. 85 and 86). At 7 days the thymus is wholly

epithelial (Figs. 87 and 88). The thymus undergoes two morphological changes between the 7th and 8th days: it separates into segments and these send out lateral lobules. These penetrate the mesenchyme at about the time the cytological transition to lymphoblasts begins (Ackerman and Knouff, 1964).

The 7 day thymus represents a great elongation of the 6 day thymus (Figs. 89 and 90). Thymus III contributes most of this. The upper or cranial tip of Thymus III (Figs. 89 and 90) is the most dorsal part. This is derived from the lateral part of the thymus primordium and presumably from its associated ectoderm and the caudal tip is derived from the medial part of the thymus primordium and the broken connection to Pharyngeal Pouch III. By analogy with the mammalian thymus, the center and the caudal tip of Thymus III should extend caudad to form the elongated thymus of day 7 (Figs. 87 and 88).

The 5 day thymus is connected mediad to the pharynx through the pharyngeal pouch and laterad it touches a mass of ectoderm (Figs. 91 to 94). In some 5 day embryos this mass is continuous with the ectoderm of Branchial Groove III and through it to the ectoderm of Branchial Groove IV, a small part of which is attached to Thymus IV (attachment not shown).

The 5 day thymus is connected to the pharynx through the pharyngeal pouch (Figs. 91 to 94). The thymus arises

as a dorsal protrusion from the crescentic lateral end of Pouch III (Fig. 92) and similarly from Pouch IV. A small mass of ectoderm which abuts Thymus III has detached from the branchial groove. This mass of ectoderm is fused to the endoderm. Its fate will require detailed studies, but its presence adjacent to the thymus primordium is evidence that ectodermal cells are sufficiently close to the thymus to contribute to it.

An earlier stage of development shows the thymus as a distinct dorsal protrusion of Pouch III (Figs. 95 to 98). At this stage the pharyngeal cavity extends into the thymus primordium (Figs. 97 and 98). The acid phosphatase reaction is intense (Figs. 99 and 100). Enzyme activity is concentrated in a band about one third of the distance from the lumen to the mesenchyme, but there are many other foci of activity in the epithelium. These other foci include debris which is at the edge of the epithelium and is, presumably, being expelled into the mesenchyme (Figs. 99 and 100). The proof of this must await electron micrographs which intercept points of extrusion. Cell deterioration and death and high acid phosphatase activity are not restricted to the thymus. Related epithelial areas, which may or may not contribute to the thymus primordium, also show deterioration and high activity (Fig. 101).

More ventral sections trace the primordium to the caudal wall of the lateral end of the pharyngeal pouch (Fig.

102). The ectoderm intrudes to a point just under the lateral extreme of the primordium (Fig. 103). In this instance the ectoderm can be traced directly to the superficial branchial ectoderm of Groove III (Fig. 103). Succeeding ventral sections cut a lateral protrusion of the ventral endoderm of the pouch (Figs. 104 to 106). This reaches to the branchial groove. The differences between Figs. 91 to 94 and Figs. 95 to 98 indicate a difference in maturity; the thymus shown in Figs. 91 to 94 is slightly more advanced. The comparison also indicates one of the practical problems in studies of this kind. The age or stage of an embryo is not an exact guide to the morphology of the thymus primordium. Figs. 91 to 94 represent the right Thymus III and Figs. 95 to 98 represent the left Thymus III of one 5 day embryo. The left thymus is the better for showing the intrusion of ectoderm and the lateral extension of endoderm, but the right thymus is the better for showing the intimate contact of ectoderm with the thymus primordium. The differences are not restricted to Thymus III and its associated membranes. The right Thymus IV (Figs. 93 and 94) is more advanced than the left Thymus IV (Figs. 106 to 108), which is just beginning its protrusion from Pouch IV. The differences between the right Thymus III and IV and the left Thymus III and IV are real and are not explained by tilting of the sections. Rarely,

if ever, are the two sides symmetrical. The different shape and the greater maturity of Thymus III as compared with Thymus IV is expected, but the different maturities of the two sides is the more fundamental contrast.

Cell degeneration is very common throughout the epithelial complexes from which the thymus is formed (Figs. 102 to 108). It is extreme medial to the thymus, where the connection to the pharynx will break, and lateral to the thymus, where the connection to the branchial groove will break (Figs. 109 and 110). It is profound in the external ectoderm which lines the grooves and the adjacent surfaces (Fig. 110). This is an area which will be enclosed by overgrowth of the hyoid arch and the surface is destined therefore to become internal. Since most of the enclosed epithelium will disappear, it seems that the degeneration of the external epithelium anticipates its inclusion within the body and cannot be viewed as a consequence of inclusion.

Intense acid phosphatase activity is found throughout the epithelia (Figs. 111 and 112). This may be compared with the acid phosphatase activity of the urodeal membrane (Fig. 113). The reality of degeneration is confirmed by the intense uptake of dye at the surface of the branchial grooves (Figs. 114 and 115). Three branchial areas take up the dye: Grooves II, III, and IV. Nearby, but separate, is the large, seemingly homogeneous (see legend, Fig. 114),

degenerating area of the wing. This area is the subject of the best description of amniote degeneration (Saunders et al., 1962). Comparison of this area with the punctate staining of the branchial grooves confirms the morphological and histochemical evidence of degeneration at the external surfaces of the grooves. The maximal intensities are about the same. The apparent homogeneity of the stained area of the wing is an artifact. The plane of focus intercepts the branchial ectoderm, but not the stained area of the wing. It is not practical to apply this technique to the internal membranes, but it seems safe to assume that the internal epithelia would stain in those areas which show morphological and histochemical evidence of degeneration.

The surface of Groove III is an area of profound degeneration (Fig. 116). The montage shows a mixture of dark, intermediate, and light cells plus debris within the epithelium, and phagocytes just outside the epithelium. Some of the light cells contain masses of very dark debris (Figs. 117 and 118) like those of the mesenchymal phagocytes (Fig. 116). Some dark cells have membranous whorls (Fig. 117) indicative of membrane destabilization and cell damage (Chen and Ruth, 1966; Carr, 1967). The dark cells may be degenerating cells and the light cells may be healthy phagocytes.

Intercellular spaces are present. These are irregular and are not accompanied by tight intercellular junctions,

desmosomes, or interdigitations (Fig. 119), in contrast to those of the urodeal membrane. The nucleoli of the dark cells are heterogeneous and contain structures which resemble the nucleolemma; this resemblance may be an accident of degeneration. The nucleoli of light cells are more homogeneous. Some are regular arrays of heavy granules (Figs. 118 and 119). The outer nuclear membrane of light cells is separated from the inner by the familiar, irregular space (Figs. 117 to 119). That of dark cells is close to the inner nuclear membrane (Fig. 119). The nuclear envelope of dark cells is indented or crenated and that of the light cells is smoother. The crenation of the dark nuclei is accompanied by a crenation of the whole cell (Figs. 116 and 119). This suggests that the opacity of dark cells is enhanced by dehydration. The crenation is, however, accompanied by a more subtle departure from normal than simple dehydration or shrinkage.

The ribosomes and the nuclear granules of light cells are larger, more opaque, and more clustered than those of dark cells (Figs. 119 and 120). The smaller and lighter granules of dark cells are scattered more evenly and do not form clusters, excepting those aligned on the endoplasmic reticulum or intracytoplasmic membranes (Fig. 120). It seems that the granules of dark cells have dissociated to give the entire cell a relatively greater and more uniform opacity. This may be a consequence or a cause of dehydration, but

these observations only indicate that two characteristics, cell shrinkage and dissociation, go together.

The impression that it is the dark, not the light, cells which are degenerate is substantiated by differences in the lipid bodies of the two cells. The lipid bodies of dark cells may have crista-like membranes (Fig. 120). Other lipid bodies in the same cells may be transitional between these and distinct, if abnormal, mitochondria (Fig. 120). The lipid bodies of light cells are relatively homogeneous (Fig. 120), there are no transitional lipid bodies, and their mitochondria look more normal (Fig. 120). This suggests that the mitochondria of dark cells degenerate into lipid bodies which contribute to those of the light cells by direct phagocytosis and modification or by dissolution and absorption of the lipid.

Similar signs of degeneration are present at the internal contacts of ectoderm with endoderm (Fig. 121). The mixed population of light and dark cells extends inward as far as these contacts. The primordium of the endodermal thymus is distinguished by the high proportion of healthy cells (Fig. 122). These are partially separated from the mesenchyme by a basement membrane (Fig. 122). Despite the presence of many healthy cells the thymus also contains many signs of degeneration (Figs. 123 and 124) and the

mesenchymal cells may contain much debris (Figs. 123 and 126). Mesenchymal cells and phagocytes have not been identified within the epithelium of the thymus primordium. This agrees with the indications in the light micrographs (Figs. 99 and 100) that the debris leaves the epithelium and is phagocytized in the mesenchyme.

The thymus primordium contains many myelin figures. One of these has not been seen in the endoderm away from the thymus, in the surrounding mesenchyme, or in the branchial ectoderm. This is the nuclear whorl (Fig. 127). Some protrude into the intercellular space (Fig. 128). Similar, but smaller, whorls have been interpreted as developing mitochondria (Pannese, C., 1966), but it is more likely that they represent destabilization of the nuclear envelope or discard of excess envelope. Small alterations of the nuclear envelope are seen in other tissues, e.g. bursa lymphocytes, but the distinctive whorls are peculiar, in this study, to the primordium of the thymus. They are interpreted as evidence of membrane instability associated with differentiation or degeneration. Since similar whorls occur in spermiogenesis (Anderson et al., 1967) it is unlikely that their presence is a necessary indication of cell death, although they may accompany a decrease in nuclear functions.

Myelin degeneration is not restricted to the nuclear envelope of the thymus cells. It is found in mitochondria (Figs. 127, 129 and 130), and in all parts of the cytoplasm.

25

The degeneration seen in the electron micrographs of internal epithelia, including the primordium of the thymus, must involve cell death as well as cell differentiation.

Although mitotic cells have been seen in the thymus they are not frequent. Yet mitosis or migration from contiguous epithelia or mesenchyme must occur in order for the thymus to grow. It is difficult to exclude cell migration, but somewhat easier to test the intensity of mitosis. Colcemid blocks mitosis and leaves the condensed metaphase chromosomes in the center of the cell as a large clump. Many such arrested metaphases may be seen in the 5 day thymus six hours after treatment of the embryo (Figs. 136 to 141). These are not distributed uniformly. In more ventral sections the arrested metaphases are separated by areas of degeneration and debris (Figs. 137 to 141). The distribution of the arrested metaphases is distinctly different from that in the pharyngeal pouches which have a zone of arrested metaphases adjacent to the lumen (Fig. 142).

IV. DISCUSSION

The immediate purpose of the work is to describe the earliest development of the primary lymphoid anlagen. The chicken embryo was selected because it has two principal lymphoid anlagen and the ages of the embryos can be controlled.

Histological and cytological methods have been used because the components of the anlagen are too small to be easily identified by any other means and too fragile for dissection.

The principal point of the observations may be stated directly. There is an intimate contact of ectoderm and endoderm in the immediate vicinity of the anlagen of the thymus and the bursa of Fabricius. Both organs begin as masses of endodermal epithelium. A direct contribution of ectoderm is not evident, but is not excluded by our observations. The regions of ectodermal-endodermal contact and the adjacent anlagen are areas of massive cell degeneration and cell death.

The occurrence of small vesicles in the urodeal membrane is the first indication of the formation of the primordium of the bursa of Fabricius. These vesicles, in most cases, are found in the 5-day chick embryo, although occasionally a very few vesicles can be identified in the 4-day embryo. In 1880 Stieda mentioned that Bornhaupt (1867) had described the appearance of the bursal vesicles on day 7 or 8 at a time when the rectum has not yet connected with the anal canal. Gasser (1880), however, maintained that the primary development of the bursa occurs earlier - its presence being evident on day 6. Wenckebach (1888) reported the occurrence, in the 5-day old embryo of Gallus, of many small cavities in a narrow crest of epithelial tissue in the posterior portion of the cloaca. In 1915 Jolly indicated that bursal vesicles are seen on the sixth day of incubation. However, vesicles appear to be

visible in his picture of the 5-day embryo (Fig. XXII, p. 398). Pera (1958) described the presence, in 5-day embryos, of numerous small and irregular cavities, separated from each other by a fairly thin epithelial wall; these appeared along with the initial development of the bursa. In 1964 Ruth et al. reported that small vesicles were present at the point of contact of the urodeal membrane and the proctodaeum in the 4-day chick embryo, and were more obvious the 5-day embryo. The present study confirms that the development of the bursal primordium of the chick embryo is evident on the fifth day of incubation.

The bursal vesicles of the 5-day embryo are most frequent in the endoderm which contacts ectoderm. They are less numerous near the cloacal lumen and do not appear in the dorsal side of the cloacal lining. These observations lead to the supposition that the ectoderm plays some role in the early development of the bursa primordium. Pera (1958) has discussed the contributions of the germ layers to the bursa of Fabricius. Many agreed that the bursa is endodermal; a view exemplified by the work of Huscke (1838), Bornhaupt (1867), Stieda (1880), Wenckebach (1888), Marshall (1893), Pomayer (1902), Boyden (1922) and others. However, other workers such as Koelliker (1879), Retterer & Balfour (1876), Vialleton (1911) considered the bursa to be ectodermal. Pera himself supported the view that the bursa is endodermal, and suggests that those workers who

considered it ectodermal probably studied the organ at too advanced a stage of development (8-9 days of incubation); that is, when the potential bursa does not show any connection with the posterior cloacal wall. Moreover, at this stage, the cavity of the bursa communicates with the proctodaeum. The separation from the cloaca and the acquisition of a secondary connection to the proctodaeum are the probable basis for the erroneous concept that the bursa is ectodermal.

Boyden (1922) reported that the regression of the caudal intestine is greatly complicated by the disintegration of the adjacent cloacal wall, the latter process resulting in the formation of the cloacal fenestra. The active disintegration begins at about 2 days and 18 hours of incubation. Jolly (1915) mentioned that the post-anal intestine (caudal intestine) undergoes regression on the third or fourth days. No caudal intestine was seen in 4- or 5-day embryos used in the present study. The regression of the caudal intestine is not related to the formation of the urodeal membrane: the latter grows by fusion of the two cloacal walls starting from the floor of the cloaca immediately adjacent to the proctodeal lumen and extending to the posterior end of the cloaca. The fact that the bursal vesicles appear in the urodeal membrane close to the proctodeal lumen and (later) along the boundary between the urodeal membrane and the mesenchyme indicates that the

bursa does not develop from the caudal intestine. However, Stieda (1880) and Jolly (1915) described work supporting the conclusion that the bursa comes from the caudal intestine. In 1880 Stieda wrote "The epithelium of the bursa of Fabricius develops from the epithelial elements which originally belong to the caudal intestine". In 1915 Jolly presented evidence that the first primordium of the bursa exactly occupies the position of the post-anal intestine (caudal intestine) and is oriented in the same way. He added that one might even say that this primordium is identical with what remains of the post-anal intestine, and one might consider the bursa as representing the remainder of the caudal intestine which arises posteriorly, turns towards the head, and undergoes a subsequent development to form a true cloacal caecum.

Pera (1958) writes in his discussion "In the embryos of Gallus domesticus the bursa starts growing in that narrow region of the posterior cloacal wall, from which at an earlier stage, the caudal intestine protruded. More precisely, some nests of epithelial cells are observed in embryos 3 days and 2 hours and 3 days and 18 hours old, when the caudal intestine has almost regressed to a small thin cord. These nests proliferate actively and generate a small ovoid, epithelial protuberance in embryos of 4 days and 4 days and 4 hours. This protuberance represents the potential bursa of Fabricius". The protuberance, described by Pera as extending from the

floor of the cloaca toward the proctodeal lumen (Fig. 18, Pera, 1958) has not been seen in the present study (see Figs. 39-42). The urodeal membrane seen between the floor of the cloaca and the proctodeal lumen is easily demonstrated in 4-day chick embryos (Figs. 39-42), and the protuberance seen by Pera may be just a part of the newly formed urodeal membrane.

Many papers dealing with the development of the bursa of Fabricius were published in the late 19th century and early 20th century. However, there were very few of these accounts which dealt with the problem of how the bursa vesicles are formed. No doubt this was partly due to the limitations of the light microscope. In 1880 Stieda mentioned that the atrophy of cells in the center of the solid spherical body, which he thought to be the first primordium of the bursa, forms a small cavity, which later communicates with the anal canal. The present studies show that cell degeneration occurs in the urodeal membrane and the proctodeal ectoderm, but the vesicles are not simply the spaces vacated by dying cells. Many distended intercellular spaces are seen with the electron microscope. These distended intercellular spaces coalesce to form larger spaces or bursa vesicles, the latter being large enough to be seen with the light microscope. Cell debris is not present in the distended intercellular spaces or bursal vesicles, and it seems clear that cell deaths do not result in the formation of the bursal vesicles.

Conversely, the vesicles seem to be produced by secretion of fluid by healthy cells. This may be accompanied by the release of fluid cytoplasm (Fig. 66).

The exact function of the bursa is not clear. Because the development of the bursa is inverse to that of the gonads - full-grown before sexual maturity and involuted at sexual maturity - some authors have attempted to relate the bursa to reproduction. Jolly (1928) reported that castration retards the involution of the bursa in the male chicken. In 1943 Selye reported that injection of sexual hormones accelerates the involution of the bursa in the cock. Kirkpatrick and Andrews (1944) obtained the same result in the pheasant. It was, however, the work of Glick et al. (1956) which assigned an important function to the bursa as an immune organ. The chick bursectomized within two weeks of hatching and the chick embryo treated with androgen to prevent development of the bursa show serious impairment of antibody production (Mueller et al., 1960).

The primordia of the chicken thymus arise from thickenings of the third and fourth pharyngeal pouches. A thickening of the epithelium of the dorsal part of the second pouch was mentioned by Kastschenko (1887). This epithelial thickening was again reported by Scothorne in 1957 in six other species of birds. Since the thickening disappears without undergoing any specific differentiation and is the anatomical homologue of Thymus II of lower vertebrates, it has been

termed an abortive thymus.

Mall (1887) described the endoderm of the third pharyngeal pouches as the only anlagen of the chicken thymus, but Verdun (1898) reported that the primordium of the chick thymus develops from the third and fourth pharyngeal pouches. The dual origin from the third and fourth pouches is generally accepted and is confirmed in this study. The two anlagen on each side combine to form a thymus on each side of the animal (Hammond, 1954).

On the basis of his observation that the second closing membrane of a visceral cleft forms laterad to the original closing membrane, Kastschenko (1887) concluded that the ectodermal epithelia of the third and fourth branchial grooves probably contribute to the formation of the chick thymus. This has been tested by Schrier and Hamilton (1952) and Hammond (1954). Schrier and Hamilton (1952) described experiments in which carbon particles, placed on the branchial surface, found their way to the thymus and parathyroids. They concluded that the ectoderm may contribute to the formation of the thymus anlagen. Hammond observed (1) a marked reduction in the development of the thymus following the removal of the branchial ectoderm, even when the wound closes over well enough to permit attachment of the pouches to the reconstituted ectoderm, and (2) that rudiments of the thymus cannot be found if the pouches fail to attach to ectoderm. He claimed that

the thymus in the chick is a derivative of the branchial ectoderm related to the dorsal part of Pharyngeal Pouches III and IV, and that the pharyngeal pouches do not give rise to the thymus if the branchial ectoderm and the pouches do not make proper contact. Hammond is probably correct in pointing out that the thymus development requires the normal relation between the pouches and their respective branchial ectoderm. The branchial ectoderm could, however, be required for the normal development of its respective pouch, but might not be essential to the formation of the derivatives of the thymus rudiments. The removal of branchial ectoderm interferes with the normal development of the pouches and this alone might explain the absence of the thymus rudiment. The base of the major thymus rudiment arises from the endodermal cells of the pouches just at the discernible limit of the branchial ectoderm. The ectodermal part of Branchial Membrane III separates from the body surface, but remains attached to Thymus III. Thus ectodermal cells of Membrane III may contribute to the formation of Thymus III, but it is clear that the greater portion of the rudiment arises from the dorsal part of the pouch. Thymus IV behaves in a similar way.

The function of the thymus remained obscure for a long time. The situation changed about 1950 when systematic removal of various organs showed that thymectomy of the young mouse blocks the onset of lymphatic leukemia (Ruth et al.,

1965). Beginning in 1957, Fichtelius and his colleagues published a series of isotopic studies which indicated that immunologically competent cells may emigrate from the thymus as they differentiate (Ruth, 1960). Additionally, the thymus may play a continuing role in the humoral control of lymphoid homeostasis (Miller, 1964; Metcalf, 1964). The initial indication of this is seen in the early invasion of the thymus by blood-borne cells which proliferate within the organ (Moore and Owen, 1967).

The present study differs from previous studies by inclusion of electron micrographs of the earliest anlagen of the bursa and the thymus. These confirm the impression of cell degeneration and death evident in light micrographs. Numerous lipid droplets of irregular shapes are observed in the proctodeal ectoderm, urodeal membrane, and the area of contact between branchial ectoderm and pharyngeal endoderm. The significance of this is not clear. Kremer also noted that degenerating cells often contain fat (Glucksmann, 1951). The proctodeal ectoderm, the urodeal membrane and the cloacal endoderm contain cell debris and numerous foci of cytoplasmic degradation similar to those found in the branchial ectoderm and the pharyngeal endoderm. Foci of cytoplasmic degradation are morphologically similar to the autophagic vacuoles of de Duve (1963) and cytolysosomes of Novikoff (1960). What is the significance of focal cytoplasmic degradation? Evidence is available to show that cytolysosomes or autophagic vacuoles

contain hydrolytic enzymes (de Duve, 1959; Novikoff et al., 1960) and are sites of digestion. The varied appearance of these cytolysosomes is due to differences in the stages of their degradation and to the presence of different cell organelles in them. In the present study, some of them, in an advanced stage of degradation, are seen occupying the major part of the cell. The occurrence of cytolysosomes and cell debris is indicative of cell degeneration. (Cytolysosomes are frequent in cells injured experimentally, Hruban et al., 1963; Swift et al., 1964; Novikoff et al., 1964; Miller et al., 1964). Hruban et al. (1963) have suggested that focal cytoplasmic degradation involves the enclosure of small portions of cytoplasm in smooth membranes within which digestion occurs. Novikoff et al. (1964) also suggested that autophagic vacuoles originate from the endoplasmic reticulum.

The multivesicular bodies and the Golgi apparatus of the bursa primordium may be related to the formation of lysosomes. The appearance of multivesicular bodies close to the Golgi apparatus and the similarity of the inner vesicles of the multivesicular body to the Golgi vesicles are suggestive of an intimate relationship. Novikoff et al. (1964) proposed that Golgi vesicles may contribute to the formation of multivesicular bodies, and may be considered to be the primary lysosomes. The inner vesicles of multivesicular bodies frequently resemble Golgi vesicles in size and appearance. The individual vesicles of multivesicular bodies

of rat cells possess acid phosphatase activity. It may be that the multivesicular body receives acid hydrolases from the Golgi vesicles, some of which appear intact within the body.

Bruni and Porter (1965) observed multivesicular bodies in the early stage of their formation. The vesicles are identical in size and content to the vesicles released from the Golgi lamellae, and Golgi vesicles are very close to and even attached to the multivesicular bodies. They propose that vesicles are released from the Golgi apparatus, lose their surface coating, and fuse into aggregates which transform into multivesicular bodies. It might be expected that Golgi vesicles would also transport lysosomal hydrolases to autophagic vacuoles, but thus far no observations suggestive of this have been encountered.

A distention of the nuclear envelope or nuclear blebbing has been seen occasionally in the cells from the urodeal membrane (Fig. 72). Small vesicles or granules were seen in the nuclear blebs (Figs. 65 and 76). These vesicles differ from Golgi vesicles and MVB vesicles. Possibly, they contribute to the intracellular bursa vesicles. The bursa vesicles seem to exert pressure on the surrounding cells as though these cells form the bursa vesicles by actively secreting fluid which cannot escape. The electron micrographs show the tight junctions between the cells which enclose the bursa vesicle. The tight junctions are seen only near the luminal aspect of the apposed cell surfaces.

In contrast to the urodeal membrane and other epithelia, the cells in the growing tip of the thymus are loosely packed together. The numerous, irregular, intercellular spaces are penetrated by many long, slender cytoplasmic protrusions. The thymus is partly separated from the surrounding mesenchyme by an incomplete basement membrane and fluffy extracellular substance (Fig. 122). Cells are actively proliferating as shown by the large number of blocked metaphases in Colcemid-treated embryos. Ovoid nuclei with large nucleoli are seen in the dorsal part of the thymus (Fig. 122). Nuclei with irregular outline are found in the ventral part of the thymus (Fig. 123). Tubular endoplasmic reticulum and mitochondria are moderately frequent. Cell debris is common and phagocytes containing cell debris are seen close to or beside the thymus. Free cell debris also occurs close to the thymus. This supports light microscopic indications that some cell debris is expelled from the thymus and other epithelia into the mesenchyme where it is phagocytized by mesenchymal cells.

The thymus contains many myelin figures connected to the nuclear envelope as whorls. Other myelin figures are connected to mitochondria, endoplasmic reticulum, Golgi membrane, and plasma membrane. Myelin figures may be indicative of membrane destabilization or membrane degeneration, and may be a step in the elimination of excess membrane. Nuclear whorls similar to those of the thymus appear during spermiogenesis (Nicander and Bane, 1962; Fawcett and Ito, 1965; Anderson et al., 1967)

and in the spinal ganglia of the chick embryo (Pannese, 1966). Myelin figures have been found in normal cells as well as in degenerating or experimentally treated cells (Cecio, 1964). Although myelin figures are demonstrated more readily in glutaraldehyde-osmium tetroxide fixed materials than in other fixatives (Carr, 1967), they are also found in the materials fixed in osmium tetroxide alone (Cecio, 1964) or in permanganate (Stoeckenius, 1958; Campiche, 1960). For example, myelin figures connected with the nuclear envelope have been found in spermatozoa fixed in osmium tetroxide alone (Nicander and Bane, 1962; Fawcett and Ito, 1965). Richter and Moize (1966) reported that myelin figures were present in the bladders of all adult mice but were not seen in bladders of the rat, guinea pig, rabbit, dog, cat or human. They were always present in the intermediate layer of epithelial cells but never in the basal or superficial layers. They did not occur in newborn mice but appeared by 10 to 14 days of age. Myelin figures are not, therefore, a simple artifact of glutaraldehyde fixation. They must be present before fixation or they must arise during fixation as a consequence of a physical peculiarity of the membranes which is expressed during fixation as nuclear whorls or myelin figures.

Two types of cells have been observed in the region of contact of the branchial ectoderm and the endoderm of the pharyngeal pouch: light and dark cells (Figs. 116 and 121). The recognition of two types is based on the profound alteration of the electron-scattering potential of the nuclear and

cytoplasmic matrices of entire cells. Light and dark cells are also found in the liver parenchymal cells under various experimental conditions: after ligation of the common bile duct in the liver of rat (Steiner et al., 1962); after the administration to rats of toxic agents such as ethionine (Herman et al., 1962) and carcinogens such as naphthylisothiocyanate (Steiner and Baglio, 1963). Steiner and Baglio (1963) did not consider the occurrence of light and dark cells to be due to an artifact produced by the buffer used in the preparation of the fixative. There is as yet no acceptable explanation, although it seems clear that light and dark cells mainly appear when tissues or cells are not in normal condition. In the normal developing embryo their occurrence may be due to tissues or cells undergoing some special alteration.

The cytoplasmic granules of dark cells are more evenly distributed than those of light cells, which suggests that polyribosomal clusters are present in light cells, but absent from dark cells. The smaller size of the granules of dark cells indicates that the ribosomes have dissociated into their subunits. Such dissociation is thought to occur whenever the ribosome loses its attachment to messenger RNA (Guthrie and Nomura, 1968). Thus the appearance of the dark cell can be interpreted to mean that it is not synthesizing protein. For this and other reasons, the dark cell is regarded as a degenerating cell and the light cell is regarded as metabolically

active.

Cell deaths are encountered in: (1) the pharyngeal pouch and contact of the branchial ectoderm and the pharyngeal pouch during the development of the thymus primordia; (2) proctodeal ectoderm and the urodeal membrane during the development of the bursa primordium; (3) the posterior part of the cloaca during its regression; and (4) the fusion of the amniotic folds. The occurrence of the degenerating cells is so apparent that it cannot be accidentally or artifactually produced during the tissue preparation. The appearance of the degenerating cells was noted during the examination of the tissues with the phase contrast microscope and was further confirmed by electron microscopic and histochemical observations. There is no reason, therefore, to doubt their actual existence.

The fact that cell death accompanies differentiation suggests that cell degeneration is a consequence, or a necessary accompaniment of morphogenesis. A comprehensive review of cell death in normal embryonic development has been made by Glucksmann (1951) who classified the cell degenerations according to their developmental functions into three groups - morphogenetic, histiogenetic and phylogenetic degenerations. Many reports on observations of degenerating cells during embryogenesis and organogenesis are listed in Glucksmann's review (1951). The cell degeneration observed in the present study can be considered as a morphogenetic

degeneration, according to Glucksmann's classification.

Saunders et al. (1962) have also pointed out the role of cell death in the shaping of the upper arm and forearm during morphogenesis of the avian wing.

As for the explanation for the death of embryonic cells Glucksmann (1951) and Ernst (1926) have different viewpoints. Ernst (1926) has suggested that endogenous and exogenous factors might cause the death of embryonic cells. He thought that the life energy of embryonic cells might become exhausted like that of adult blood cells, epidermal cells, and die. Glucksmann (1951) considered that Ernst's comparison is not very apt, since embryonic cells are able to rejuvenate themselves by division while the differentiated adult cells are incapable of division. Experimental embryological and genetic observation suggests that certain stimuli for the proliferation and differentiation of organs are active for limited periods only, and it is thus reasonable to assume that when these stimuli cease, cells fail to divide and complete their specialization, thereby aging and subsequently dying (Glucksmann, 1951). With regard to exogenous factors Ernst (1926) has considered the pressure of neighboring mitotic cells and the displacement of cells by changes in the shape of organs which may lead to nutritional disturbances, and result in death. Glucksmann (1951) thought that although Ernst's view may apply in a few instances, it certainly would not account for the majority of morphogenetic degenerations.

Some previous reports (Hamburger and Levi-Montalcini, 1949; Hamburger, 1958; Gasseling and Saunders, 1961) appear to support the view that cell death is the result of certain tissue interactions (Saunders et al., 1962). In general, however, the causation of the morphogenic degenerations is still obscure. Cell degeneration mentioned above is presumably under genetic control, but this is not defined. However, some cases apparently depend on particular genes (Gluecksohn-Schoenheimer, 1942, 1945).

The cell degeneration evident in the urodeal membrane during the formation of bursa vesicles is accompanied by intensive acid phosphatase activity. When the bursa separates from the urodeal membrane the enzyme activity decreases and the signs of cells degeneration are greatly reduced. The enzyme activity reappears in the bursa epithelium during the formation of the follicles and the follicles show signs of cell deterioration. This parallel between acid phosphatase activity, cell deterioration, and differentiation, during the formation of the bursa epithelium and later during the formation of the follicles, suggests that the three processes are intimately, if not necessarily, related.

The cell degeneration in the ectodermal branchial grooves, the endodermal pharyngeal pouches and the thymus primordium is closely associated with acid phosphatase activity. The enzyme activity in the thymus decreases greatly after the

seventh day of incubation. The release of the acid phosphatase or other lysosomal hydrolases is not necessarily the cause of cell death. The lysosomes may become activated after the cells die. The time at which lysosomal hydrolases begin to act in cell degeneration is unknown. The cell debris appears to be phagocytized or absorbed by neighboring epithelial cells or extruded into the mesenchyme and phagocytized by the mesenchymal cells.

The fact that the mitotic cells of the pharyngeal pouch appear along the inner lining of the pouch, as revealed by the Colcemid method (Fig. 142) and the fact that acid phosphatase activity is concentrated basal to the mitotic figures of the pouch (Figs. 99 and 100) suggest that the acid phosphatase activity may be associated with cell division rather than cell degeneration. De Duve and Wattiaux (1966) emphasize the perinuclear rearrangement of the lysosomes during mitosis (Dougherty, 1964; Robbins and Ganatas, 1964; Kent et al., 1965) and the activation of lysosomes in lymphocytes by phytohemagglutinin (Hirschhorn et al., 1964) as indicative that acid phosphatase may play a role in mitosis. Nevertheless, the acid phosphatase activity of the branchial and cloacal epithelia is always intense in areas of cell degeneration and is particularly intense around visible debris. Unless this association with debris represents an artifact of enzyme localization it is more likely that

intense acid phosphatase activity in the branchial and cloacal epithelia is related primarily to the formation and disposal of debris. This is substantiated by the intense activity in mesenchymal cells which contain debris and the weak activity in proliferating lymphoid tissue.

V. SUMMARY

1. The thymus and the bursa of Fabricius, the first lymphoid organs of the chicken, appear on the fifth day of incubation as proliferations of endodermal epithelia.

2. The bursa appears in the caudal half of the urodeal membrane. The urodeal membrane is a small, thin partition between the right and left halves of the body in the region ventral to the caudal end of the gut. The dorsal part of the urodeal membrane is cloacal endoderm and the ventral part is proctodeal ectoderm. The bursa appears as a median chain of intercellular vesicles subjacent to the proctodeal ectoderm and just within the endoderm. These vesicles enlarge and fuse to become the lumen of the bursa. The surrounding endodermal cells proliferate to form the lining of the bursa. The vesicles at the anterior of the urodeal membrane may not contribute to the lumen of the bursa.

The posterior part of the urodeal membrane probably represents the eventual opening of the bursa into the proctodaeum and the anterior part represents the eventual opening of the embryonic cloaca.

3. The number and size of the bursa vesicles suggest that active secretion of fluid occurs throughout the urodeal membrane. Their light microscopic clarity indicates that they are not deposits of cell debris. The borders of the bursa vesicles are lined by numerous tight junctions. The tight

coupling of these cells and the symmetry of the vesicles suggest that the fluid of the vesicles is under pressure. The enlarged and fused bursa vesicles form a bursa sac caudad to the urodeal membrane and the cloaca. The blind end of the bursa sac expands dorsally towards the vertebral column. The bursa lymphoid follicles first appear in the bursa epithelium on the 13th day of incubation.

4. Cell degeneration and cell death are common in the proctodeal ectoderm and the urodeal membrane. Since degeneration is associated with the activity of lysosomal enzymes, the activity of the most definitive of these was examined through the early development of the bursa. The acid phosphatase activity of the bursa epithelium is very active at 7 days, 13 days and 14 days, and inactive at 9, 10, 11, and 12 days. The times at which the epithelium of the bursa has high activity are the times of active differentiation: the formation of the definitive bursa epithelium and its transformation into follicles. The high activity in the proctodeal ectoderm and the subjacent urodeal membrane is associated with the formation of the anus and the bursa stalk.

5. The acid phosphatase activity in the tunica propria is mainly attributed to the immature heterophil granulocytes and partly to the mesenchymal cells.

6. The thymus appears as four separate proliferations. These arise from the dorsal, lateral extremes of pharyngeal

pouches III and IV. Each of these proliferations lies just dorsal and medial to the medial end of a small, transverse membrane connecting the pharyngeal pouch to the corresponding branchial groove. The dorsal part of Membrane III is a tube of ectoderm which intrudes mediad from Groove III and the ventral part is a tube of endoderm which protrudes laterad from the ventral part of Pouch III. The contact of ectoderm with endoderm is continuous from just beneath the body surface to a point just ventral and lateral to Thymus III. Membrane IV does not have a ventral, endodermal part. The contact of ectoderm with endoderm is restricted to the area just ventral and lateral to Thymus IV. There is no chain of vesicles.

7. Cell degeneration is very common throughout the epithelial complexes from which the thymus is formed. It is extreme medial to the thymus, where the connection to the pharynx will break, and lateral to the thymus, where the connection to the branchial groove will break. Intense acid phosphatase activity is found throughout the epithelium and in the early thymus, but not in the thymus after the seventh day of incubation. The reality of degeneration is confirmed by the intense uptake of dye at the surface of the branchial groove. The branchial areas which take up dye are Grooves II, III, and IV.

8. The Colcemid-treated embryos show that cell proliferation is concurrent with cell degeneration in the early thymus

primordium.

9. Two types of cells have been observed in the region of contact of the branchial ectoderm and the endoderm of the pharyngeal pouch: light and dark cells.

The recognition of two types is based on the profound alteration of the electron-scattering potential of the nuclear and cytoplasmic matrix of entire cells.

10. In thymus cells, nuclear whorls are commonly seen. Myelin figures appear in connection with mitochondria, endoplasmic reticulum and Golgi membrane. Nuclear whorls and myelin figures are an indication of membrane degeneration.

BIBLIOGRAPHY

- Ackerman, G. A., and R. A. Knouff. 1959. Lymphocytopoiesis in the bursa of Fabricius. *Am. J. Anat.*, 104: 163-206.
- Ackerman, G. A., and R. A. Knouff. 1964. Lymphocyte formation in the thymus of the embryonic chick. *Anat. Rec.*, 149: 191-216.
- Anderson, W. A., A. Weissman and R. A. Ellis. 1967. Cyto-differentiation during spermiogenesis in *Lumbricus terrestris*. *J. Cell Biology*, 32: 11-26.
- Auerbach, R. 1961. Experimental analysis of the origin of cell types in the development of the mouse thymus. *Dev. Biol.*, 3: 336-354.
- Baillif, R. N. 1949. Thymic involution and regeneration in the albino rat following injection of acid colloidal substances. *Am. J. Anat.*, 84: 457-510.
- Barger, J. D., and E. D. De Lamater. 1948. The use of thionyl chloride in the preparation of Schiff's reagent. *Science*, 108: 121.
- Barka, T. 1960. A simple azo-dye method for histochemical demonstration of acid phosphatase. *Nature*, 187: 248-249.
- Beard, J. 1900. The source of leucocytes and the true function of the thymus. *Anat. Anzeiger*, 18: 550-561.
- Beard, J. 1900. The thymus placode of the spiracle of *Raja batis*. *Anat. Anzeiger*, 18: 359.

- Bornhaupt, T. 1867. Untersuchungen über die Entwicklung der Urogenitalsystems beim Hühnchen. In Diss., Riga. (Quoted from Stieda, 1880).
- Boyden, E. 1922. The development of the cloaca in birds, with special reference to the origin of the bursa of Fabricius, the formation of a urodeal sinus, and the regular occurrence of a cloacal fenestra. Amer. J. Anat. 30: 163-202.
- Bruni, C., and K. R. Porter. 1965. The fine structure of the parenchymal cell of the normal rat liver. Amer. J. Pathol. 46:691.
- Campiche, M. 1960. Les inclusions lamellaires des cell alveolaires dans le poumon du raton. Relations entre l'ultrastructure et la fixation. J. Ultrastructure Res. 3: 302-312.
- Carr, I. 1967. Nuclear membrane whorls. Zeitschrift für Zellforschung. 80: 140-144.
- Cecio, A. 1964. Electron microscopic observations of young rat liver. I. Distribution and structure of the myelin figures. Zeitschrift für Zellforschung, 62: 717-743.
- Chan, C., and G. Sainte-Marie. 1968. Distribution and morphology of the subcapsular and reticular cells of the ten-week-old rat thymus. J. Anat., 102: 477-491.
- Chen, L. T., and R. F. Ruth. 1966. Nuclear structure in lymphoid primordia. Nature, 209: 381-383.

- De Duve, C. 1959. Lysosomes, a new group of cytoplasmic particles. In "Subcellular Particles". T. Hayashi (ed.), Ronald, New York. P. 128.
- De Duve, C. 1963. The lysosome concept. In "Ciba Foundation Symposium on Lysosomes". De Reuck, A.V.S., and M. P. Cameron (eds.). Little, Brown & Co., Boston. Pp. 1-31.
- De Duve, C., and R. Wattiaux. 1966. Functions of lysosomes. *Ann. Rev. of Physiology*, 28:435.
- Dougherty, W. J. 1964. Fate of Gogi complex, lysosomes, and microbodies during mitosis of rat hepatic cells. *J. Cell Biol.* 23: 25A.
- Ernst, M. 1926. Über Untergang von Zellen während der normalen Entwicklung bei Wirbeltieren. *Z. ges. Anat. I. Z. Anat. Entw. Gesch.*, 79:228.
- Fawcett, D. W., and S. Ito. 1965. The fine structure of bat spermatozoa. *Amer. J. Anat.*, 116: 567-609.
- Gasseling, M. T., and J. W. Saunders, Jr. 1961. Effects of the apical ectodermal ridge on growth of the versene-stripped chick limb bud. *Dev. Biol.*, 3: 1-25.
- Gasser, P. 1880. Die Entstehung der Kloakenöffnung bei Hühnerembryonen. *Arch. f. Anat. u. Entwickl.*, S. 297-319. (Quoted from Boyden, 1922).

- Glick, B., T. S. Chang, and R. G. Jaap. 1956. The bursa of Fabricius and antibody production. *Poultry Science*, 35: 224-225.
- Glucksmann, A. 1951. Cell deaths in normal vertebrate ontogeny. *Biol. Rev.*, 26, 59-86.
- Gluecksohn-Schoenheimer, S. 1942. The morphological manifestation of a dominant mutation affecting tail and urogenital systems. *Genetics*, 28: 341-348.
- Gluecksohn-Schoenheimer, S. 1945. The embryonic development of mutants of the Sd-strain in mice. *Genetics* 30: 29-38.
- Gomori, G. 1952. In "Microscopic Histochemistry, Principles and Practice". University of Chicago Press. P. 193.
- Guthrie, C., and M. Nomura. 1968. Initiation of protein synthesis: a critical test of the 30S subunit model. *Nature*, 219:232.
- Hamburger, V., and R. Levi-Montalcini. 1949. Proliferation, differentiation and degeneration in the spinal ganglia of the chick embryo under normal and experimental conditions. *J. Exptl. Zool.*, 111: 457-502.
- Hamburger, V. 1958. Regression versus peripheral control of differentiation in motor hypoplasia. *Amer. J. Anat.* 102: 365-410.
- Hammond, W. S. 1954. Origin of thymus in the chick embryo. *J. Morphol.* 95: 501-521.

- Herman, L., L. Eber, and P. J. Fitzgerald. 1962. Liver cell degeneration with ethionine administration. In "Electron Microscopy, Fifth International Congress". Vol. 2, VV-6. S. S. Breese, Jr. (ed.), Academic Press, New York.
- Hirschhorn, R., G. Kaplan, K. Hirschhorn, and G. Weissmann. 1964. Appearance of lysosomes before mitosis induced in human lymphocytes by phytohemagglutinin. Clin. Res. 12:449.
- Holt, S. J. 1958. Indigogenic staining methods for esterases. In "General Cytochemical Methods". J. F. Danielli (ed.), Academic Press, New York.
- Holt, S. J., and R. M. Hicks. 1961. Studies on formalin fixation for electron microscopy and cytochemical staining purposes. J. Biophys. Biochem. Cytol. 11: 31 and 47.
- Hruban, Z., B. Spargo, H. Swift, R. W. Wissler, and R. G. Kleinfeld. 1963. Focal cytoplasmic degradation. Amer. J. Pathol. 42:657-683.
- Jolly, J. 1915. La bourse de Fabricius et les organes lymphoepitheliaux. Arch. d'anat. micr. T. 16: 363-547.
- Jolly, J., and A. Pezard. 1928. Castration retards the involution of the bursa Fabricius. C. R. de la Societe de Biologie, 98: 379-380.

- Kastschenko, N. 1887. Das Schlundspaltengluet des Hühnchens. Arch. Anat. Phy., Anat. Abt. S. 258-300. (Quoted from Hammond, 1954).
- Kent, G., O. T. Minik, E. Orfei, F. I. Volini, and F. Madera-Orsini. 1965. The movement of iron-laden lysosomes in rat liver cells during mitosis. Amer. J. Pathol., 46:803.
- Kirkpatrick, C. M., and F. N. Andrews. 1944. The influence of the sex hormones on the bursa of Fabricius and the pelvis in the ring-necked pheasant. Endocrinology, 34: 340.
- Luft, J. H. 1961. Improvements in epoxy resin embedding methods. J. Biophys. Biochem. Cytol., 9: 409-414.
- Mall, F. P. 1887. Entwicklung der Branchial Bogen und Spalten des Hühnchens. Arch. Anat. Phys., Anat. Abt. S. 1-34. (Quoted from Hammond, 1954).
- Margolis, G., and J. P. Pickett. 1956. New application of luxol fast blue myelin stain. Lab. Investigation, 5:459.
- Maximow, A. A. 1909. Untersuchungen über Blut und Bindegewebe 2. Über die Histogenese der Thymus bei Säugetieren. Arch. mikroskop. Anat. u. Entwicklungsmech. 74:525-621.
- Miller, F., and G. E. Palade. 1964. Lytic activities in renal protein absorption droplets. J. Cell Biol., 23: 519-552.

- Moore, M. A. S., and J. J. T. Owen. 1966. Experimental studies on the development of the bursa of Fabricius. *Devel. Biol.* 14: 40-51.
- Moore, M. A. S., and J. J. T. Owen. 1967. Experimental studies on the development of the thymus. *J. Exptl. Med.* 126:715.
- Mueller, A., H. R. Wolfe, and R. K. Meyer. 1960. Precipitin production in chickens. XXI. Antibody production in bursectomized chickens and in chickens injected with 19-nortestosterone on the fifth day of incubation. *J. Immunol.*, 85: 172-179.
- Nicander, L., and A. Bane. 1962. Fine structure of boar spermatozoa. *Zeitschr. Zellforsch.* 57: 390-405.
- Novikoff, A. B. 1960. Biochemical and staining reactions of cytoplasmic constituents. In "Developing Cell Systems and Their Control". Pp. 167-203. D. Rudnick (ed.), Ronald Press, New York.
- Novikoff, A. B., and E. Essner. 1960. The liver cell. Some new approaches to its study. *Amer. J. Med.*, 29: 102-131.
- Novikoff, A. B., E. Essner, and N. Quintana. 1964. Golgi apparatus and lysosomes. *Fed. Proc.* 23: 1010.
- Palade, G. E. 1952. A study of fixation for electron microscopy. *J. Exptl. Med.*, 95: 285-297.
- Pannese, E. 1966. Structures possibly related to the formation of new mitochondria in spinal ganglion neuroblasts. *J. Ultrastructure Res.*, 15: 57-65.

- Patten, B. M. 1951. Early embryology of the chick. 4th ed. The Blakiston Co., Philadelphia.
- Pera, L. 1958. Morfologia e sviluppo della bursa di Fabricia in *Gallus domesticus*. Archivio Italiano di Anatomia e di Embriologia. 63: 407-444.
- Richter, W. R., and S. M. Moize. 1966. Myelin figures in mouse transitional epithelium. Fed. Proc. 25:534.
- Robbins, E., and N. K. Gonatas. 1964. The ultrastructure of a mammalian cell during the mitotic cycle. J. Cell Biol. 21:429.
- Ruth, R. F. 1960. Ontogeny of the blood cells. Fed. Proc. 19: 579-585.
- Ruth, R. F., C. P. Allen, and H. W. Wolfe. 1964. The effect of thymus on lymphoid tissue. In "The Thymus in Immunobiology". R. A. Good and A. E. Gabrielsen (eds.) Harper and Row, Philadelphia.
- Ruth, R. F., E. O. Hohn, and G. R. J. Law. 1965. Ontogeny of the lymphoid tissue. Scand. J. Haematol. 8:29.
- Sabatini, D. D., K. G. Bensch, and R. J. Barrnett. 1962. New fixatives for cytological and cytochemical studies. In "Proceedings of Fifth International Congress for Electron Microscopy". 2:L3. S. S. Breese, Jr. (ed.), Academic Press, New York.
- Saunders, J. W., Jr., M. T. Gasseling, and L. C. Saunders. 1962. Cellular death in morphogenesis of the avian wing. Devel. Biol. 5:147-178.

- Schrier, J. E., and H. L. Hamilton. 1952. An experimental study of the origin of the parathyroid and thymus glands in the chick. *J. Exptl. Zool.* 119:165.
- Scothorne, R. J. 1957. Observation on the so-called Thymus II of birds. *J. Anat.*, 91: 13-24.
- Selye, H. 1943. Morphological changes in the fowl following chronic overdosage with various steroids. *J. Morph.* 73:401-418.
- Steiner, J. W., J. S. Carruthers, and S. R. Kalifat. 1962. Observations on the fine structure of rat liver cells in extrahepatic cholestasis. *Zeitchr. Zellforsch.* 58: 141.
- Steiner, J. W., and C. M. Baglio. 1963. Electron microscopy of the cytoplasm of parenchymal liver cells in alpha-naphthylisothiocyanate-induced cirrhosis. *Lab. Invest.* 12: 765-790.
- Stieda, L. 1880. Über den Bau and die Entwicklung der Bursa Fabricii. *Zeitschr. f. Wiss. Zool.*, Bd. 34, S. 296-309.
- Stoeckenius, W. 1958. Fixierung von Myelinfiguren aus Phosphatiden und Eiweiß mit OsO_4 und KMnO_4 . Fourth Int. Conf. E. M., Berlin. 2: 174-177.
- Swift, H. and Z. Hruban. 1964. Focal degradation as a biological process. *Fed. Proc.* 23: 1026-1037.
- Verdun, P. 1898. Sur les derives branchiaux du poulet. *C. R. Soc. Biol., Paris.* 5: 243-244. (Quoted from Hammond, 1954).

- Watson, M. L. 1958. Staining of tissue sections for electron microscopy with heavy metals. J. Biophy. Biochem. Cytol., 4: 475-478.
- Wenckebach, K. F. 1888. De Ontwikkeling en de Bouw der Bursa Fabricii. Proefschrift. Leiden. (Quoted from Boyden, 1922).

Fig. 1. Dextral view of a 4-day chick embryo. A few drops of two percent osmium tetroxide solution have been added to the embryo in order to increase the contrast. This treatment is also applied to the embryos illustrated in Figs. 2 and 3.

X 7.8

Fig. 2. Dextral view of a 5-day chick embryo.

X 6

Fig. 3. Dextral view of a 6-day chick embryo.

X 7

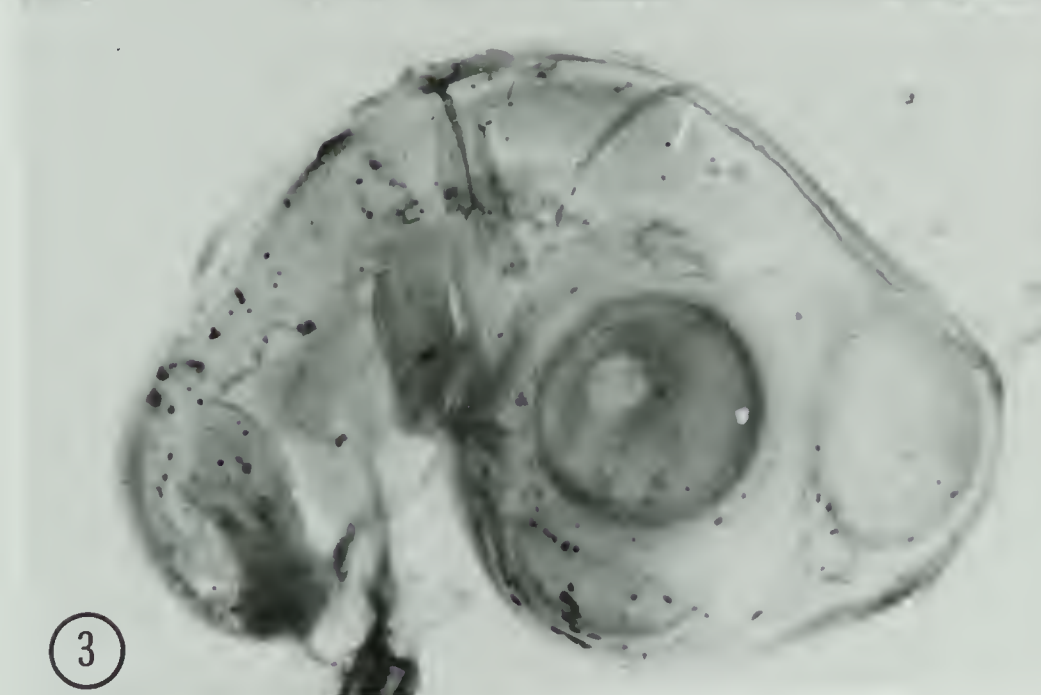
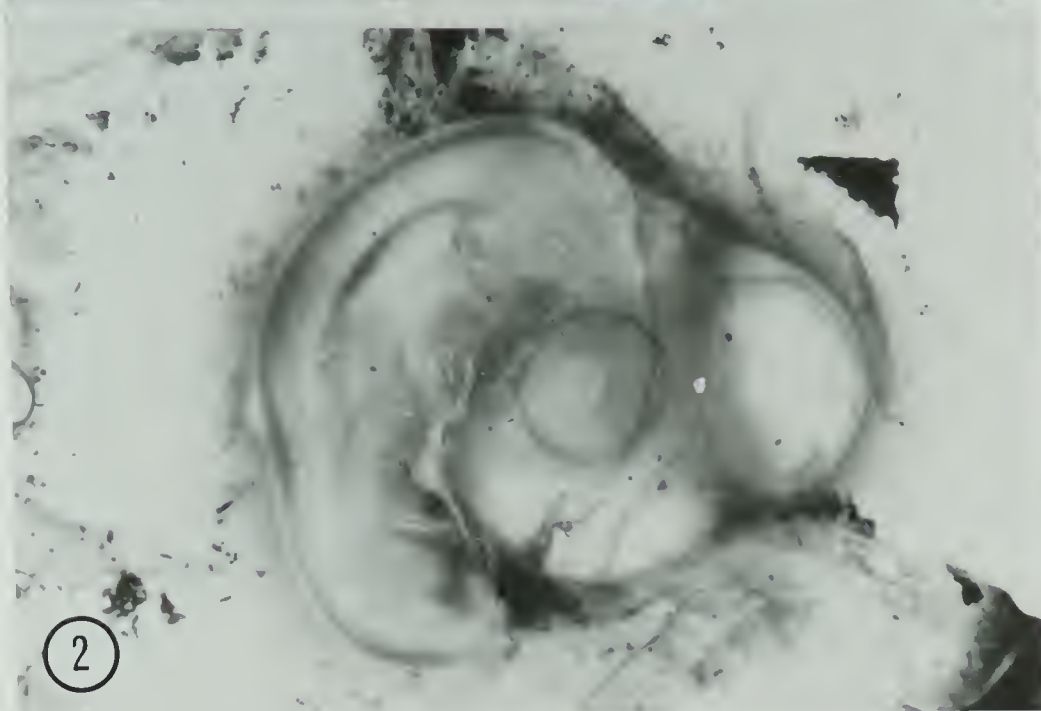
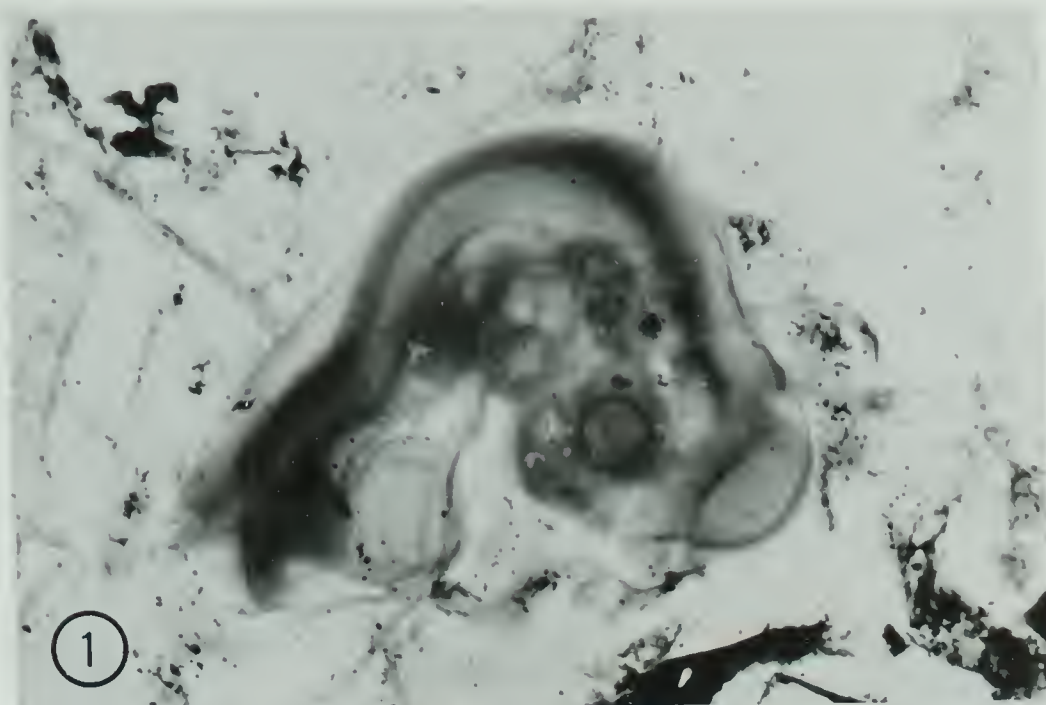
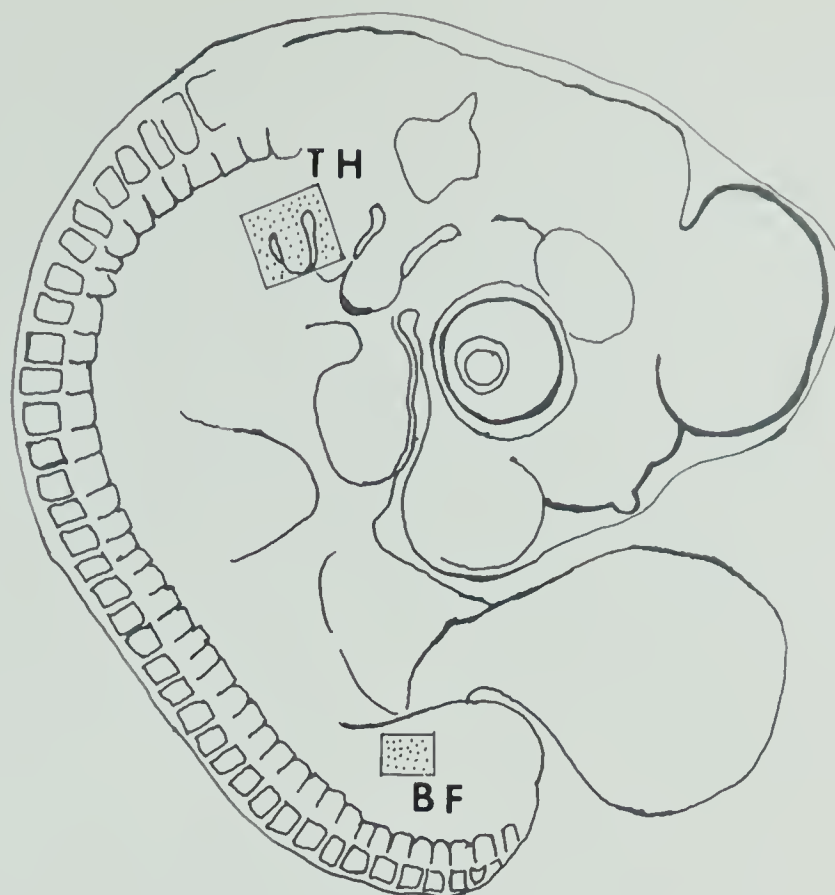


Fig. 4. A diagram of the dextral view of a 4-day chick embryo. The locations of the primordia of the thymus (TH) and the bursa of Fabricius (BF) are shown in the stippled rectangles.

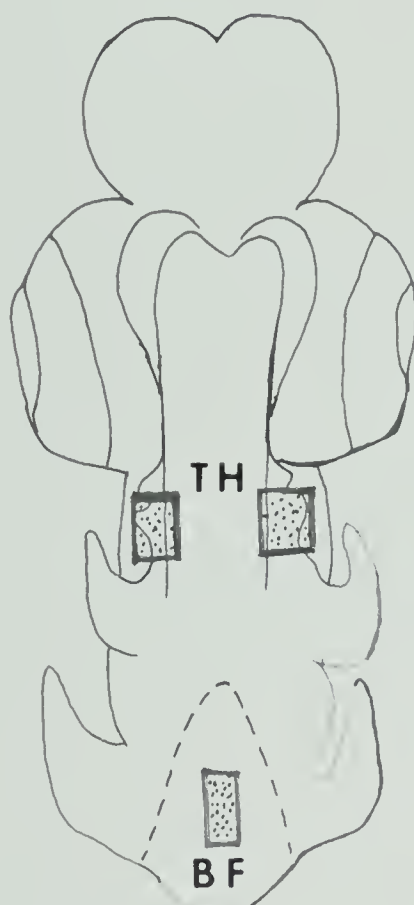
X 16

Fig. 5. A diagram of the dorsal view of a 5-day chick embryo. The locations of the primordia of the thymus (TH) and the bursa of Fabricius (BF) are shown in the stippled rectangles.

X 9



4



5

Fig. 6. Internal organs of a 4-day chick embryo drawn from a wax-plate reconstruction after Patten (1958) to show the locations of the primordia of the thymus (TH) and the bursa of Fabricius (BF).

X 25

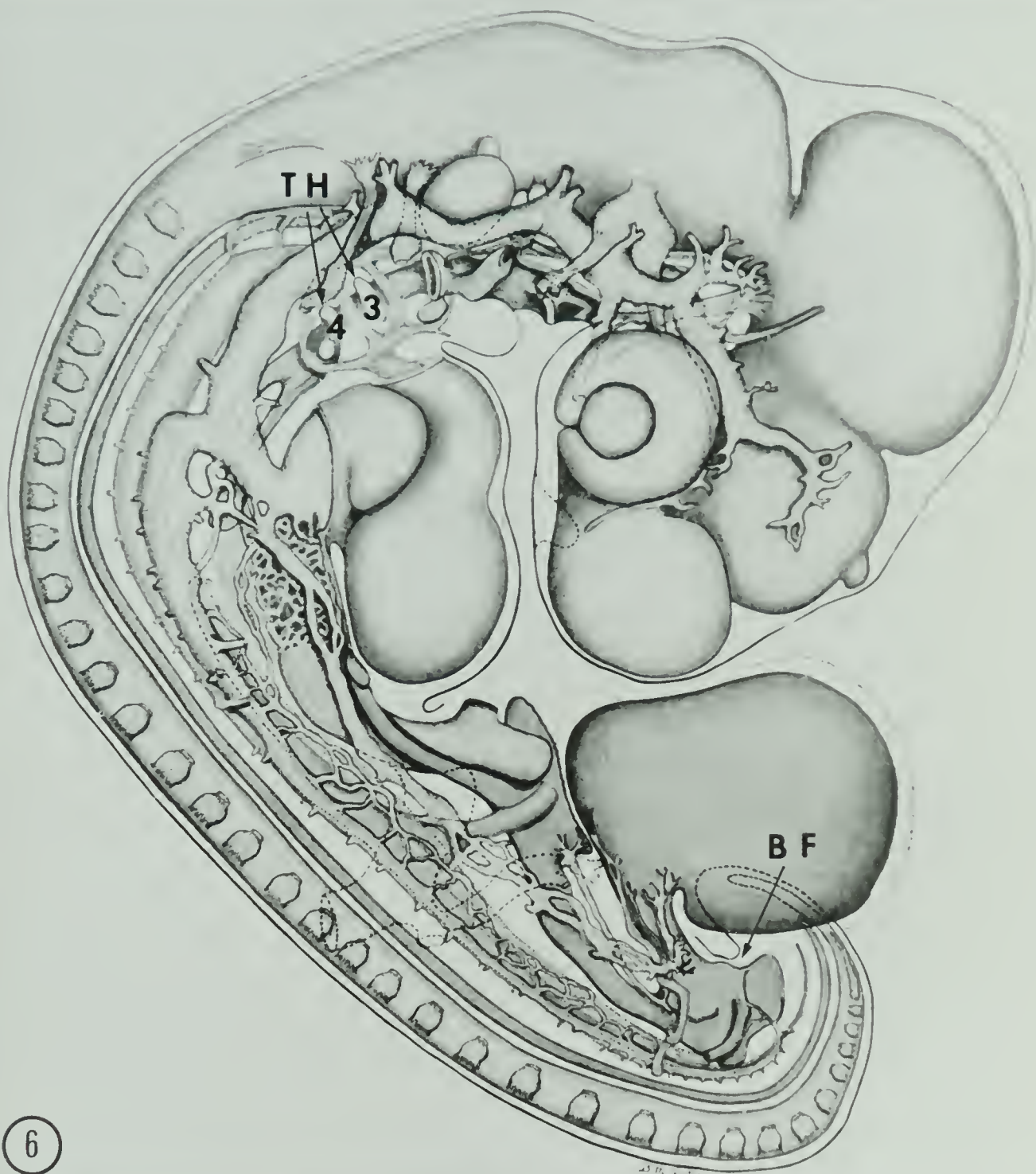
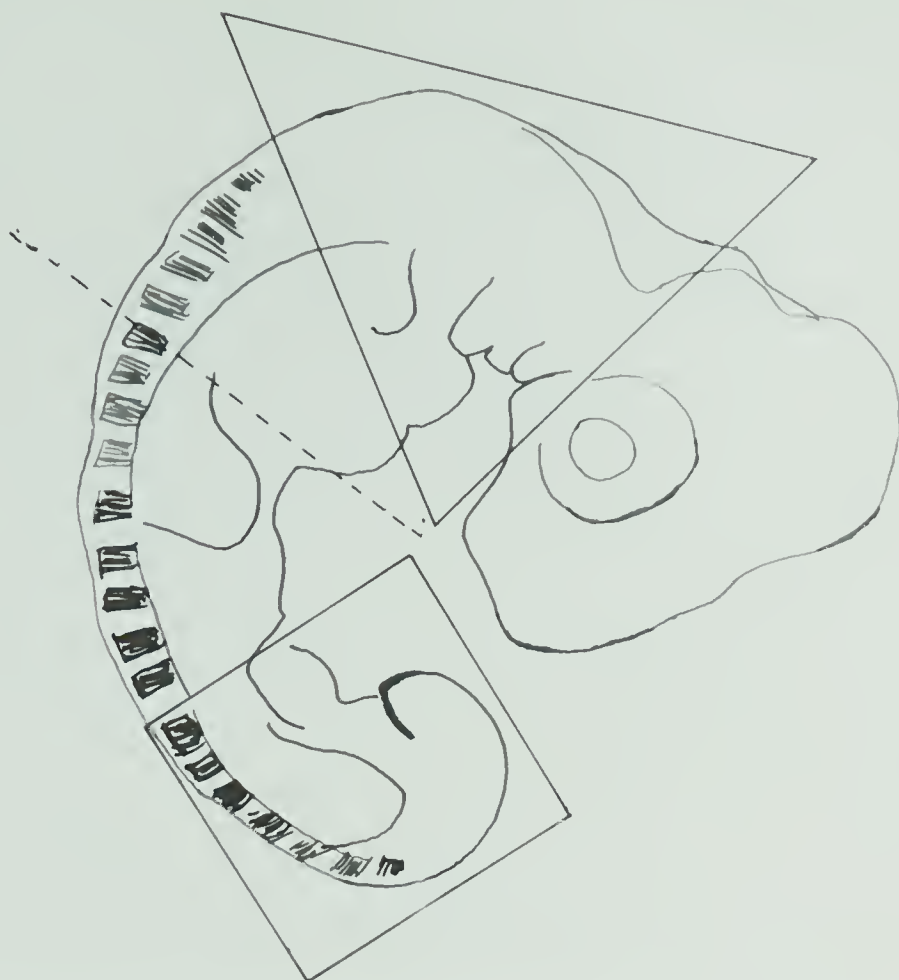


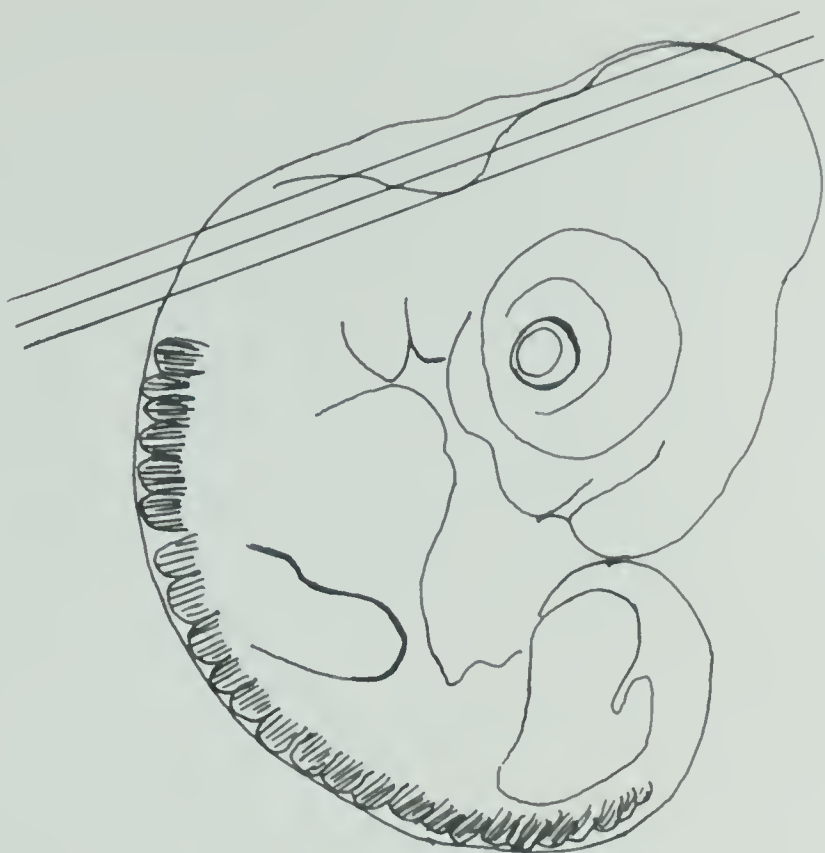
Fig. 7. A diagram of the dextral view of a 4-day chick embryo. The embryo is cut in halves (broken line) after brief fixation (to harden the embryo) and the branchial region (triangle) and the cloacal region (square) are cut out and fixed for microscopy.



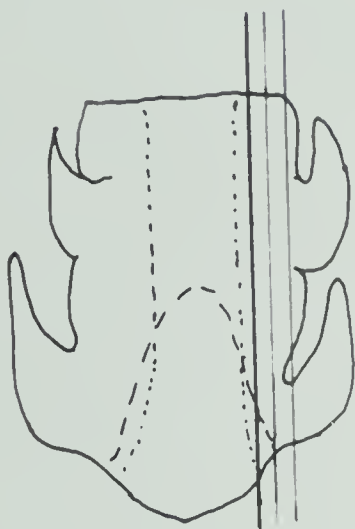
7

Fig. 8. A diagram of the dextral view of a 5-day chick embryo to indicate the planes of the sections through the branchial region. The uppermost line indicates the plane of the first section which is perpendicular to the page. The sections are frontal with respect to the pharynx.
X 10

Fig. 9. A diagram of the dorsal view of the posterior part of a 5-day chick embryo to indicate the planes of the sections through the cloacal region. The sections are parasagittal, or sagittal, with respect to the axis of the body. The diagram does not indicate the slight curvature of the tail to the right.
X 10



8



9

Fig. 10. Part of a bursa lymphoid follicle of the 19-day chick embryo showing a part of a degenerating cell. (DC) in the medulla of the lymphoid follicle. The medulla is separated from the cortex by the basement membrane (BM). The medulla is at the right of the figure, the cortex at the left. Note the dark reticular cells along the basement membrane.

BM: basement membrane

DC: degenerating cell FB: fibroblast

Glutaraldehyde-osmium tetroxide, Epon,
and uranyl acetate.

X 9,600



Figs. 11-12. Phase contrast photomicrographs of parts of the bursa of Fabricius of a 13-day chick embryo. Note that numerous cells which are darker than epithelial cells are distributed evenly throughout the tunica propria. Lymphoid follicles (LF) appear to be composed of two parts: the medulla (M) and the cortex. The boundary between the medulla and cortex of follicle is recognizable.

| | |
|---|------------------------|
| B: boundary between medulla and cortex of lymphoid follicle | CA: bursal lumen |
| C: cortex of follicle | M: medulla of follicle |
| MU: muscularis | TP: tunica propria |

Osmium tetroxide, Araldite, and unstained.

X 198

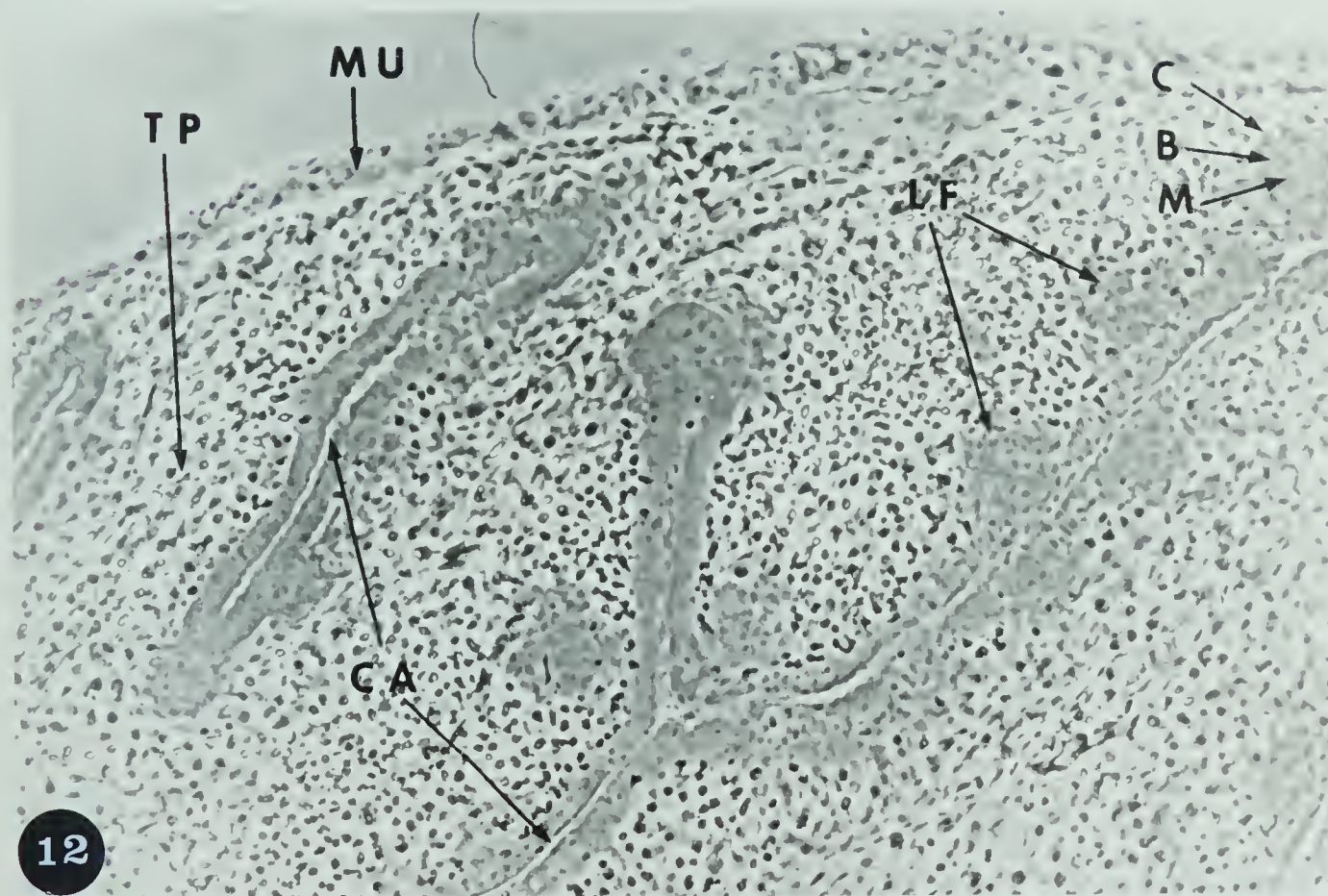
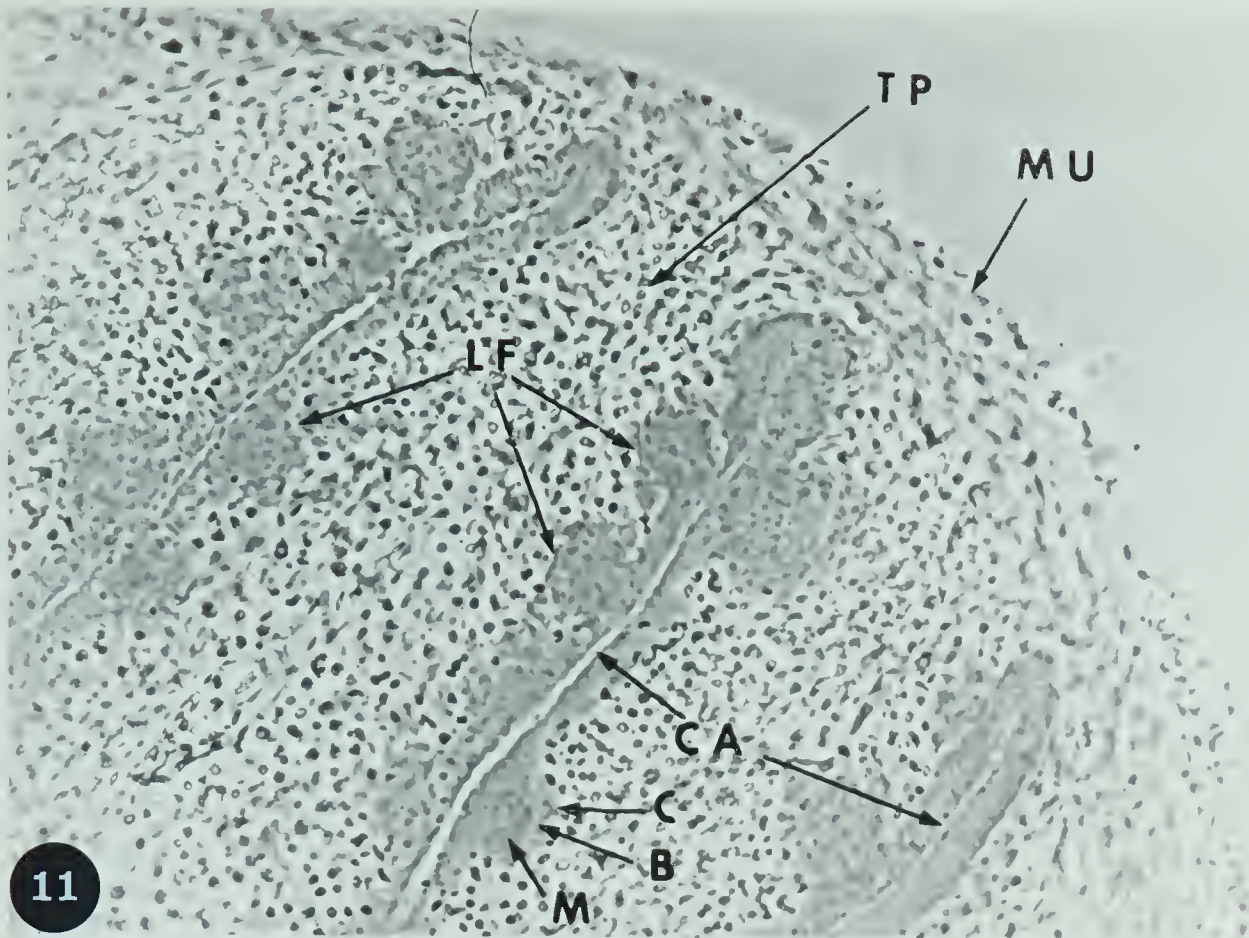


Fig. 13. Part of a bursa lymphoid follicle of the 19-day chick embryo showing a lymphoblast surrounded by a dark reticular cell (RC). A lymphocyte is seen in the upper right hand corner. An erythrocyte (ER) is shown at the lower left hand corner. The basement membrane (BM) separates the medulla of the lymphoid follicle (upper half) from the cortex (lower half).

BM: basement membrane LM: lymphocyte

EC: erythrocyte N: nucleus

LB: lymphoblast

Glutaraldehyde-osmium tetroxide, Epon, and uranyl acetate.

X 21,000

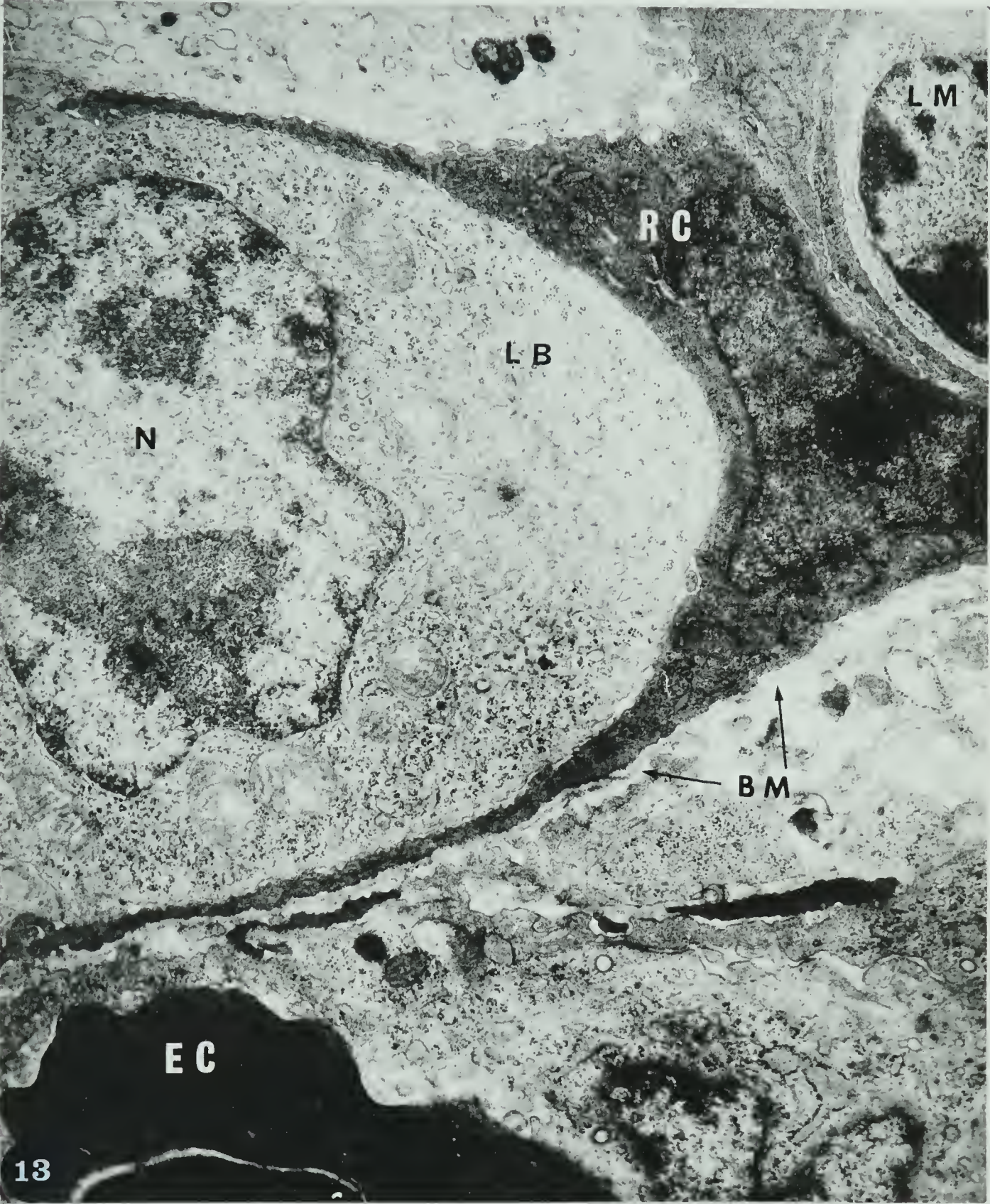


Fig. 14. A part of a lymphoid follicle of the bursa of Fabricius of a 19-day chick embryo showing the medulla of the lymphoid follicle (upper half of the figure) separated from the cortex (lower half) by the basement membrane (BM). A pyknotic nucleus (PN) and a desmosome are seen in the medulla.

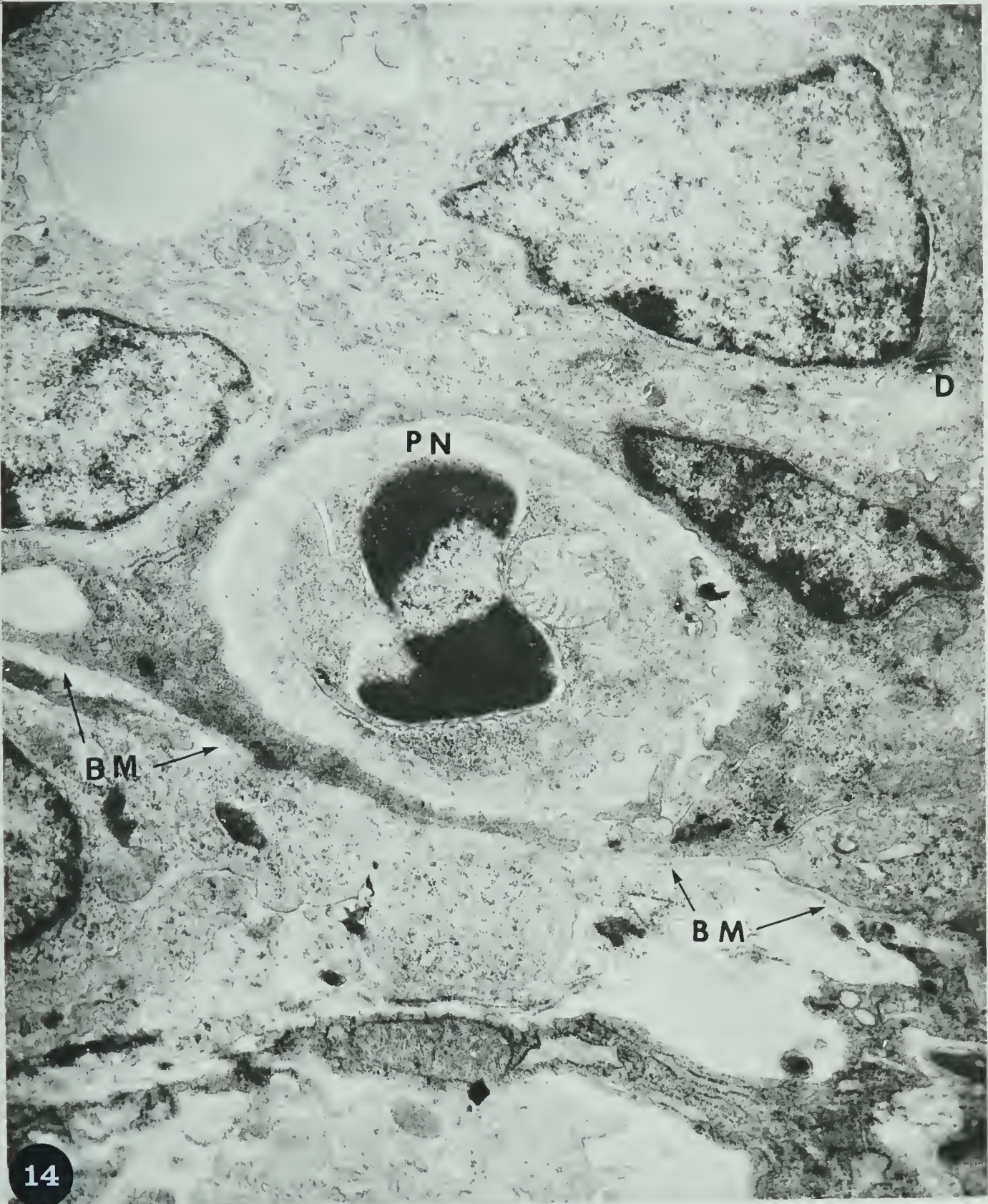
BM: basement membrane (basal lamina)

D: desmosome

PN: pyknotic nucleus

Glutaraldehyde-osmium tetroxide, Epon, and uranyl acetate.

X 21,000



Figs. 15-16. Part of the medulla of a bursa lymphoid follicle of a 19-day chick embryo showing two cytolysosomes (Fig. 15) and a degenerating cell (Fig. 16). Many myelin figures are seen in the cytoplasm of the degenerating cell. Glutaraldehyde-osmium tetroxide, Epon, and uranyl acetate.

X 36,000

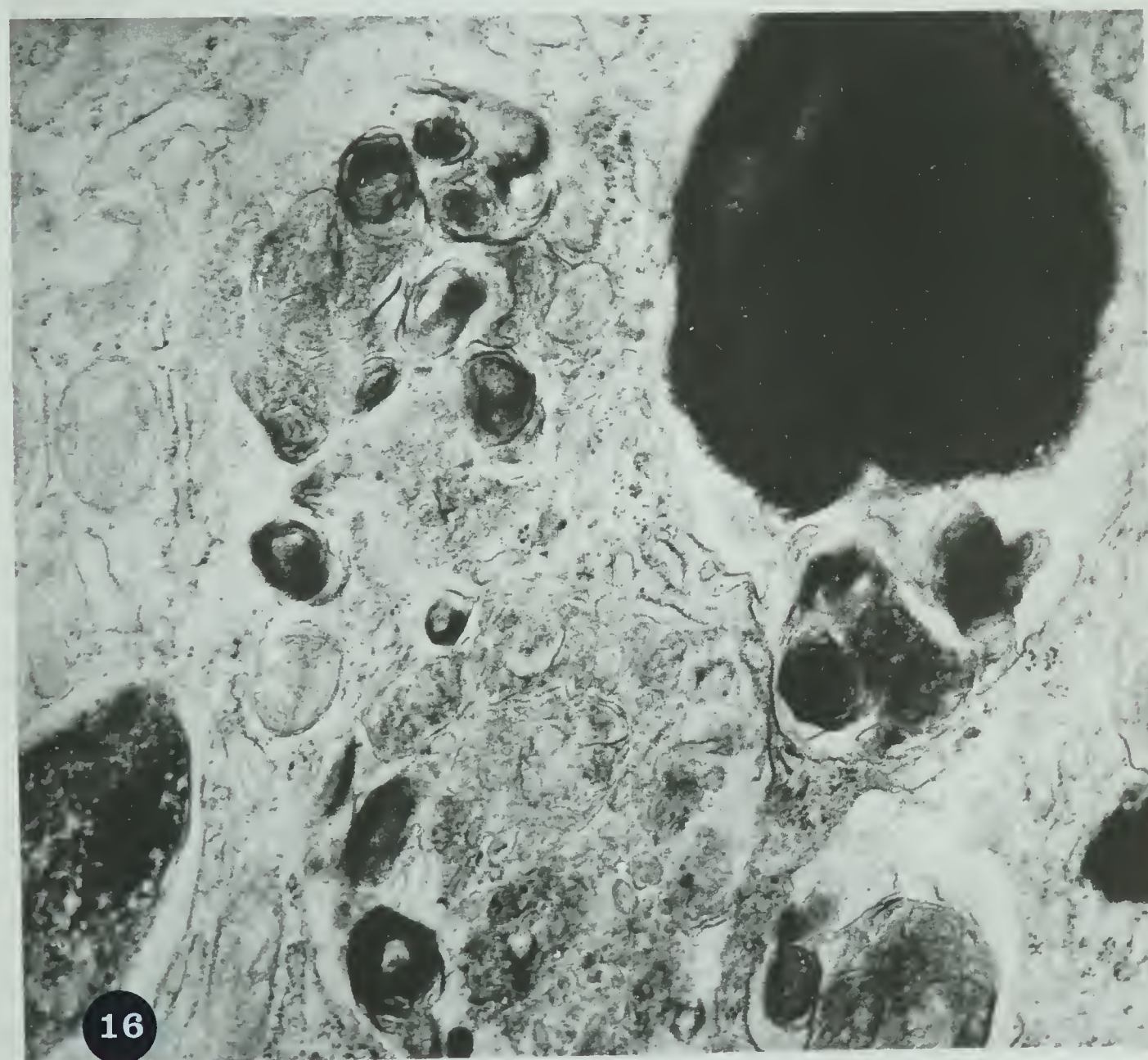
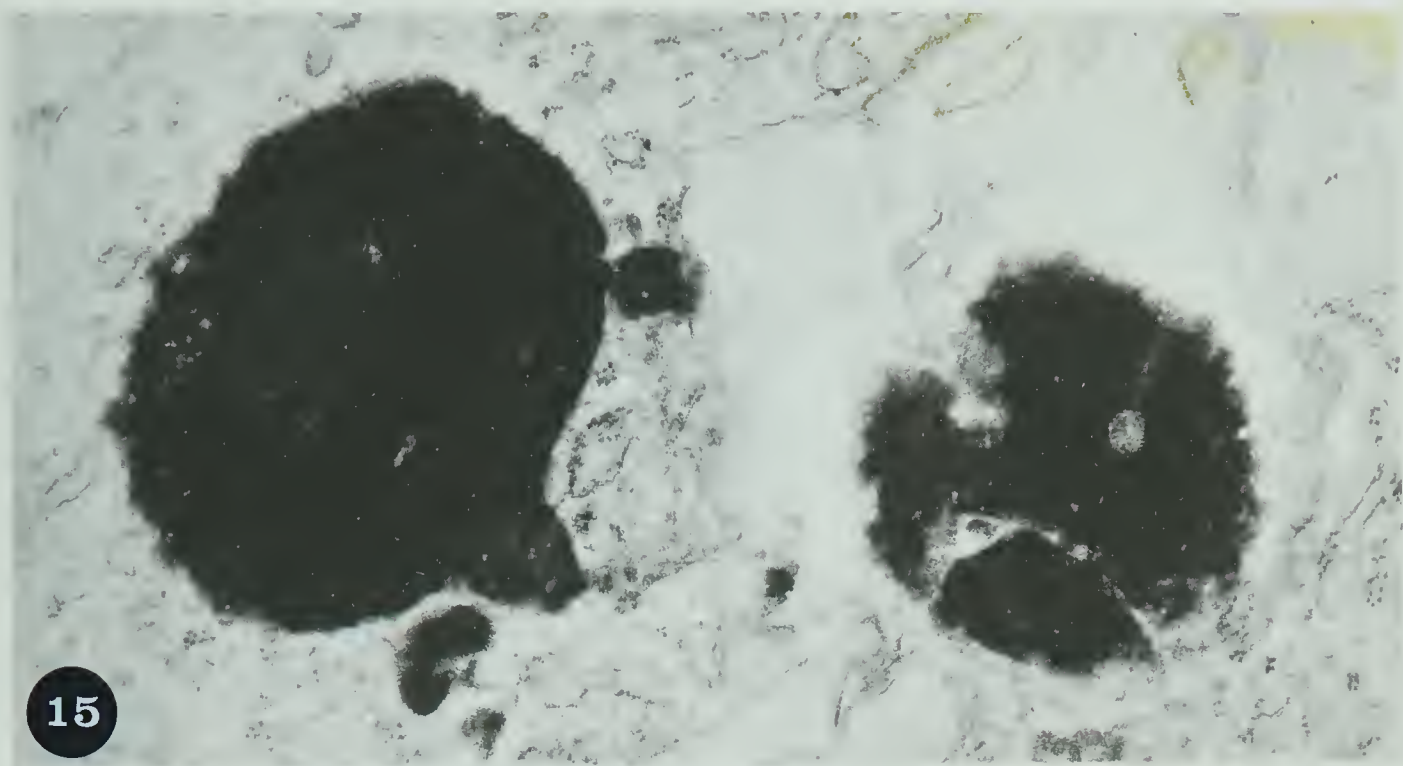


Fig. 17. The acid phosphatase activity of clusters of granulocytes (arrows) in the tunica propria (TP) of a 12-day bursa.

TP: tunica propria BL: lumen

Barka medium for acid phosphatase, no counterstain.

X 235

Fig. 18. The acid phosphatase reaction in the epithelium, the tunica propria, and the lymphoid follicles (LF) of a 13-day bursa.

Section preparation as in Fig. 17.

X 235

Fig. 19. High acid phosphatase activity in the lymphoid follicles and the tunica propria of a 14-day bursa. Section preparation as in Fig. 17 plus methyl green counterstain.

X 235

Fig. 20. Moderate acid phosphatase activity in the lymphoid follicles of a 19-day bursa.

Section preparation as in Fig. 19.

X 110

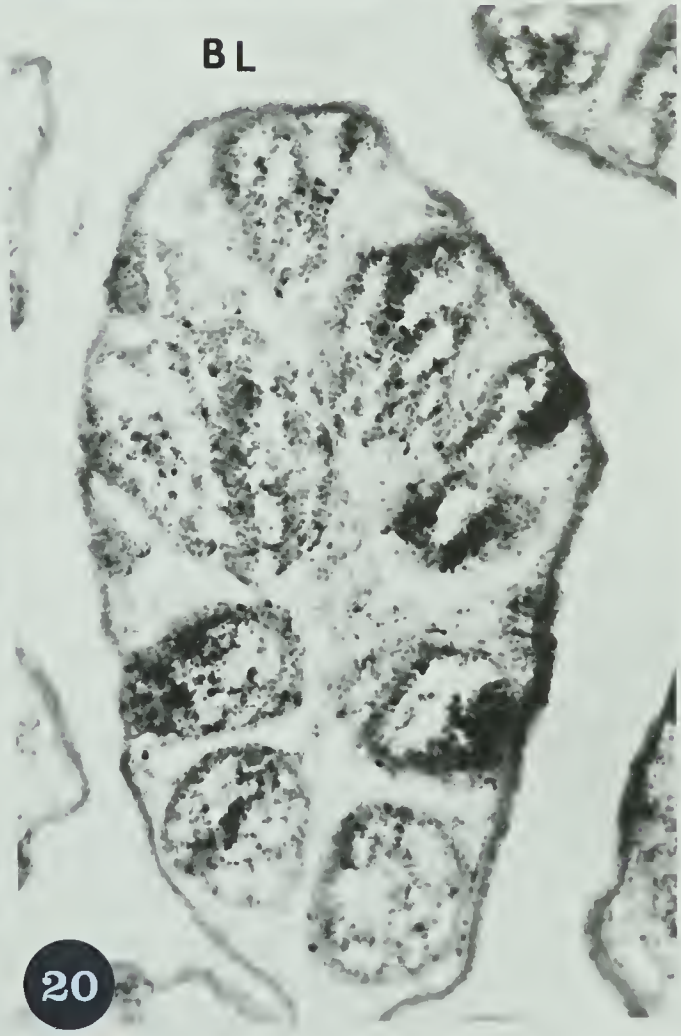
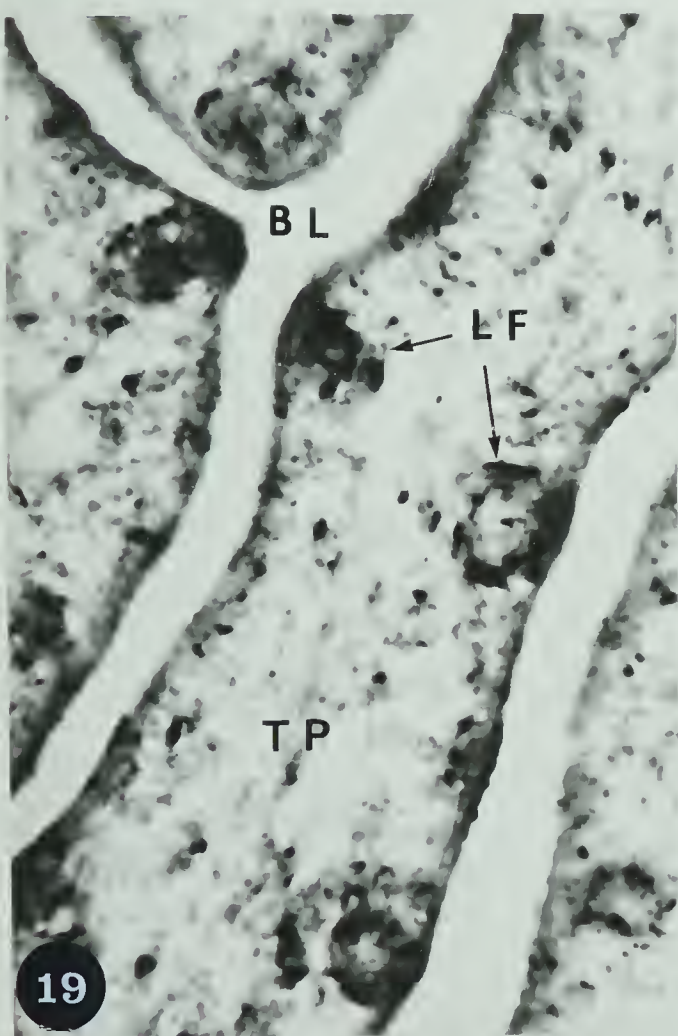
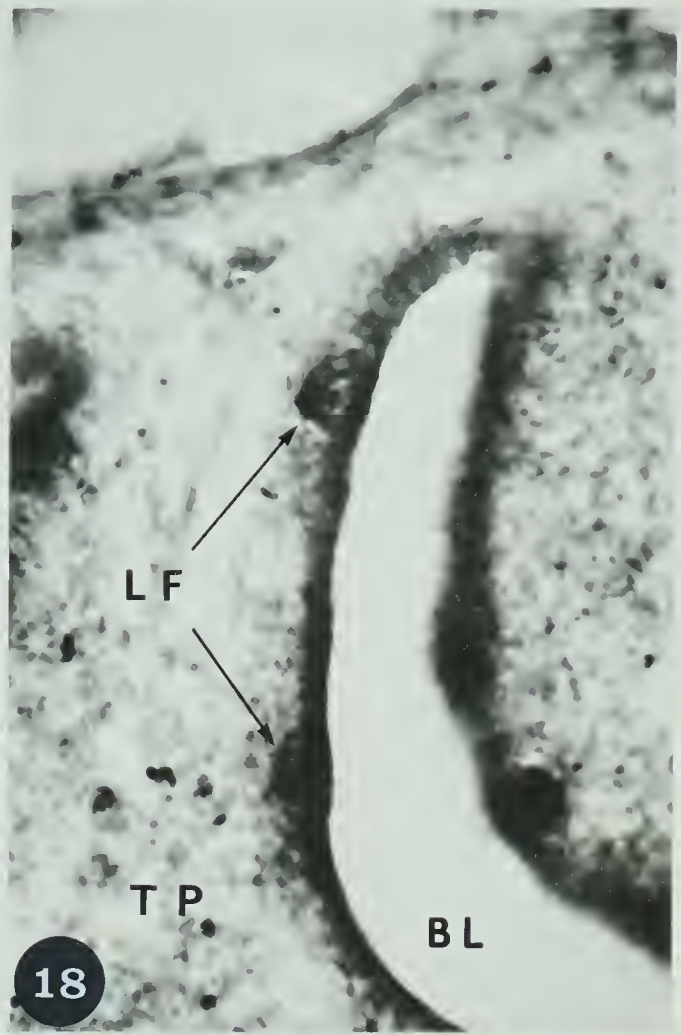
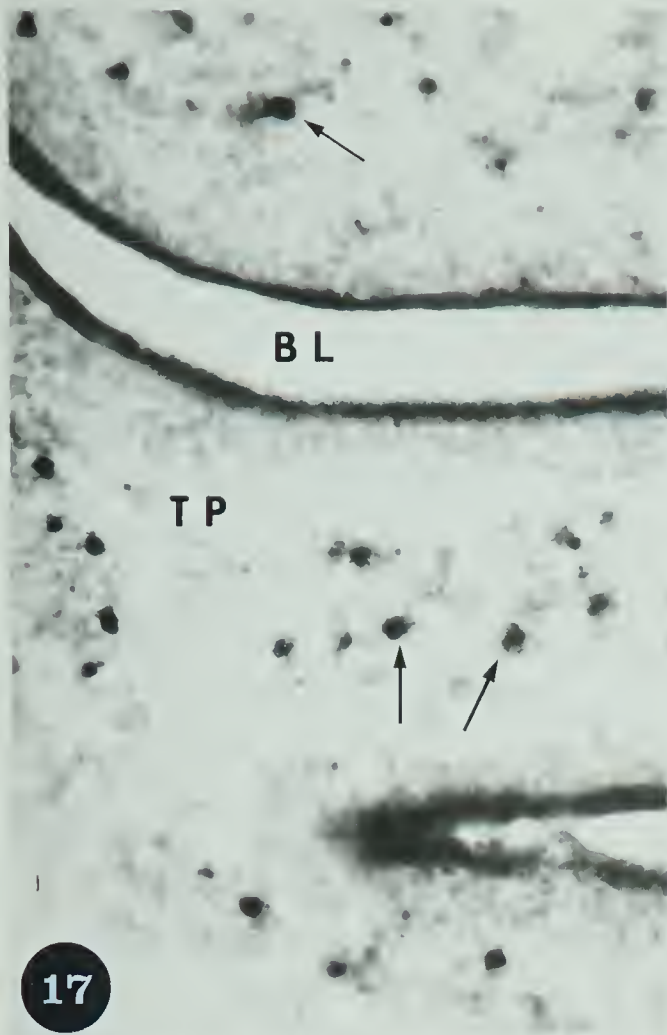


Fig. 21. Mature granulocytes in the 14-day bursa. The immature granulocytes are larger than mature ones and have, instead of pink to red, purple cytoplasmic granules. A small area of the tunica propria is shown at higher magnification in Fig. 22.

Frozen section, Giemsa stain, color photomicrograph. X 110

Fig. 22. Part of the tunica propria of the bursa shown in Fig. 21. A cluster of immature granulocytes with purple cytoplasmic granules is seen close to the blood vessel in the center of this figure. Some immature granulocytes have a mixture of purple and red granules. (Mature granulocytes contain red cytoplasmic granules.) The nuclei stain pale blue.

Frozen section, Giemsa stain, color photomicrograph. X 600

Fig. 23. Acid phosphatase activity in the lymphoid follicles and in the tunica propria of a 14-day bursa.

Barka medium, no counterstain. X 110

Fig. 24. Acid phosphatase in a lymphoid follicle (upper left) and in the granulocytes. Some mature granulocytes have low activity.

Barka medium for acid phosphatase, no counter-stain.

X 600

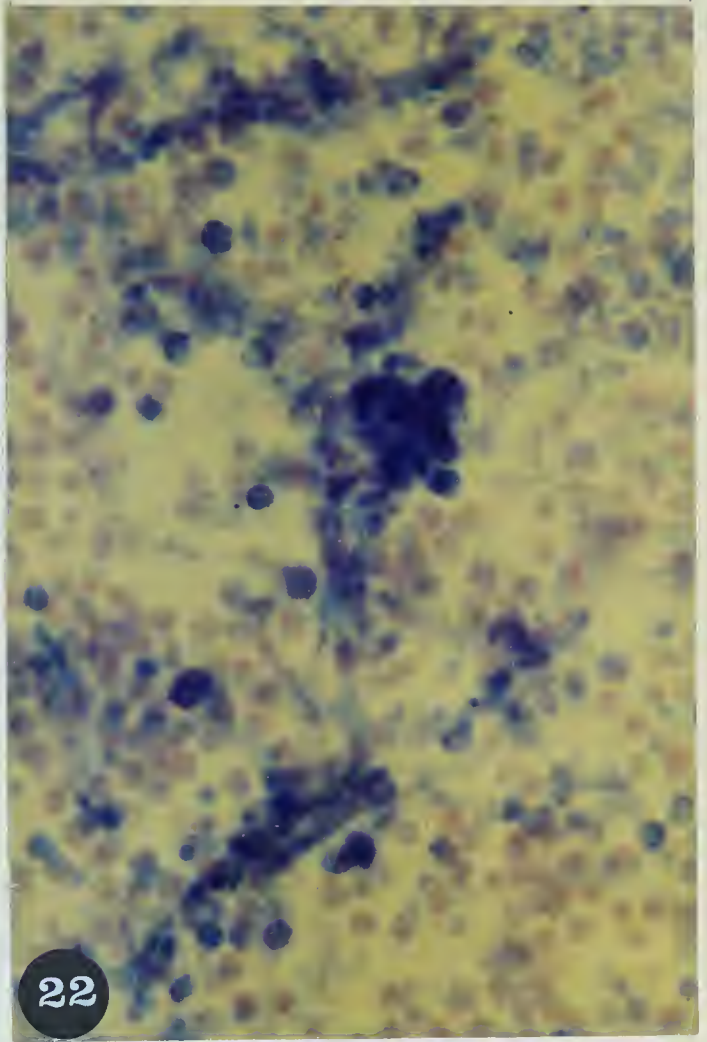
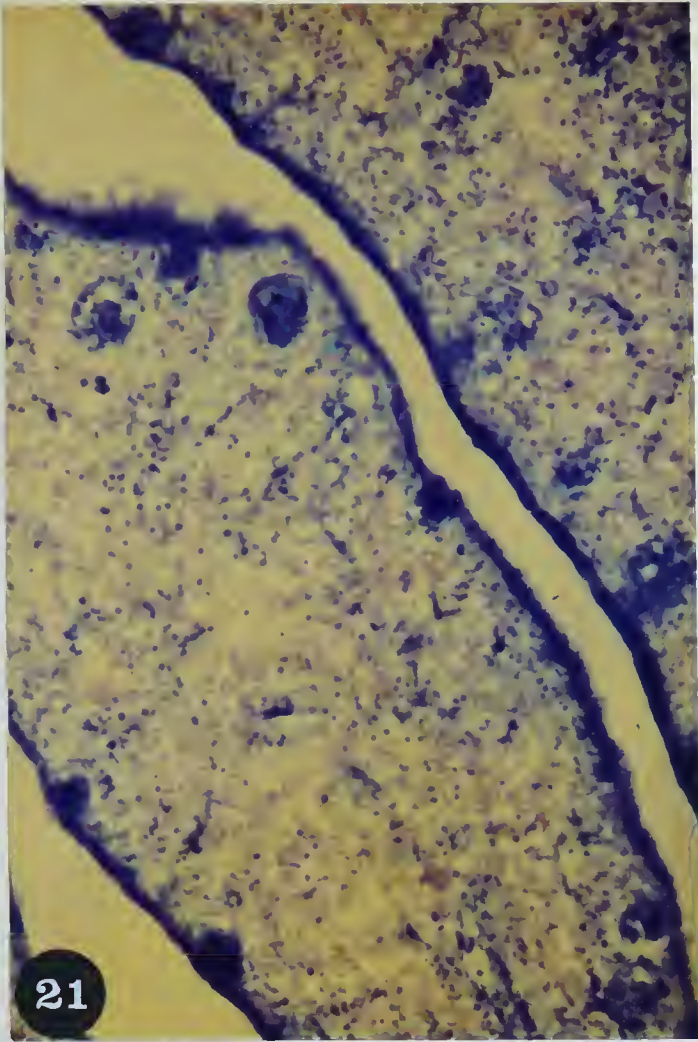


Fig. 25. A heterophil granulocyte in the tunica propria of a 19-day bursa. There are three types of ovoid, membrane-bound granules: "a" granules which are full of dense, fine micro-granules and are identical with the azurophil granules seen after Wright staining; "b" granules which have fewer and larger micro-granules and may represent a transition from "a" to "c"; and "c" granules which have less dense, smaller micro-granules and may be the specific granules of Wright preparations.

Glutaraldehyde-osmium tetroxide, Epon, and uranyl acetate.

X 36,000



Fig. 26. Two eosinophils in the tunica propria of the 20-day bursa. Some granules contain an excentric spherical core. The acid phosphatase reaction produces lead phosphate deposits in the granule and on its limiting membrane (a).

N: nucleus

Glutaraldehyde, Gomori's medium, post-fixation in osmium tetroxide, Epon, and unstained.

X 21,600

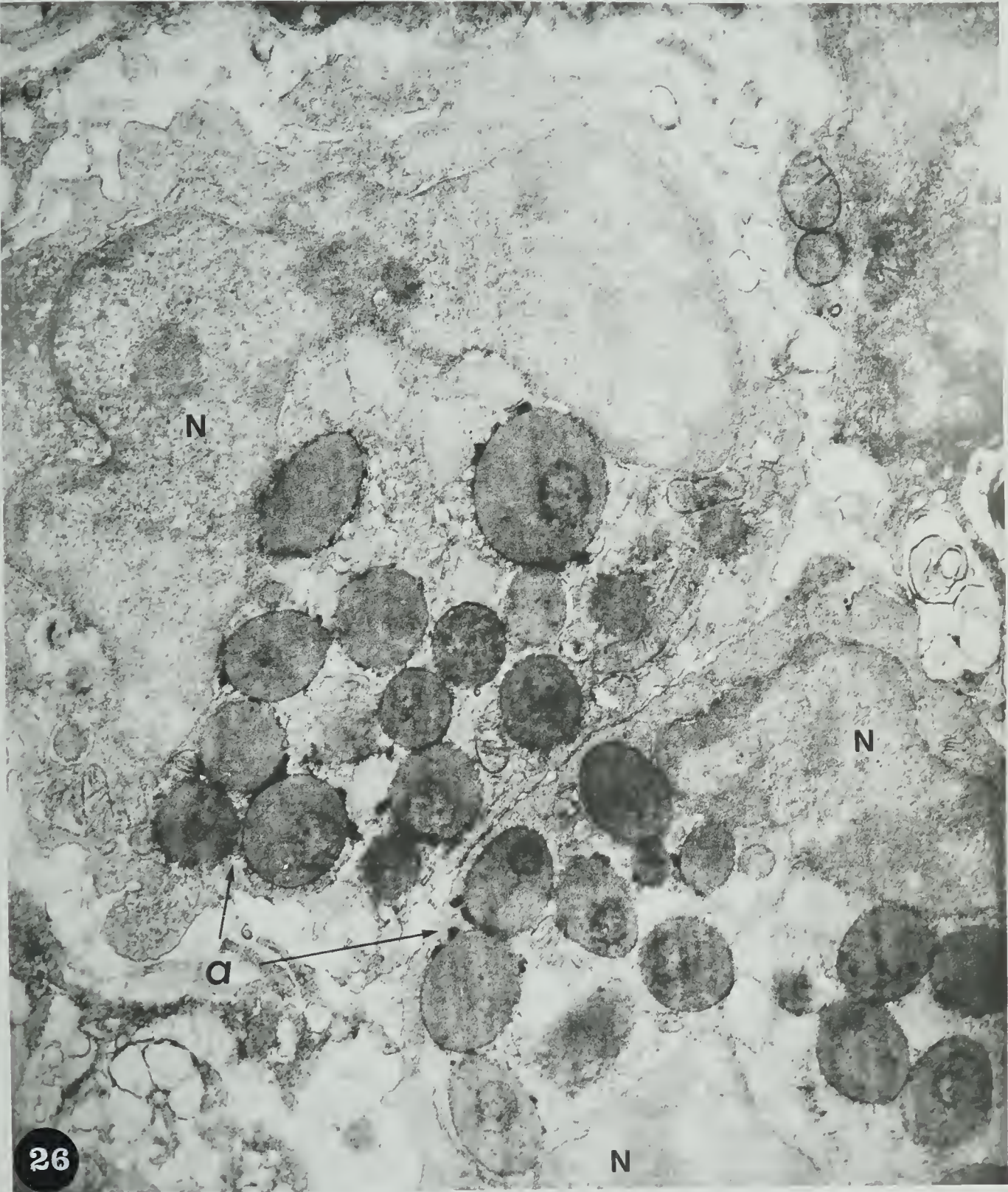


Fig. 27. Acid phosphatase in a 14-day bursa when follicles are abundant.

BF: bursa of Fabricius

Barka medium, and counterstained with methyl green.

X 10

Fig. 28. Acid phosphatase in a 13-day bursa when follicles are few. Bursa plicae are seen.

Barka medium, no counterstain.

X 10

Fig. 29. Acid phosphatase in a 12-day bursa when follicles are not yet formed. A part of the urodeal membrane (unlabelled arrow) is illustrated at higher magnification in Fig. 38.

R: rectum An: anus

Preparation as in Fig. 28.

X 10

Fig. 30. Acid phosphatase in an 11-day bursa. (This figure is darker than most others. The greater darkness of the bursa epithelium is not indicative of high acid phosphatase activity.)

Section preparation as in Fig. 27.

X 10

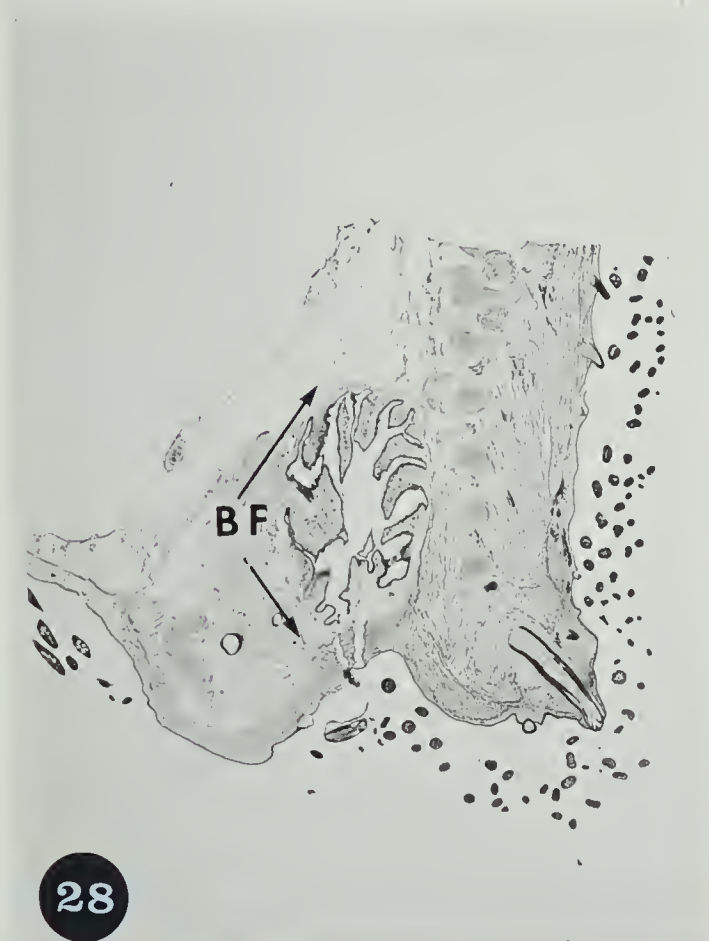
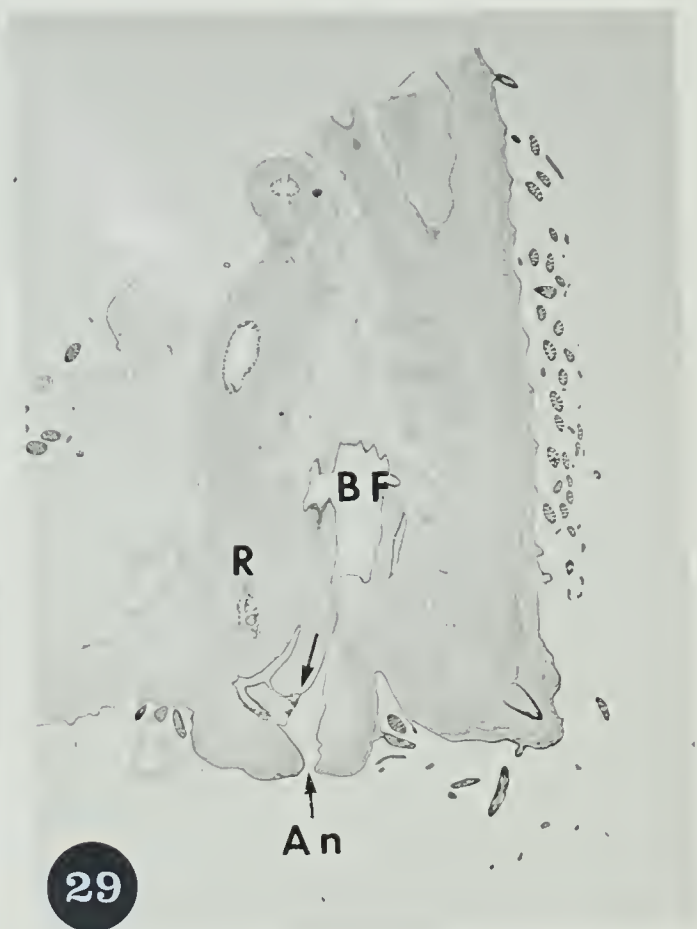
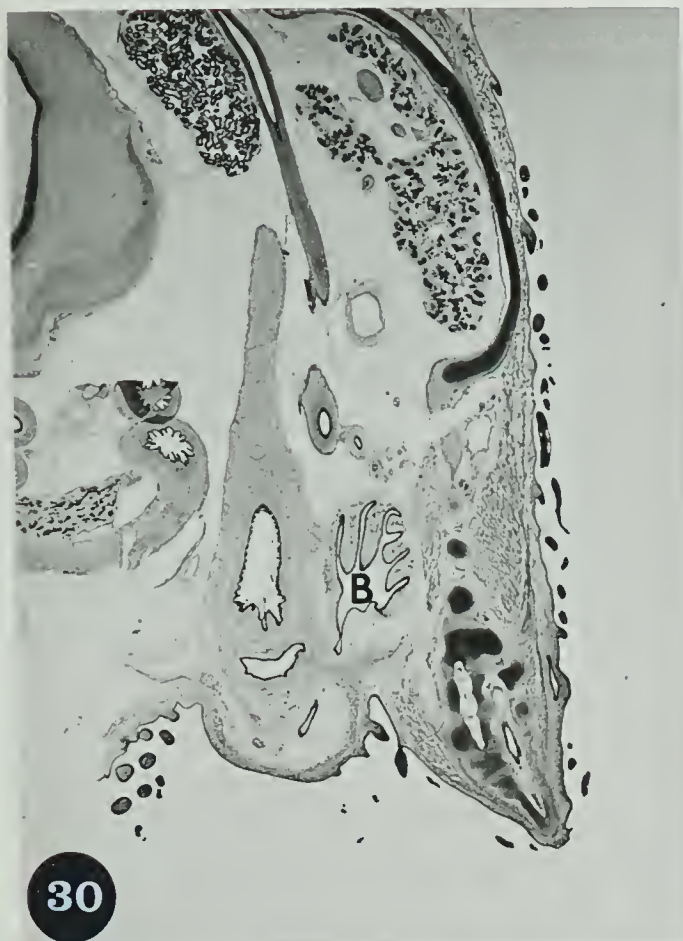
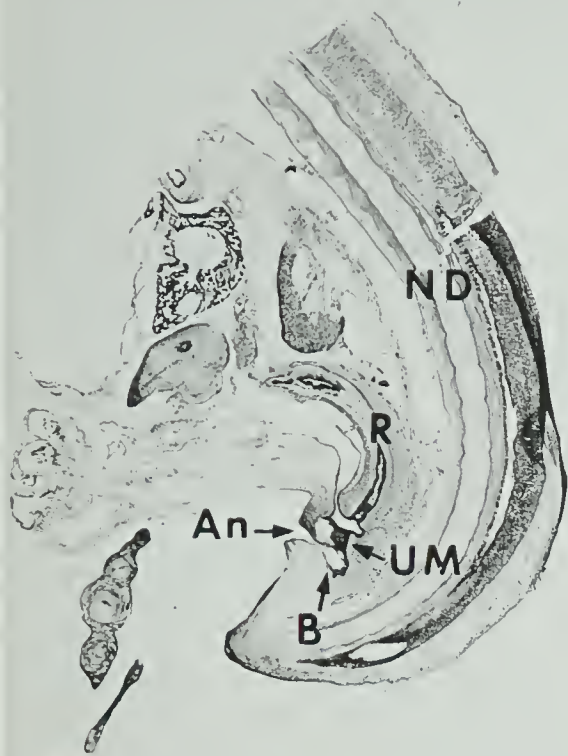


Fig. 31. A sagittal section of a 10-day embryo showing the expansion of the bursa between the rectum and the vertebral column. Intense acid phosphatase activity is noted in the urodeal membrane and the rectum. The urodeal membrane (arrow) is illustrated at higher magnification in Fig. 37. Barka medium, no counterstain. X 10

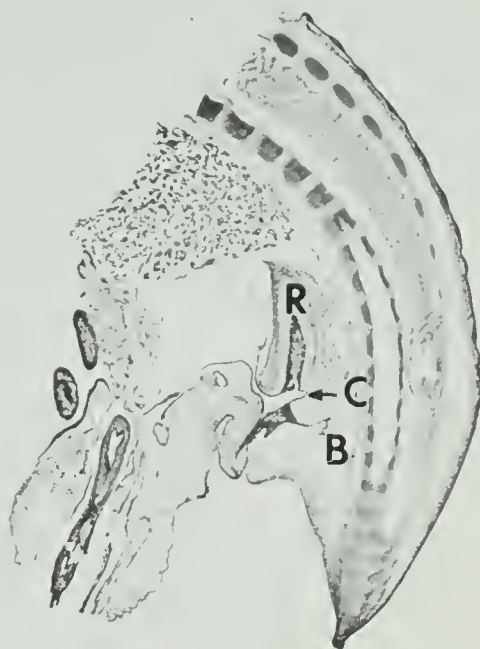
Fig. 32. The 9-day bursa is a flattened sac just ventral to the vertebral column. Intense acid phosphatase activity occurs in the urodeal membrane (unlabelled arrow) and the rectum (R), which are shown at higher magnification in Figs. 35 and 36. Section preparation as in Fig. 31. X 10

Fig. 33. The blind end of an 8-day bursa (B) extends dorsad toward the vertebral column.
C: cloaca R: rectum
Frozen section, Giemsa stain. X 10

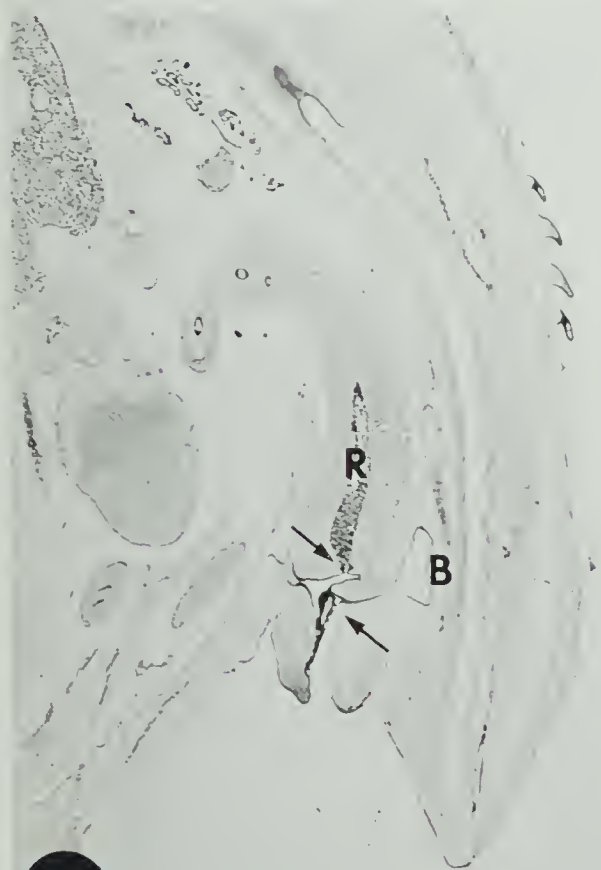
Fig. 34. At seven days the primordium of the bursa (B) extends as a blind sac away from the urodeal membrane (UM). Intense acid phosphatase activity is present in the urodeal membrane and the rectum.
AN: anus ND: notochord
Section preparation as in Fig. 31. X 10



34



33



32



31

Fig. 35. Acid phosphatase in the 9-day urodeal membrane (UM).

ME: mesenchyme

BS: lumen of the bursa stalk

Section incubated in Barka medium for acid phosphatase localization, no counterstain.

X 235.

Fig. 36. Acid phosphatase in the 9-day rectum.

R: rectum

Section preparation as in Fig. 35.

X 235

Fig. 37. Acid phosphatase in the urodeal membrane of a 10-day embryo.

Section preparation as in Fig. 35.

X 235

Fig. 38. Acid phosphatase in the 12-day urodeal membrane.

X 620

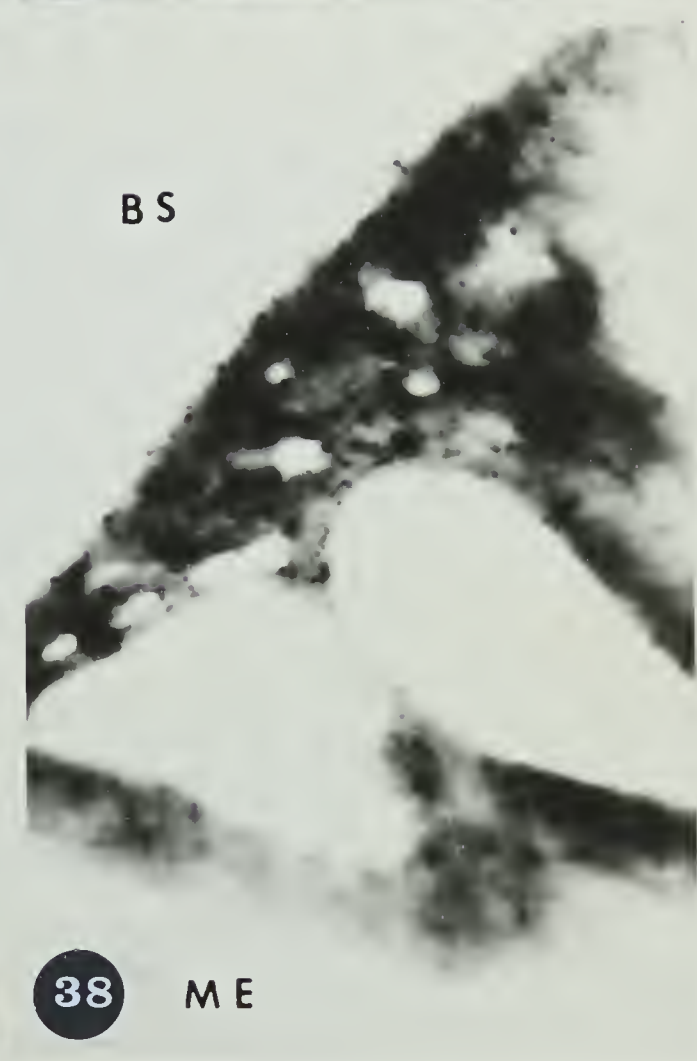
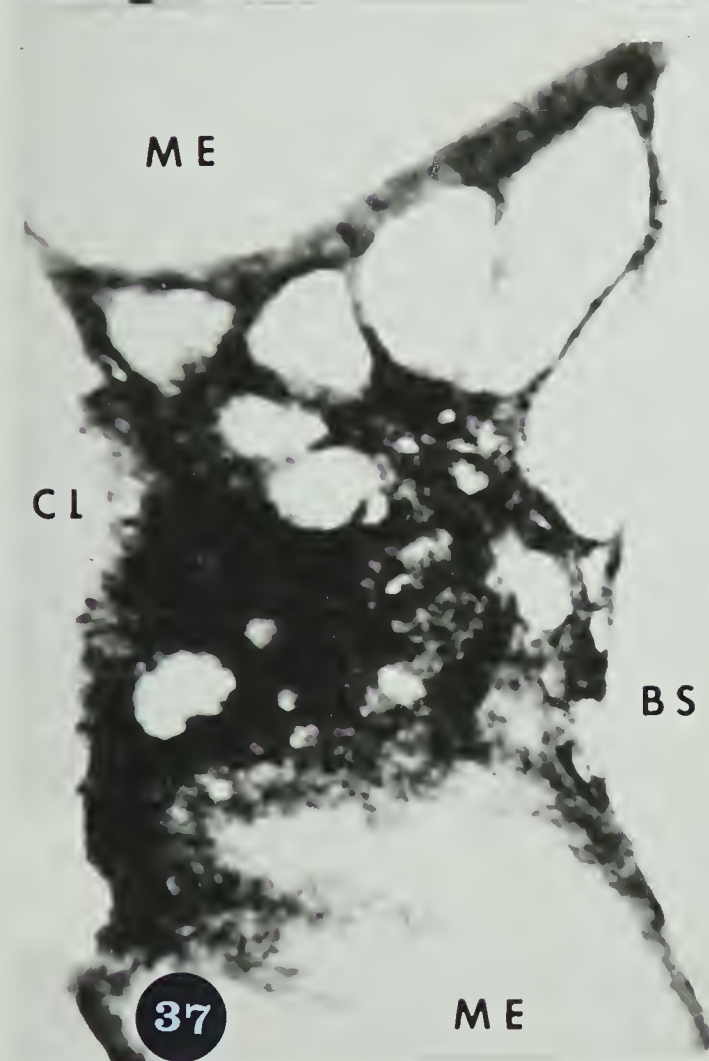
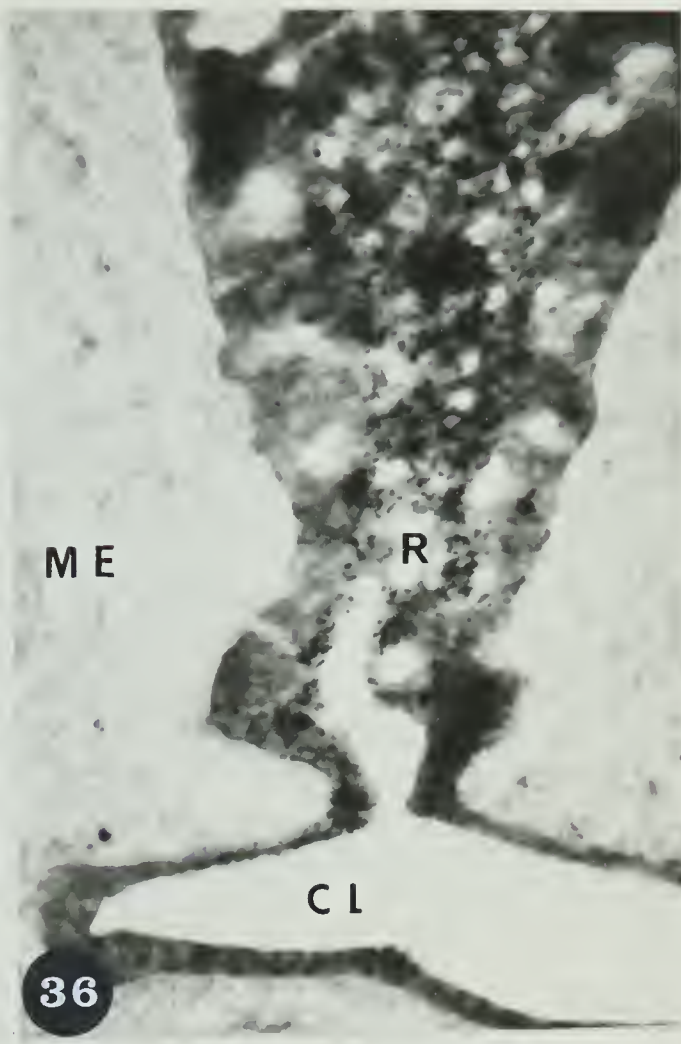
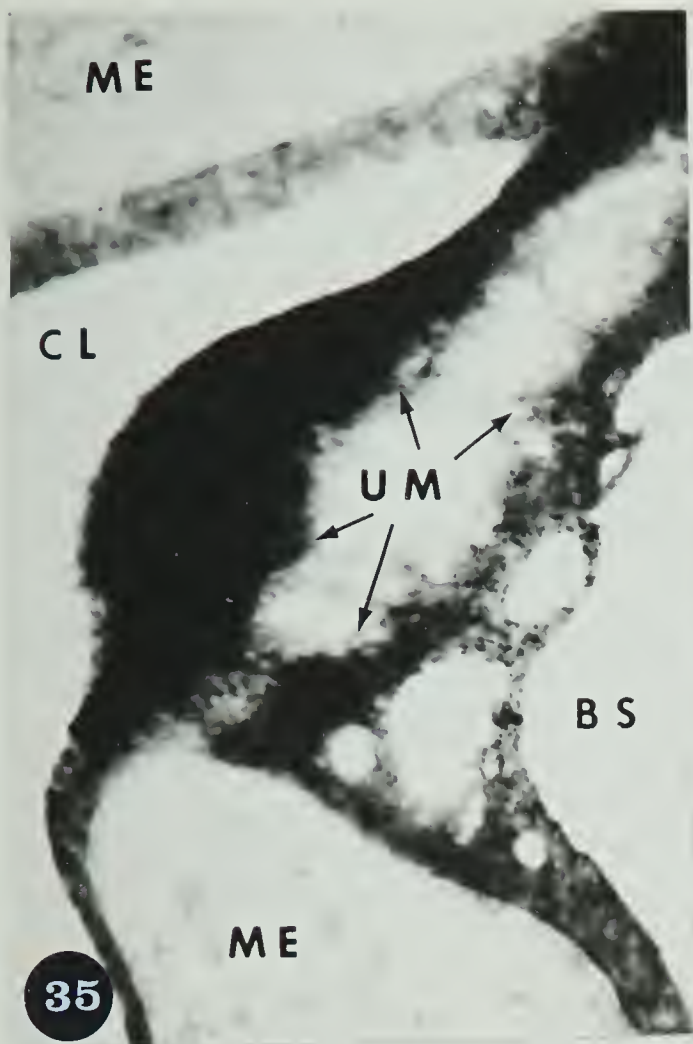


Fig. 39-42. A series of phase contrast photomicrographs taken from serial parasagittal sections of a 4-day cloaca showing the cloacal fenestra (CF).

CF: cloacal fenestra

ME: mesenchyme

UM: urodeal membrane

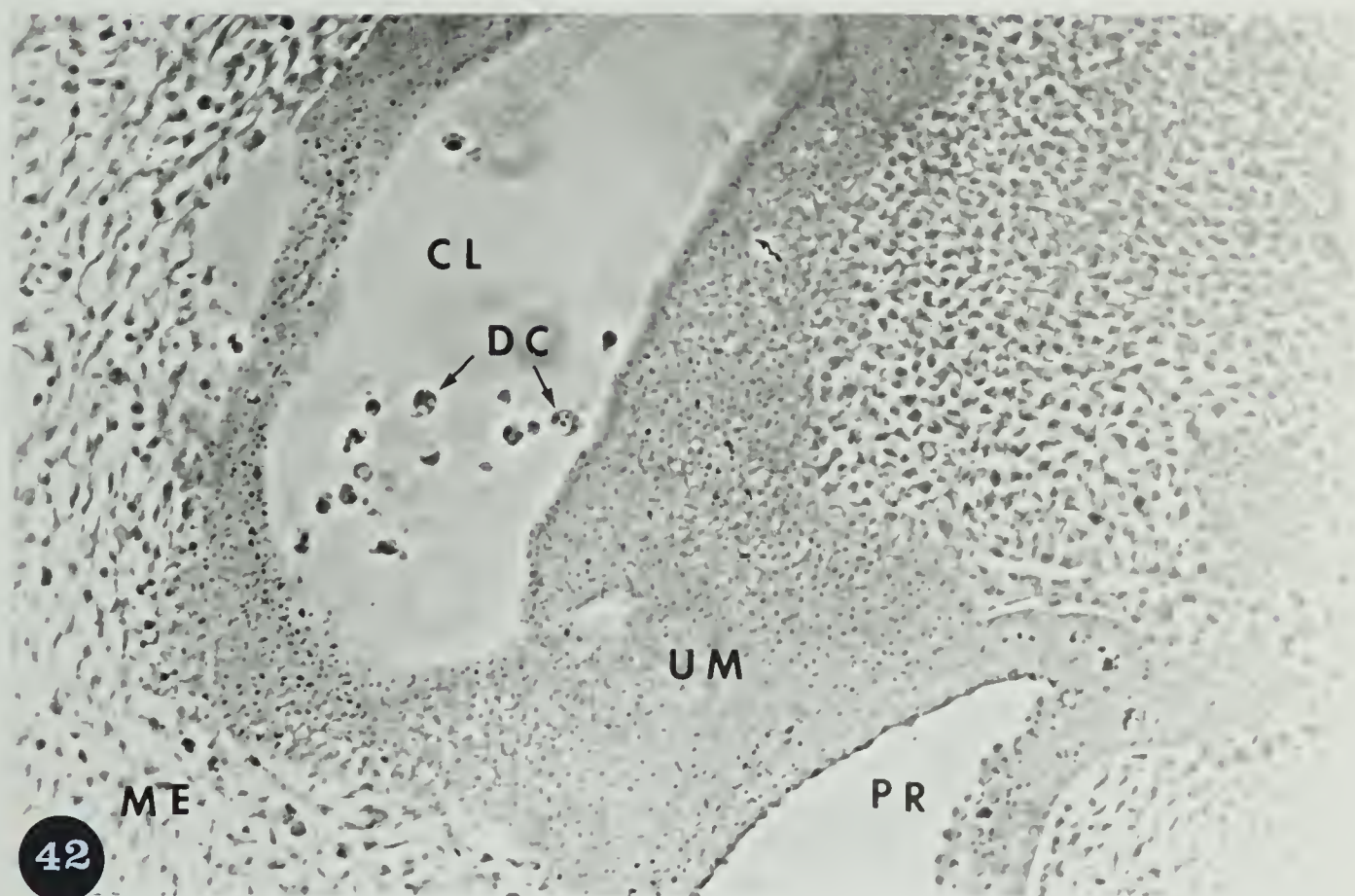
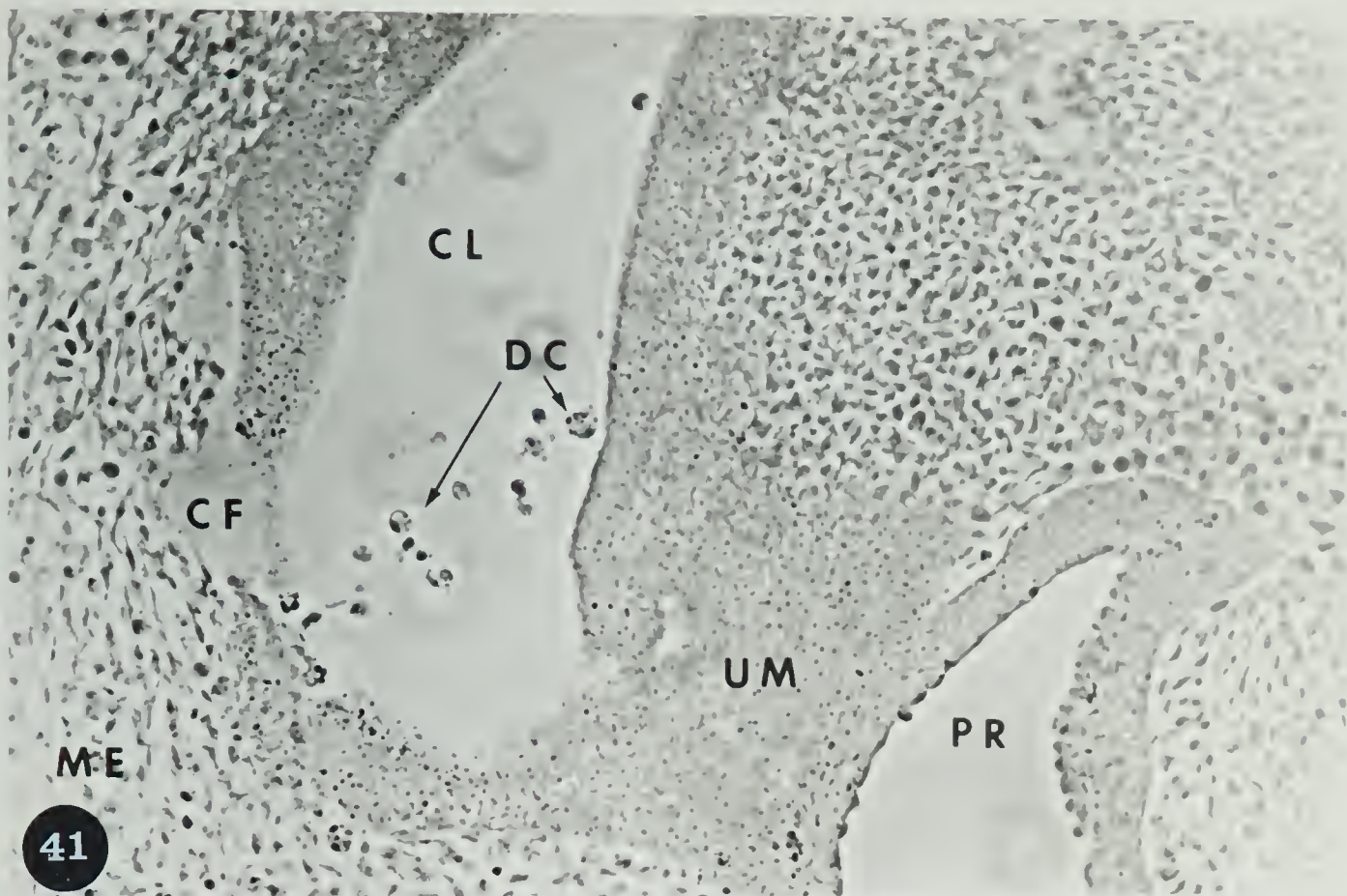
DC: degenerating cell

PR: proctodaeum

Osmium tetroxide, Araldite, and unstained.

X 198





Figs. 43-44. Higher magnification of the sections following that illustrated in Fig. 42. Note the degenerating cells (DC) and the bursal vesicle (BV).

Osmium tetroxide, Araldite, and unstained; phase contrast.

X 405

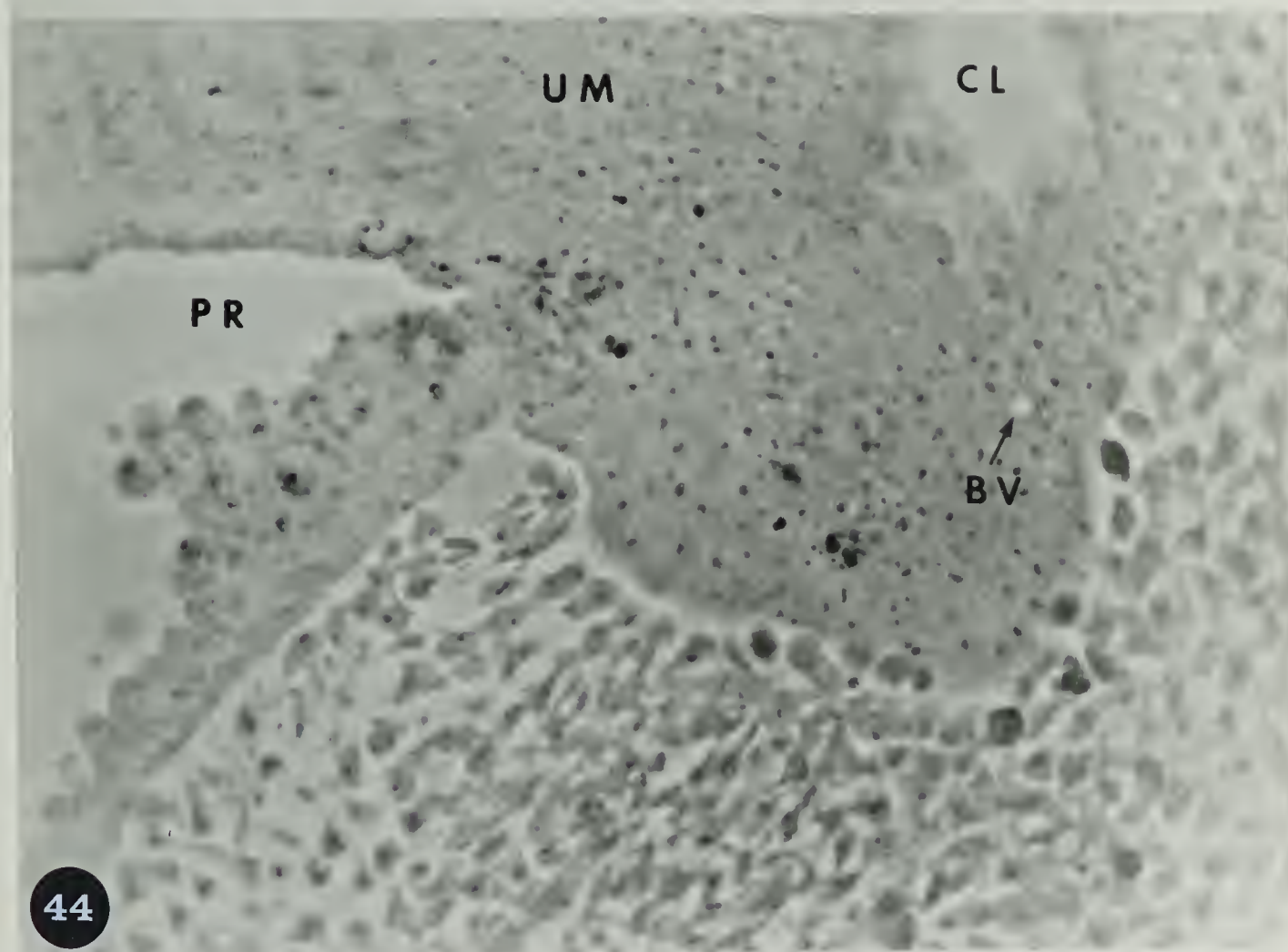
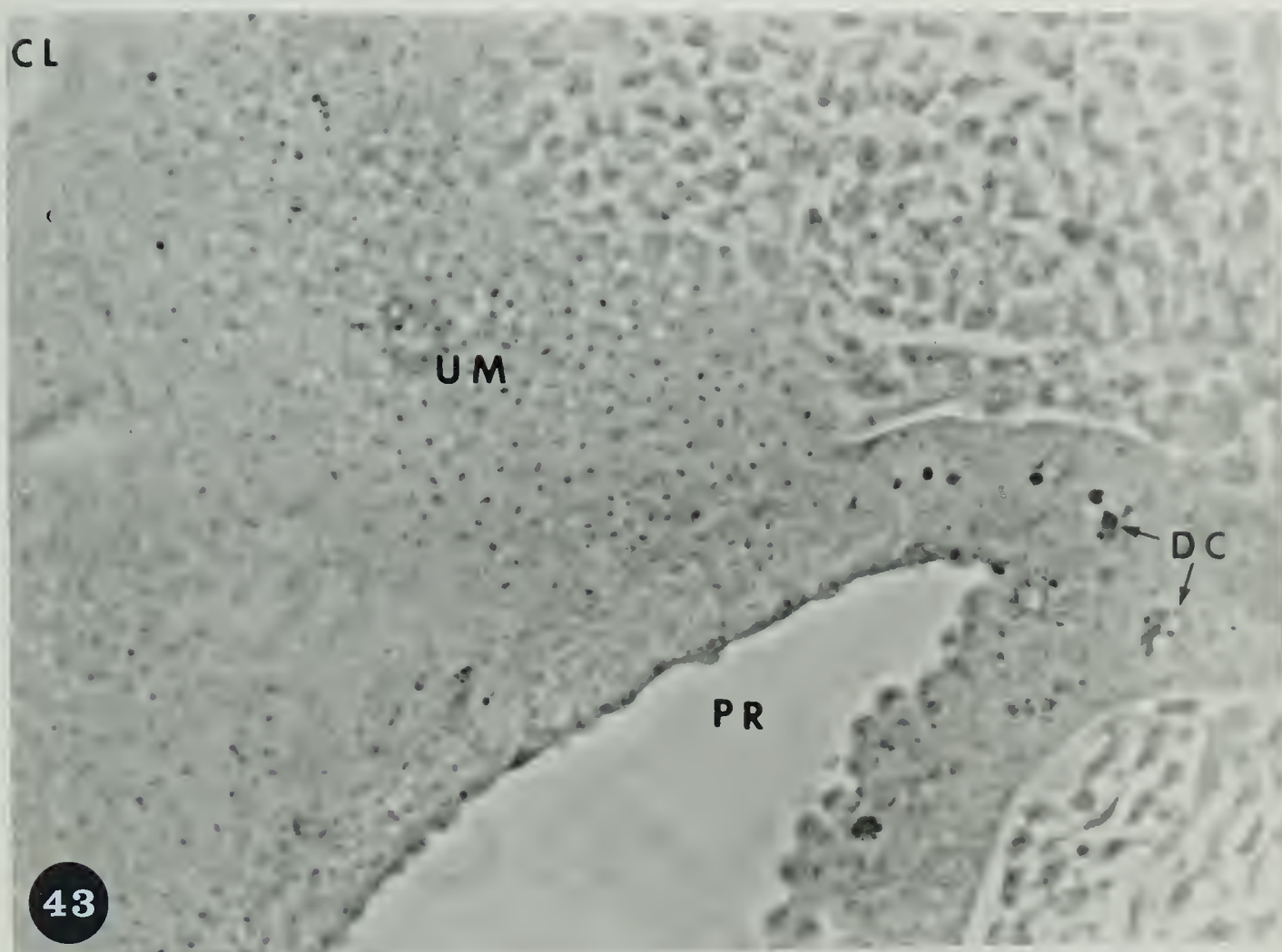


Fig. 45. A diagram of a representative sagittal section through the cloaca and proctodeal ectoderm of a 4-day chick embryo. The rectangle indicates the locale of a series of photomicrographs (Figs. 46-51).

AM: posterior amniotic fold DA: dorsal aorta
ND: notochord NT: neural tube
X 50

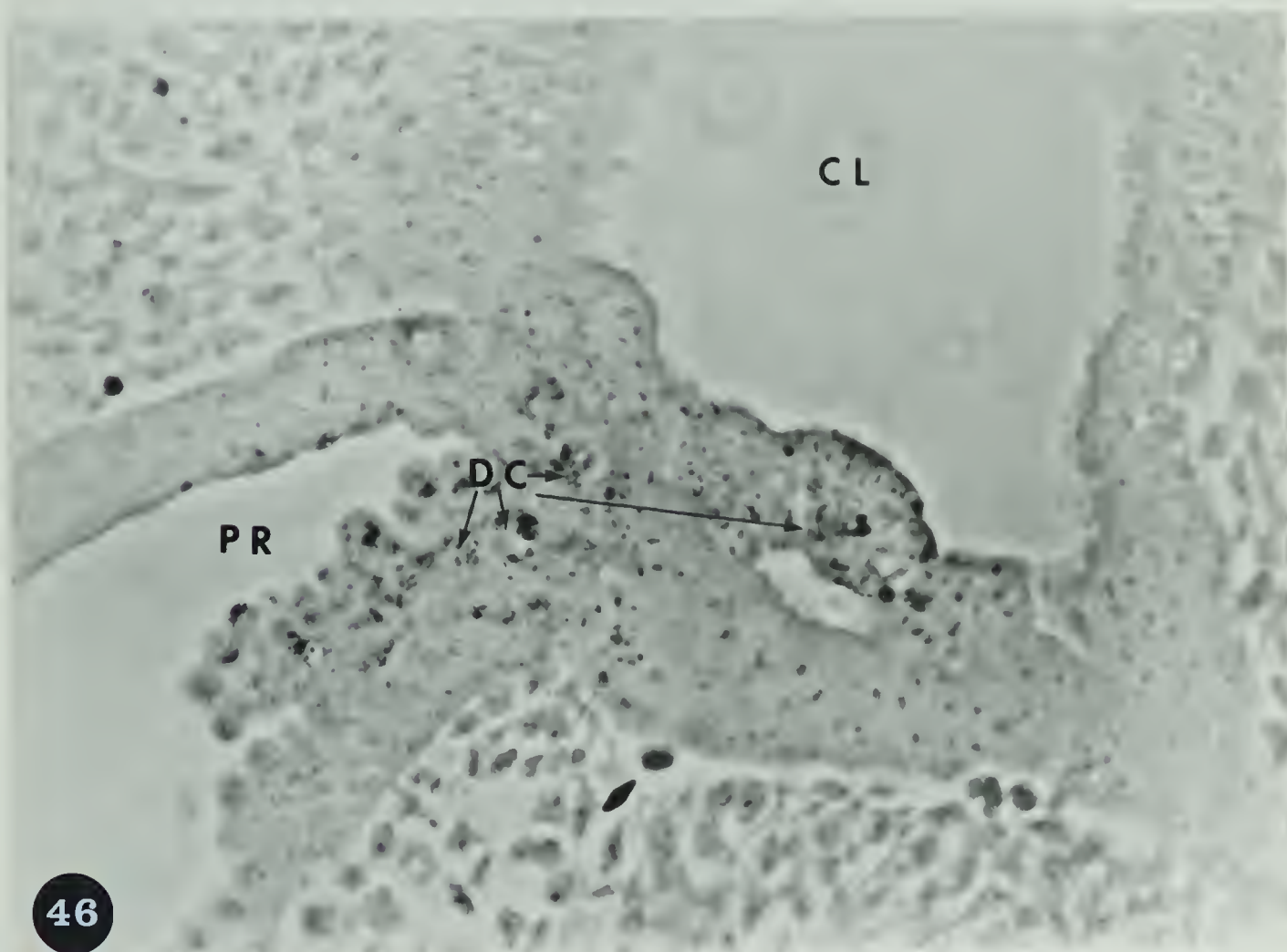
Fig. 46-51. A series of phase contrast photomicrographs taken from serial parasagittal sections of a 4-day cloaca showing the contact of the ectodermal proctodeal epithelium and the endodermal cloacal epithelium. Note the protrusion of cells from the floor of the cloaca into the lumen of the cloaca.

PR: proctodaeum CL: cloacal cavity
AL: allantois DC: degenerating cell
Osmium tetroxide, Araldite, and unstained.

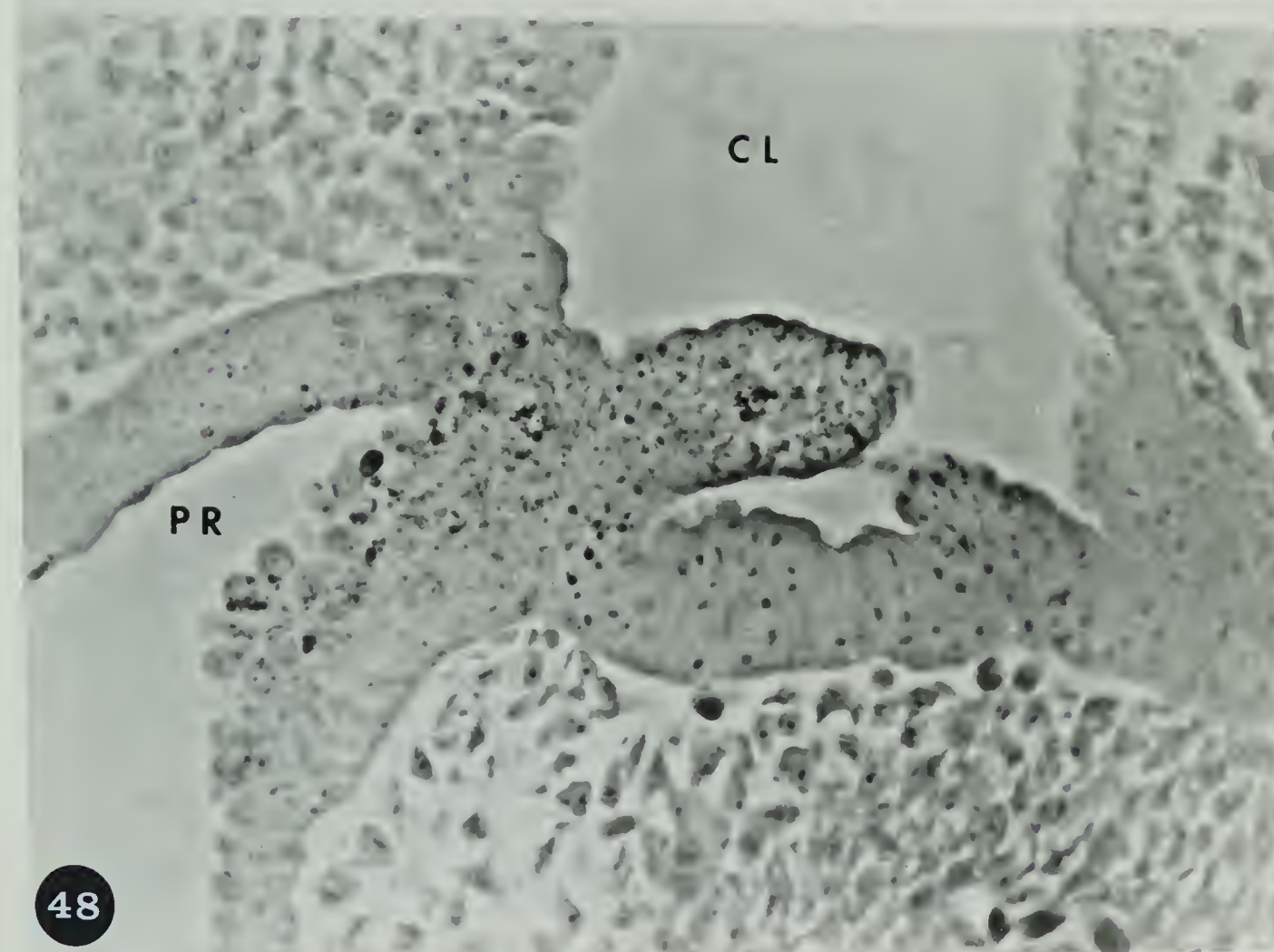
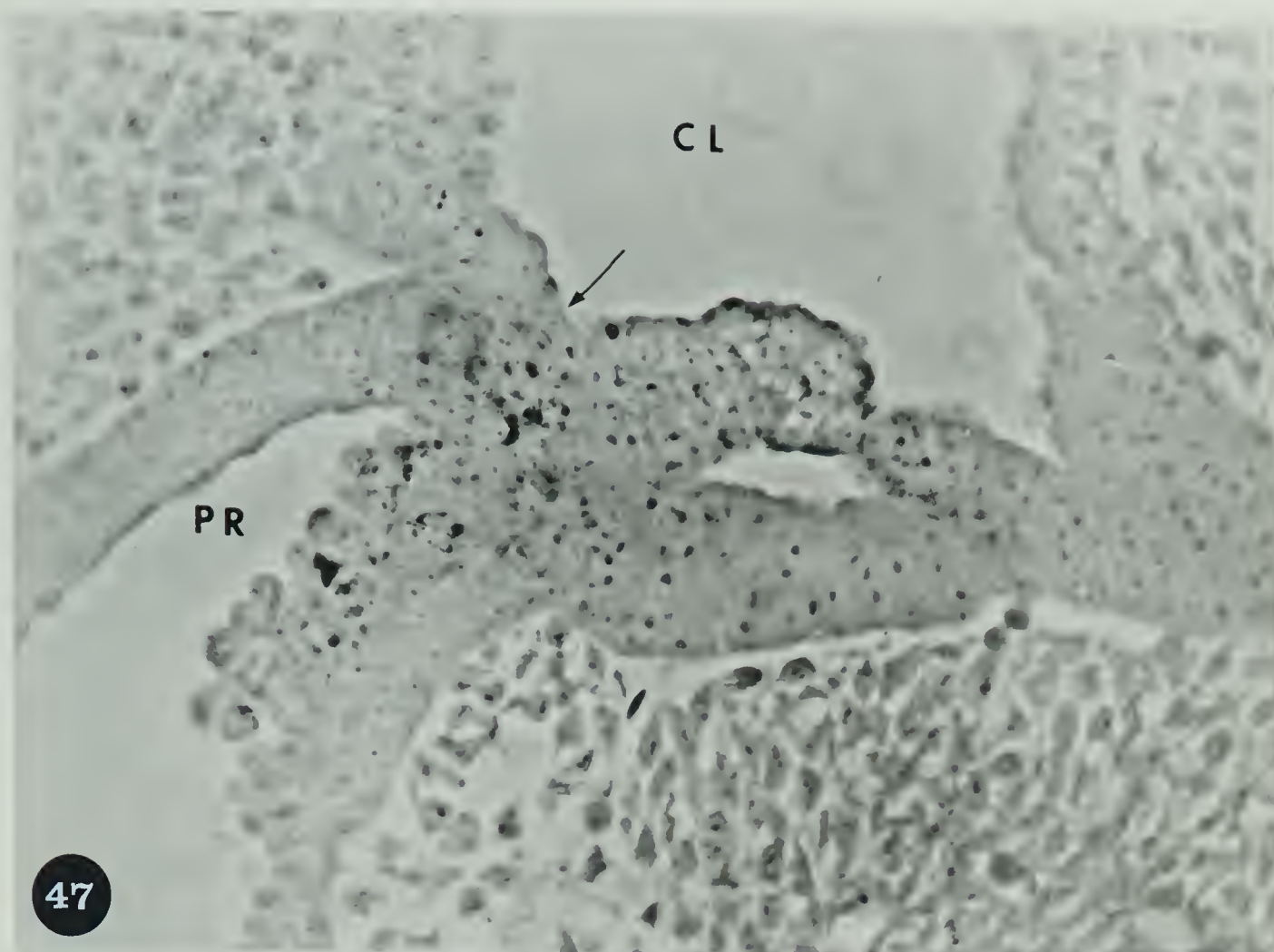
X 405

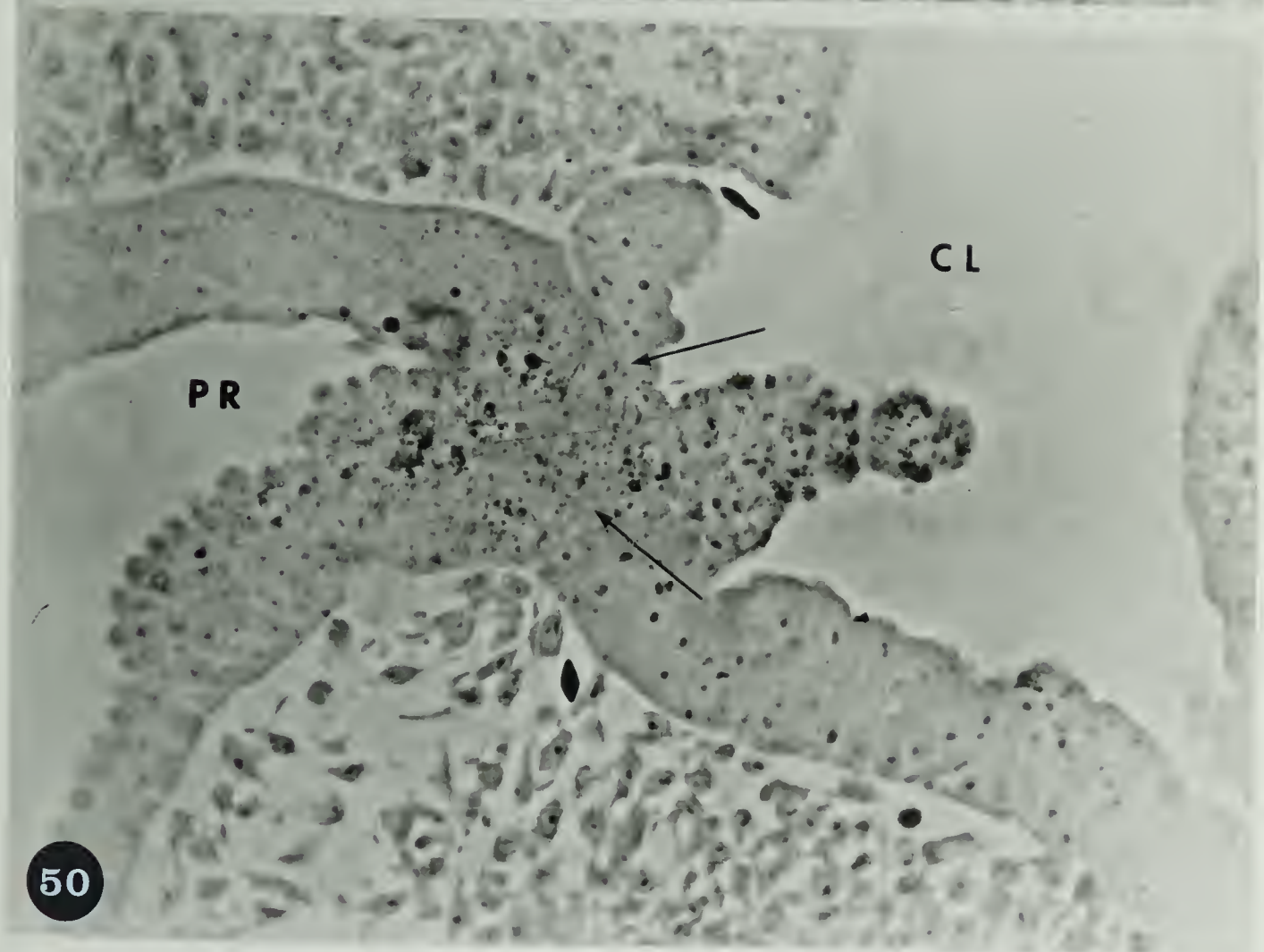
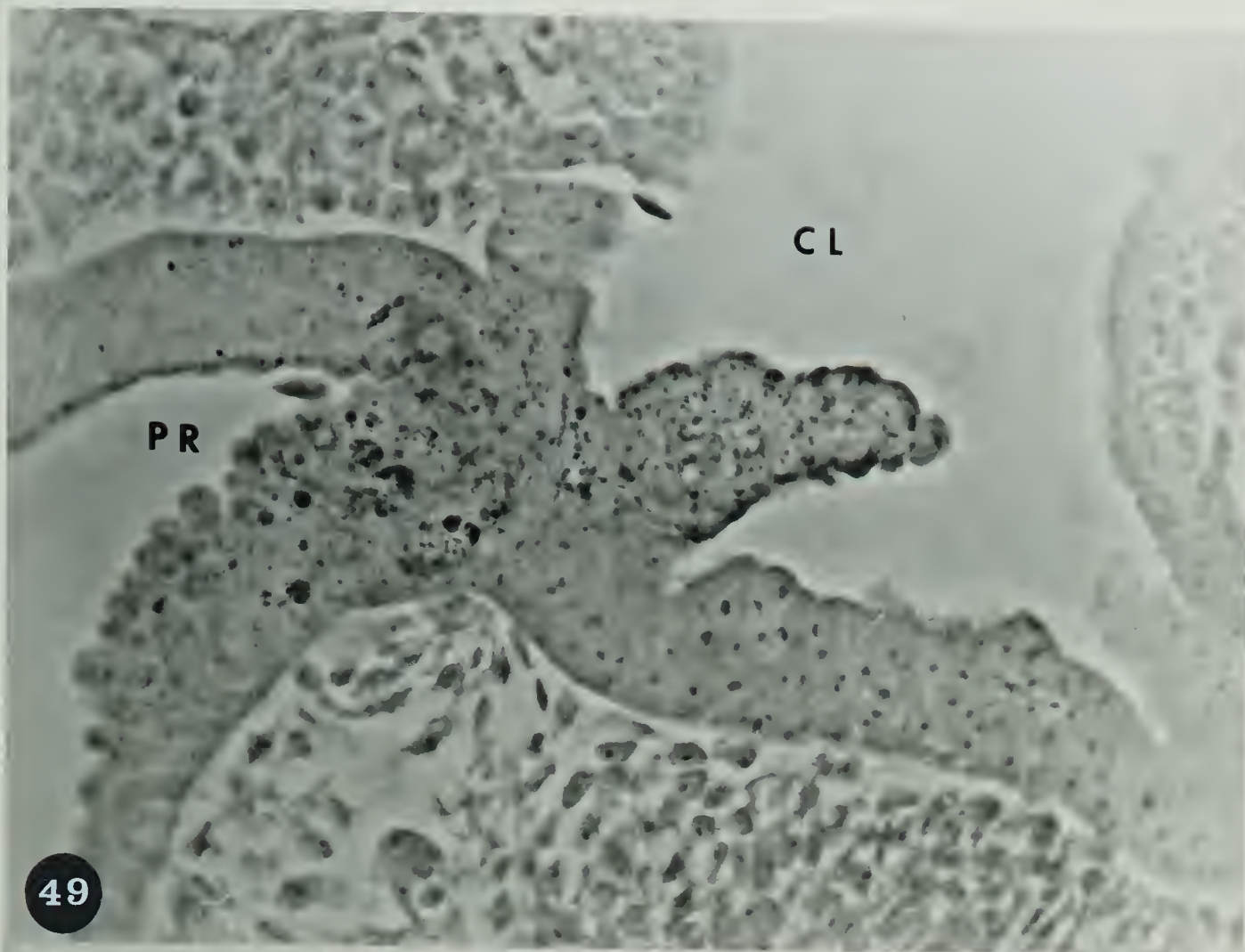


45



46





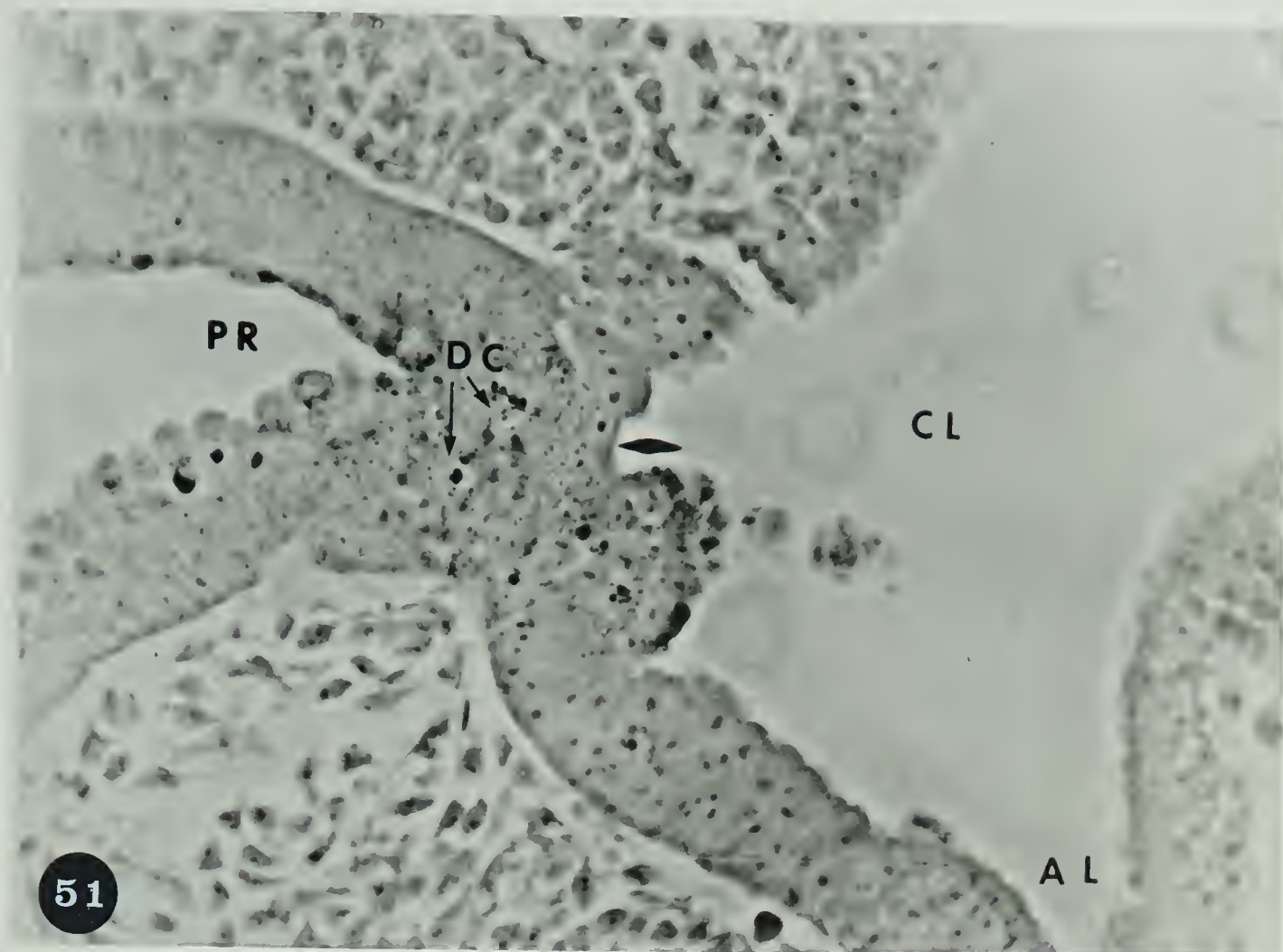


Fig. 52. A diagram of a representative sagittal section through a 5-day urodeal membrane. The rectangle indicates the location of the series of photomicrographs (Figs. 53-57).

| | |
|-----------------|----------------------|
| AL: allantois | CL: cloacal lumen |
| ND: notochord | NT: neural tube |
| PR: proctodaeum | UM: urodeal membrane |
| R: rectum | |

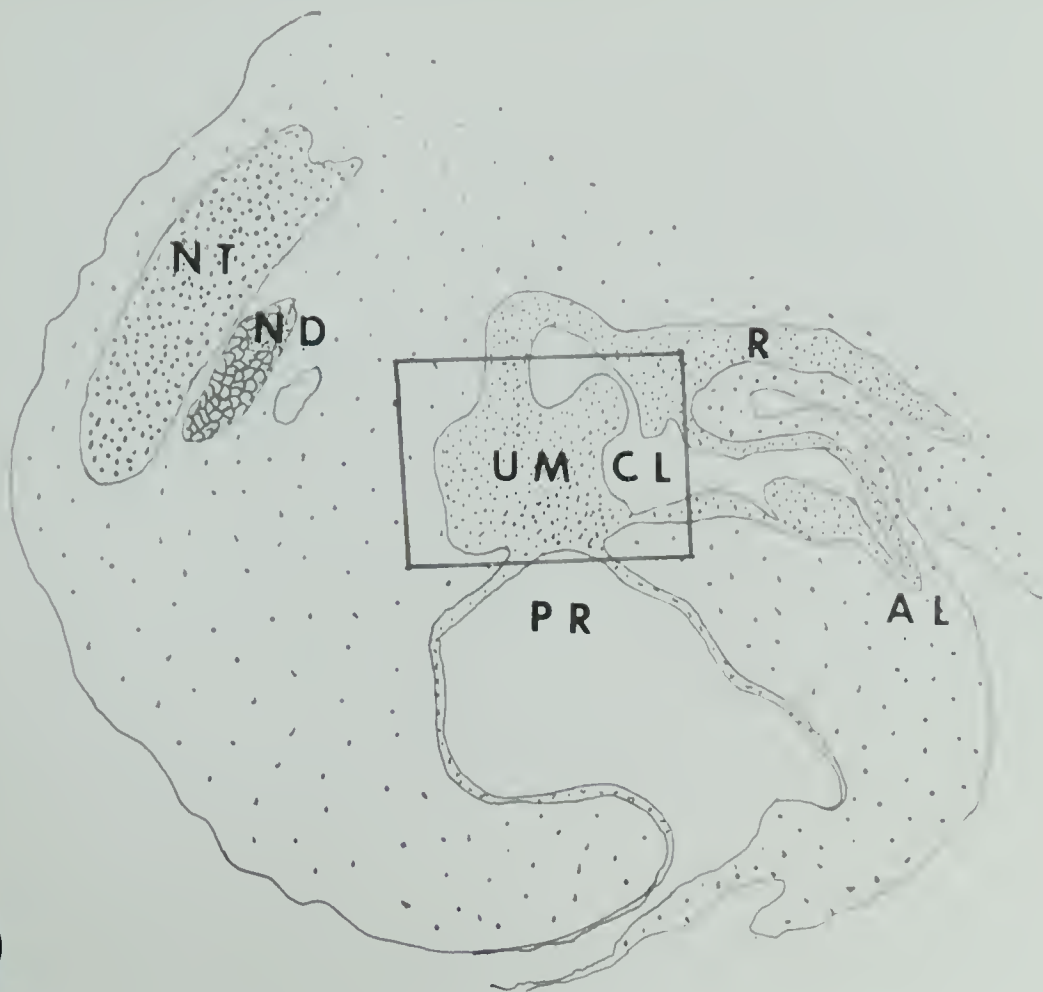
X 45

Figs. 53-57. A series of phase contrast photomicrographs taken from serial parasagittal sections of the posterior part of a 5-day chick embryo showing the topological relationship of the proctodeal ectoderm, urodeal membrane and the cloacal lining. Bursal vesicles are seen in the urodeal membrane.

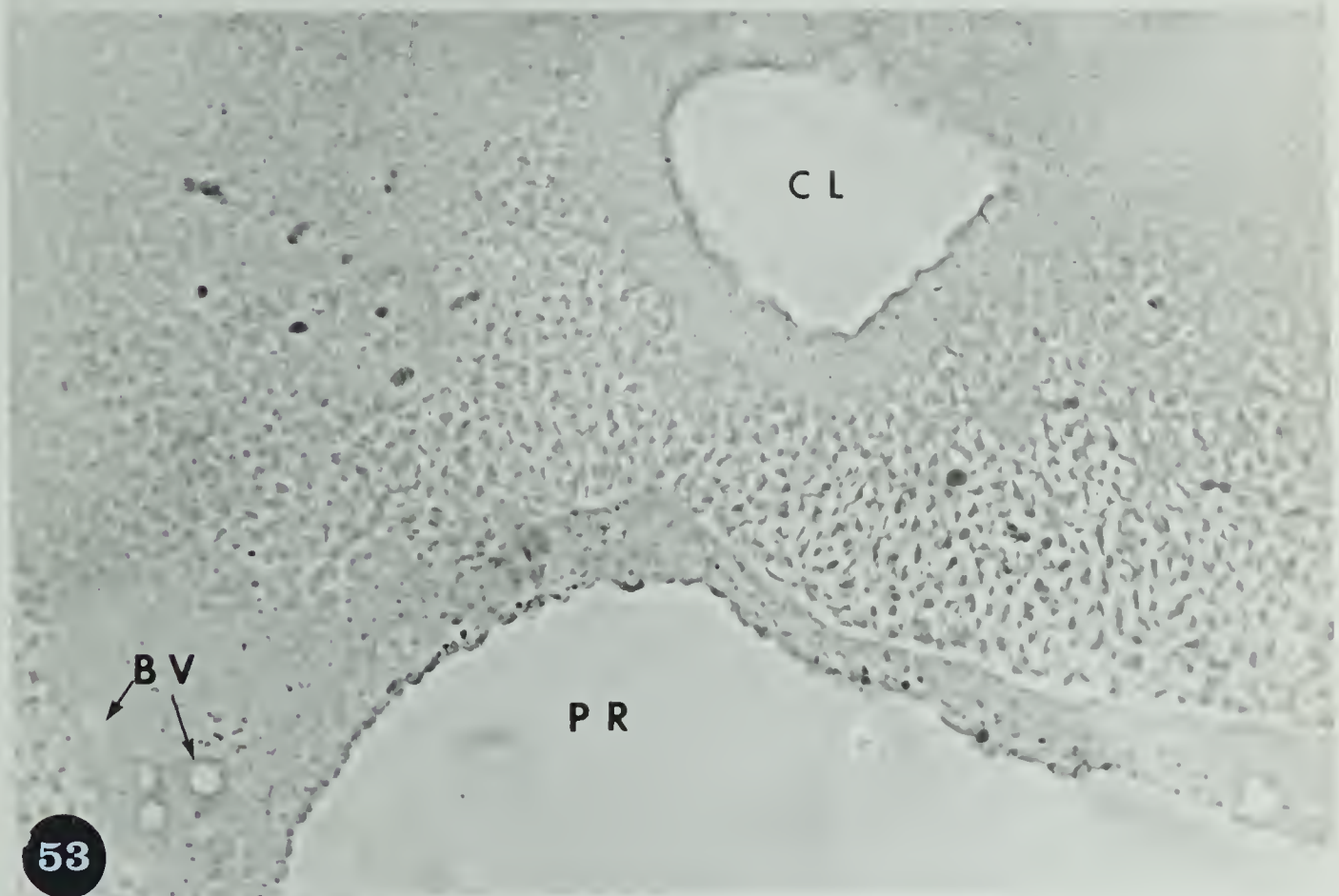
| | |
|-------------------|----------------------|
| AL: allantois | BV: bursal vesicle |
| CL: cloacal lumen | ME: mesenchyme |
| PR: proctodaeum | UM: urodeal membrane |

Osmium tetroxide, Araldite, and unstained.

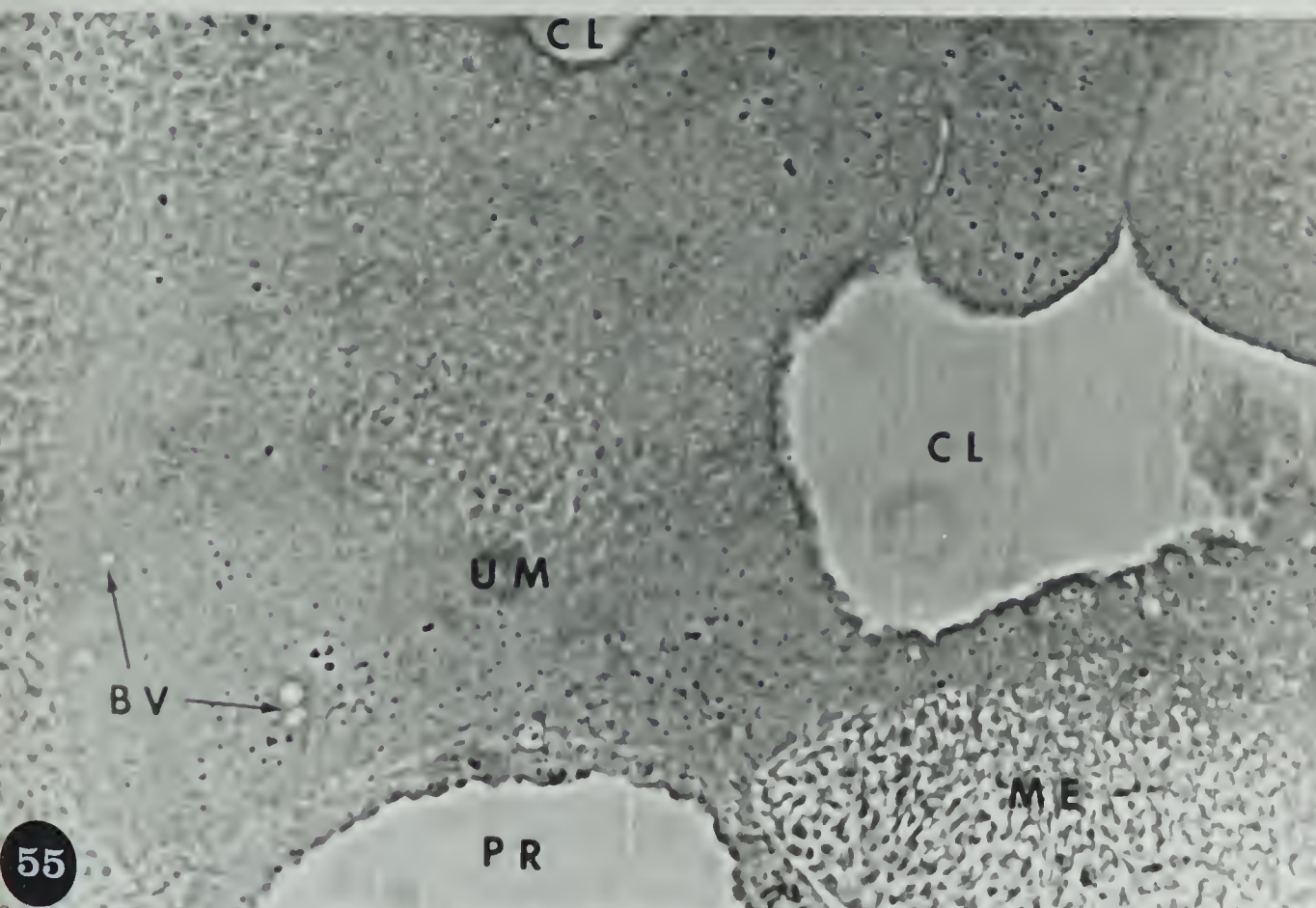
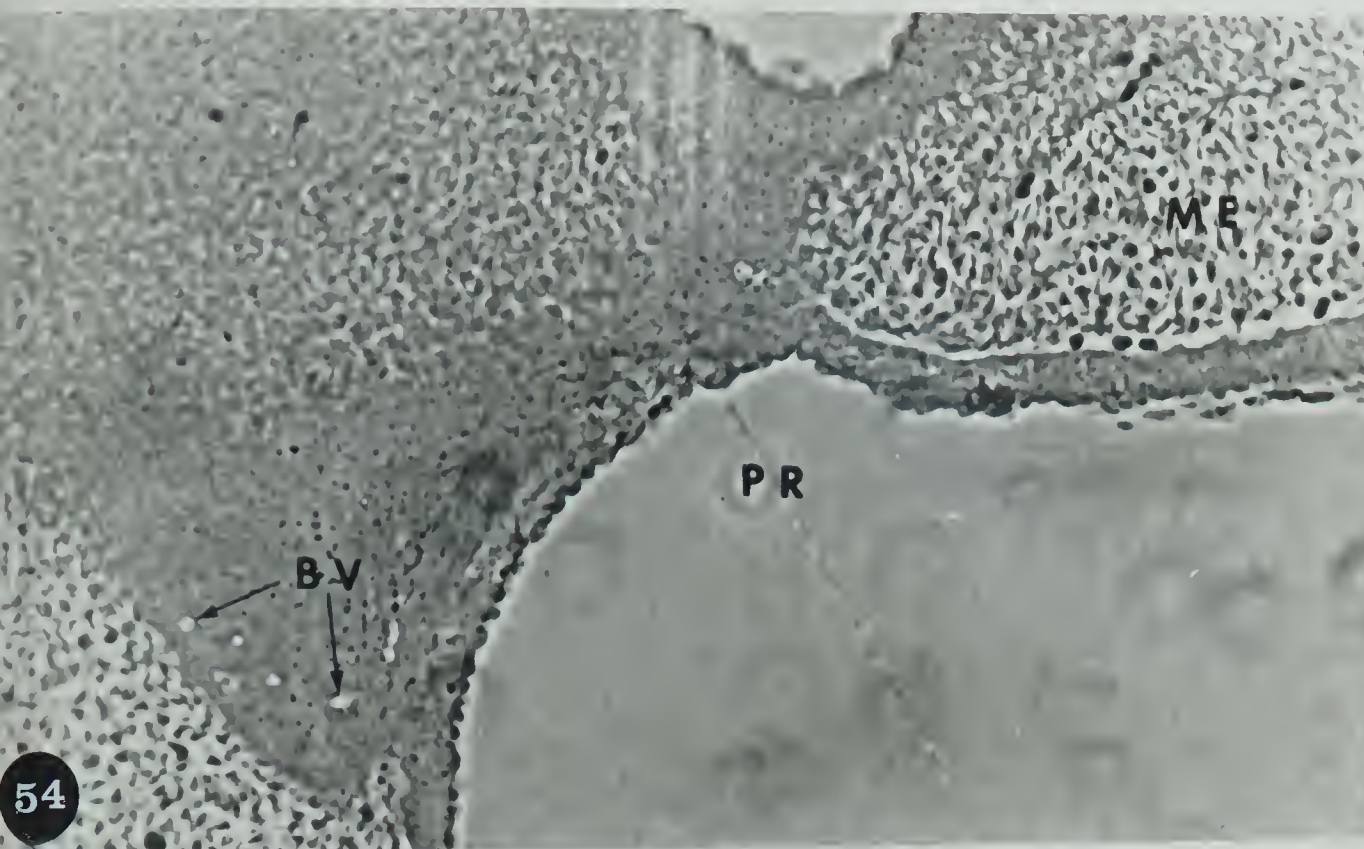
X 198

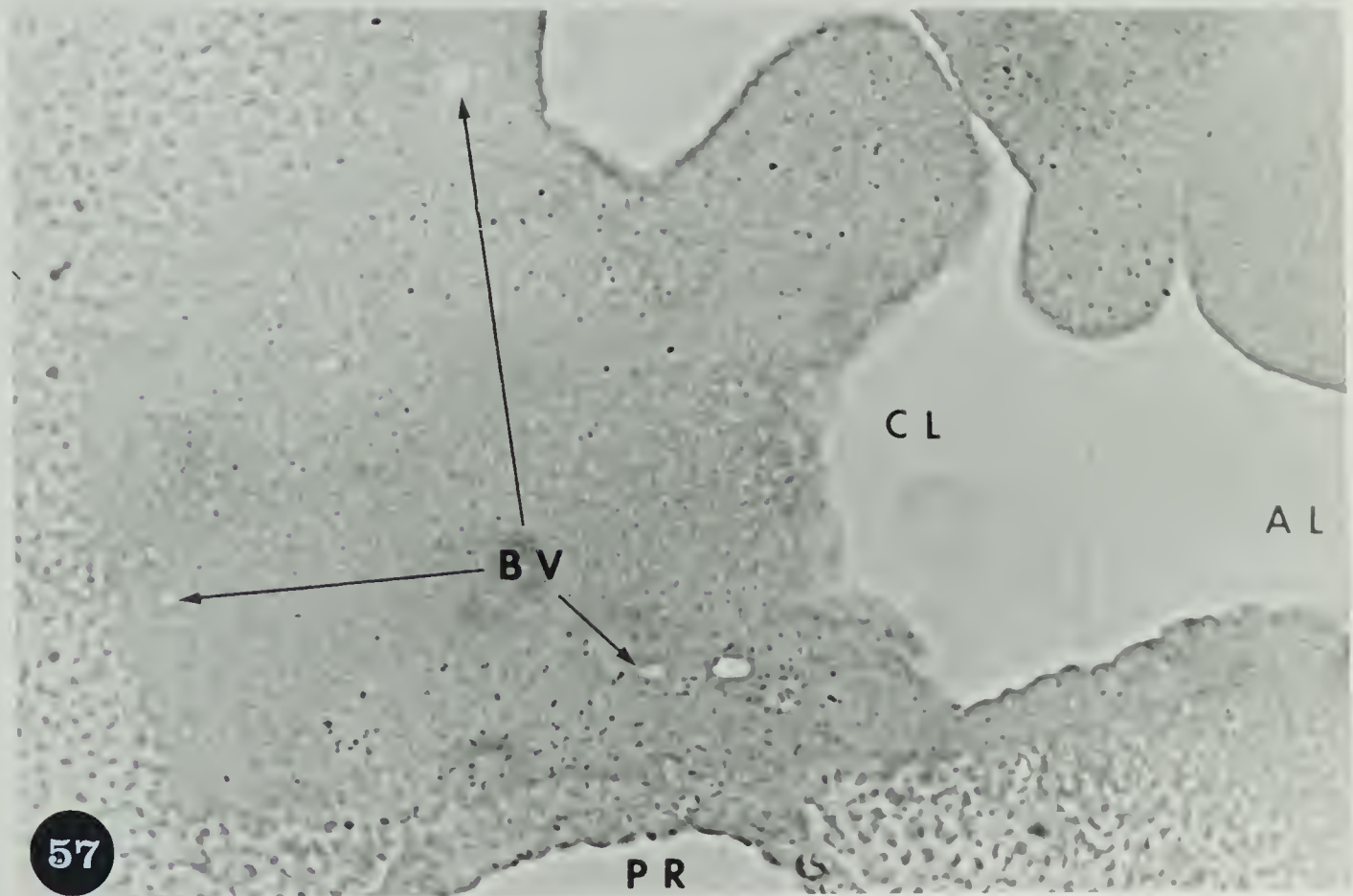
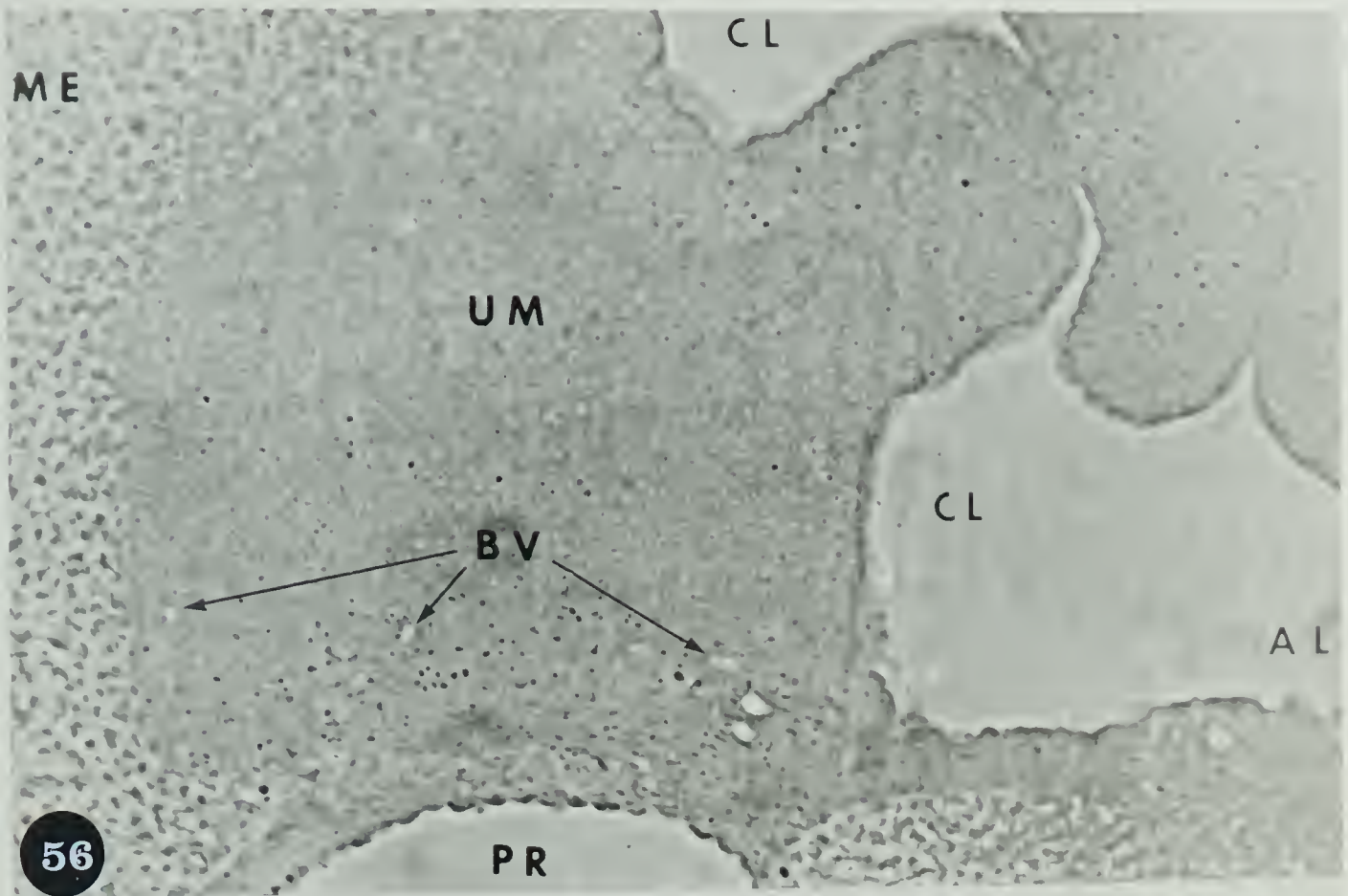


52



53





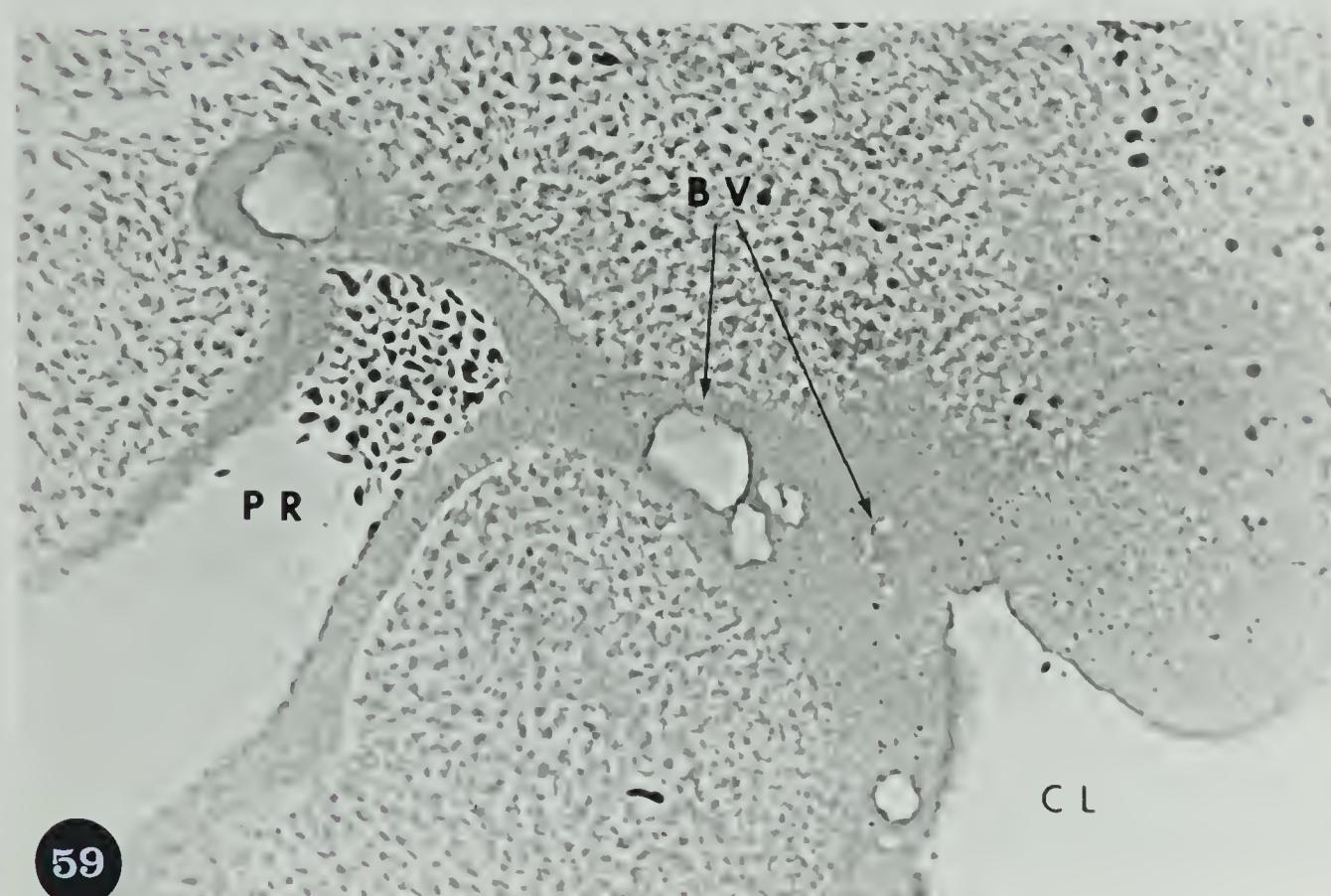
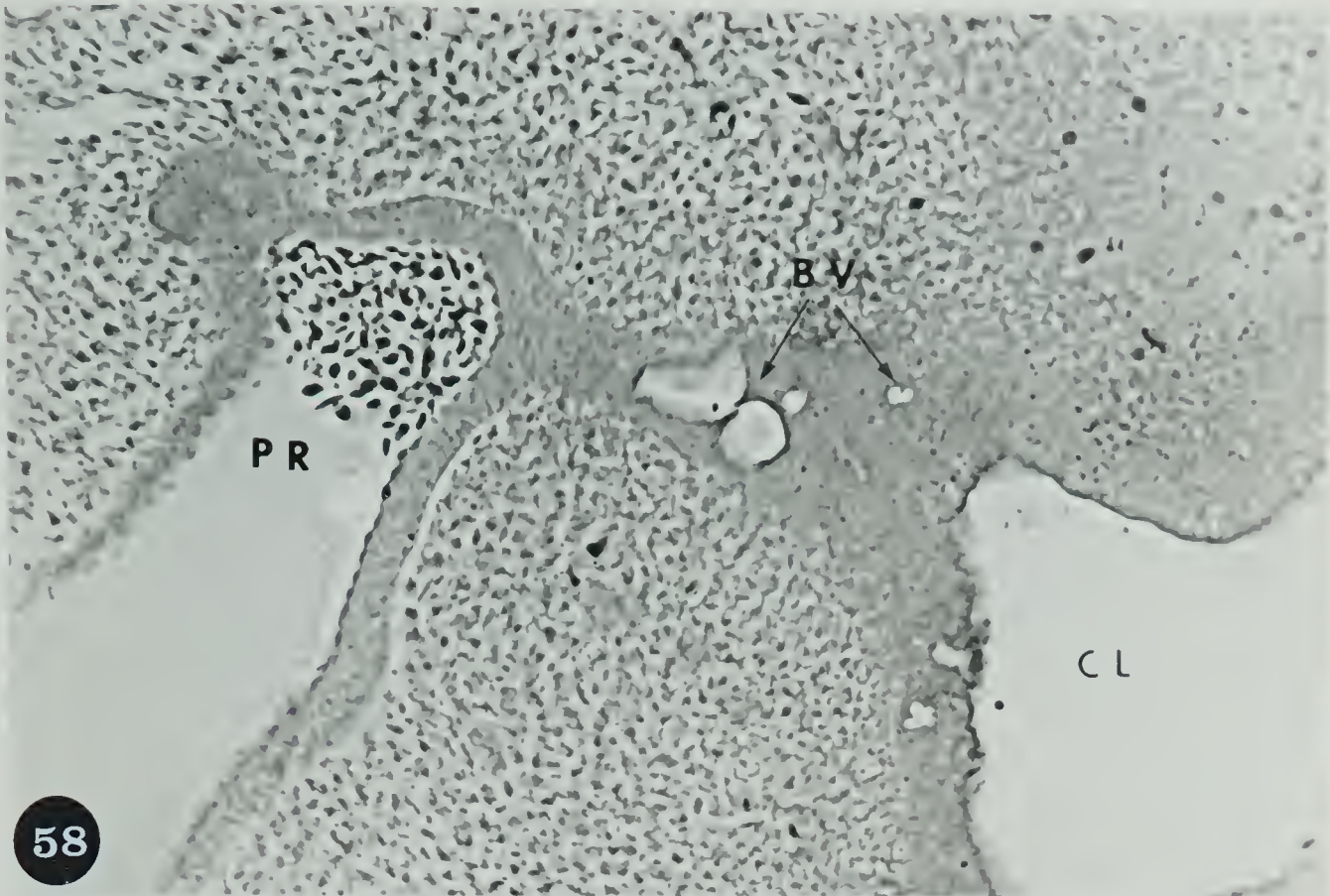
Figs. 58-63. A series of phase contrast photomicrographs taken from serial parasaggital sections of the posterior part of a 6-day embryo showing bursal vesicles (BV) throughout the urodeal membrane.

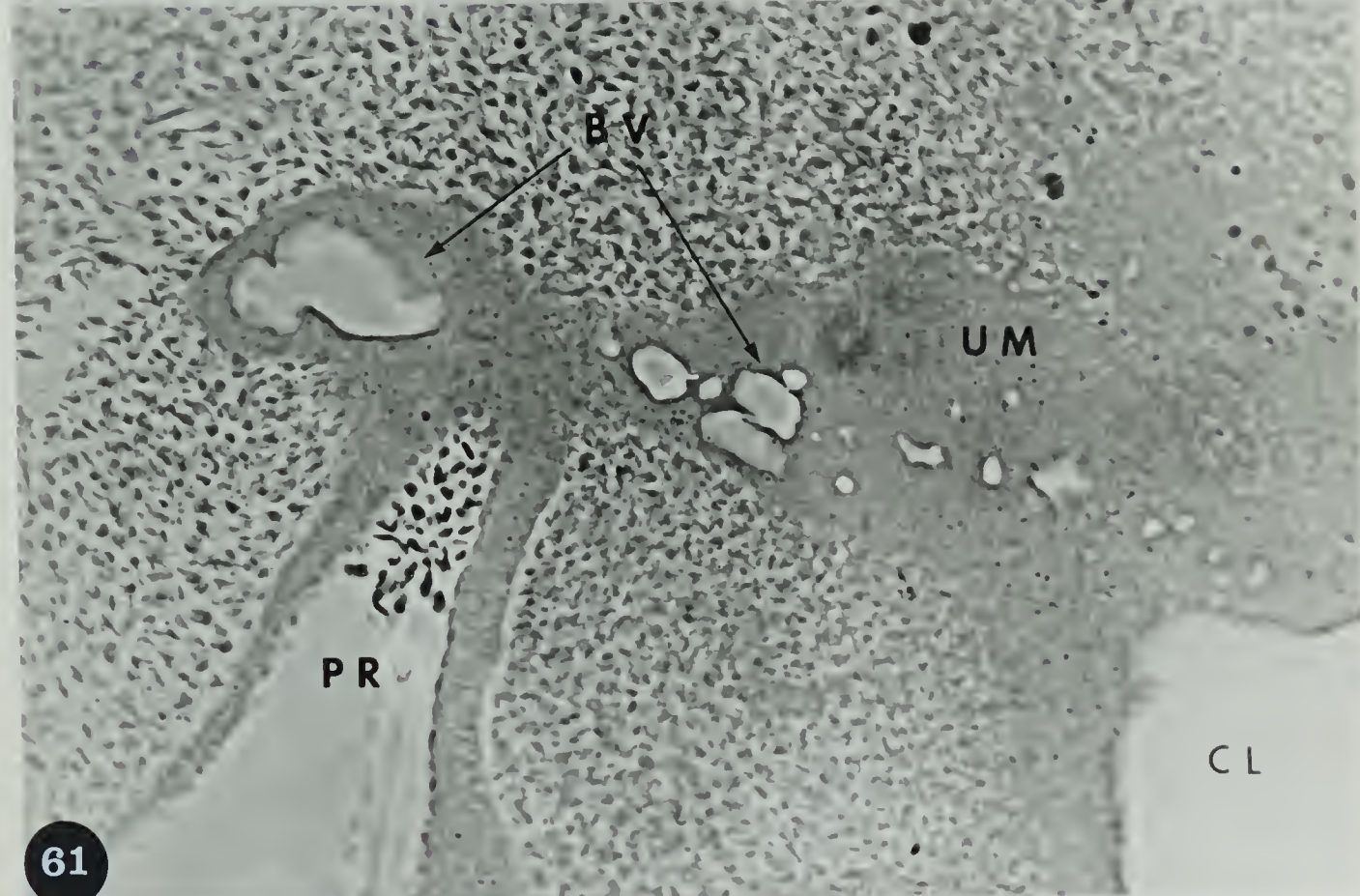
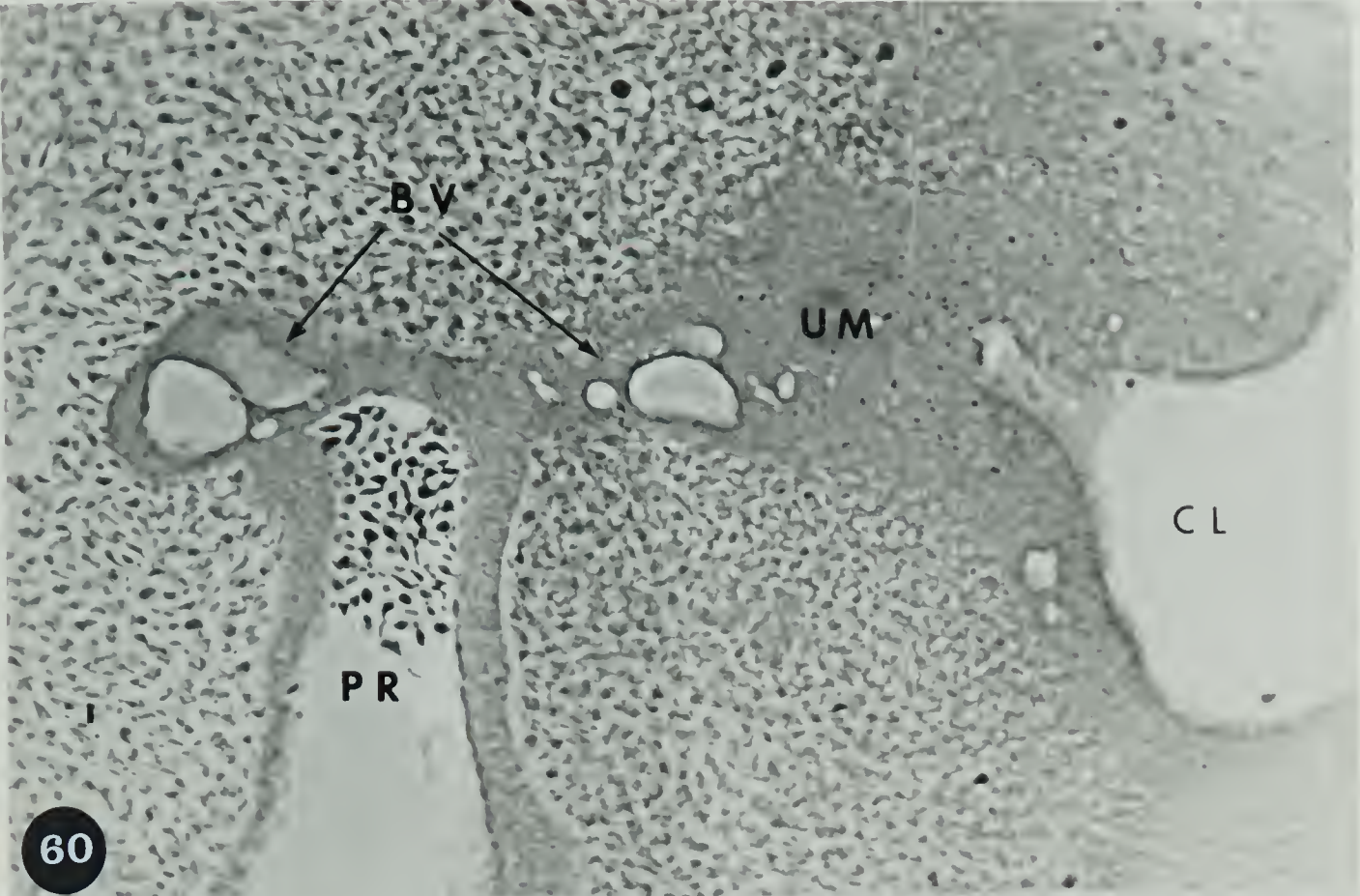
BV: bursal vesicle CL: cloacal cavity

UM: urodeal membrane PR: proctodaeum

Osmium tetroxide fixation, Araldite, and unstained.

X 198





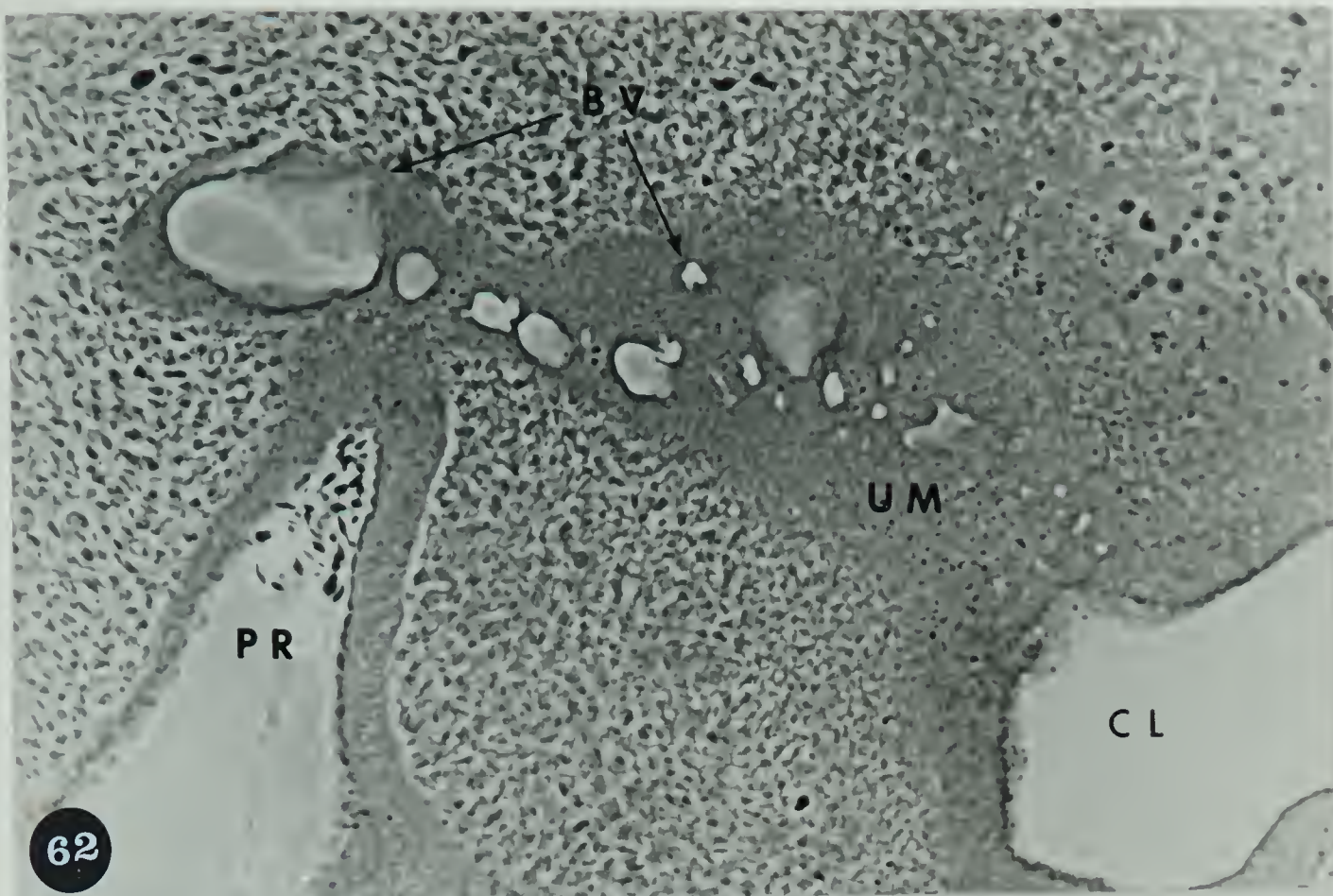


Fig. 64. Ectodermal cells of the proctodaeum. A cytolysome (CL) is seen near the lower right corner. Note the pinocytotic vesicles (PV), the Golgi apparatus (G) near the cell surface, vesicular endoplasmic reticulum and interdigitations of the cell surface of adjoining cells.

CL: cytolysome

CM: cell membrane

G: Golgi apparatus

IS: intercellular space

L: lipid droplet

PR: proctodaeum

PV: pinocytotic vesicle

Osmium tetroxide, Araldite, and uranyl acetate.

X 22,400

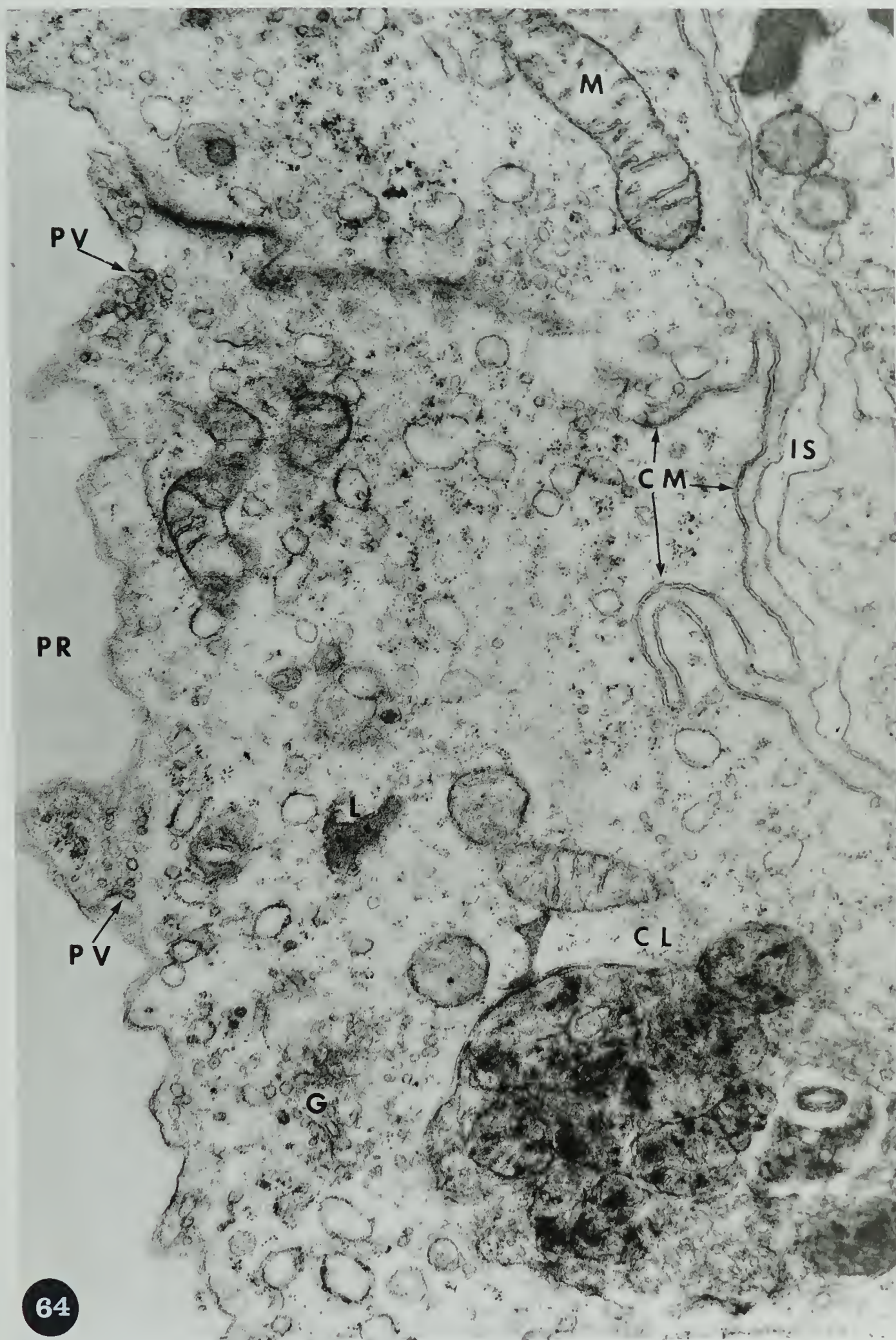


Fig. 65. Ectodermal cells of the proctodeal epithelium showing numerous lipid droplets (L) of irregular shape, tight junctions (TB), desmosomes (D), Golgi apparatus (G), intercellular space (IS) and cytolysosomes (CL).

PR: proctodaeum N: nucleus

Osmium tetroxide, Araldite, and uranyl acetate.

X 12,120

P R

L

D

T B

D

G

IS

D

N

C L

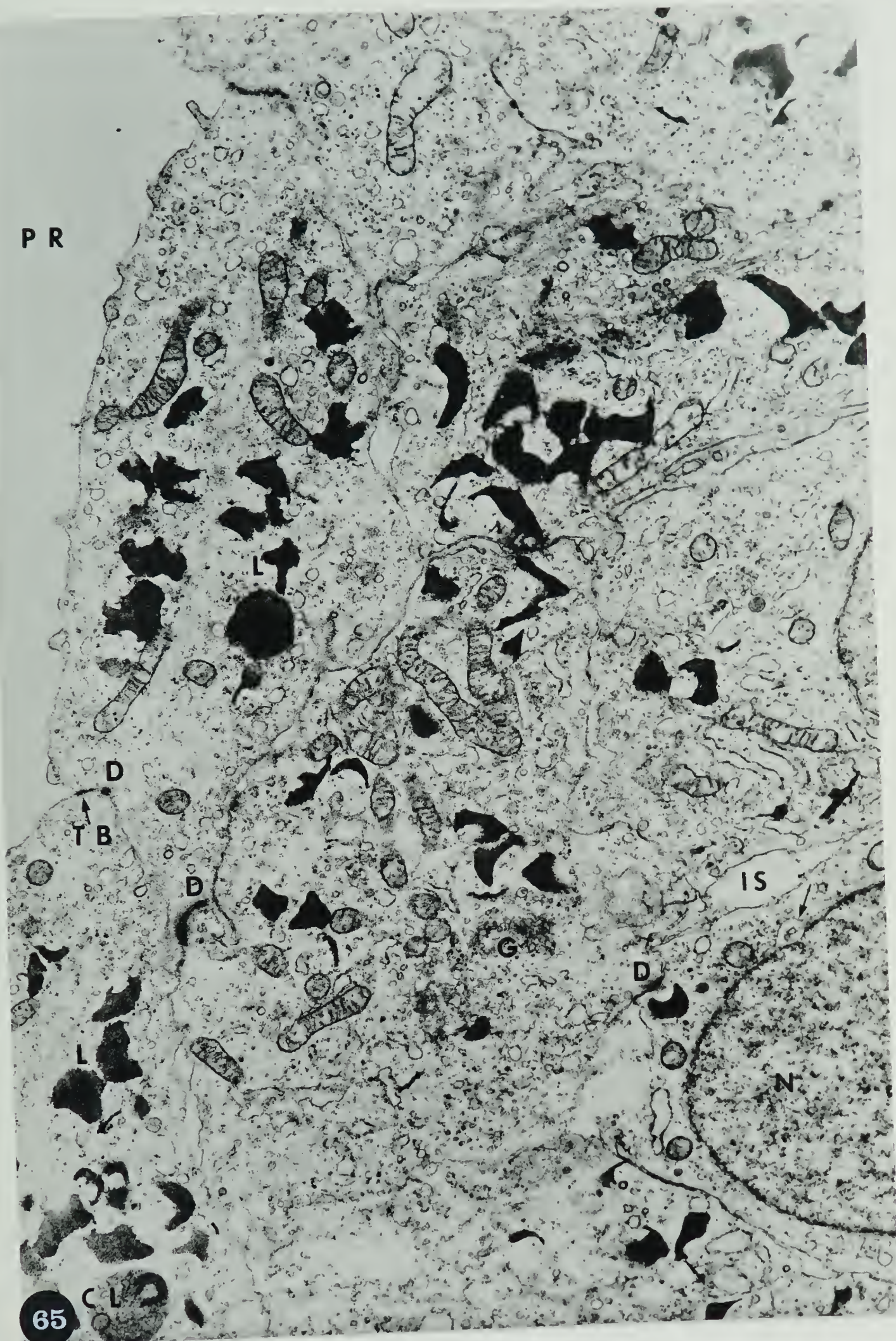


Fig. 66. A part of the urodeal membrane near the proctodaeum showing multivesicular bodies (MVB), Golgi apparatus (G), nuclear pores (arrows), desmosomes (D), and an intercellular space (IS) the border of which resembles those of bursa vesicles. Note the sharp contrast of the parts of the border and the diffuse character of adjacent parts where cytoplasmic granules have entered the intercellular space. The interrupted border may be artifactual, but such interruptions are not seen at the proctodeal and cloacal surfaces. The diffuse parts may be the portals through which cytoplasmic granules contribute to the bursa vesicles.

N: nucleus

Osmium tetroxide, Araldite, and uranyl acetate.

X 26,600

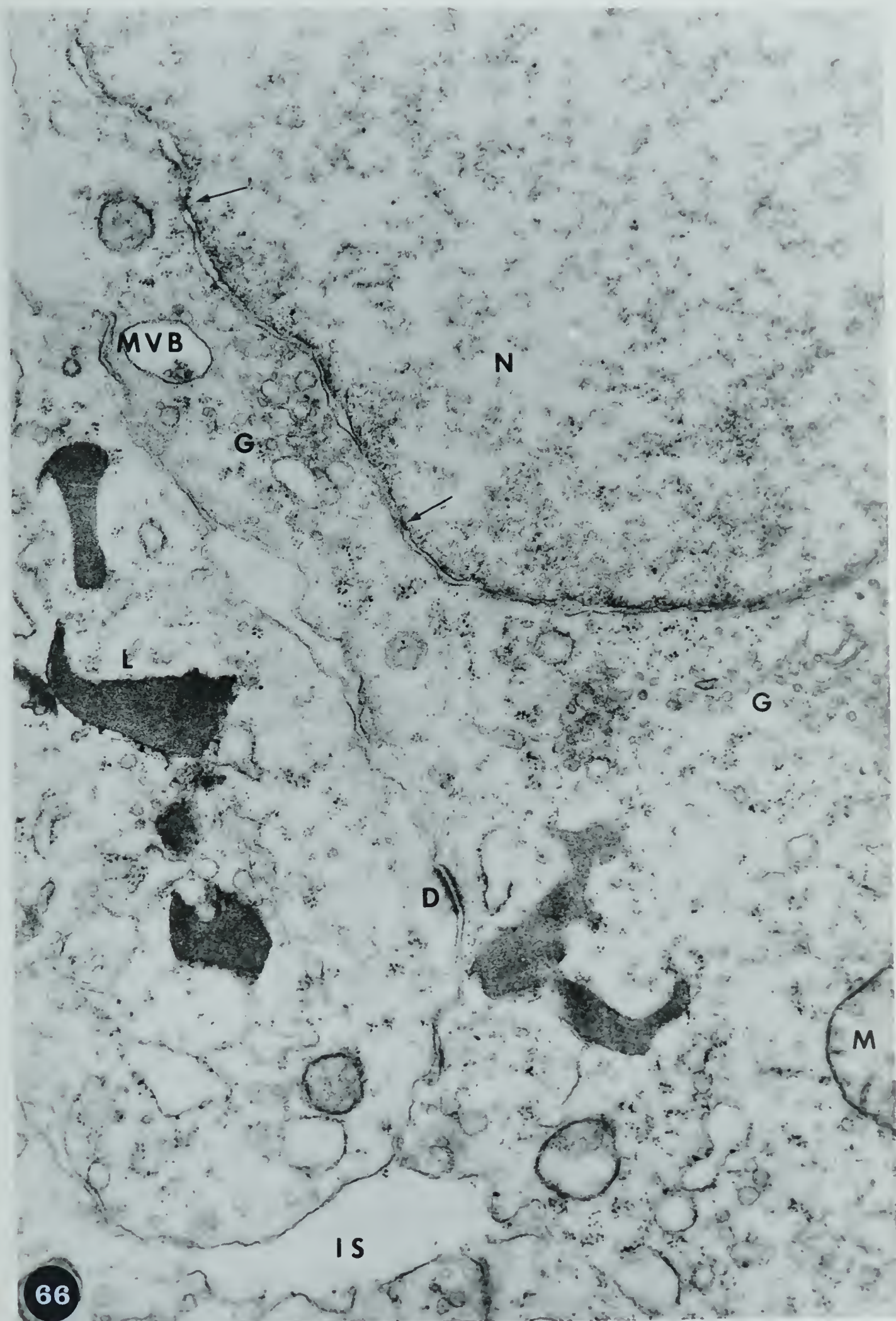


Fig. 67. An area of urodeal membrane near the proctodaeum showing a degenerating cell (CL) surrounded by normal cells.

CL: cytolysome G: Golgi apparatus

D: desmosome CO: Collagen-like

IS: intercellular space material

NL: nucleolus N: nucleus

Osmium tetroxide, Araldite, and uranyl acetate.

X 14,850

Fig. 68. Epithelial cells near the proctodaeum. A degenerating cell is seen in the center and is surrounded by four normal cells at four corners. Degraded mitochondria and enlarged endoplasmic reticulum (ER) are recognizable in the degenerating cell. Osmium tetroxide, Araldite, and unstained. X 16,800

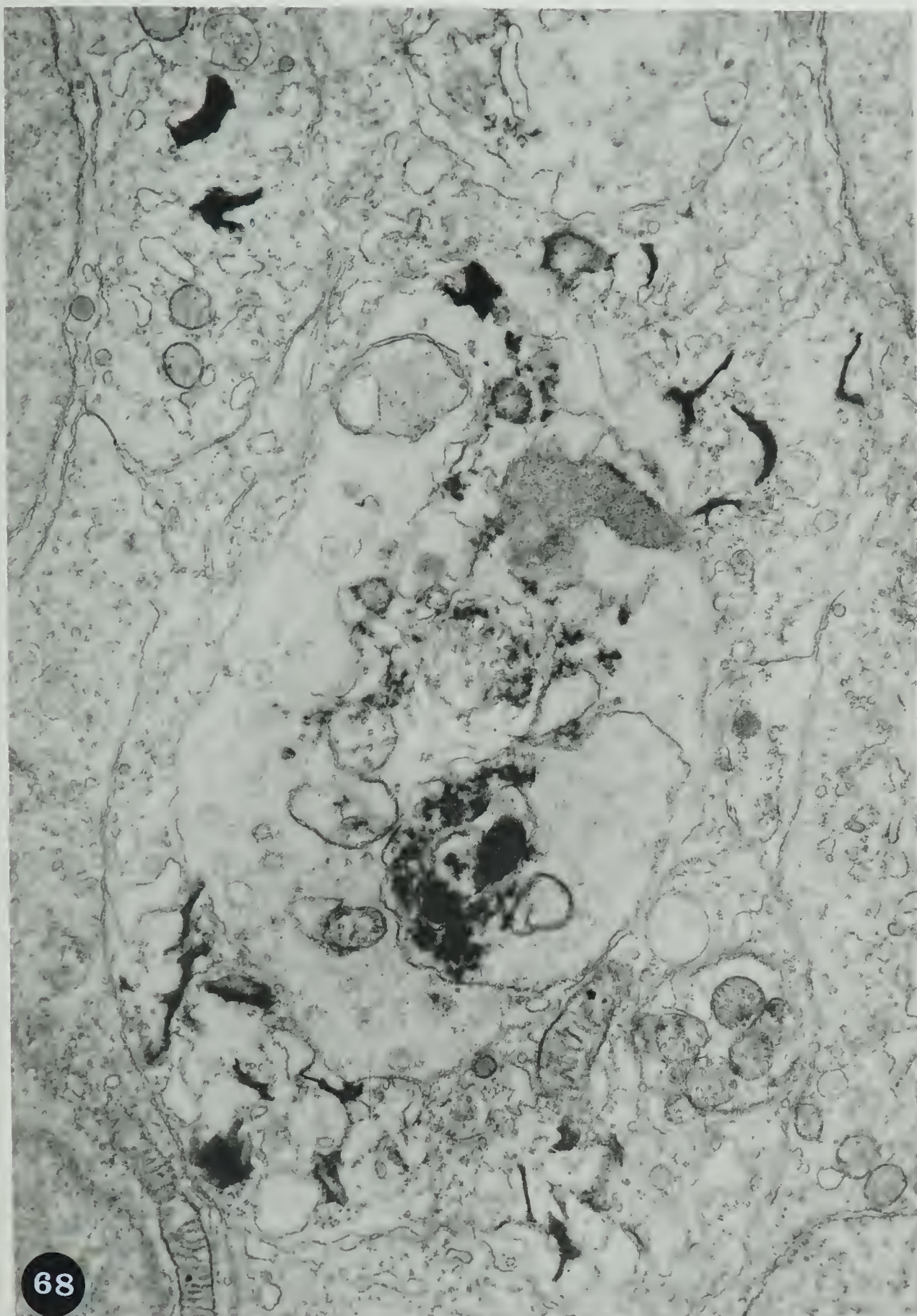


Fig. 69. An area of the urodeal membrane showing numerous aggregations of ribosomes (R), granular endoplasmic reticulum, multivesicular bodies (MVB), and distended intercellular spaces (IS).
Osmium tetroxide, Araldite, and uranyl acetate.
X 24,960

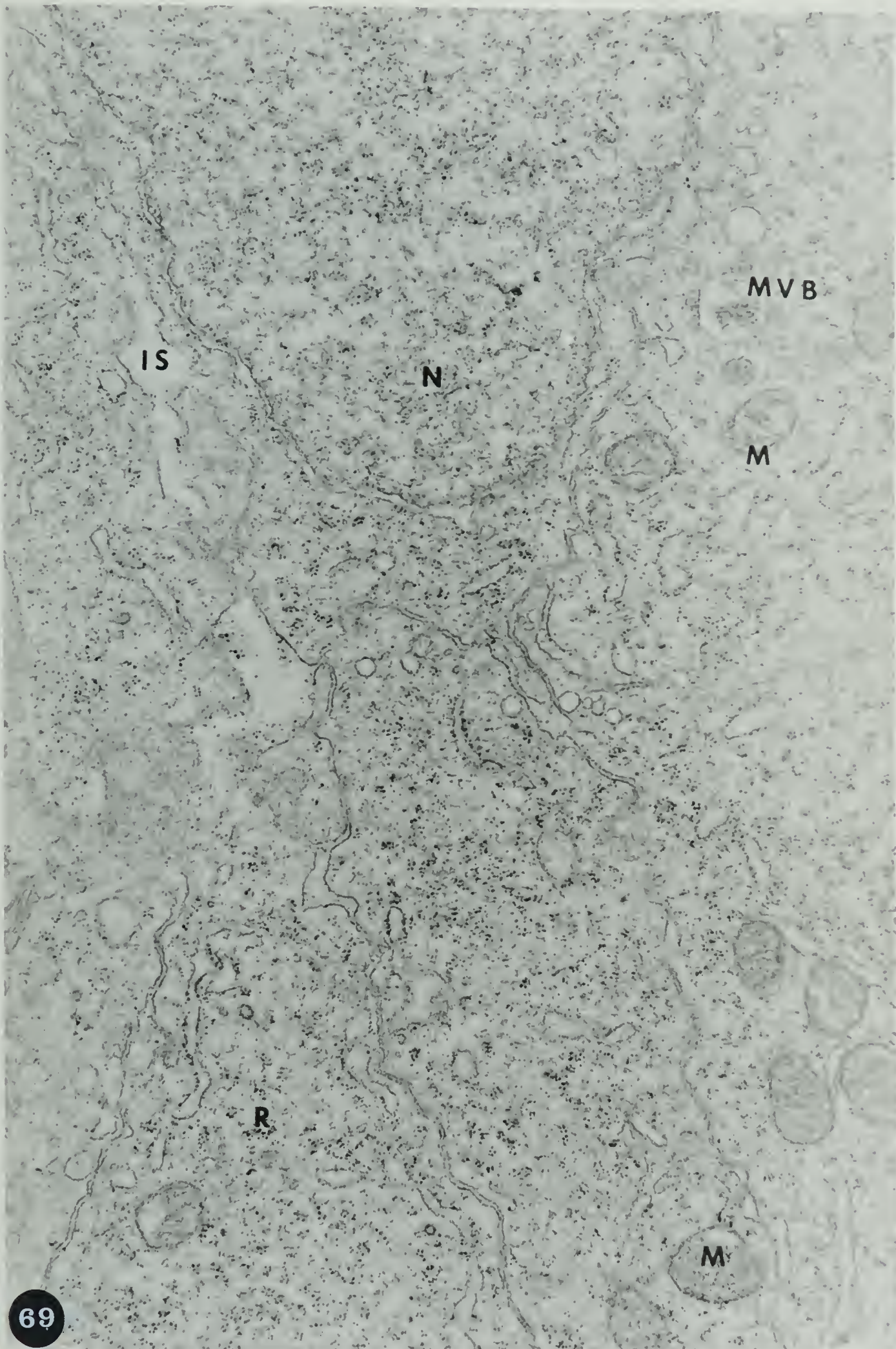


Fig. 70. Part of Fig. 71 enlarged to show multivesicular bodies (MVB), numerous ribosomes (R), and irregular lipid droplets (L). The fusion of a Golgi vesicle with the limiting membrane of the multivesicular body is indicated by an arrow. Note the close attachment of the cell containing large MVB with the cell below it. The lower cell has either been damaged during fixation or naturally in the region of attachment. There is a band of amorphous material extending from D to the right of R. The limiting membrane of the MVB nearest this diffuse area is ruptured, perhaps artifactually. The proximity of these two unusual alterations in an area which otherwise seems to be moderately well fixed suggests that the MVB of the superior cells may have contributed to the alteration of the lower cell. Osmium tetroxide, Araldite, and uranyl acetate. X 22,400

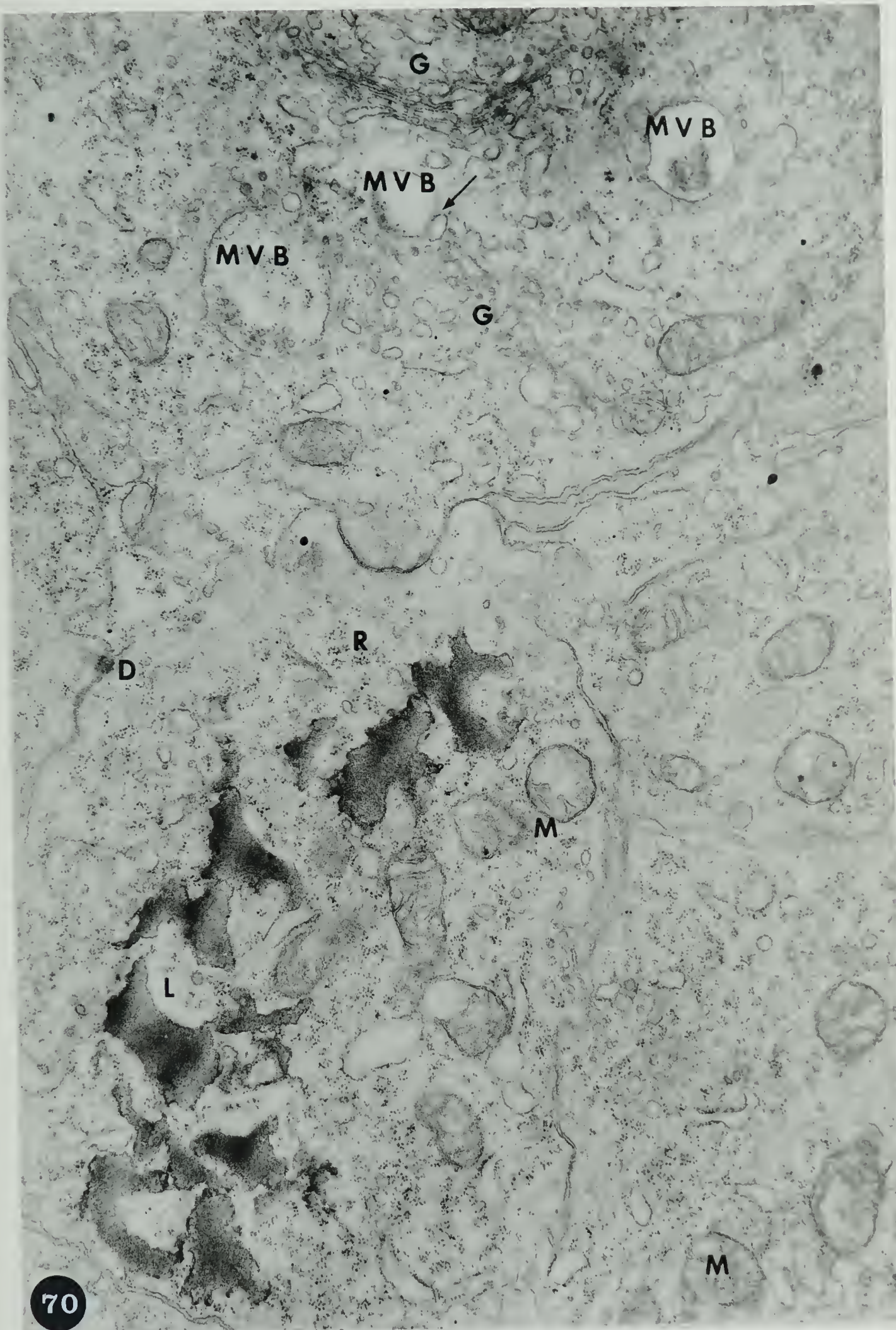


Fig. 71. An area of the urodeal membrane. Part of a bursal vesicle (BV) is seen at the lower left corner. Note the extensions of some cells (arrows).

D: desmosome L: lipid droplet

N: nucleus

Osmium tetroxide, Araldite, and uranyl acetate.

X 13,938

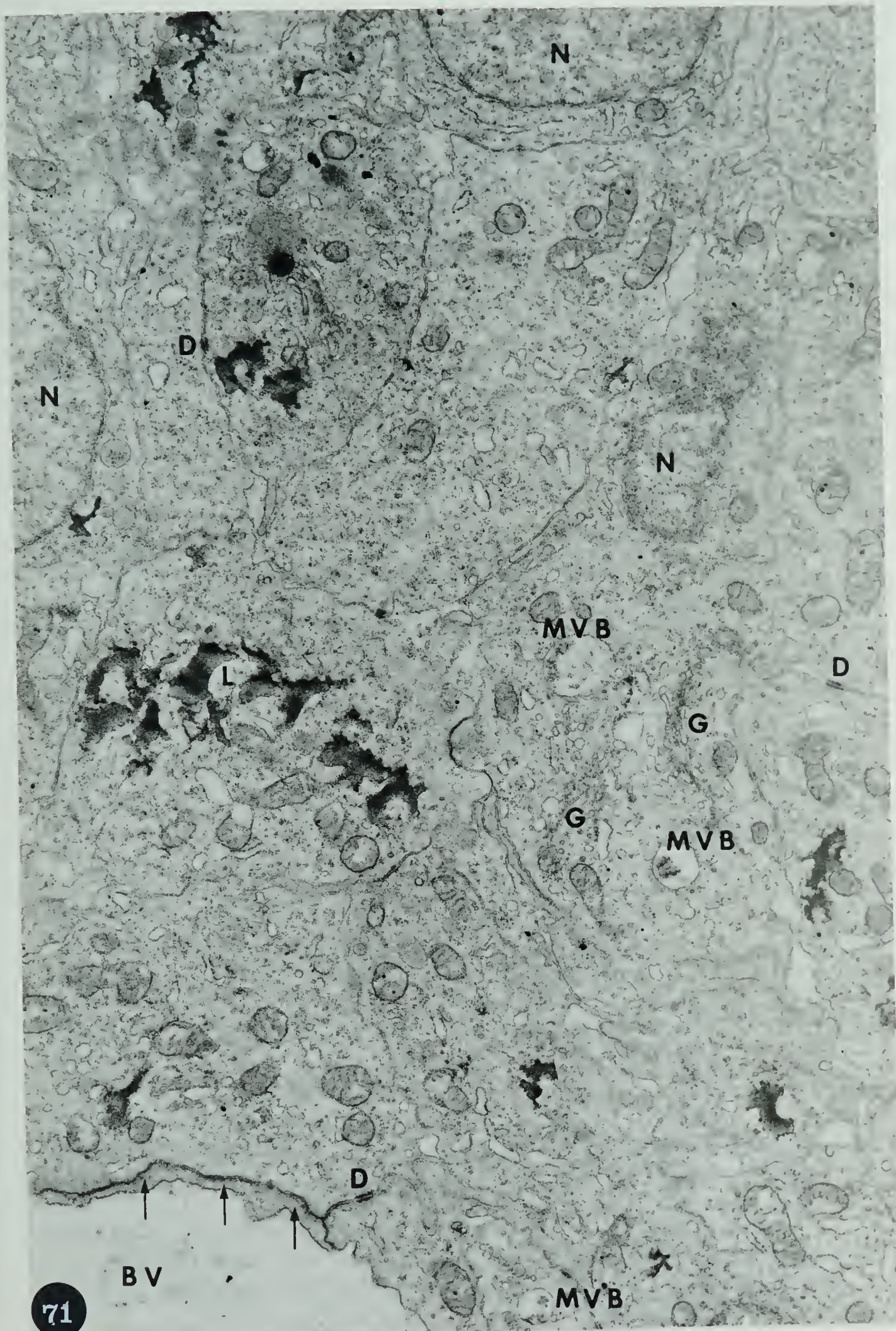


Fig. 72. Part of a bursal vesicle and adjacent cells.

Granular material is present in the bursal vesicle (BV). The plasma membrane facing the bursal vesicle has alternate dense and diffuse parts which resemble the alternate dense and diffuse parts of the border of some intercellular spaces (Fig. 66). The outer membrane of the nuclear envelope comes so close to the cytoplasmic membrane that it may almost appear continuous with it (arrows).

Osmium tetroxide, Araldite, and uranyl acetate.

X 27,600

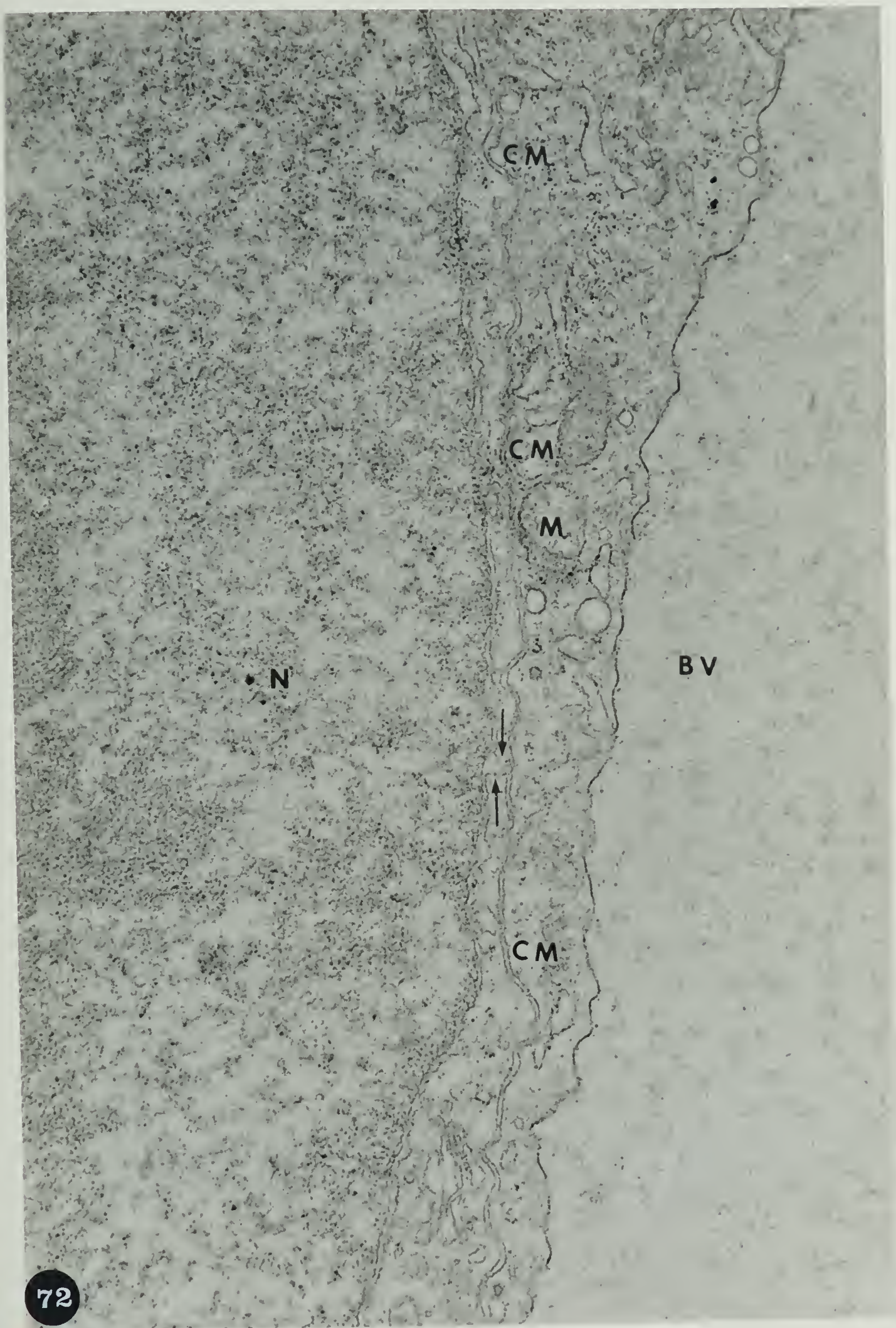


Fig. 73. A part of the urodeal membrane and the cloaca.

The oblique or cross section of the tight junction of cells near the bursa vesicles is shown in the upper center between two thick arrows. The perpendicular view of the tight junction of the bursa vesicle is indicated by thin arrows as seen in the lower center. The tight junction also appears between cells facing the cloacal lumen.

The cytoplasm adjacent to tight junctions shows a slight condensation. The plasma membrane facing the cloacal lumen is darker than the rest of the plasma membrane except the junctional complex of the epithelial cells.

Osmium tetroxide, Araldite, and unstained.

X 9,000

Insert: A higher magnification of a plasma membrane at the cloacal lumen (CL). It shows the asymmetrical unit membrane. The darker and thicker line of the unit membrane is facing the cloacal lumen, the light and thin line faces the cytoplasm.

Uranyl acetate.

X 100,000



Fig. 74. Cells of the urodeal membrane, near the lumen of the cloaca, showing interdigitations and numerous clusters of ribosomes.

| | |
|--------------------------|-------------------|
| D: desmosome | CM: cell membrane |
| G: Golgi apparatus | M: mitochondrion |
| MVB: Multivesicular body | N: nucleus |
| NL: nucleolus | |

Osmium tetroxide, Araldite, and uranyl acetate.

X 11,363

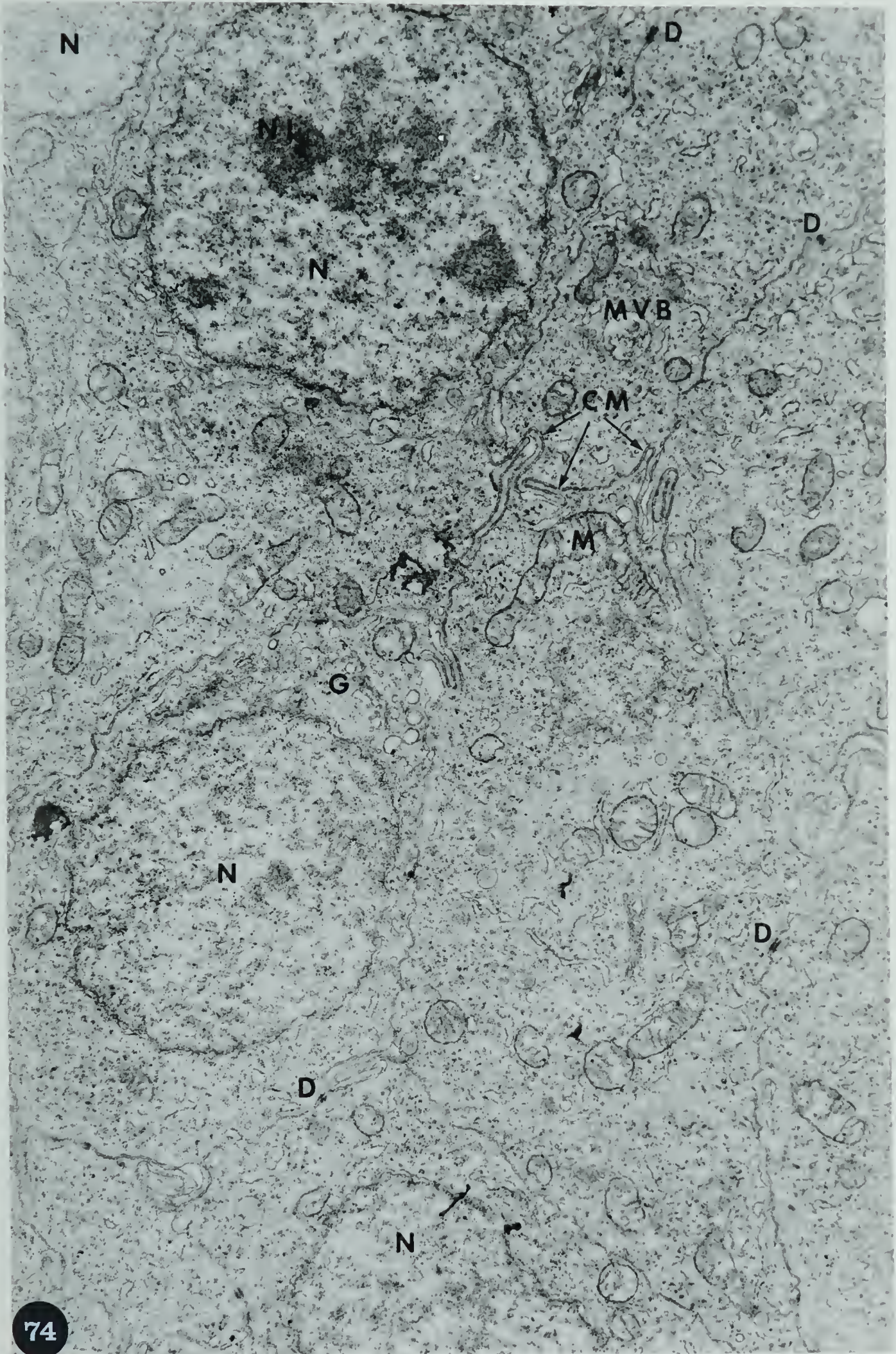


Fig. 75. Part of a cell of the urodeal membrane, near the lumen of the cloaca, showing a cytolysosome (CL) and clusters of ribosomes (R).
Osmium tetroxide, Araldite, and uranyl acetate.
X 45,000

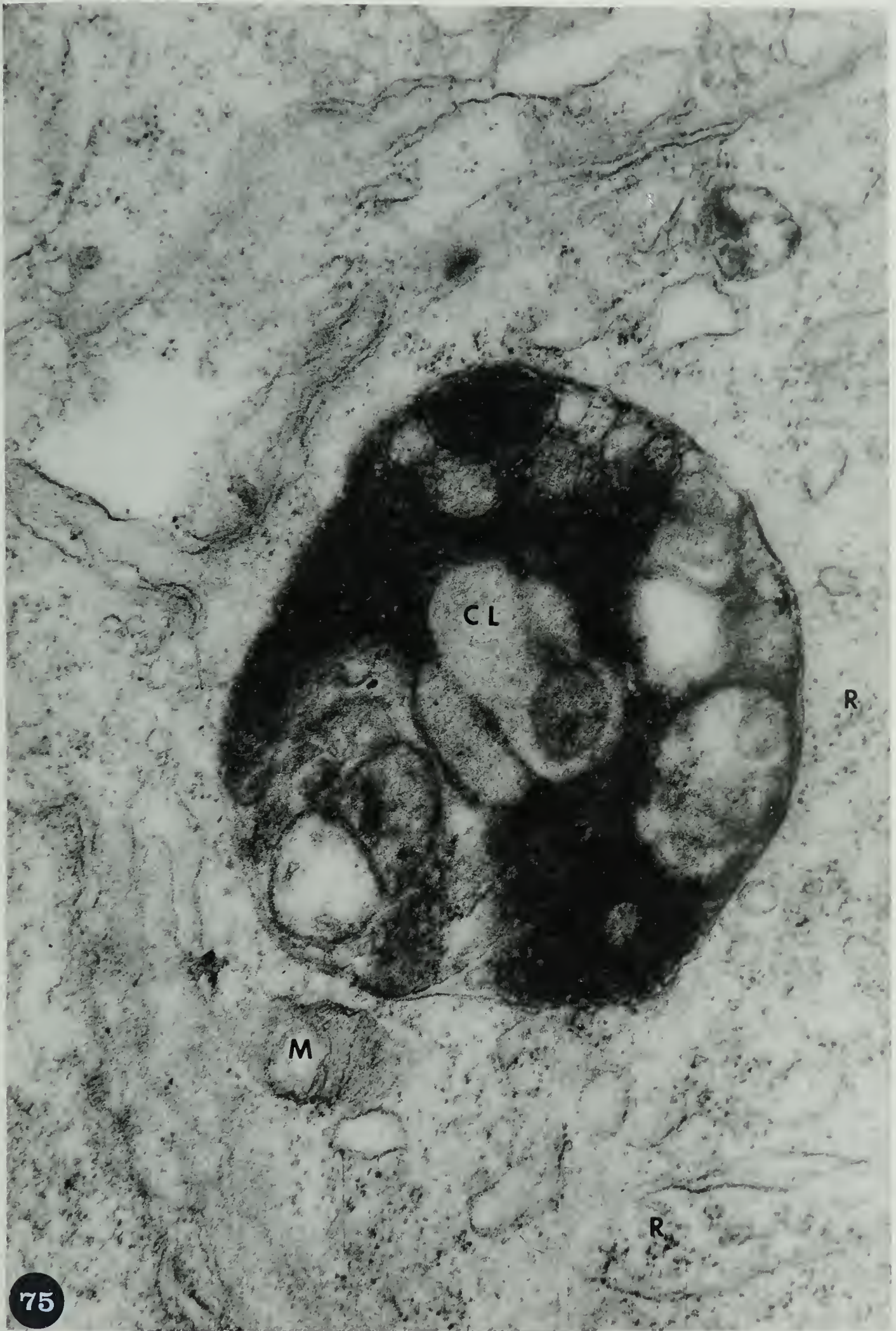


Fig. 76. Cells of the urodeal membrane adjacent to the mesenchyme. Note the elongate form of the cells. Swelling of the nuclear envelope is seen (thick arrow). Small vesicles seem to pinch off from the outer membrane of the nuclear envelope (thin arrow). This is an unstained section. The appearance of ribosomes is not so distinct as that seen in stained sections.

BM: basement membrane

NL: nuceolus

D: desmosome

M: mitochondrion

MB: microbody

L: lipid droplet

N: nucleus

MVB: multivesicular
body

Osmium tetroxide, Araldite, and unstained.

X 14,640

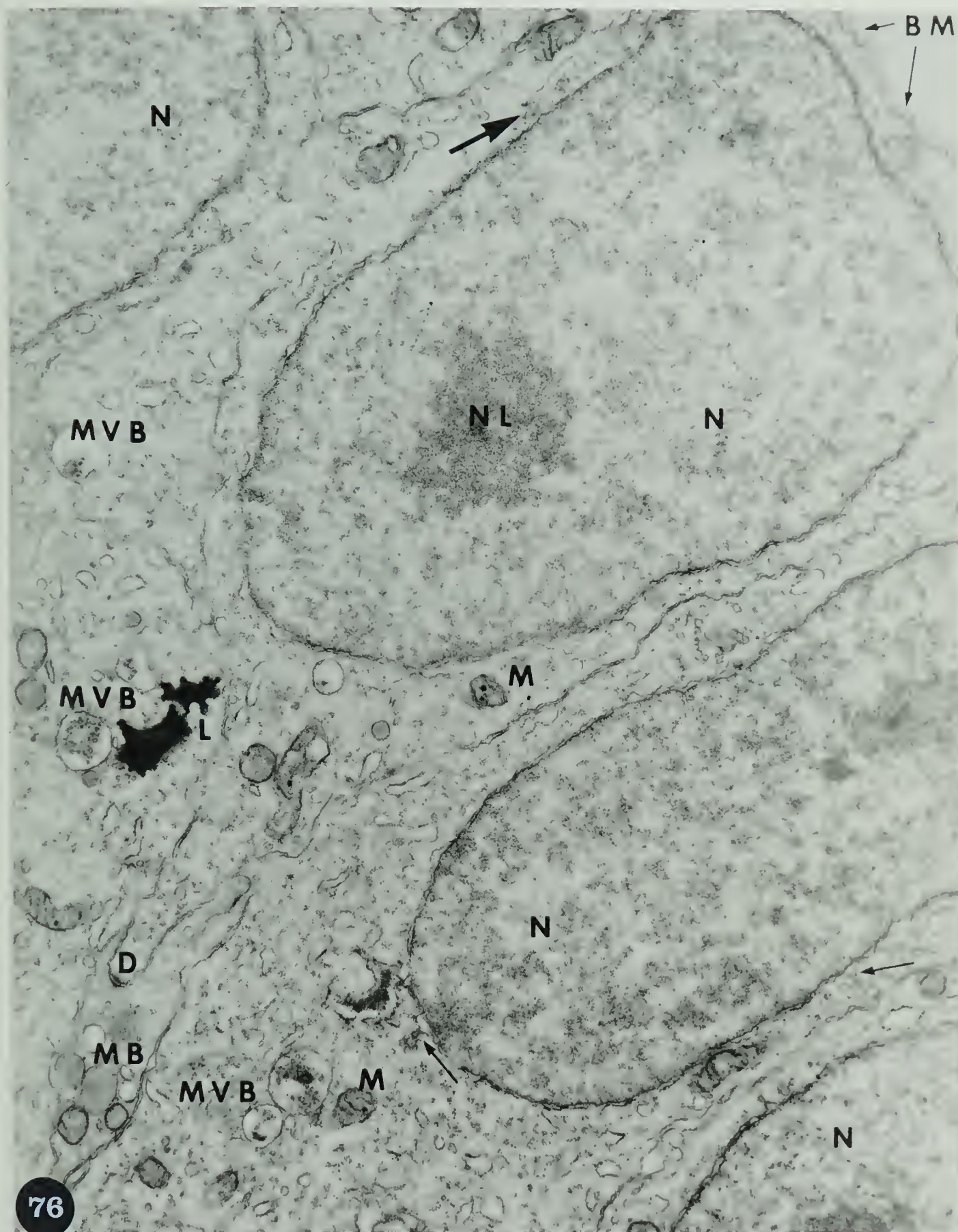


Fig. 77. A frontal section of a 13-day embryo showing the thymus lying along both sides of the neck. The acid phosphatase activity is low; the darkness of the thymus is due to the counterstain. Barka medium and counterstained with methyl green. X 10

Fig. 78. Part of the thymus illustrated in Fig. 77 showing scattered punctate acid phosphatase (see arrows). X 250



Fig. 79. The neck region of a 12-day embryo showing the thymus lying along the neck (a-f). Part of the thymus indicated by an arrow is illustrated at higher magnification in Fig. 80.

Barka medium, no counterstain.

X 10

Fig. 80. Part of the thymus shown in Fig. 79 illustrating punctate acid phosphatase activity in the mesenchyme and very little in the thymus.

X 250

Fig. 81. A frontal section of the neck region of an 11-day embryo to show the thymus lying along the neck (a-d). Part of the thymus indicated by an arrow is illustrated at higher magnification in Fig. 82.

Barka medium, no counterstain.

X 10

Fig. 82. Part of the thymus shown in Fig. 81 illustrating punctate acid phosphatase in the mesenchyme and very little in the thymus.

X 250

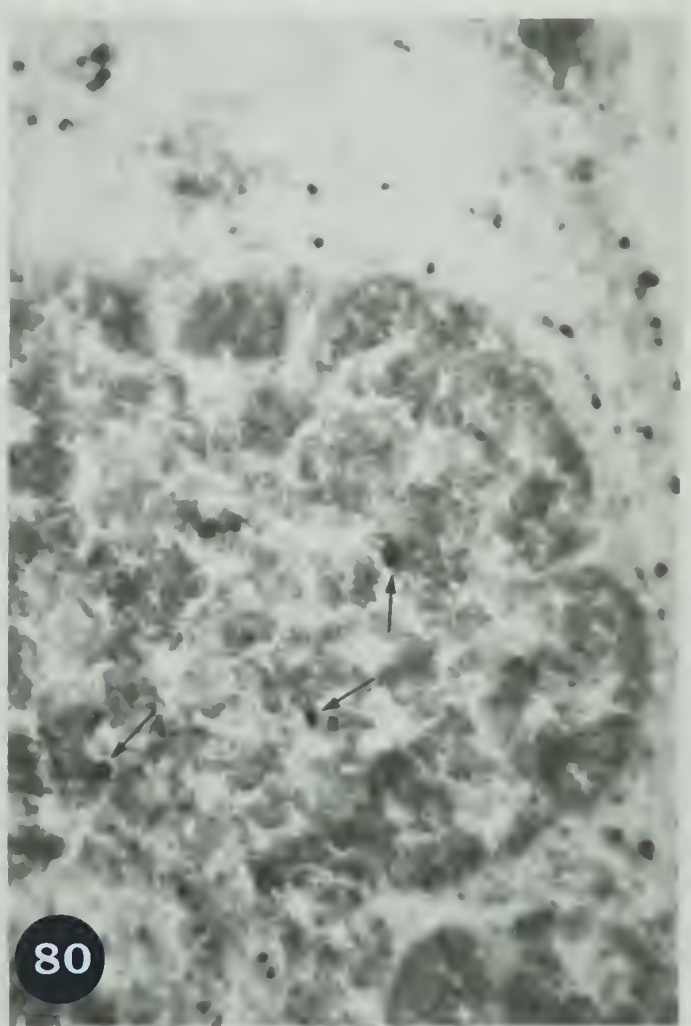
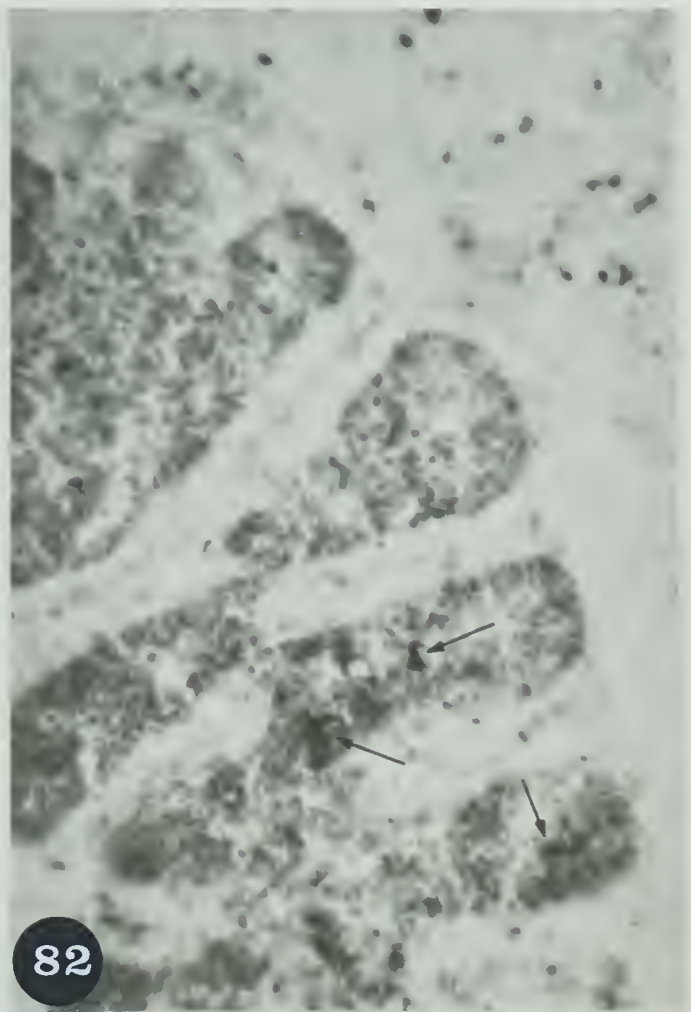
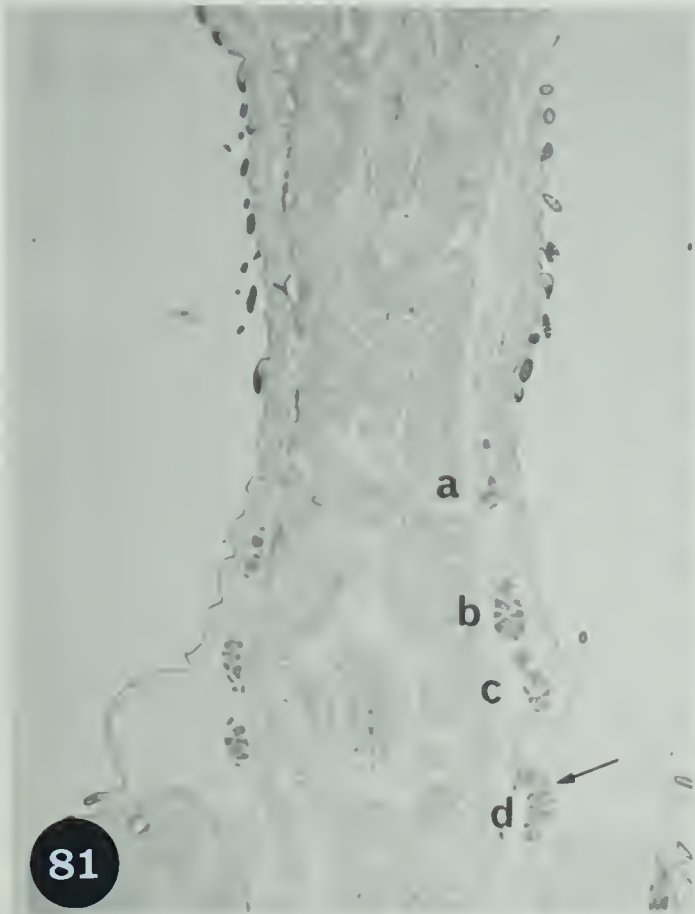


Fig. 83. A frontal section of the neck of a 10-day embryo showing three lobes of the thymus (a-c). Part of the thymus indicated by an arrow is shown at higher magnification in Fig. 84.

Barka medium, no counterstain. X 10

Fig. 84. Part of the thymus shown in Fig. 83 illustrating punctate acid phosphatase in the mesenchyme and very little in the thymus (see arrows).

X 250

Fig. 85. A frontal section of the neck region of an 8-day embryo to show the lobulation of the thymus (a-e). One lobe of the thymus indicated by an arrow is shown at higher magnification in Fig. 86.

Barka medium, no counterstain.

X 10

Fig. 86. Part of the thymus shown in Fig. 85 illustrating punctate acid phosphatase in the mesenchyme and very little in the thymus. The figure shows the thymus at an incipient stage of lymphopoiesis when it has just begun to lobulate. The upper lobules appear more epithelial and the lower appear more lymphoidal.

X 250

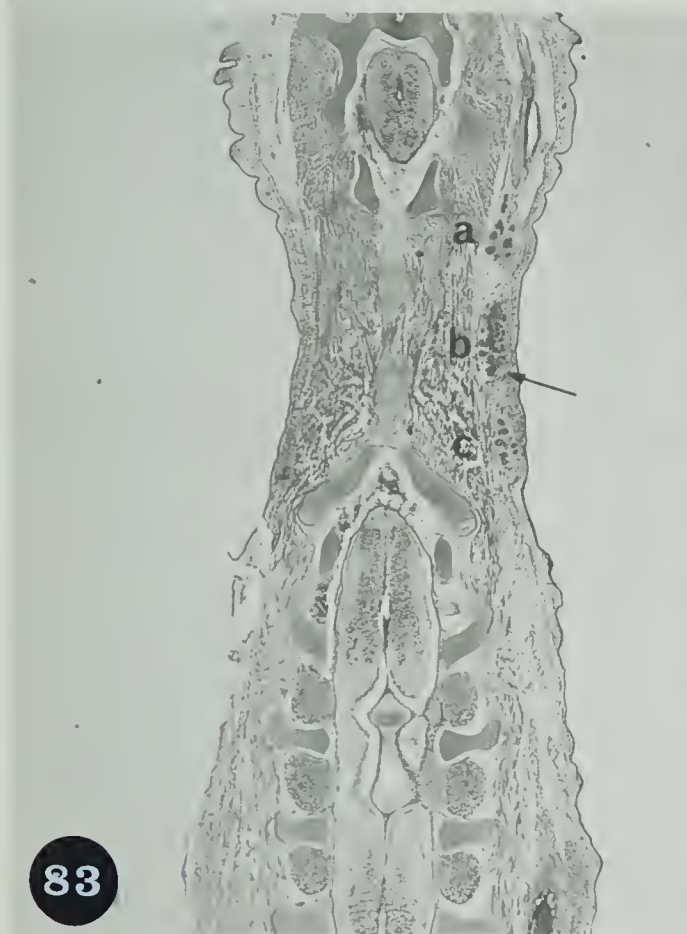
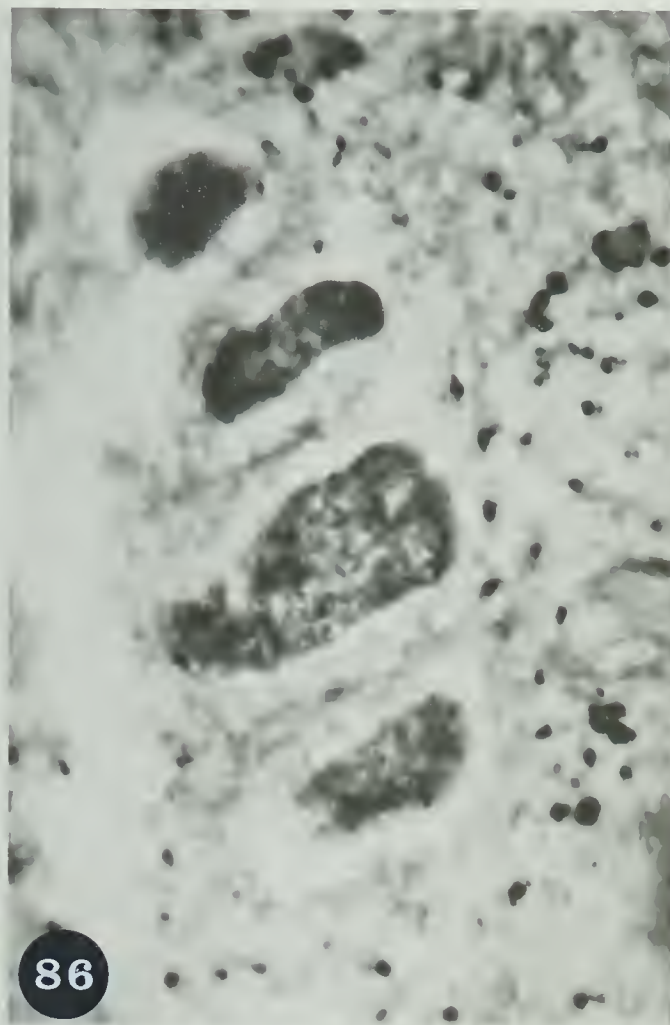
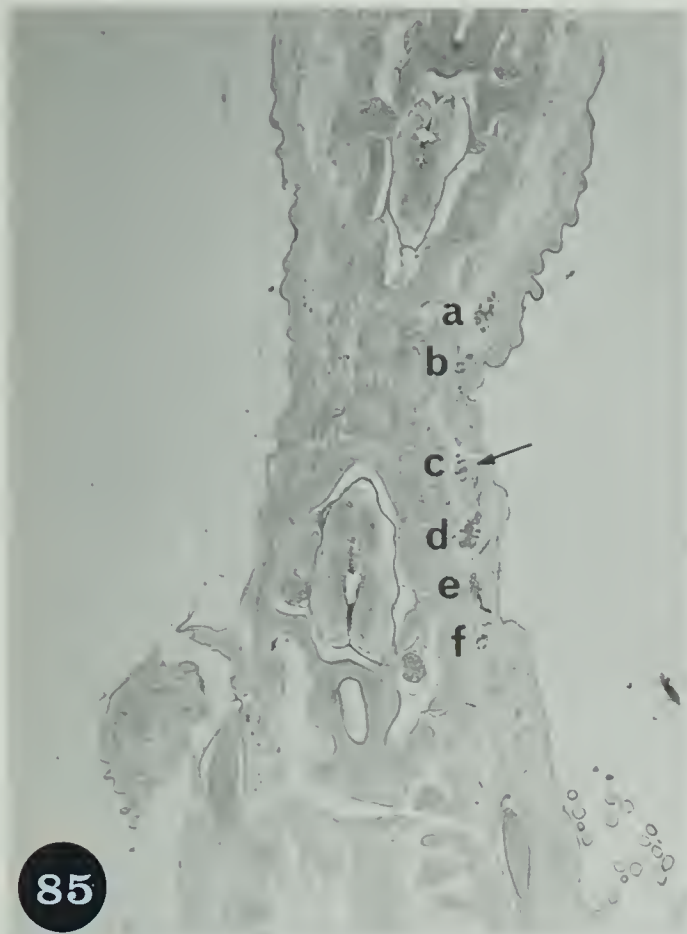


Fig. 87. A frontal section of the neck region of the 7-day embryo showing the slender thymus primordium (indicated by two arrows) which is illustrated at higher magnification in Fig. 88.

Frozen section and methylene blue staining.

X 10

Fig. 88. A part of Fig. 87 showing the slender thymus primordium (TH) at higher magnification.

X 250

Fig. 89. A frontal section of the 6-day embryo showing the thymus primordia (arrow) which is illustrated at higher magnification in Fig. 90.

Barka medium, no counterstain.

X 10

Fig. 90. Thymus III (TH3) and Thymus IV (TH4) show intense acid phosphatase activity. Punctate activity is present in the mesenchyme.

AA3: third aortic arch

AA4: fourth aortic arch

TH3: Thymus III

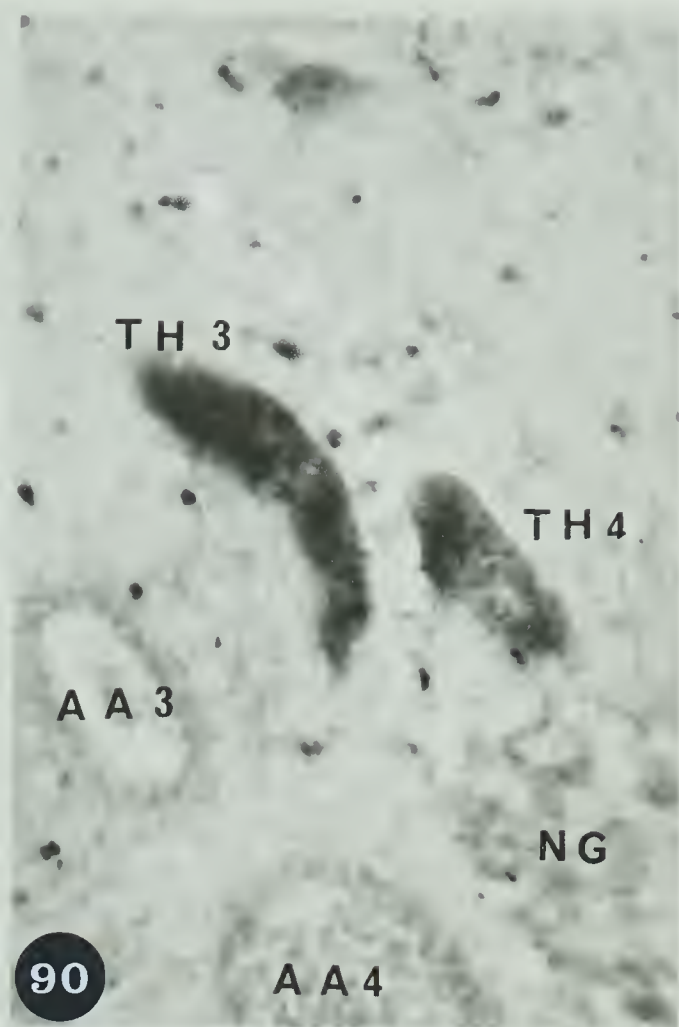
TH4: Thymus IV

NG: nodosal ganglion

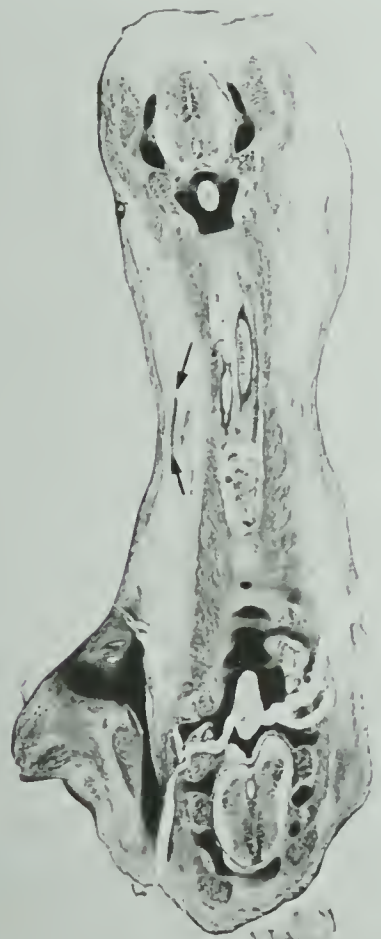
X 250



89



90



87



88

Fig. 91. A diagram of a representative section through the branchial region of a 5-day embryo. The series of photomicrographs of Figs. 92-94 are taken from the area indicated by the rectangle.

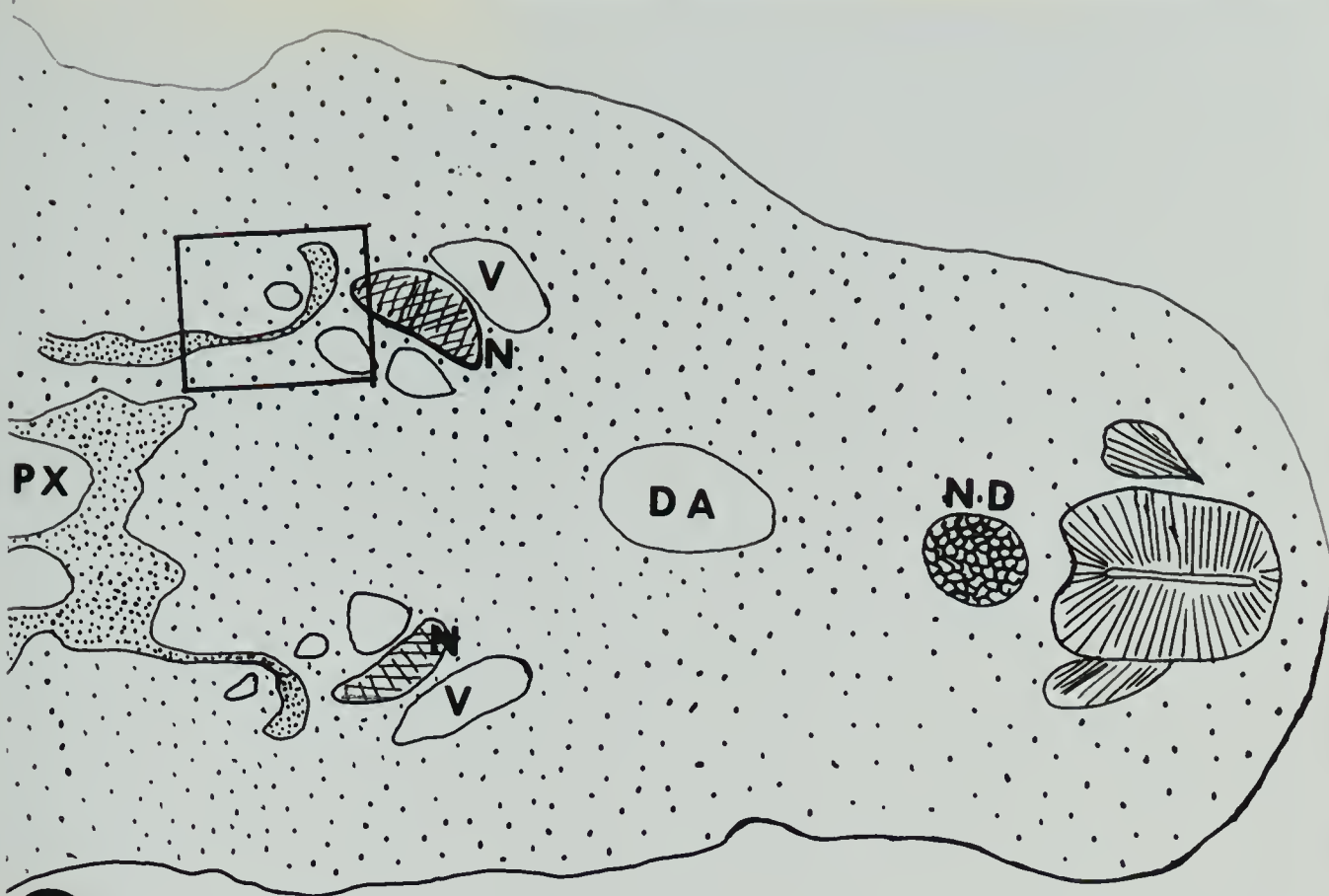
| | |
|--------------------|---------------|
| DA: dorsal aorta | PX: pharynx |
| N: nodose ganglion | ND: notochord |
| V: jugular vein | |

X 60

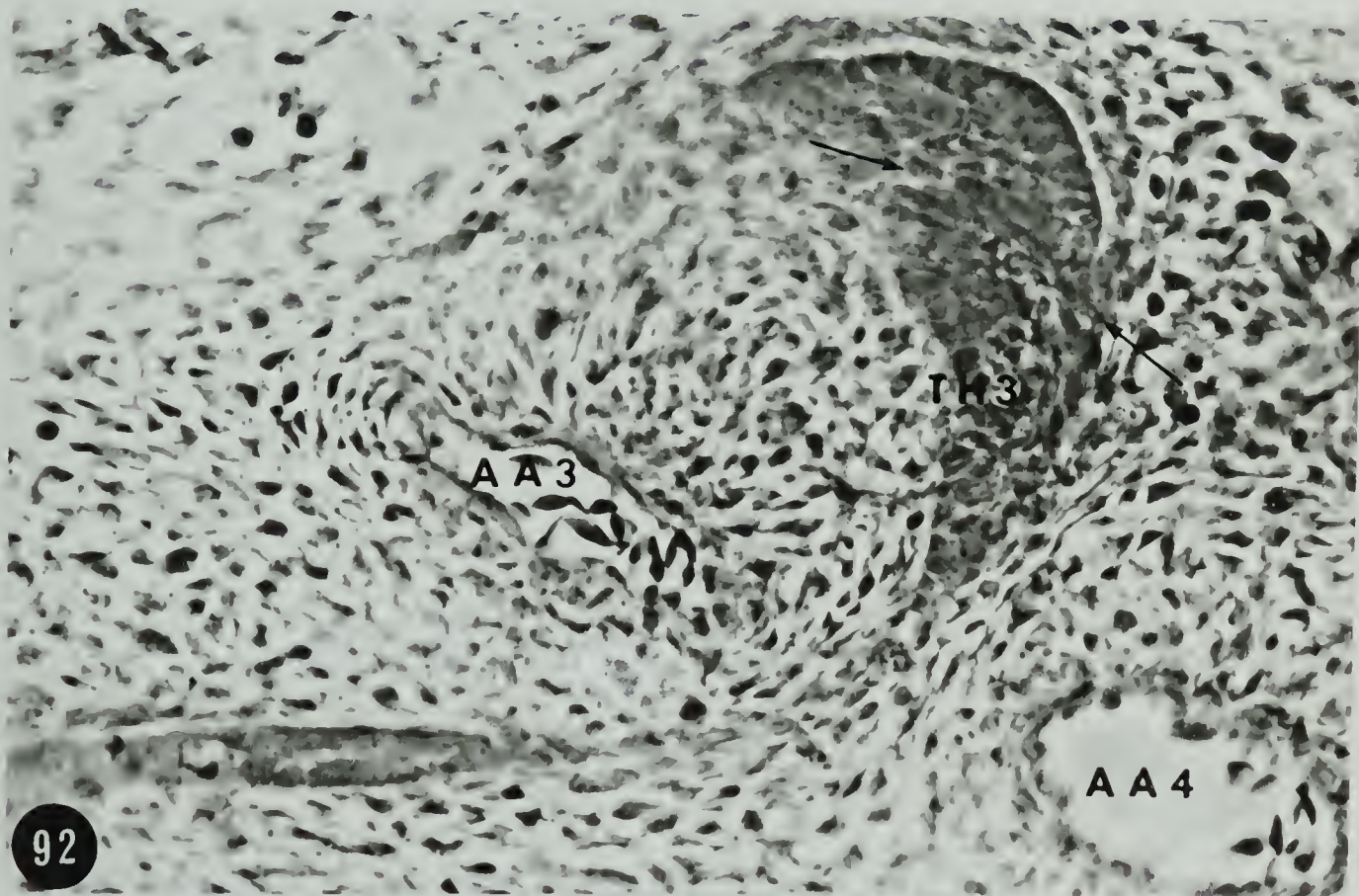
Figs. 92-94. A series of phase contrast photomicrographs taken from serial frontal sections through the branchial region of a 5-day chick embryo, arranged in a dorsoventral sequence. Visible parts of the thymus primordium are a dorsolateral part (TH3) of the third pharyngeal pouch, and its appended ectoderm, and a dorsolateral part (TH4) of the fourth pharyngeal pouch. The epithelial tissue above the arrows is branchial ectoderm.

| |
|-------------------------|
| AA3: third aortic arch |
| AA4: fourth aortic arch |

X 405



91



92

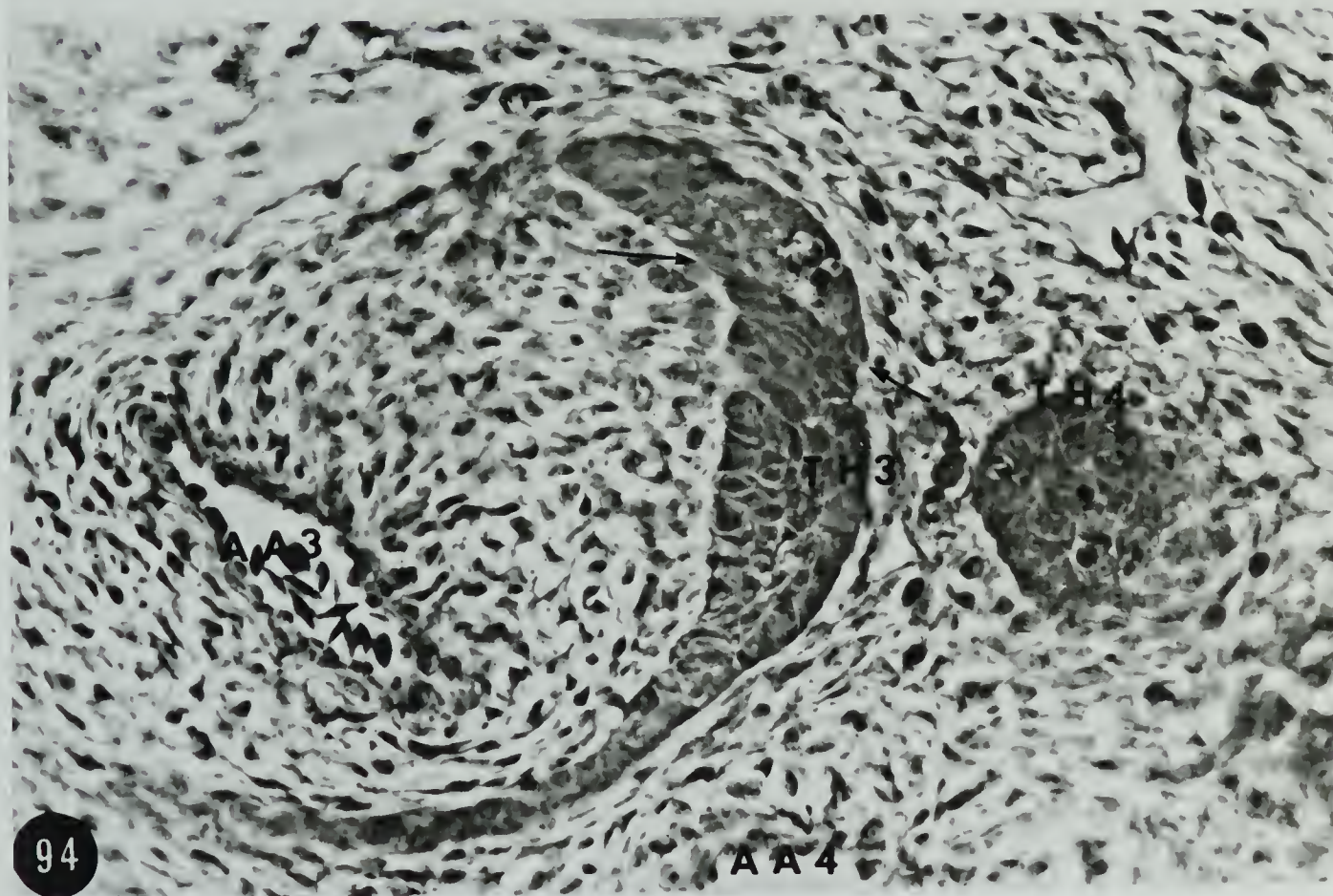
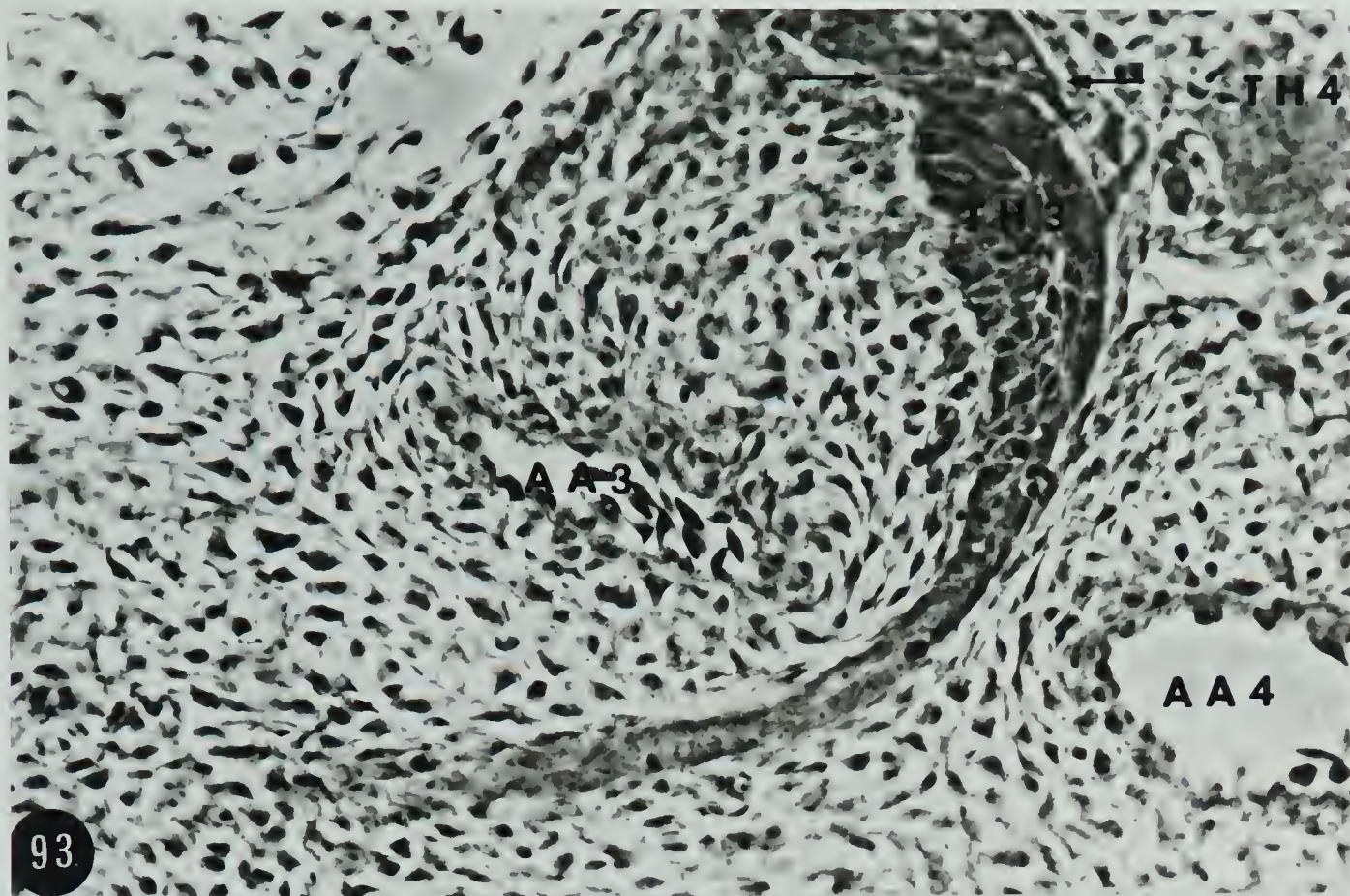


Fig. 95. A diagram of a representative frontal section through the branchial region of a 11-4 hour embryo. The rectangle indicates the location of the series of photomicrographs, Figs. 96-98, and 102-108.

DA: dorsal aorta

PX: pharynx

V: jugular vein

X 40

Figs. 96-98. Phase contrast photomicrographs taken in dorsoventral sequence. The endodermal primordium of Thymus III is seen in Fig. 96. The lumen of a third pharyngeal pouch extends into the dorsal protrusion of the pouch (PH3) (Figs. 97 and 98).

AA3: third aortic arch

PH3: Pharyngeal Pouch III

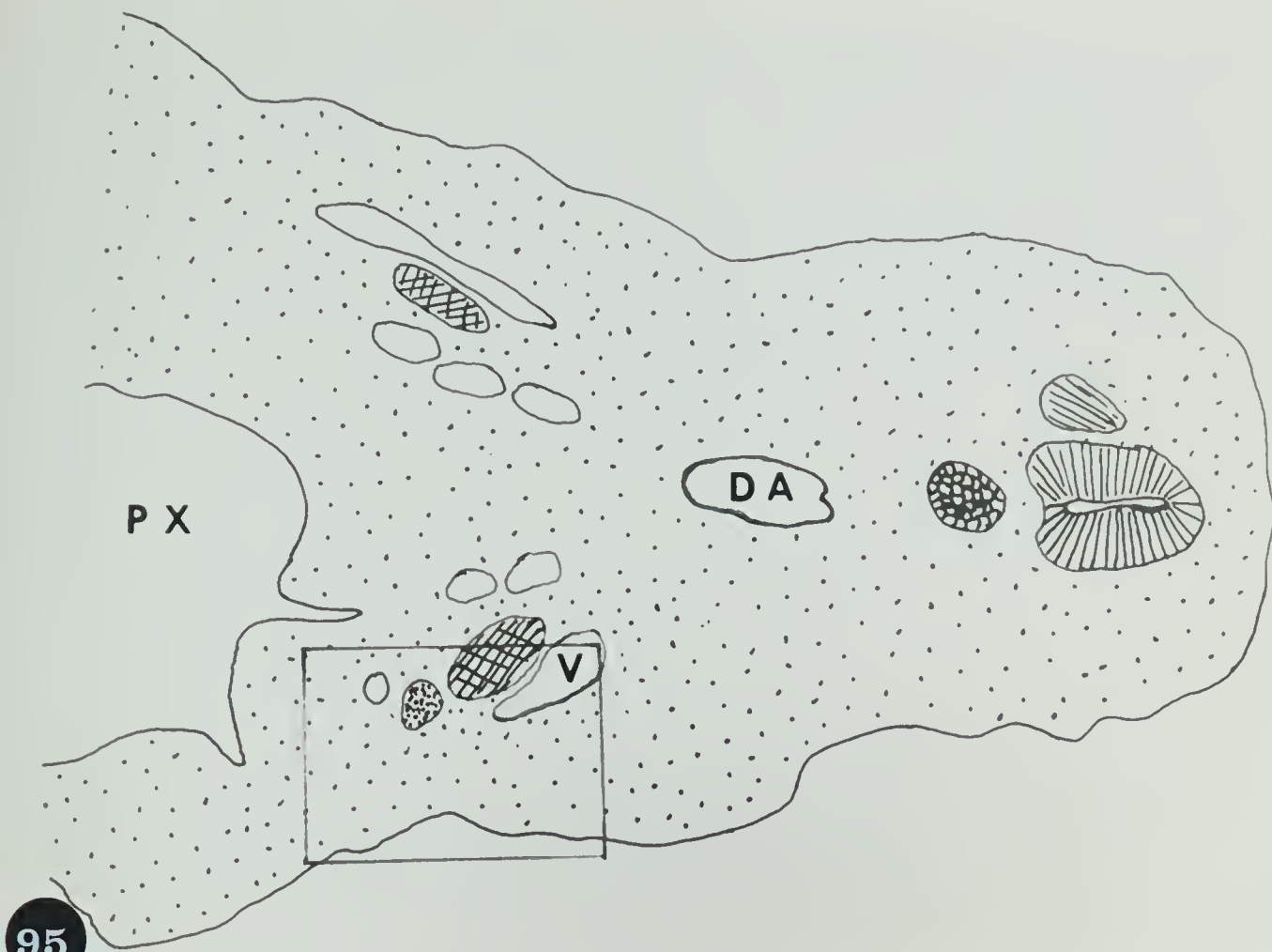
NG: nodosal ganglion

TH3: Thymus III

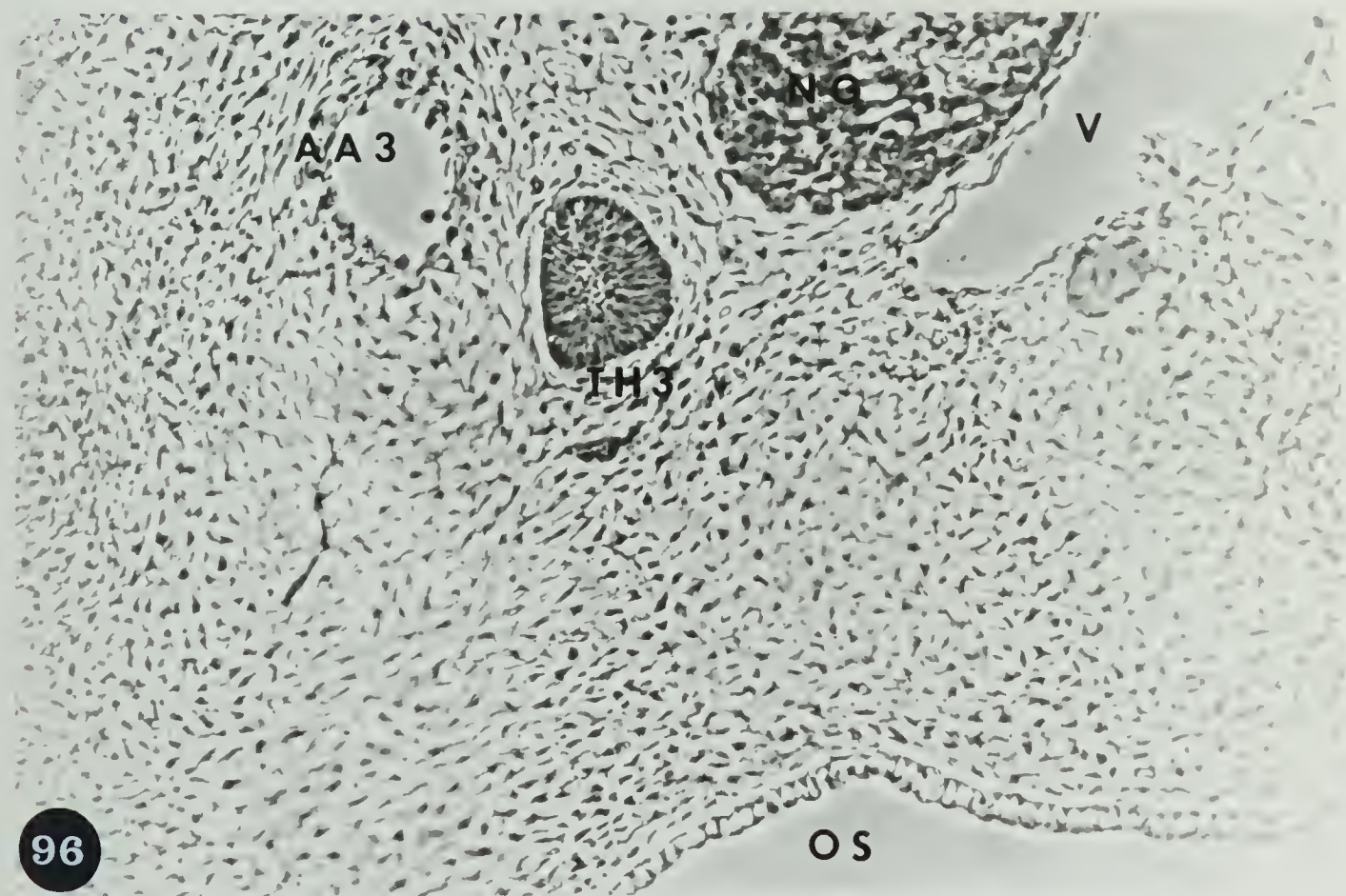
OS: external body surface

V: jugular vein

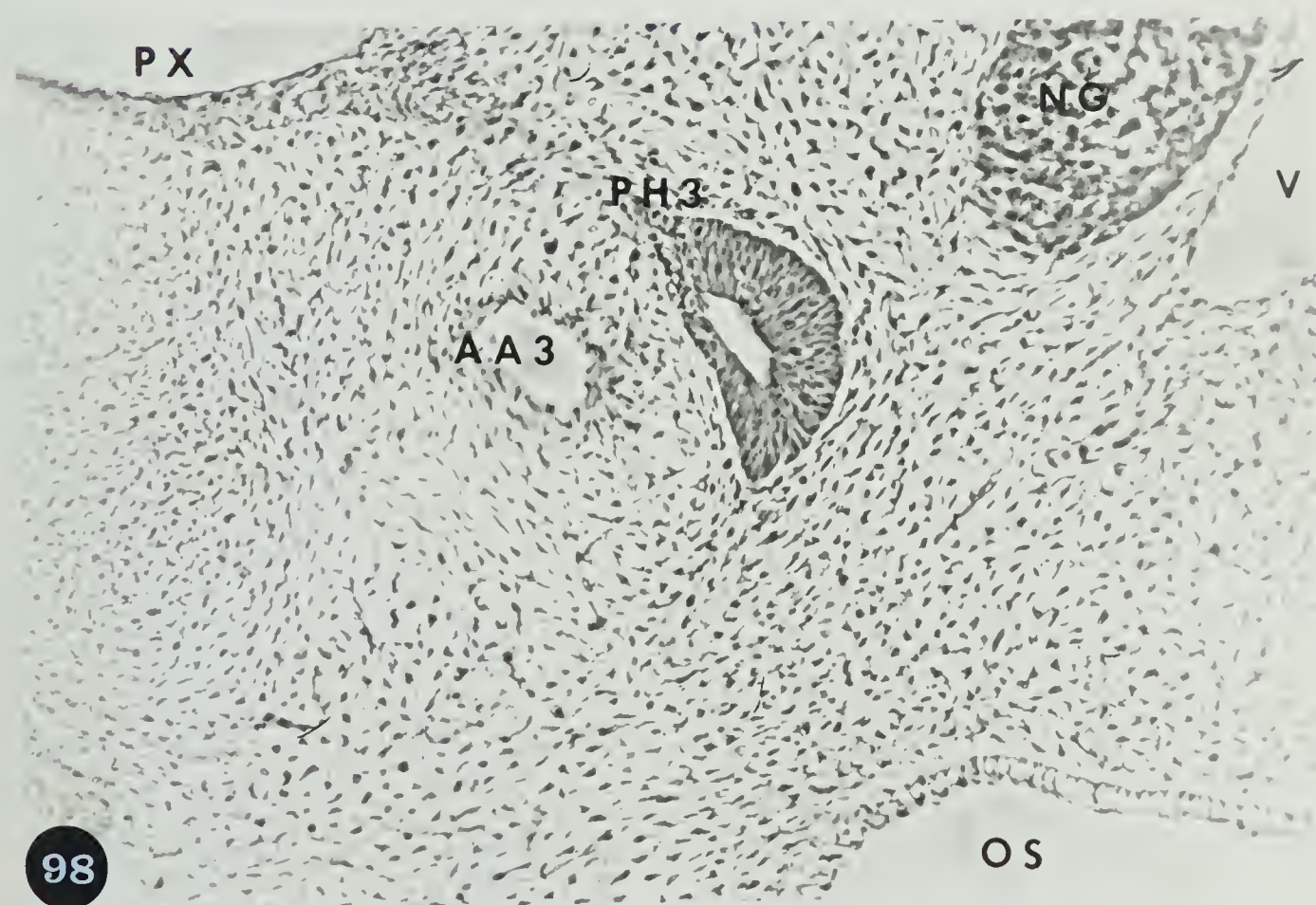
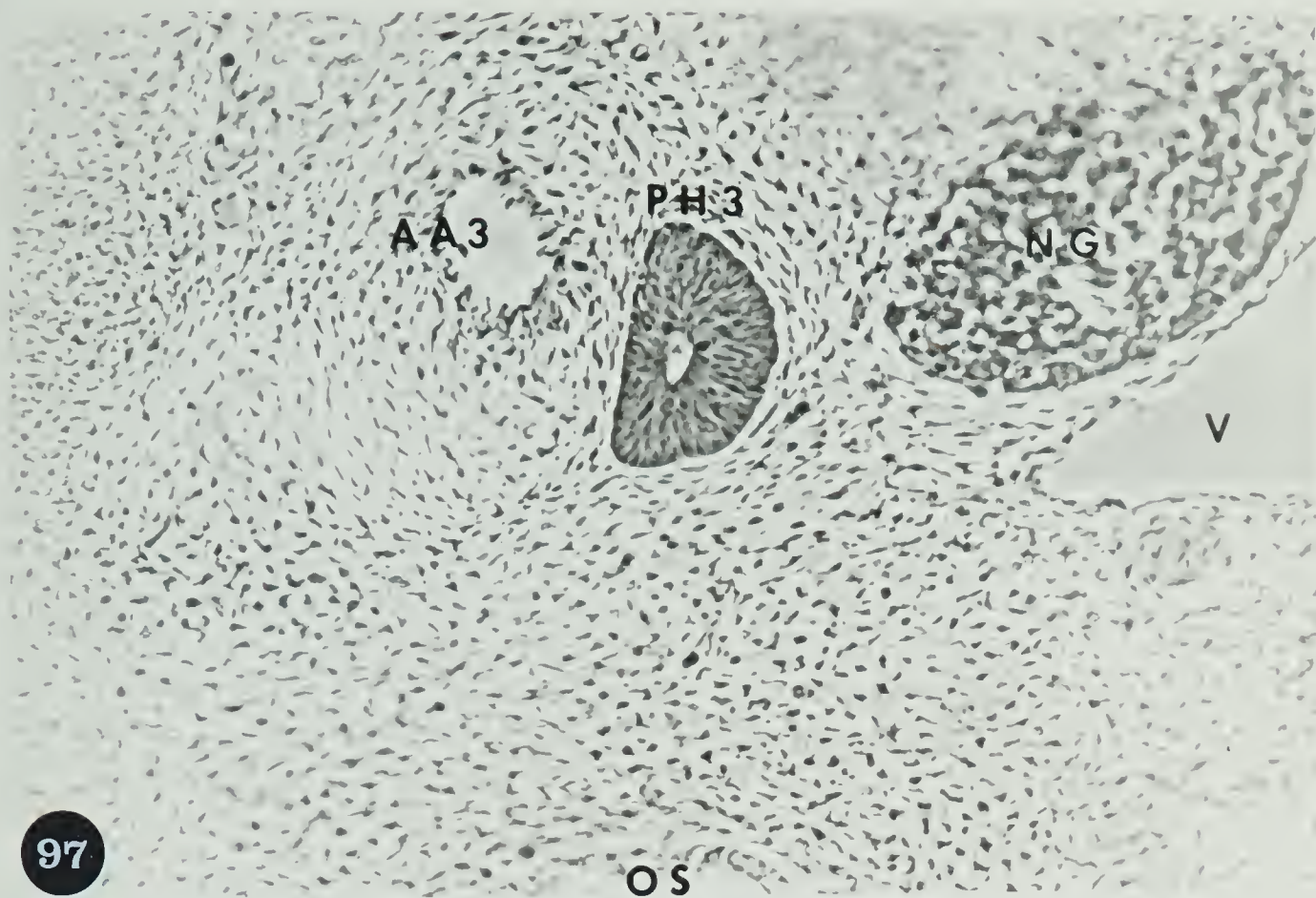
X 198



95

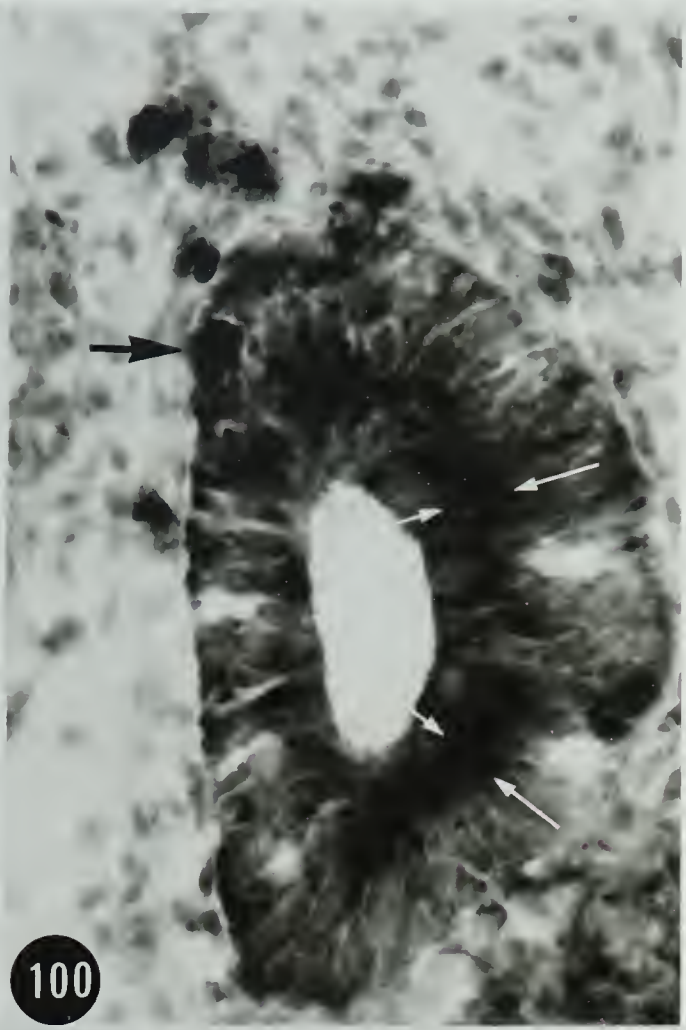
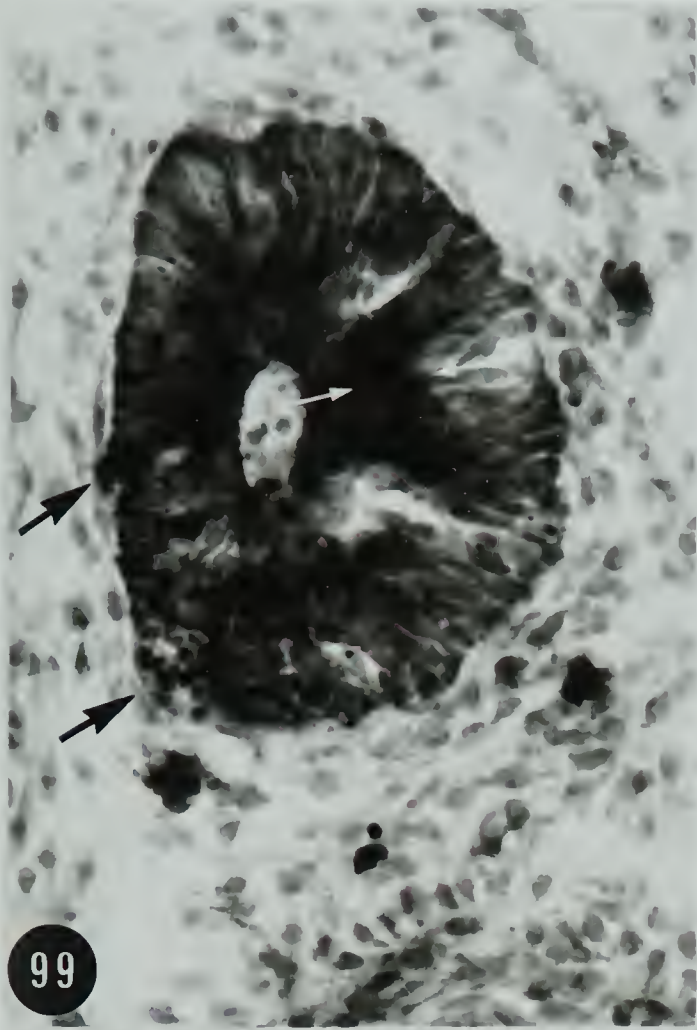


96



Figs. 99 and 100. Pharyngeal Pouch III at the base of the endodermal primordium of the thymus of a 5-day embryo. Acid phosphatase activity is intense in the epithelial cells, and forms a band around the lumen (white arrows). Intensely reactive extrusions (black arrows) are thought to represent debris and dead epithelial cells. Barka medium, no counterstain. X 580

Fig. 101. Pharyngeal Pouch III of a 5-day embryo in contact with its Ectobranchial Groove III (ED3). Both epithelia have high activity. Barka medium, no counterstain. X 580



Figs. 96-98 and 102-108. A series of phase contrast photomicrographs taken from serial frontal sections of the branchial region of a 114 hour embryo, arranged in a dorso-ventral sequence. The primordium of Thymus III is seen in Fig. 96. The lumen of the third pharyngeal pouch extends into the dorsal protrusion of the pouch (PH3) (Figs. 97 and 98). The contact of the dorsal part of the third pharyngeal pouch (PH3) and the third ectobranchial duct (ED3) is shown in Fig. 103. Figs. 104 and 105 show the solid form of the ventral part of the third pharyngeal pouch (PH3) in contact or fusing with the ectobranchial duct. Figs. 106-108 show the dorsal part of the fourth pharyngeal pouch coming into contact with the fourth ectobranchial duct. Many degenerating cells are recognizable in the branchial ectoderm and the pouch.

AA3: third aortic arch

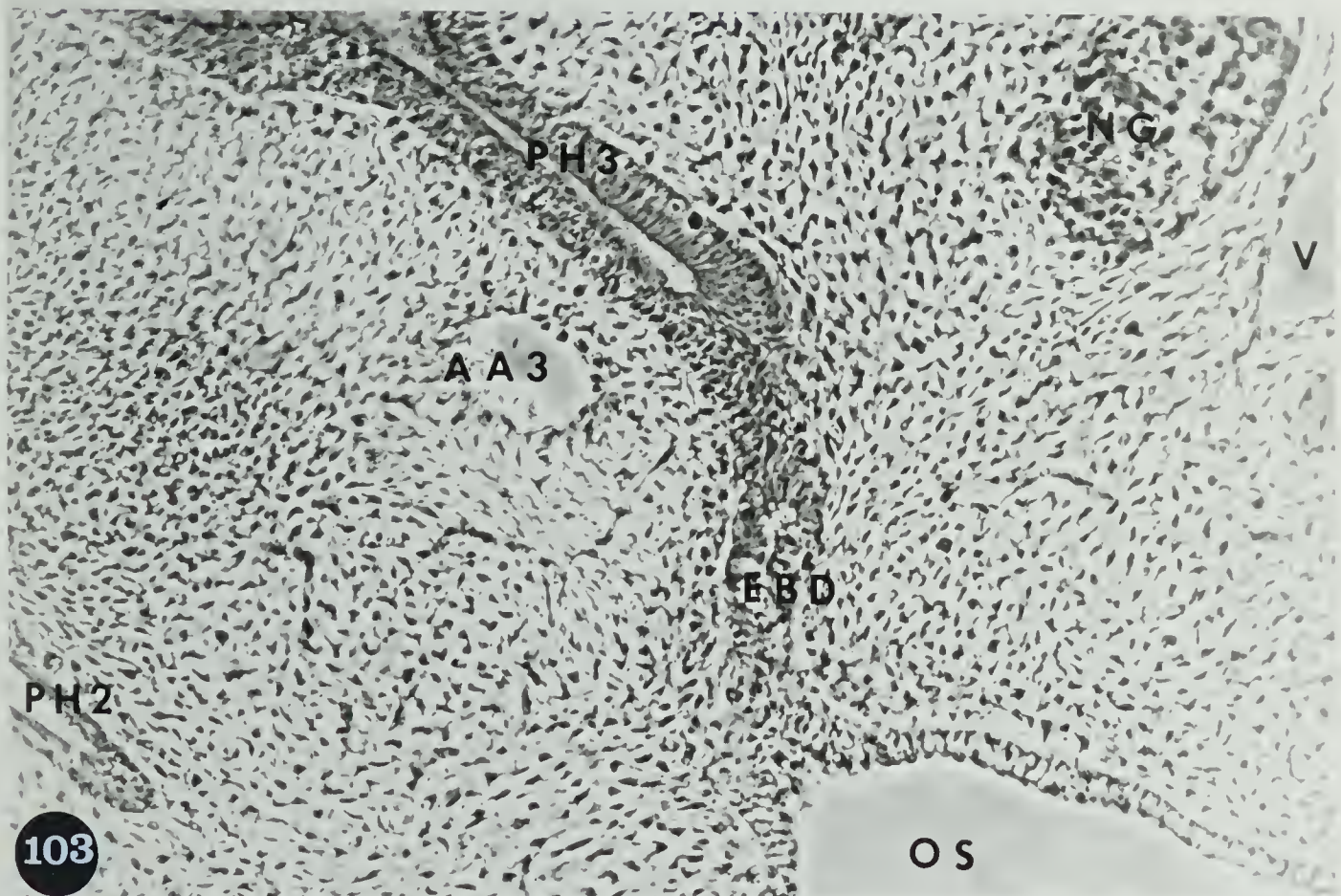
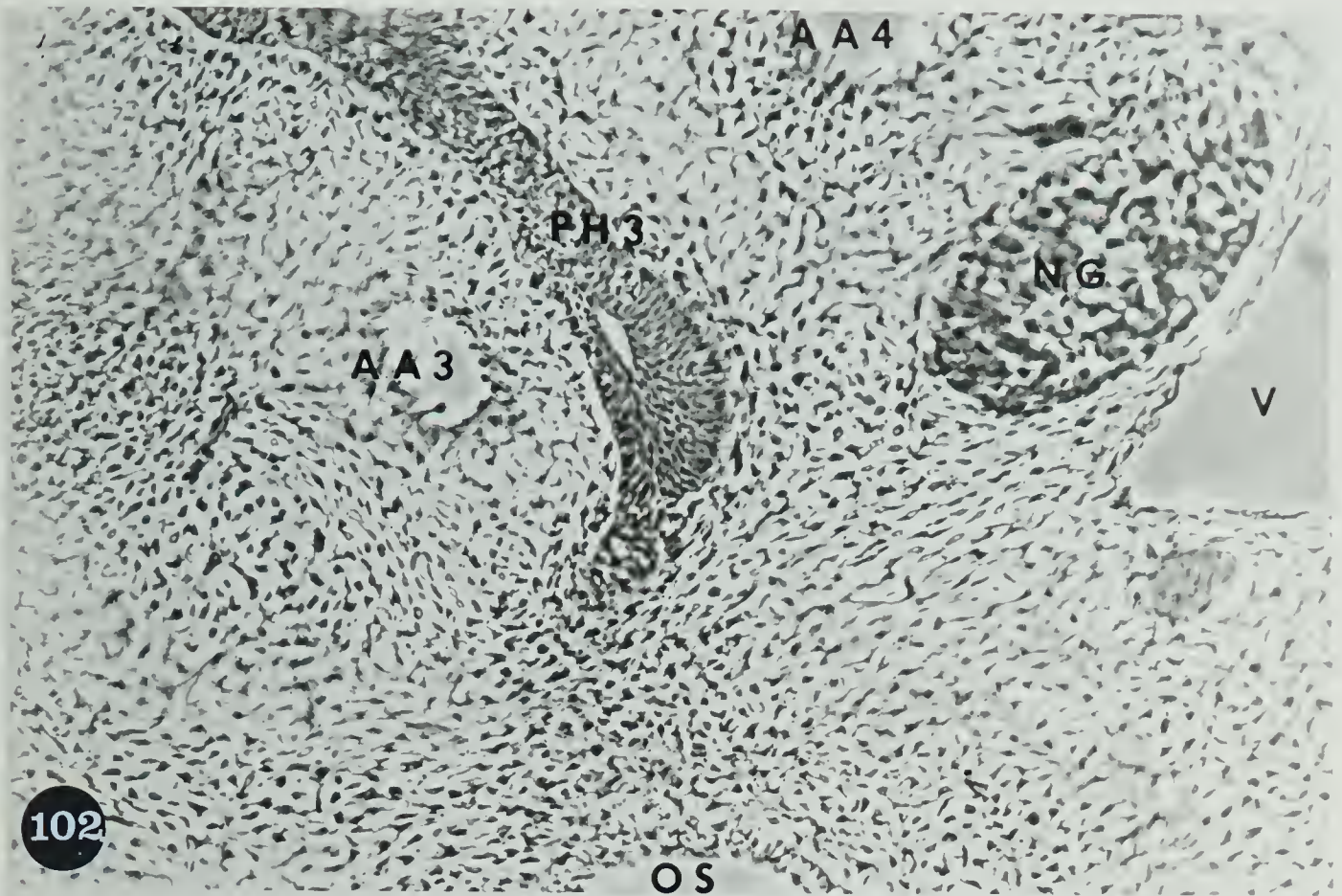
NG: nodosal ganglion

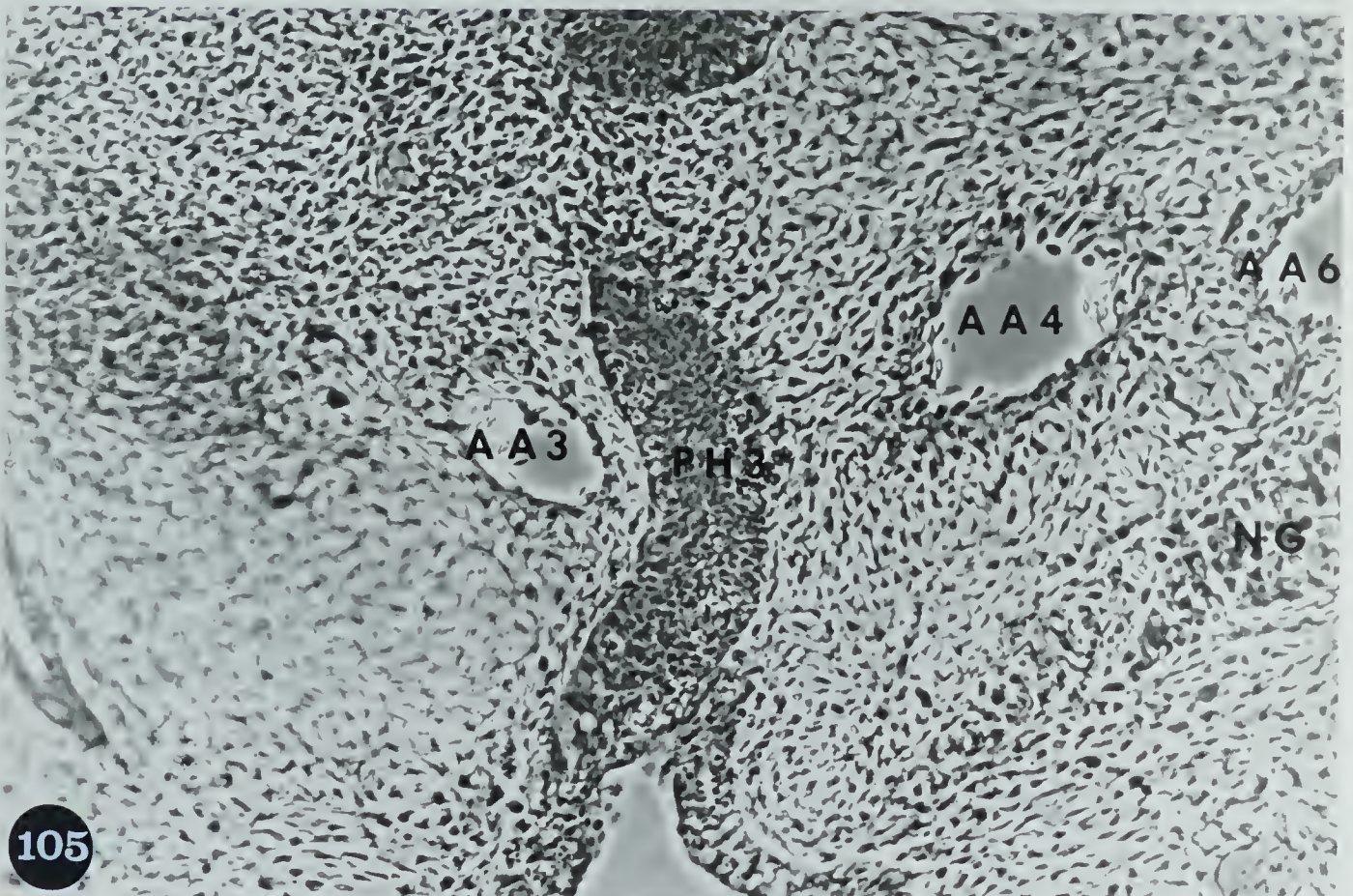
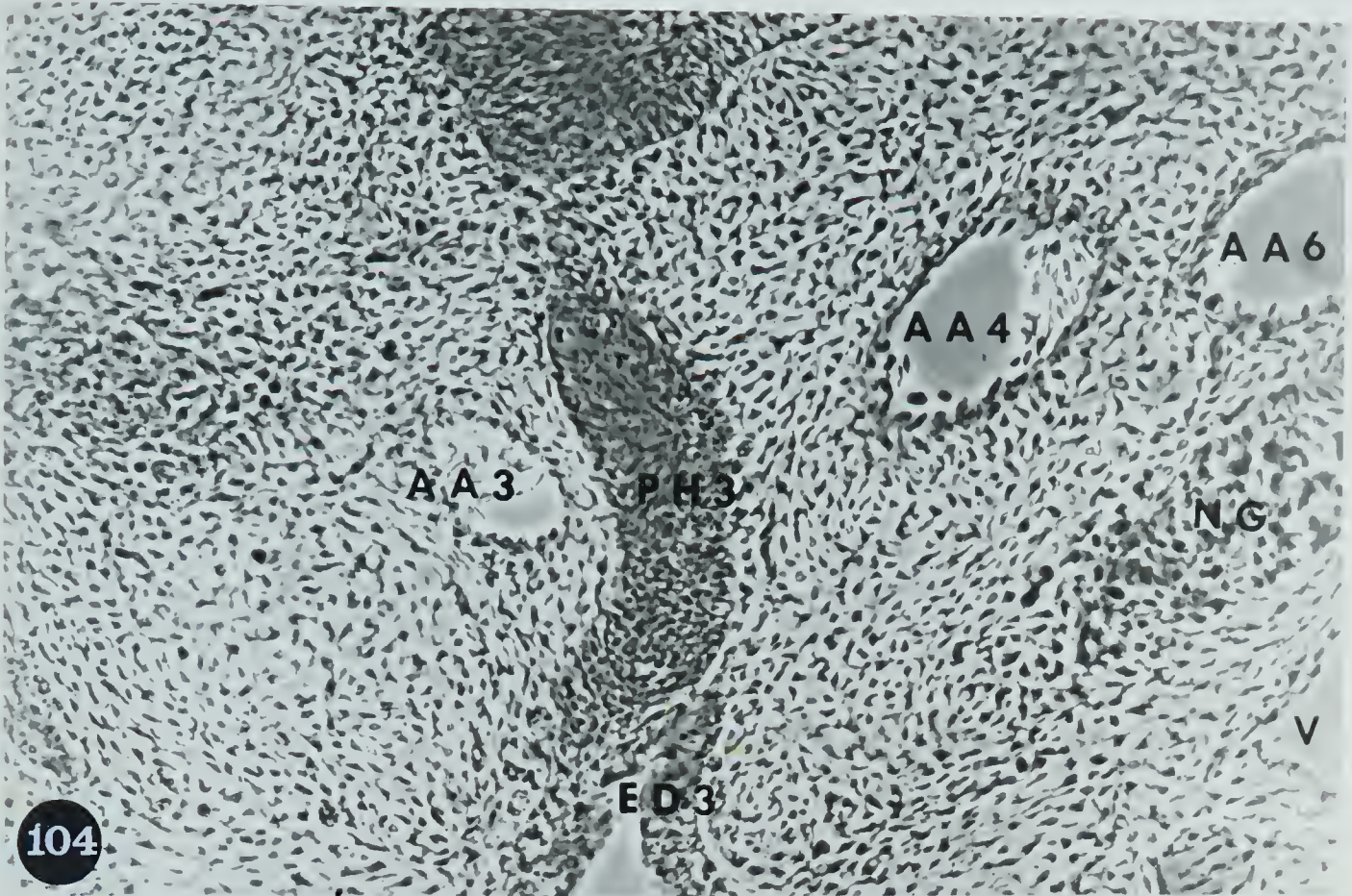
OS: outside the body surface

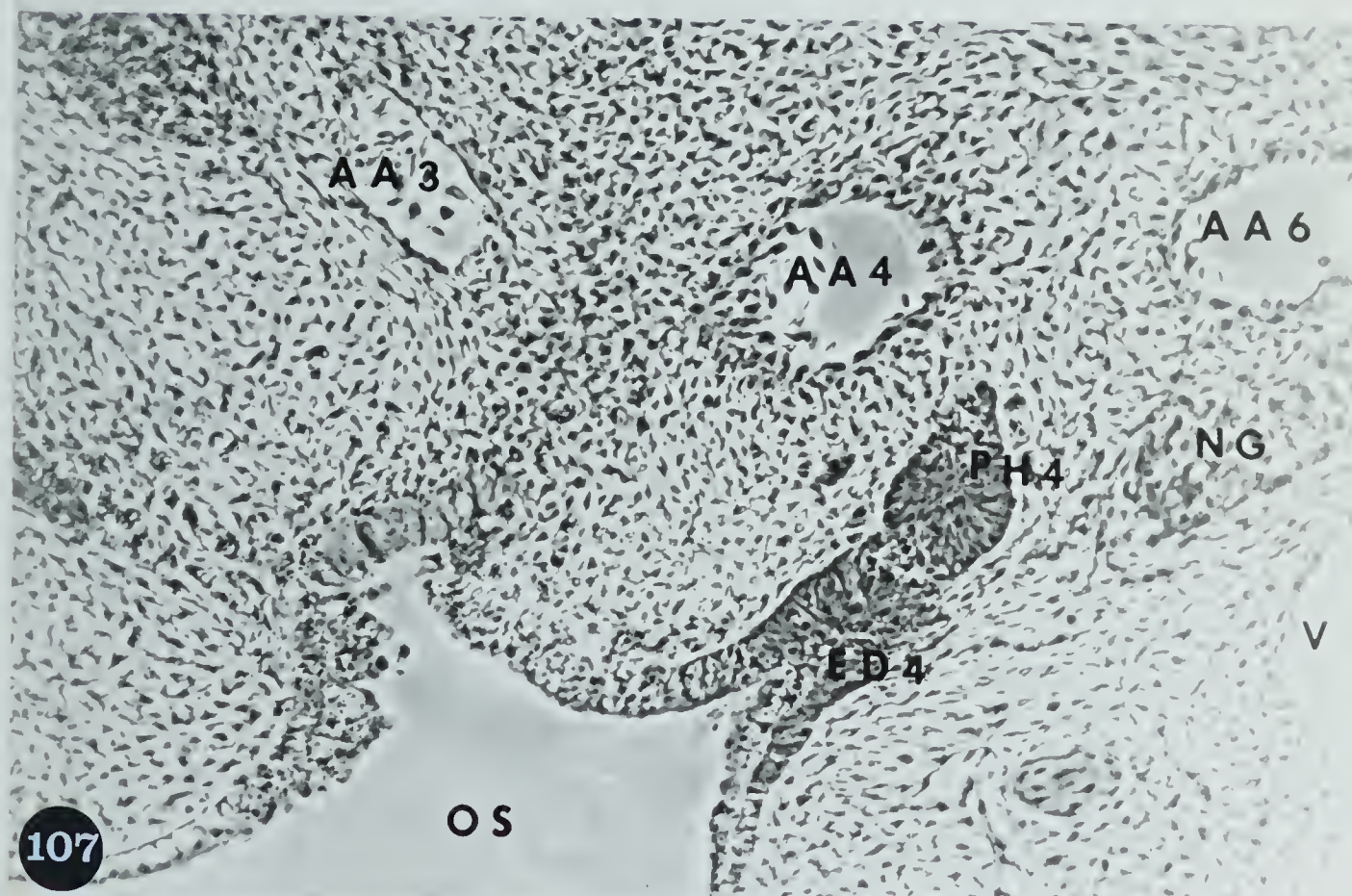
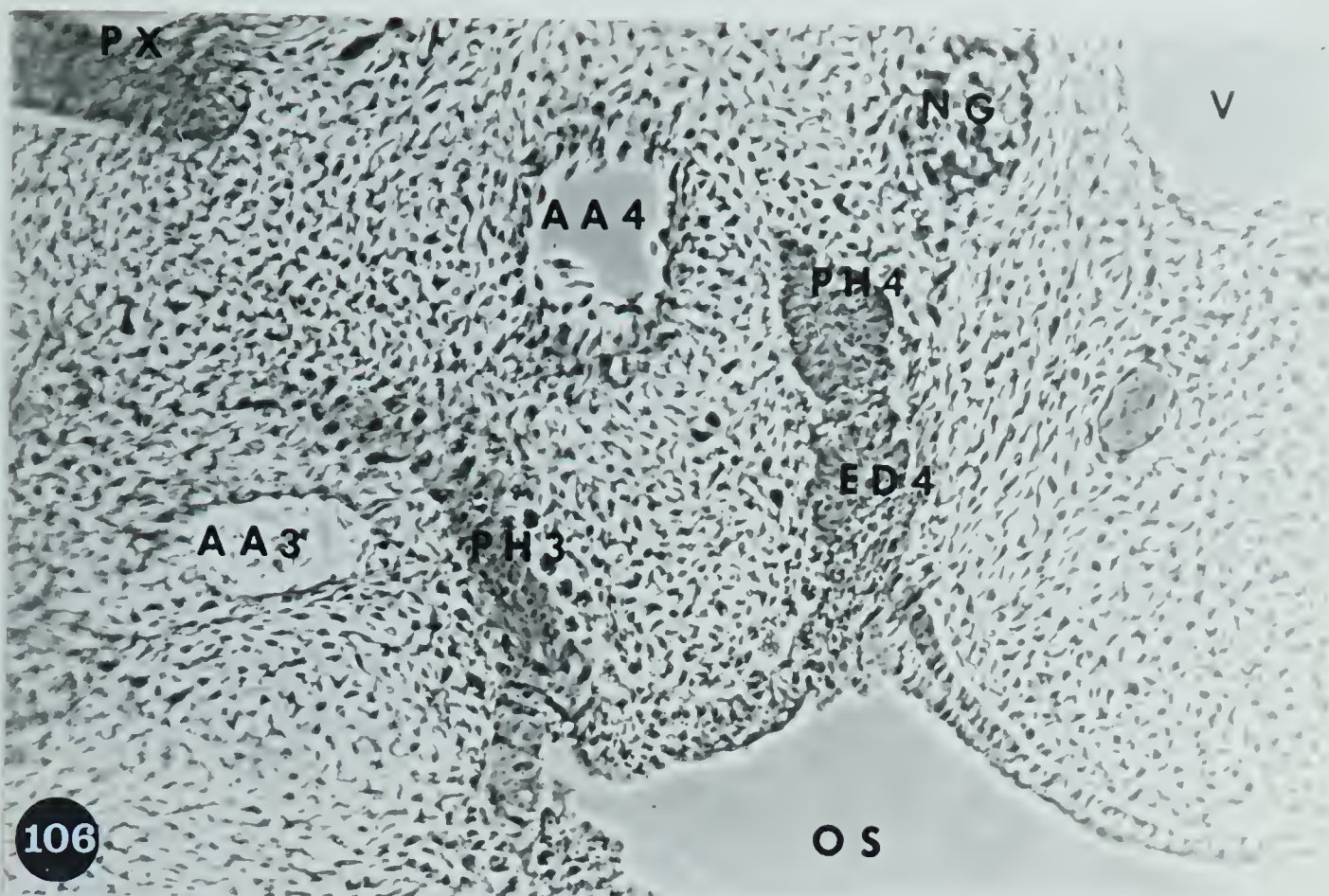
PH3: third pharyngeal pouch

TH3: Thymus III

V: jugular vein







Figs. 102-108. A series of phase contrast photomicrographs taken from serial frontal sections of the branchial region of a 114 embryo, arranged in a dorsoventral sequence. The contact of the dorsal part of Pharyngeal Pouch III (PH3) and the Ectobranchial Duct III (ED3) is shown in Fig. 103. Figs. 104 and 105 show the solid lateral extension of the ventral part of the Pharyngeal Pouch III (PH3) in contact with the ectobranchial duct. Figs. 106-108 show the dorsal part of the Pharyngeal Pouch IV in contact with the Ectobranchial Duct IV. Many degenerating cells are recognizable in the branchial ectoderm and the pouch.

| | |
|---------------------------|-----------------|
| AA3: third aortic arch | PH3: Pharyngeal |
| NG: nodosal ganglion | Pouch III |
| OS: external body surface | TH3: Thymus III |
| V: jugular vein | |

X 198

Fig. 109. Higher magnification of the section following that illustrated in Fig. 102. It shows the degenerating cells in the pouch.

| | |
|-----------------------|---------------------------|
| DC: degenerating cell | PH3: Pharyngeal Pouch III |
| PX: pharynx | |

X 405

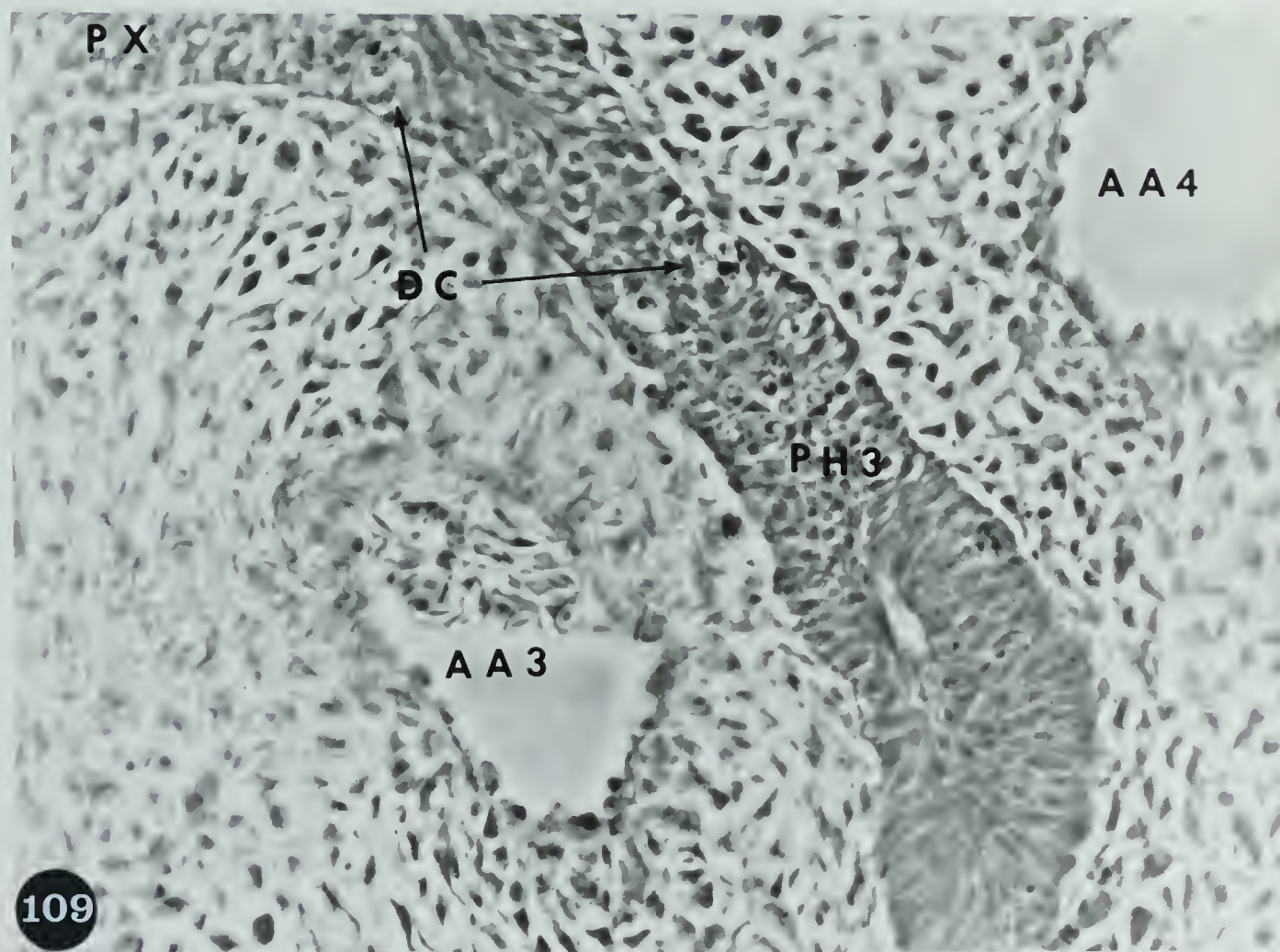
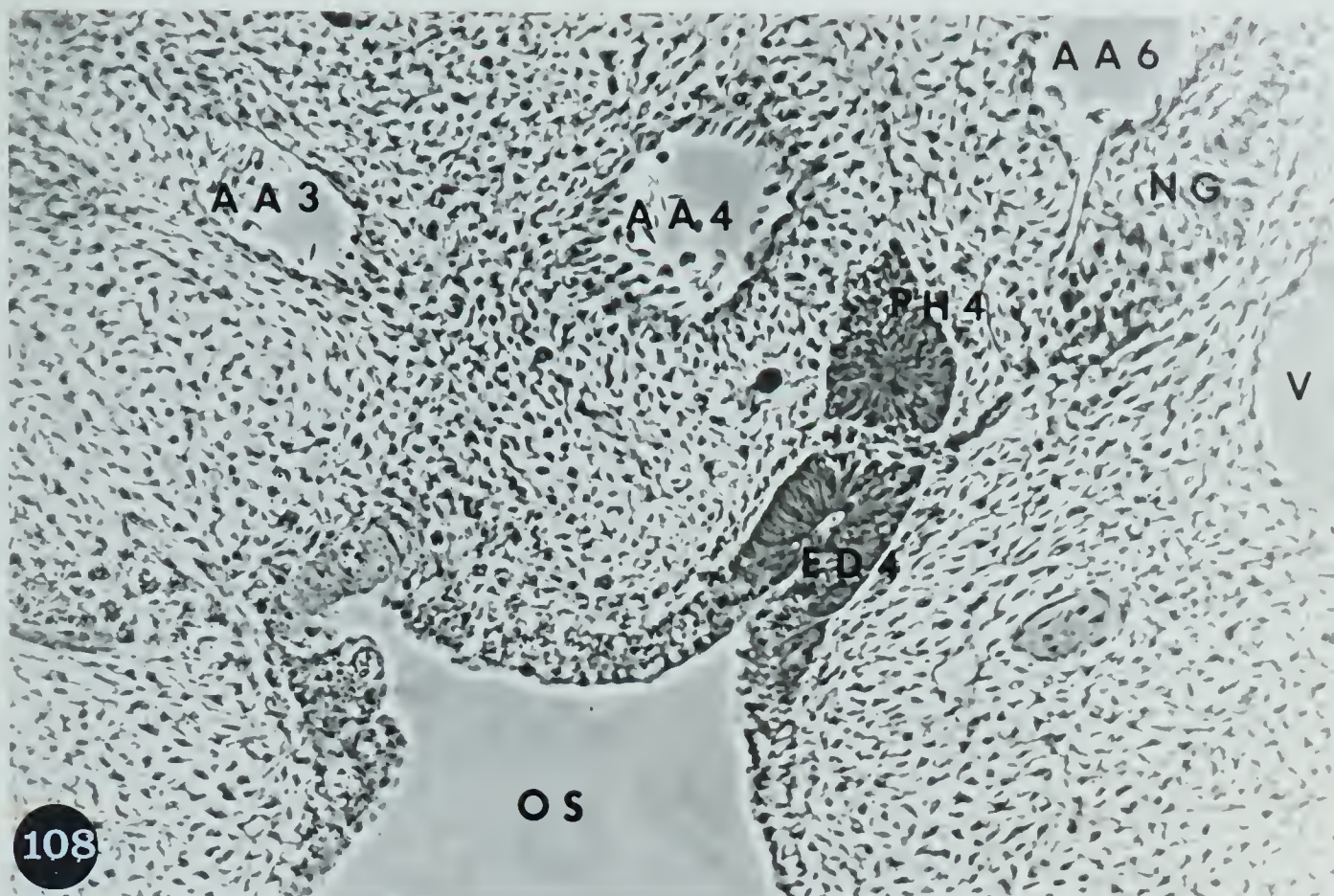


Fig. 110. Higher magnification of the section preceding that illustrated in Fig. 106. Pharyngeal Pouch III (PH3) extends to the superficial branchial ectoderm and the Pharyngeal Pouch IV (PH4) contacts the Ectobranchial Duct IV (ED4). The epithelia contain many degenerating cells.

X 405

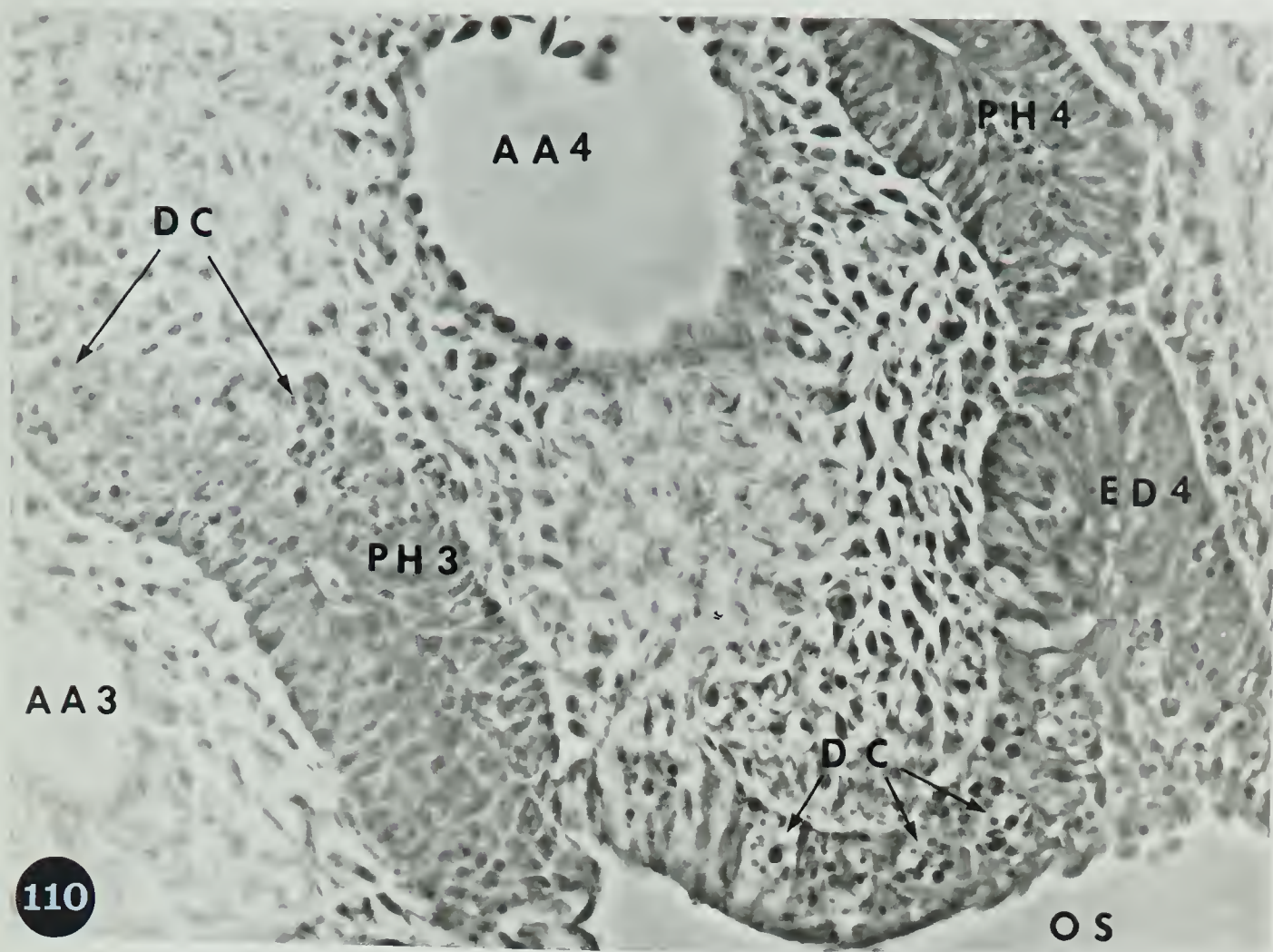


Fig. 111. Acid phosphatase activity in Thymus III of a 5-day embryo. The mesenchyme has yellowish background stain.

Barka medium, no counterstain.

X 600

Fig. 112. Acid phosphatase activity in the ectoderm on the medial side of the hyoid arch, an area which undergoes degeneration. The ectoderm on the lateral side of the hyoid arch contains little activity.

Barka medium, no counterstain.

X 110

Fig. 113. Acid phosphatase in the urodeal membrane, an area which undergoes degeneration. Three bursa vesicles are seen at the right hand side of the figure, and the cloacal lumen is seen in the upper left hand corner.

Barka medium, no counterstain.

X 600

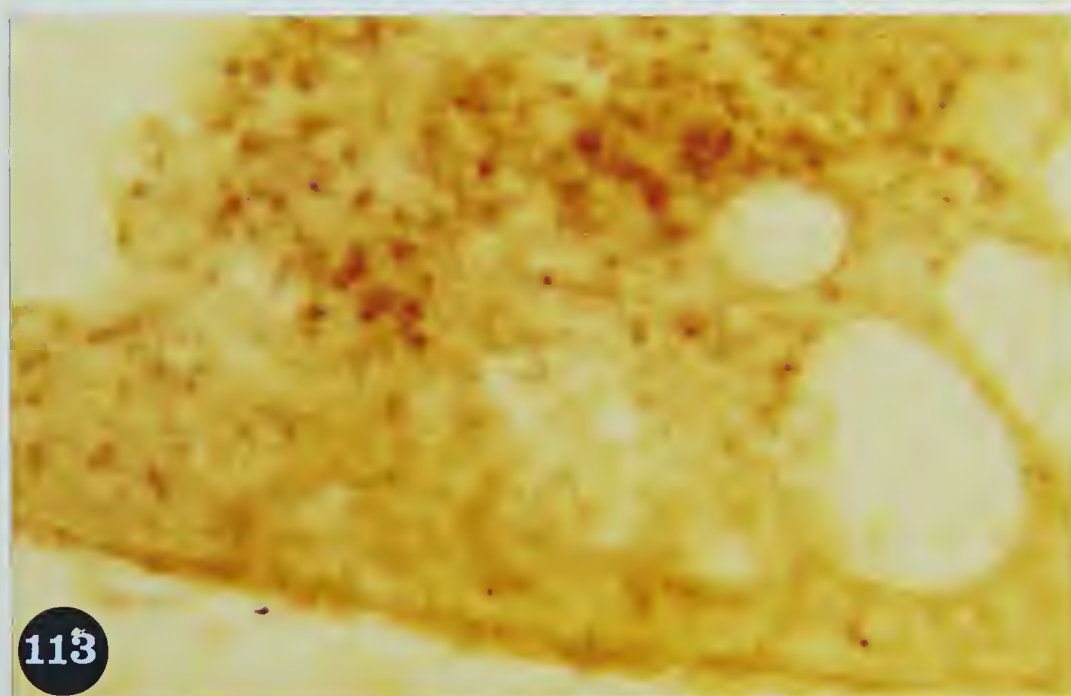
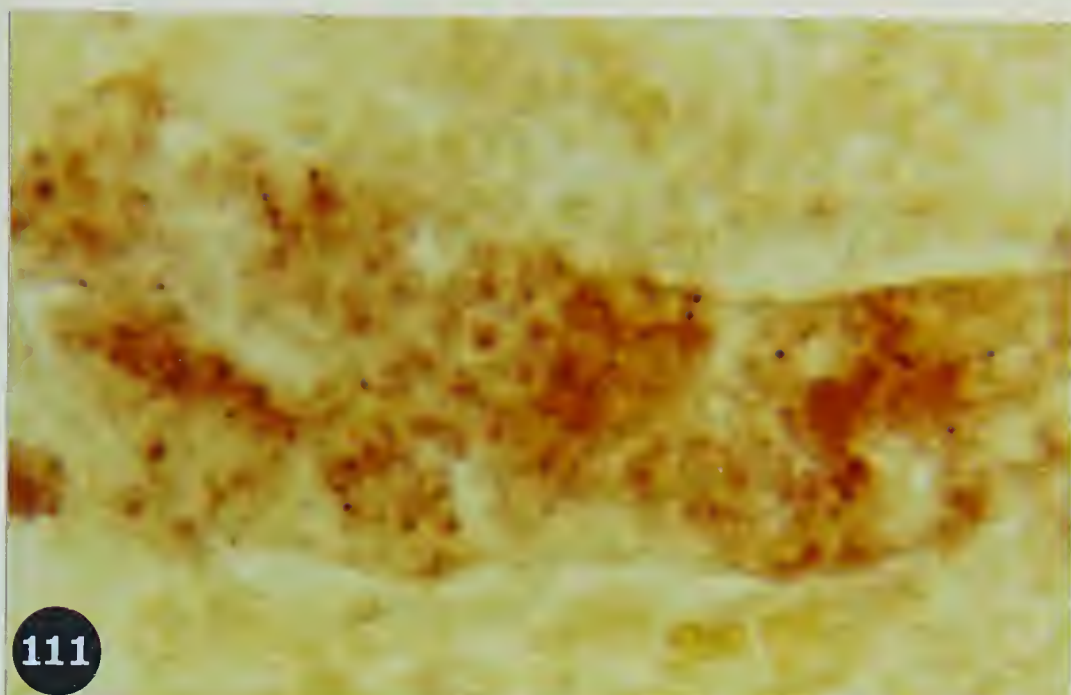


Fig. 114. The anterior part of a 5-day embryo vitally stained to detect degeneration. Degenerating cells are distributed in the branchial region (thin arrows) and in the upper edge of the forelimb (thick arrow). The head of the embryo lies to the right of the figure, the dorsal side of the embryo to the top. Part of the branchial region indicated by thin arrows is shown at higher magnification in Fig. 145.

H: heart

E: eye

Nile blue sulfate.

X 42

Fig. 115. Part of the branchial region shown in Fig. 114 to illustrate the distribution of degenerating cells at the dorsocaudal edge of the hyoid arch (thin arrow) and in the third and fourth branchial grooves (thick arrows).

Hy: hyoid arch

X 175

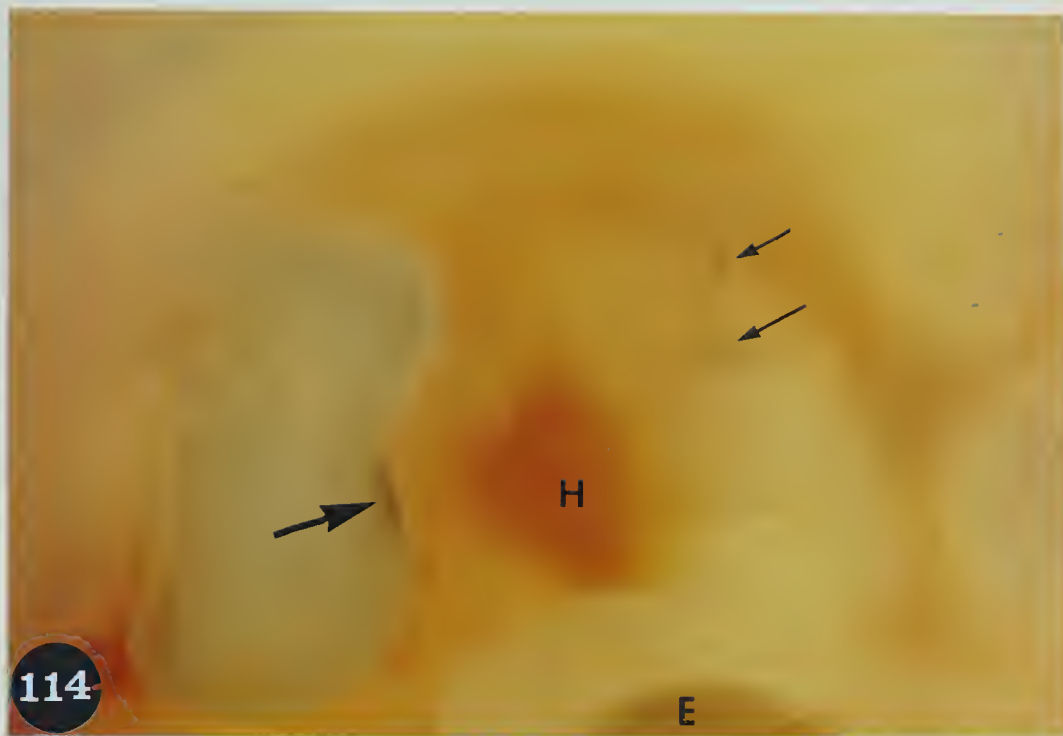


Fig. 116. A montage of several electron micrographs where the lateral extension of the ventral part of Pharyngeal Pouch III (upper left corner) meets the branchial surface. The demarcation between these two parts is not clear. Two types of cells are noticed, light (LC) and dark cells (DC). Cytolysosomes (CL) and cell debris are numerous, both in the epithelial and mesenchymal cells (ME). Glutaraldehyde-osmium tetroxide, Araldite, and uranyl acetate.
X 3000

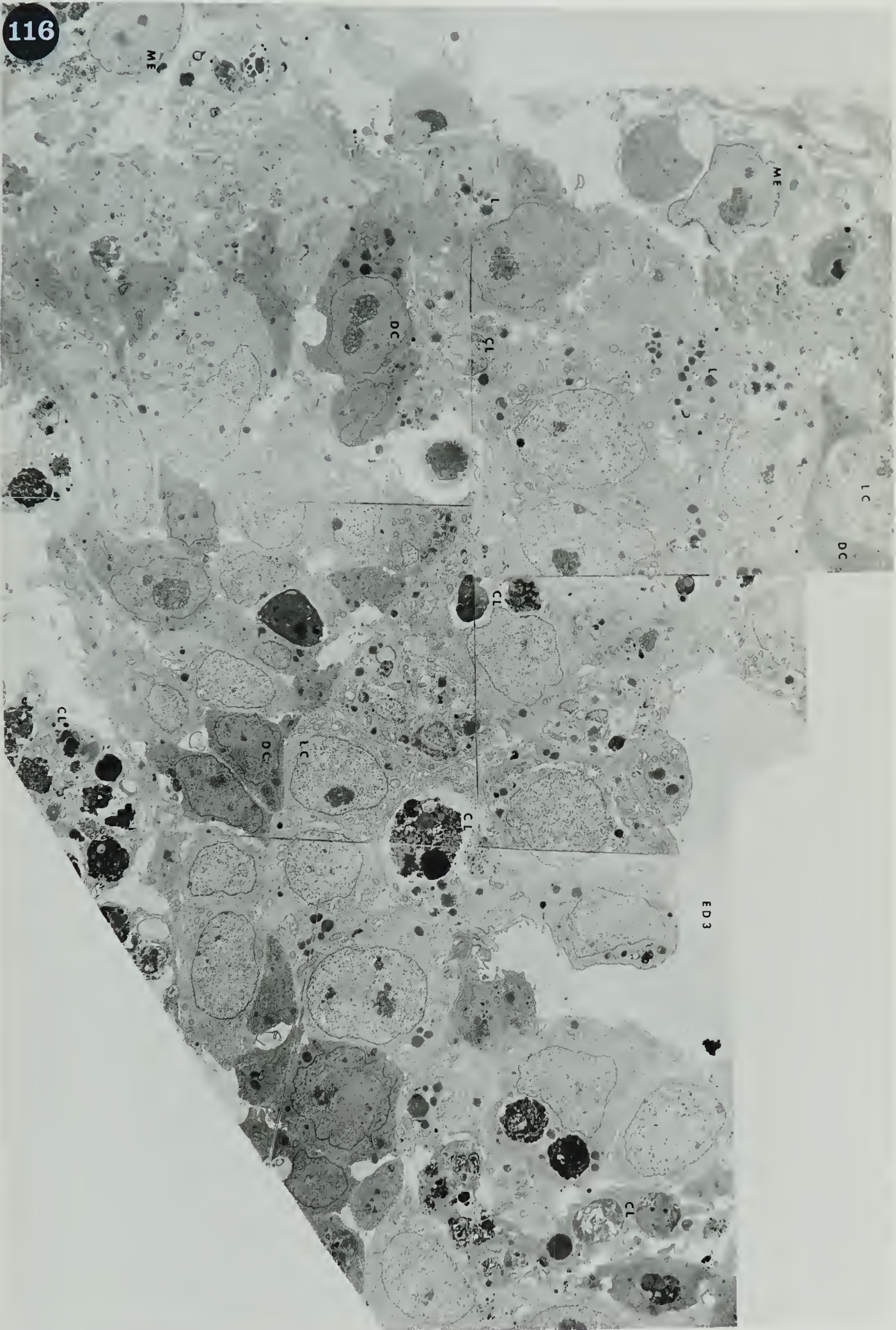
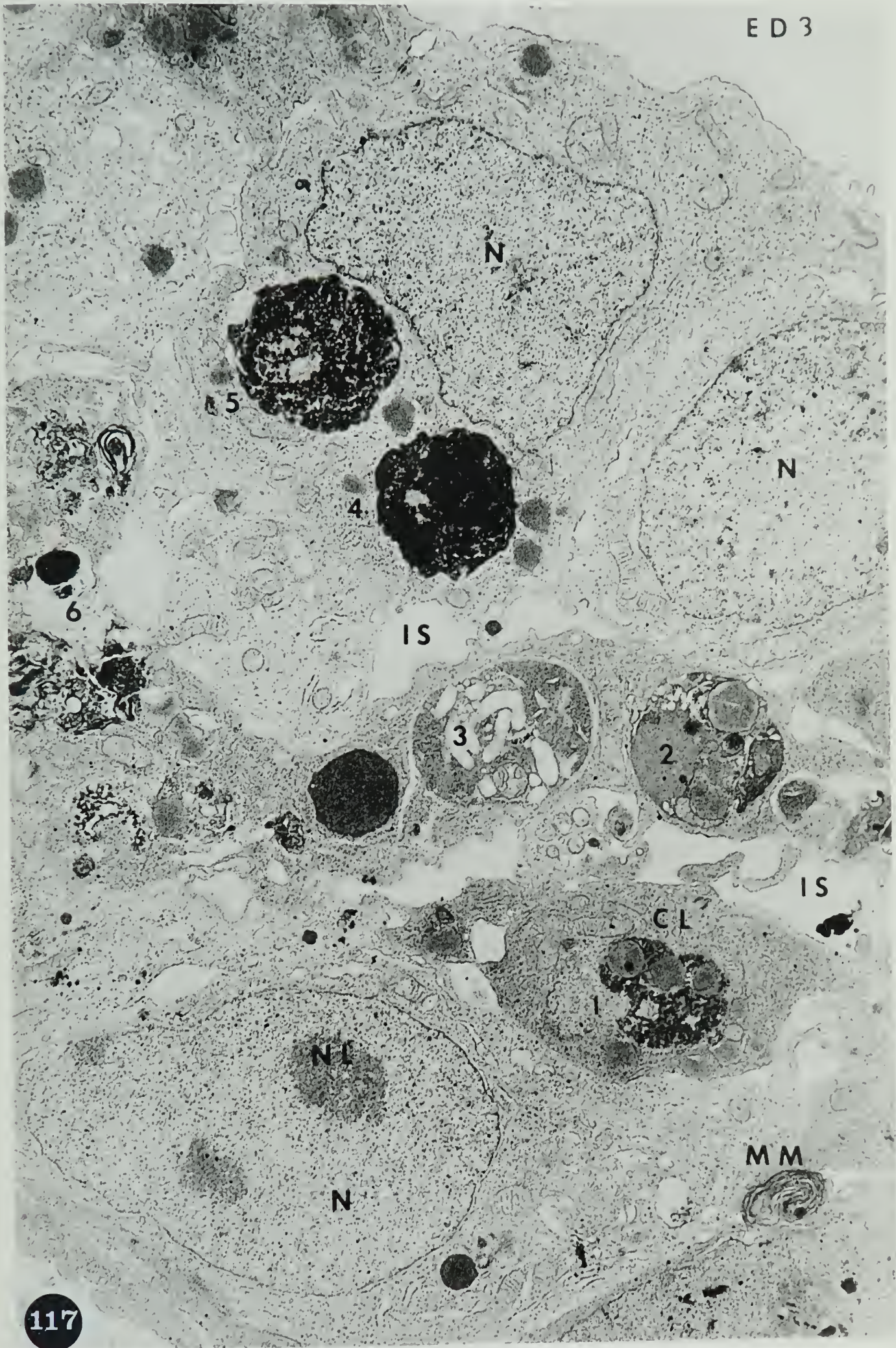


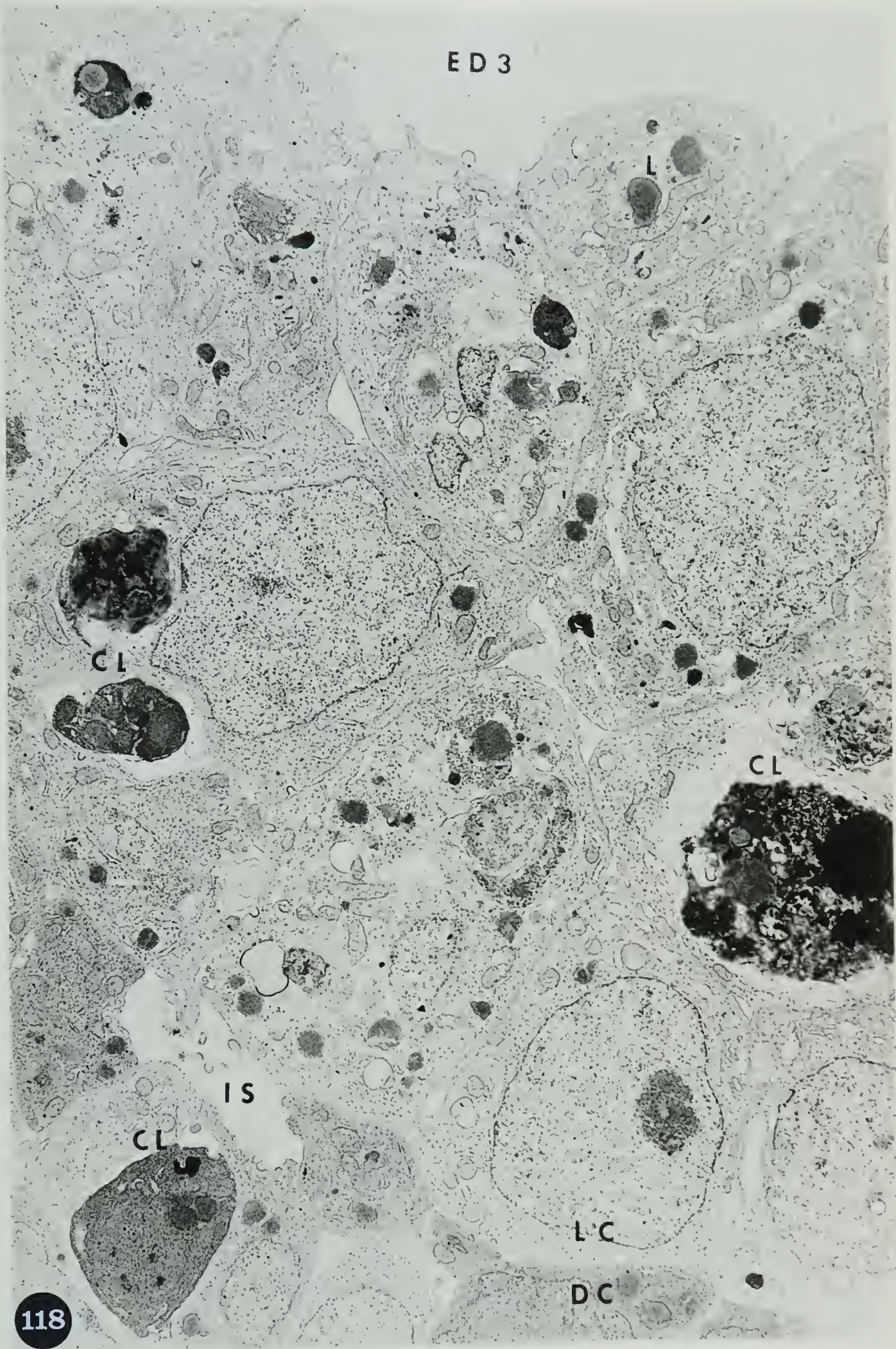
Fig. 117-119. Parts of Fig. 116 shown at higher magnification. A myeloid membrane (MM) is seen in the intercellular space but continuous with the plasma membrane (Fig. 117). Large intercellular spaces (IS) and numerous cytolysosomes (CL) of different sizes and forms are noticed. Note the light (LC) and dark cells (DC).

ED3: Branchial Groove III N: nucleus
Glutaraldehyde-osmium tetroxide, Araldite,
and uranyl acetate.

X 10,138



ED 3



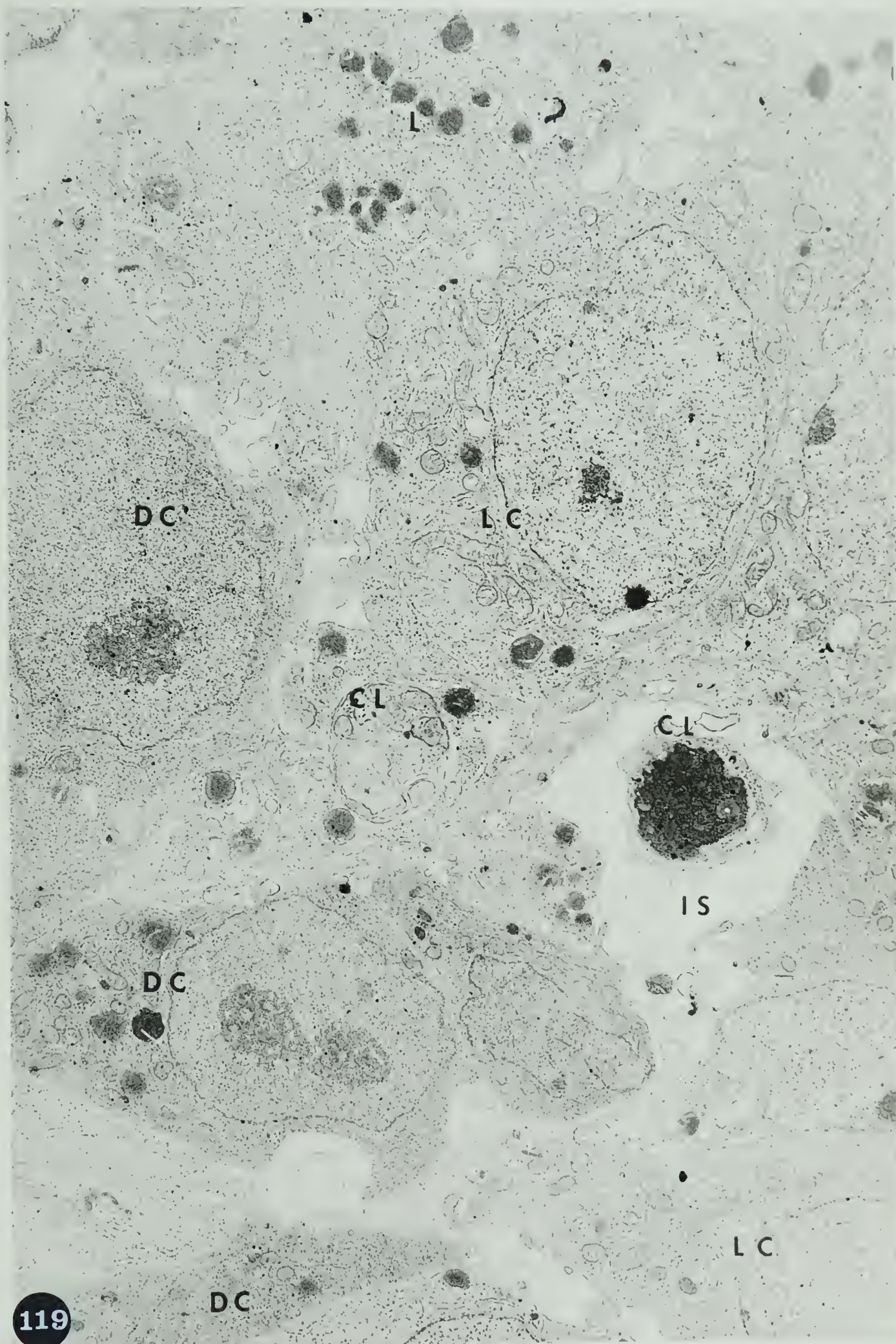


Fig. 120. Parts of light and dark cells in the area of contact of the Pharyngeal Pouch III and the Branchial Groove III. Myeloid membranes (MM) associated with the cytolysome (CL) are found in both light and dark cells. Lipid droplets (L) in dark cells contain structures similar to the cristae of mitochondria, but those of light cells are more homogeneous. This may represent a transfer of lipid from the degenerating structures of dark cells to light cells.

Glutaraldehyde-osmium tetroxide, Araldite, and uranyl acetate.

X 21,000

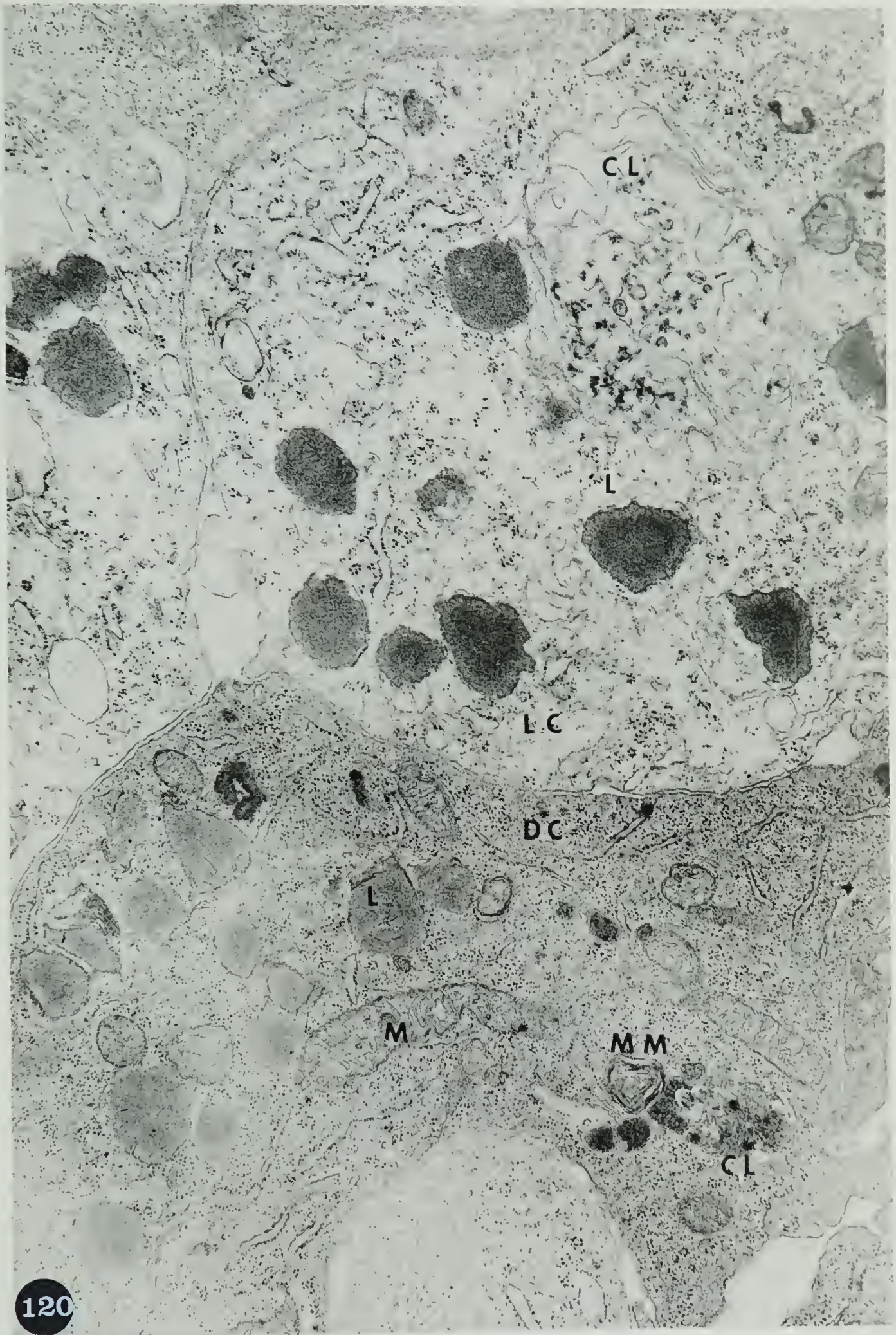


Fig. 121. Lateral part of Branchial Membrane III of a 5-day embryo showing cell debris (CL) and a mixture of dark and light cells. The light cells are larger than the dark cells, which seem crenated or partly dehydrated. Similar groups of light and dark cells are seen at the branchial surface. The two types of cells seem to occur in the vicinity of the contact between ectoderm and endoderm, but have not been seen in the deeper parts of Branchial Membrane III. The Branchial Groove is to the top of the figure, the mesenchyme is to the lower right.

Glutaraldehyde-osmium tetroxide, Epon, and uranyl acetate.

X 9,600

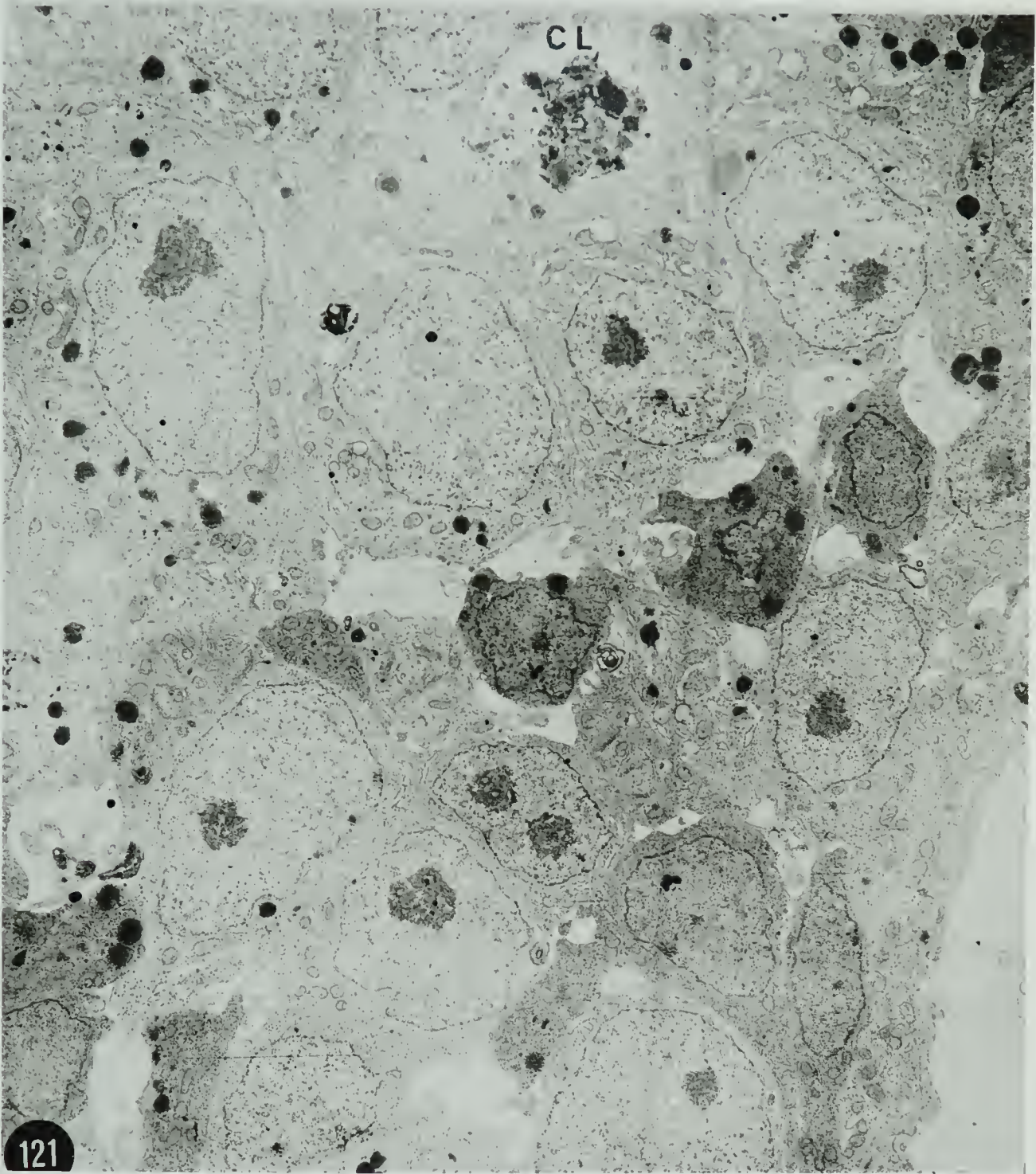


Fig. 122. Part of Thymus III of a 5-day embryo showing thymus cells near the dorsal tip of the thymus, and the incomplete basement membrane surrounding the thymus (thin arrow). One of the thymus cells has a nuclear whorl (thick arrow). These are common in thymus cells, but have not been seen in the adjacent mesenchyma. Glutaraldehyde-osmium tetroxide, Epon, and uranyl acetate.

X 10,800

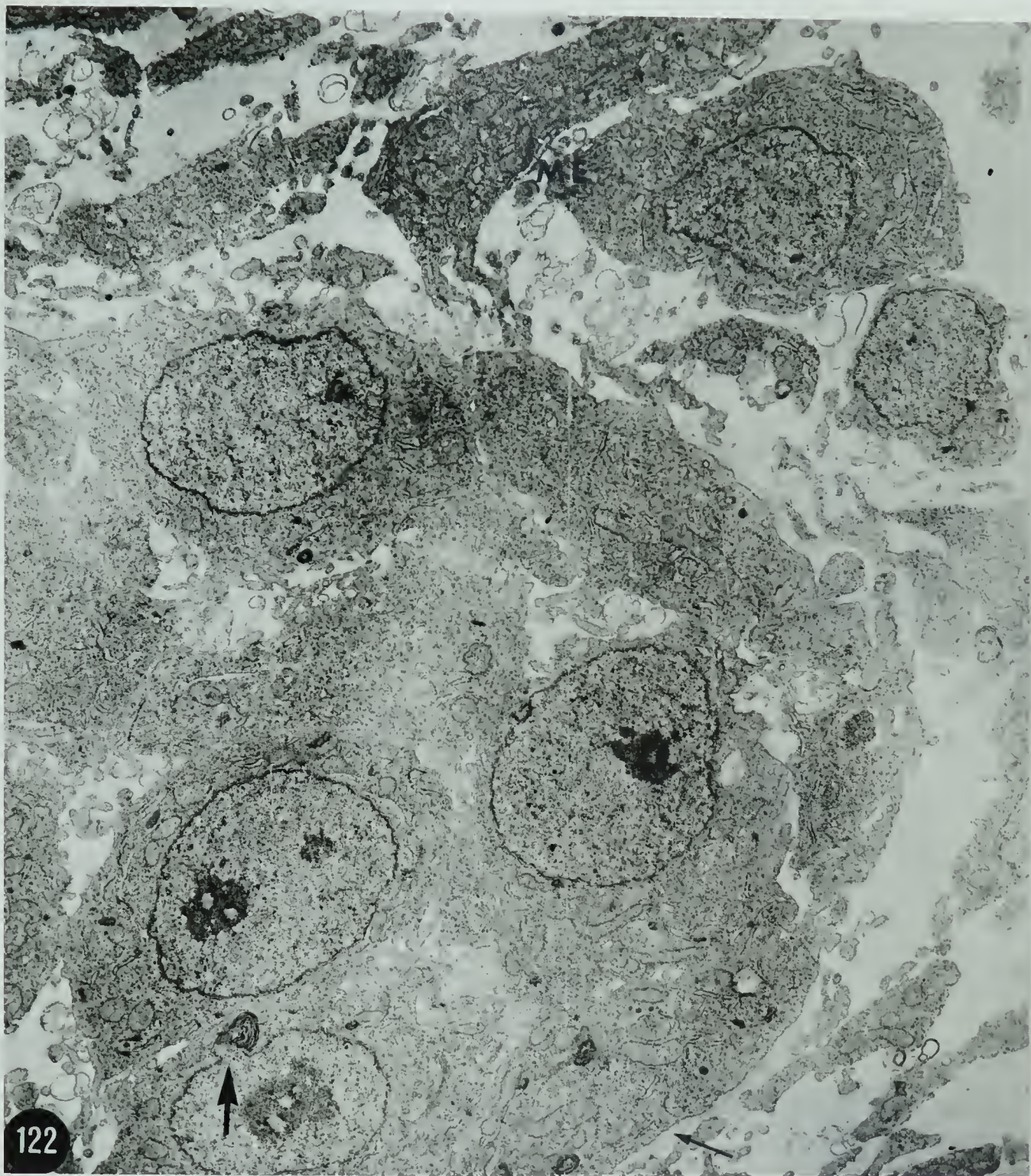


Fig. 123. Part of Thymus III of a 5-day embryo showing cell debris (D) in the upper center and a clump of cell debris in the mesenchyme probably phagocytosed by a mesenchymal cell. Glutaraldehyde-osmium tetroxide, Epon, and uranyl acetate.

X 12,600

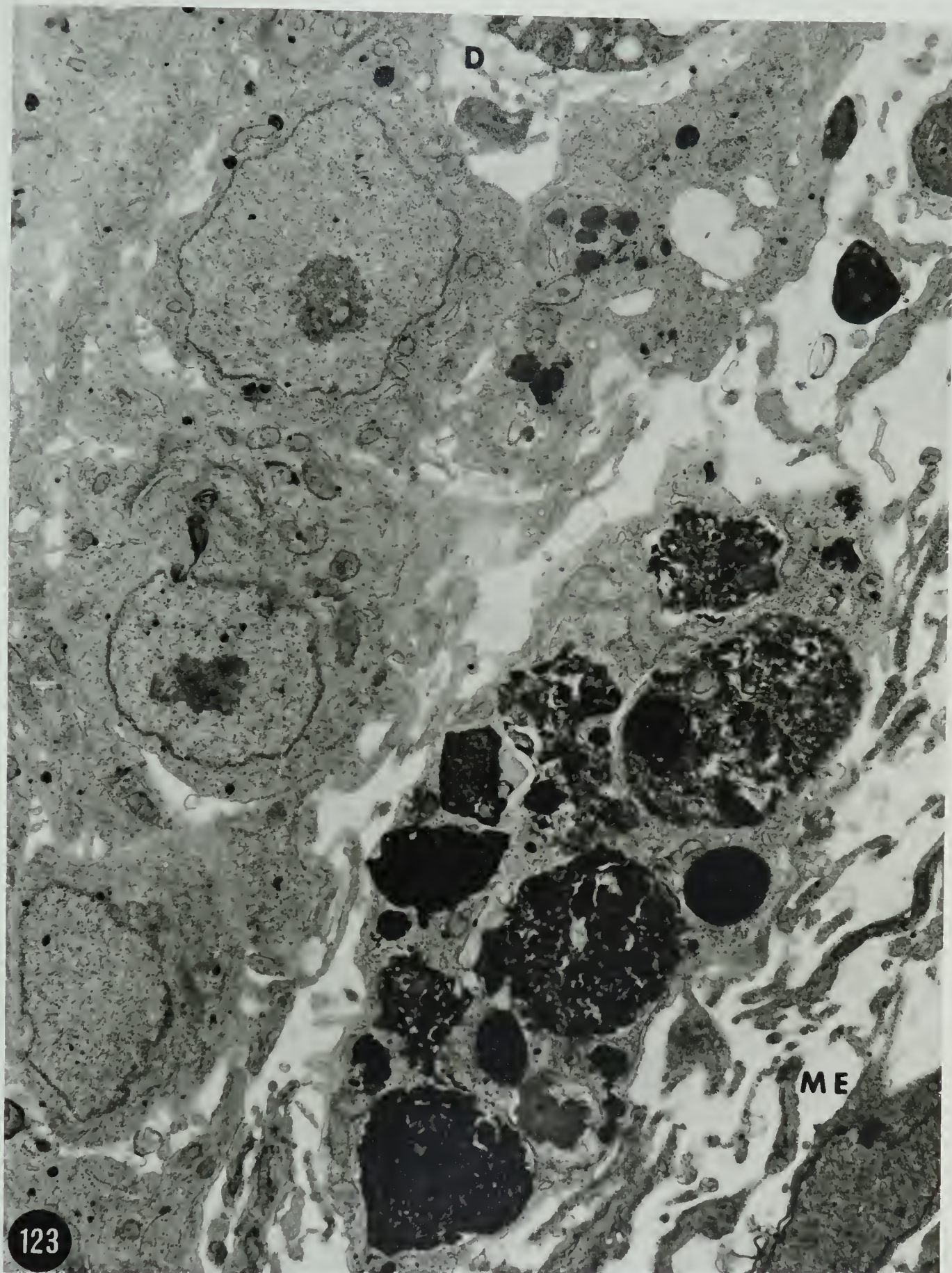


Fig. 124. Part of Thymus III of a 5-day embryo showing three cytolysomes, differing in appearance and size.

Glutaraldehyde-osmium tetroxide, Araldite, and uranyl acetate.

X 17,200

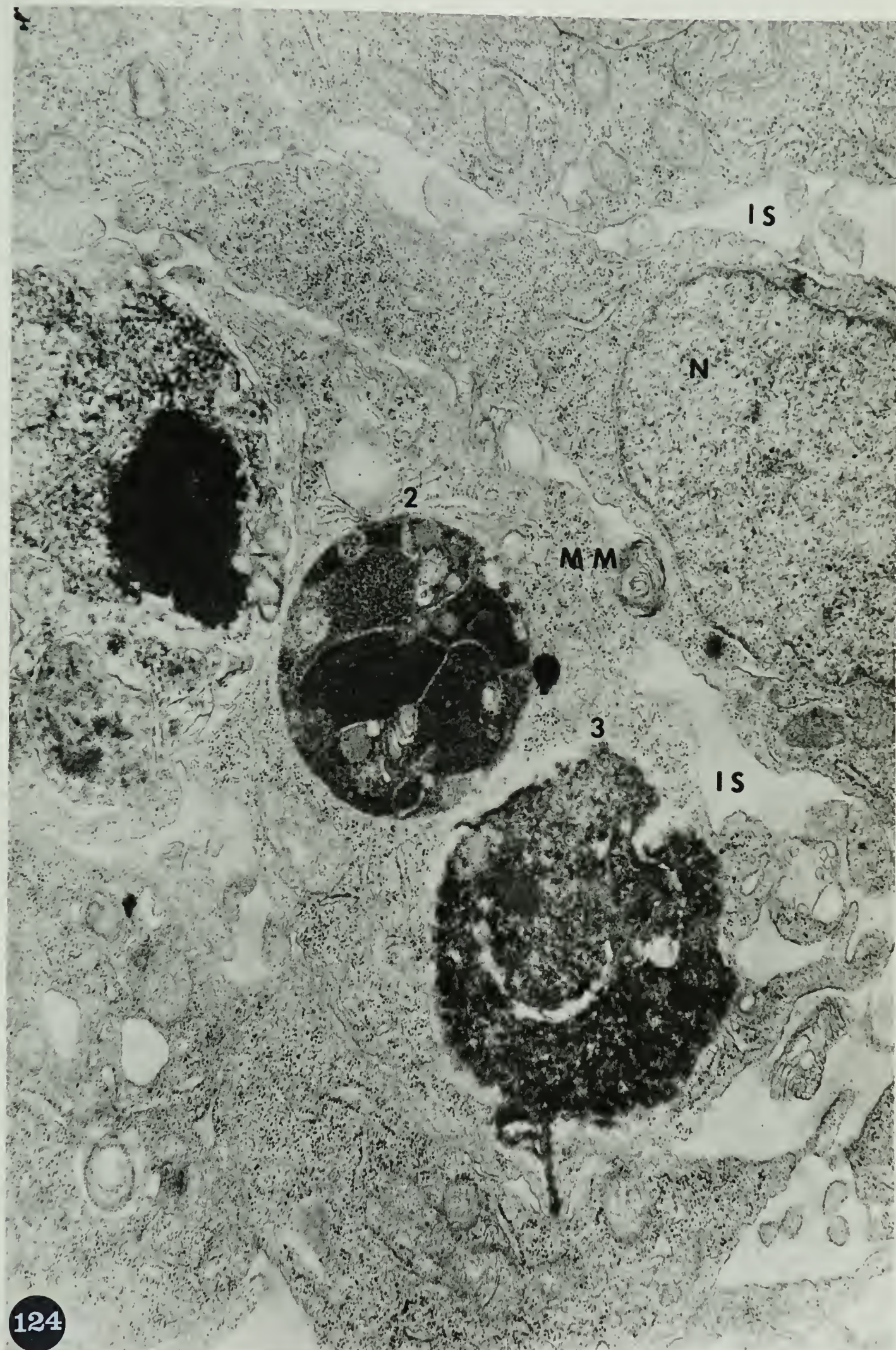


Fig. 125. Part of Thymus III of a 5-day embryo showing a thymus cell and a mesenchymal cell (ME) just outside the thymus. A basement membrane is not visible.

Glutaraldehyde-osmium tetroxide, Epon,
and uranyl acetate.

X 35,000

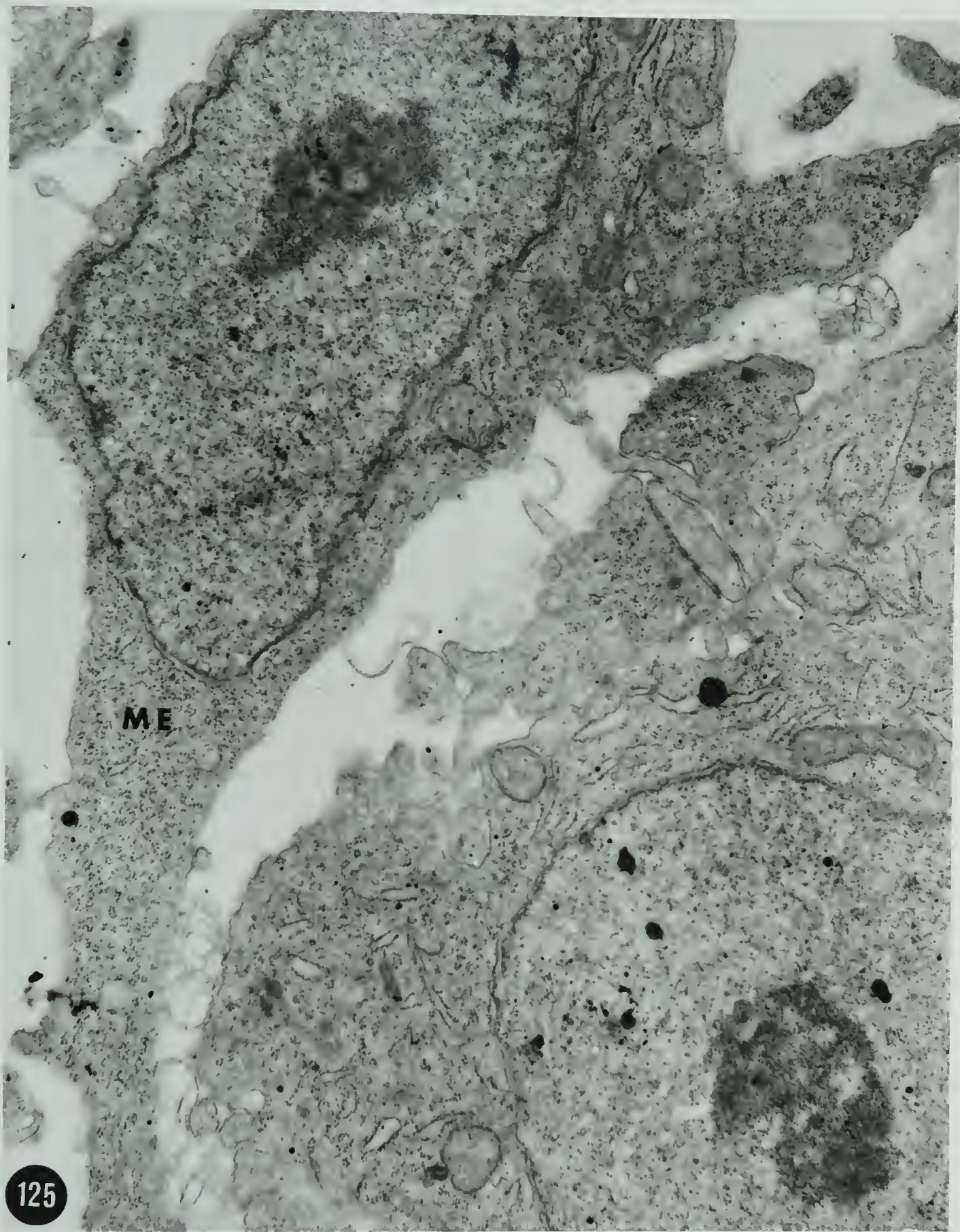


Fig. 126. A mesenchymal cell near Thymus III containing cell debris (CL).

IS: intercellular space

M: mitochondrion

N: nucleus

Glutaraldehyde-osmium tetroxide, Araldite,
and uranyl acetate.

X 17,200

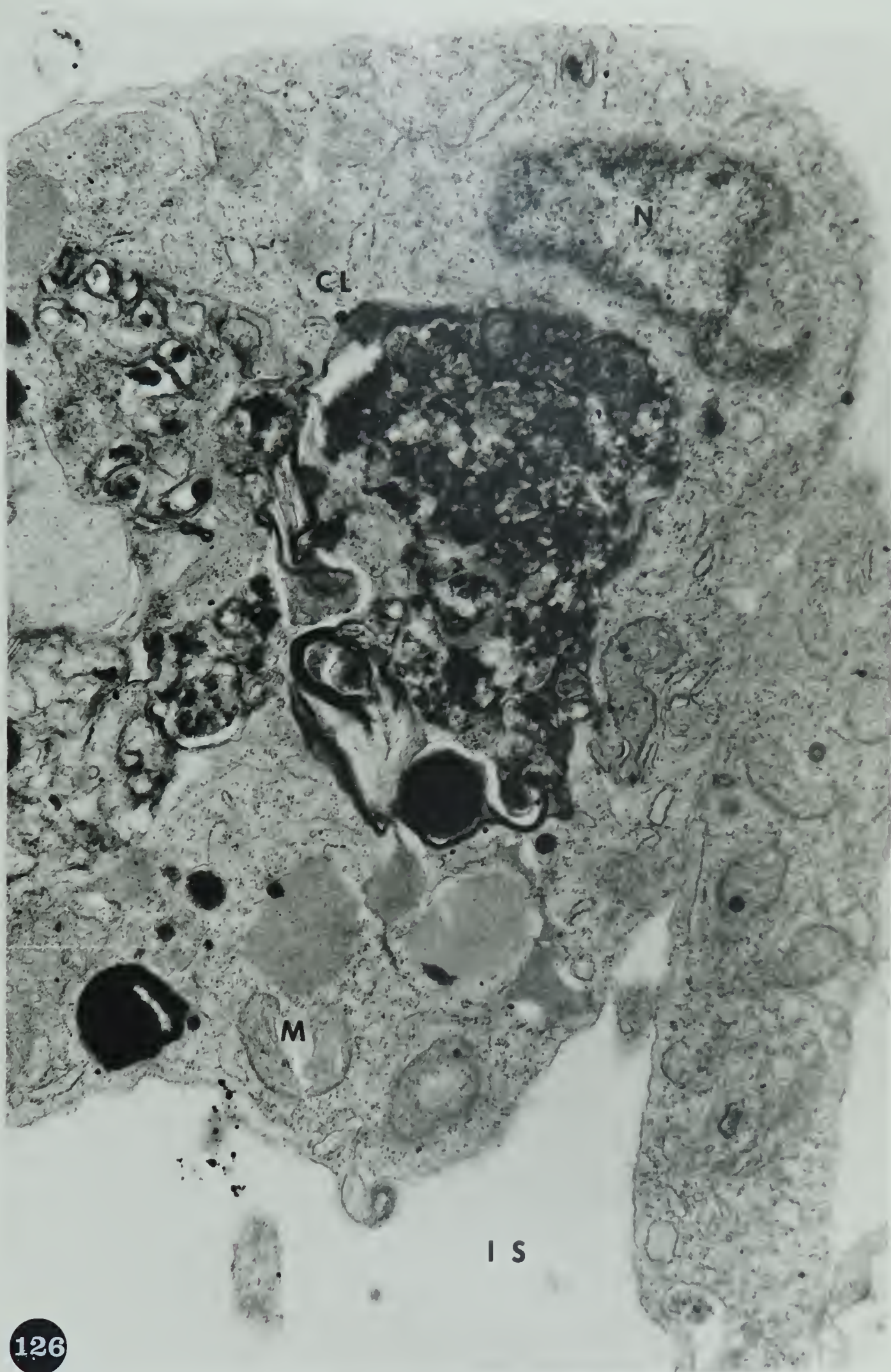


Fig. 127. Part of a cell from Thymus III of a 5-day embryo showing nuclear whorls and an altered mitochondrion (M). The presence of several nuclear pores (NP) indicates that the nuclear envelope has not been grossly damaged during fixation and preparation. The contrast between the whorls and the remainder of the nuclear envelope suggests that the whorls represent focal degradations or instability of parts of the nuclear envelope. Glutaraldehyde-osmium tetroxide, Araldite, and uranyl acetate.

X 30,000



Fig. 128. A thymus cell of a 5-day embryo showing a myelin figure which protrudes into the inter-cellular space. The proximate part of the nuclear envelope is diffuse and the base of the myelin figure does not contain polyribosomes. This suggests that the myelin figure is a protrusion of the nuclear envelope although a direct connection cannot be seen.

N: nucleus NP: nuclear pore

Glutaraldehyde-osmium tetroxide, Araldite,
and uranyl acetate.

X 35,200

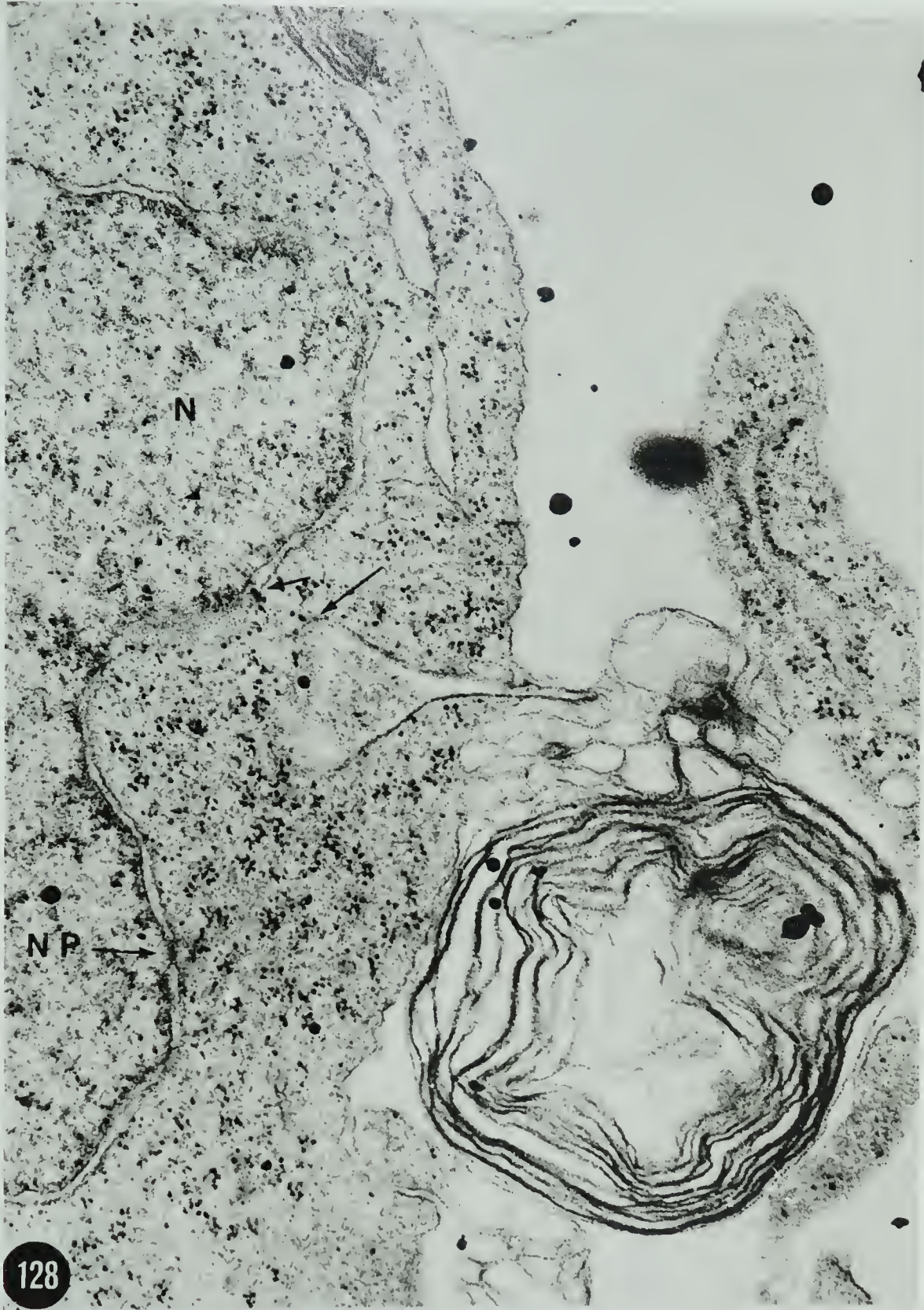


Fig. 129. Part of Thymus III of a 5-day embryo showing myelin membranes (MM) in association with a mitochondrion (M), the nuclear envelope, and the plasma membrane.

N: nucleus

Glutaraldehyde-osmium tetroxide, Araldite, and uranyl acetate.

X 32,500

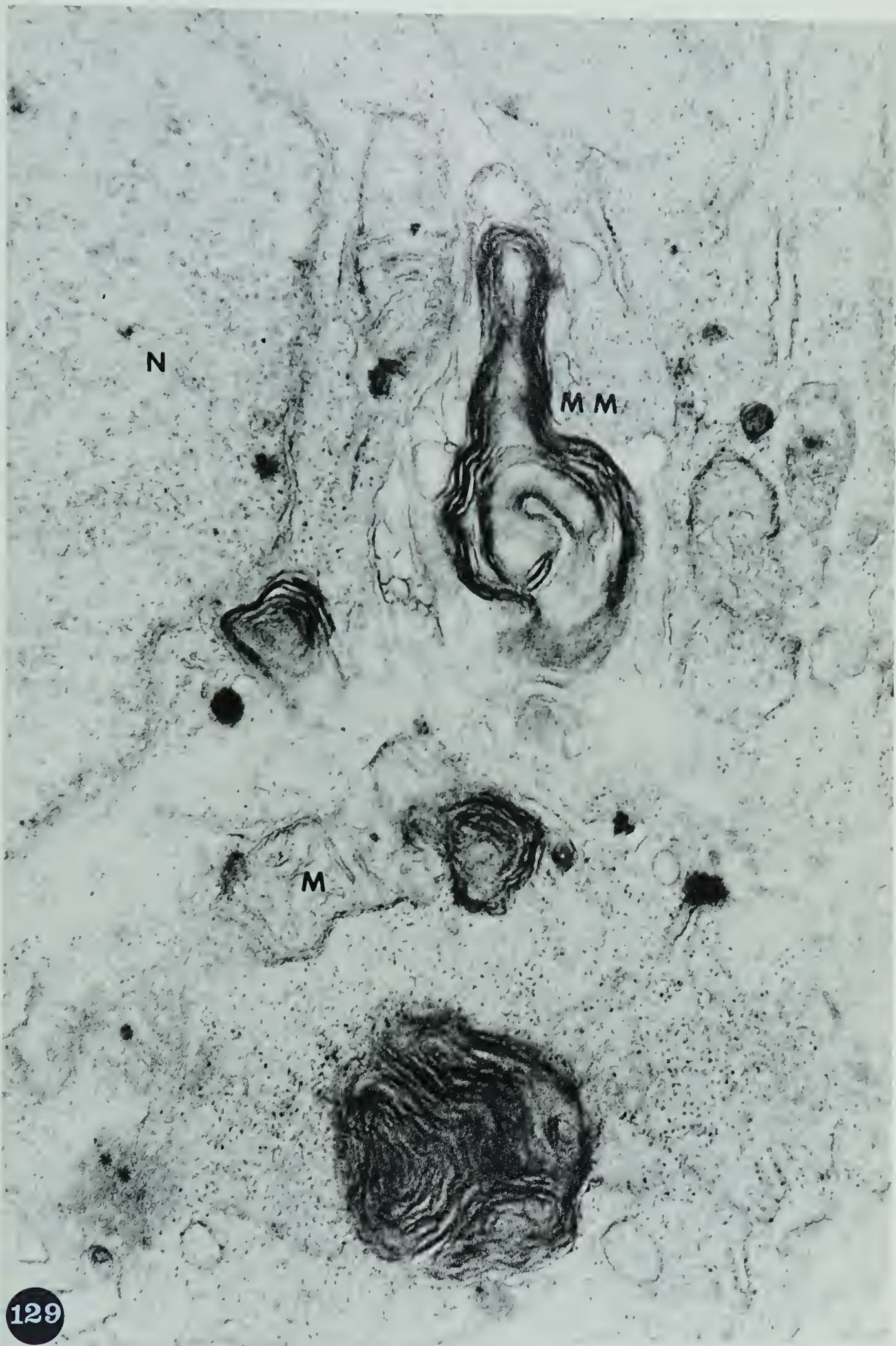


Fig. 130. Thymus cells of a 5-day embryo showing myelin membranes in association with a mitochondrion (M) and the endoplasmic reticulum (ER). Loosely packed myelin membranes (LMM) are present at the intercellular space (IS) and the plasma membrane. The nuclear envelope is not connected to the cytoplasmic myelin figure.

Glutaraldehyde-osmium tetroxide, Araldite, and uranyl acetate.

X 32,500

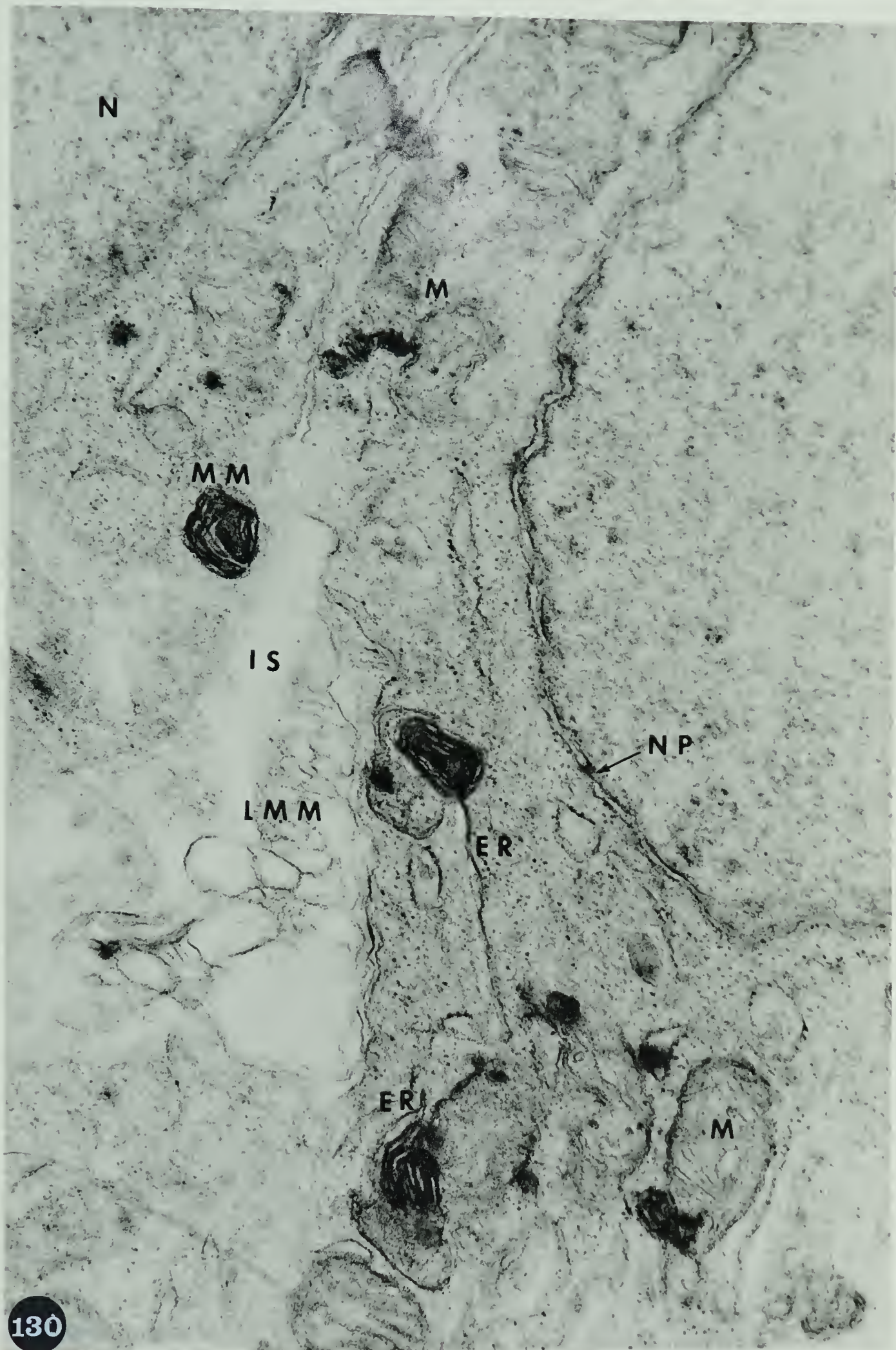


Fig. 131. Part of an endodermal cell from the dorsal part of the Pharyngeal Pouch III showing myelin membranes (MM) in continuity with the Golgi membrane (G) and with the endoplasmic reticulum (ER).

ME: mesenchymal cell

IS: intercellular space

M: mitochondrion

Glutaraldehyde-osmium tetroxide, Araldite, and uranyl acetate.

X 32,500



Fig. 132. Part of an endodermal cell from the dorsal part of the Pharyngeal Pouch III at the top, and part of a mesenchymal cell at the bottom. The endoplasmic reticulum (ER) of the mesenchymal cell approaches and may contact the plasma membrane (arrow). Tubular endoplasmic reticulum is common in the mesenchymal cells. An indentation of the nucleus (IN) of the endodermal cell is noted.

IS: intercellular space

M: mitochondrion

N: nucleus

Glutaraldehyde-osmium tetroxide, Araldite, and uranyl acetate.

X 30,000

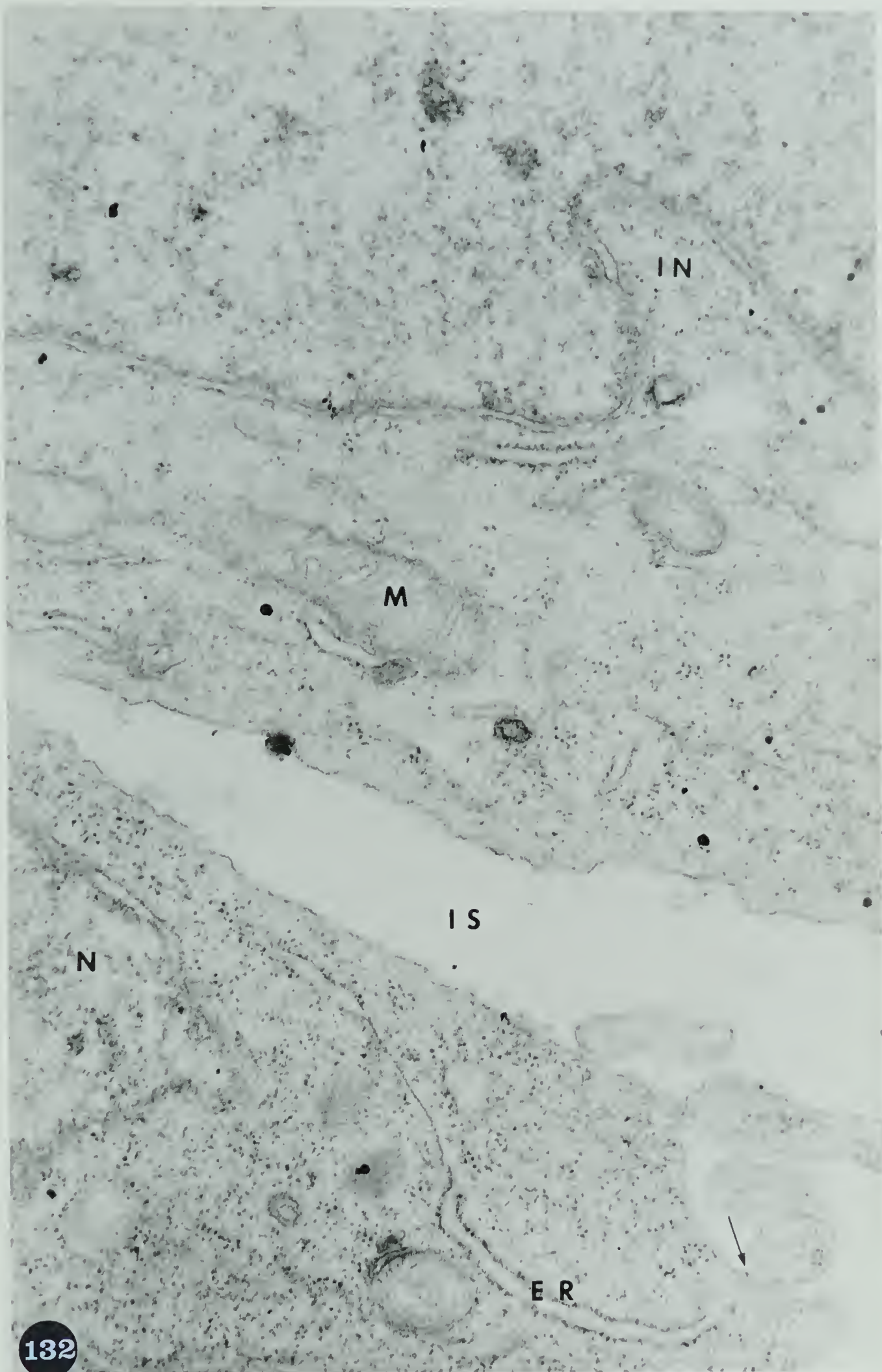


Fig. 133. A frontal through section of Thymus IV of a 5-day embryo showing Feulgen-positive pyknotic debris (arrows). The pyknotic debris is darker than normal nuclei.

Feulgen reaction for DNA, counterstained with luxol fast blue.

X 580

Fig. 134. Branchial Groove IV (ED4) of a 5-day embryo showing Feulgen-positive pyknotic debris (arrows) in the ectodermal epithelium.

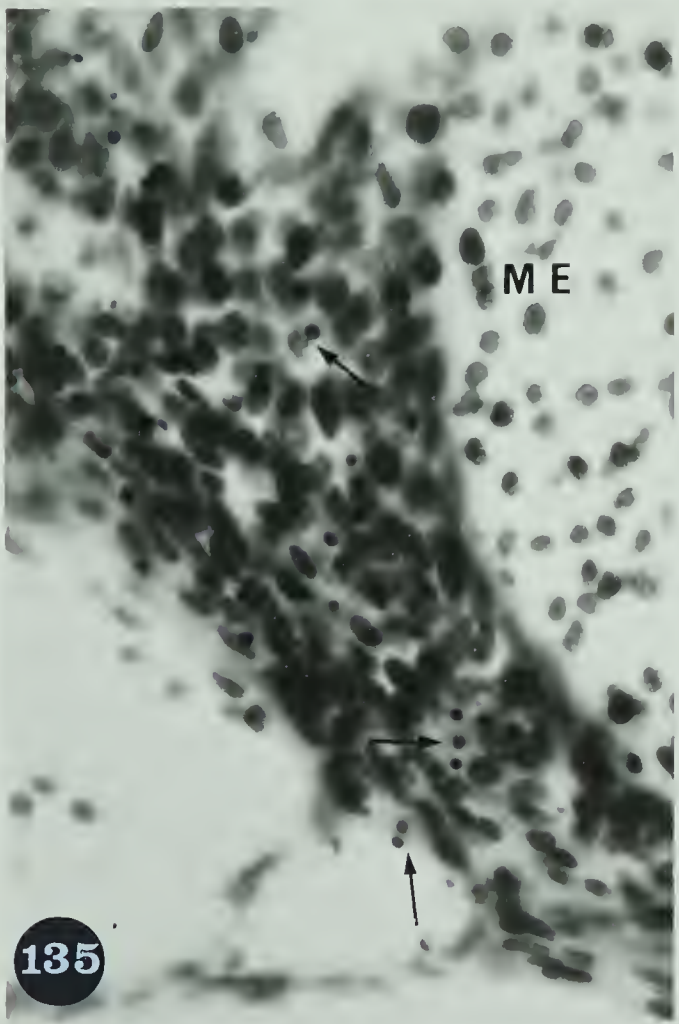
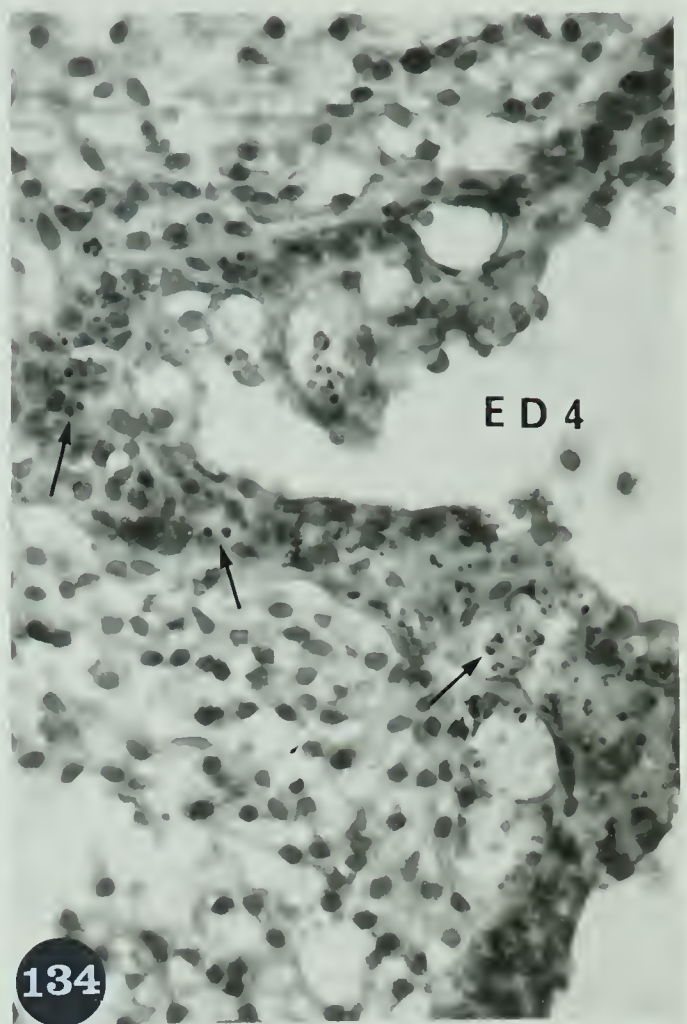
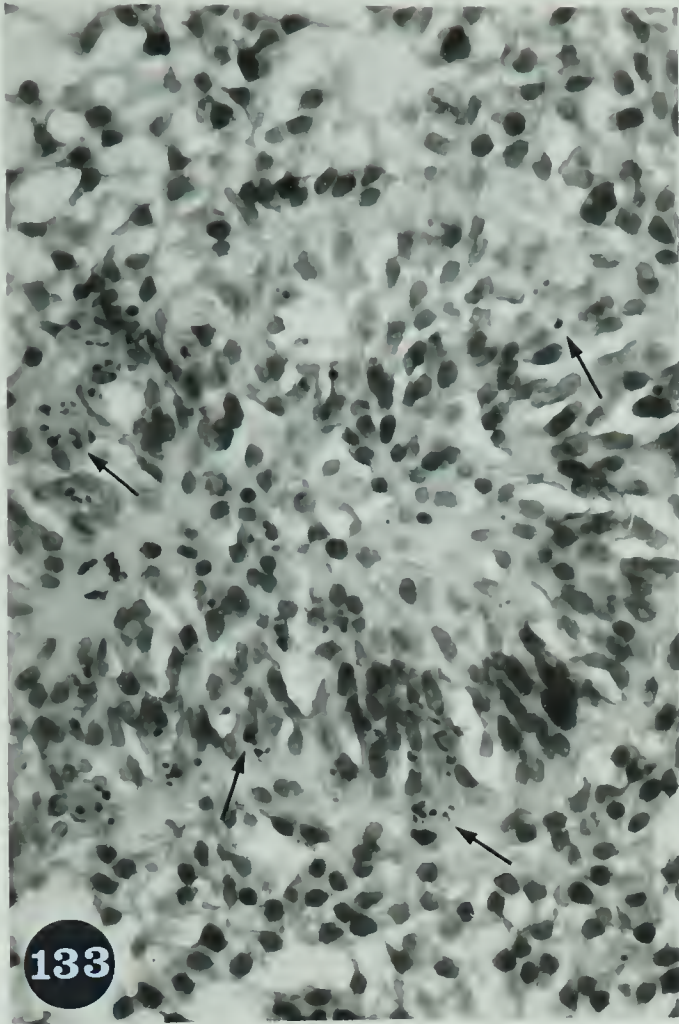
Feulgen reaction for DNA, counterstained with luxol fast blue.

X 580

Fig. 135. Part of the urodeal membrane of a 9-day embryo to show the Feulgen-positive pyknotic nuclei (arrows).

Feulgen reaction for DNA, counterstained with luxol fast blue.

X 580



Figs. 136-141. Representative serial paraffin sections of Thymus III of a 5-day embryo showing Colcemid-arrested metaphases (long arrows) and pyknotic debris (short arrows). Arrested metaphases are also seen in the mesenchyme.

AA3: third aortic arch

ME: mesenchyme

JV: jugular vein

Colcemid treatment for six hours before killing, formalin-calcium, stained with Erhlich haematoxylin.

X 580

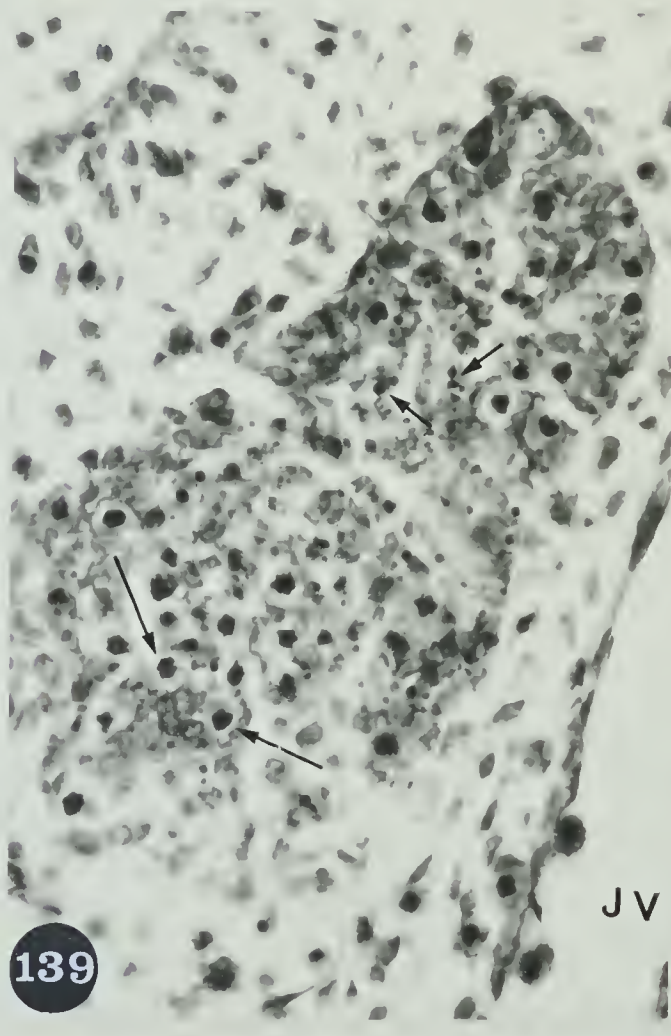
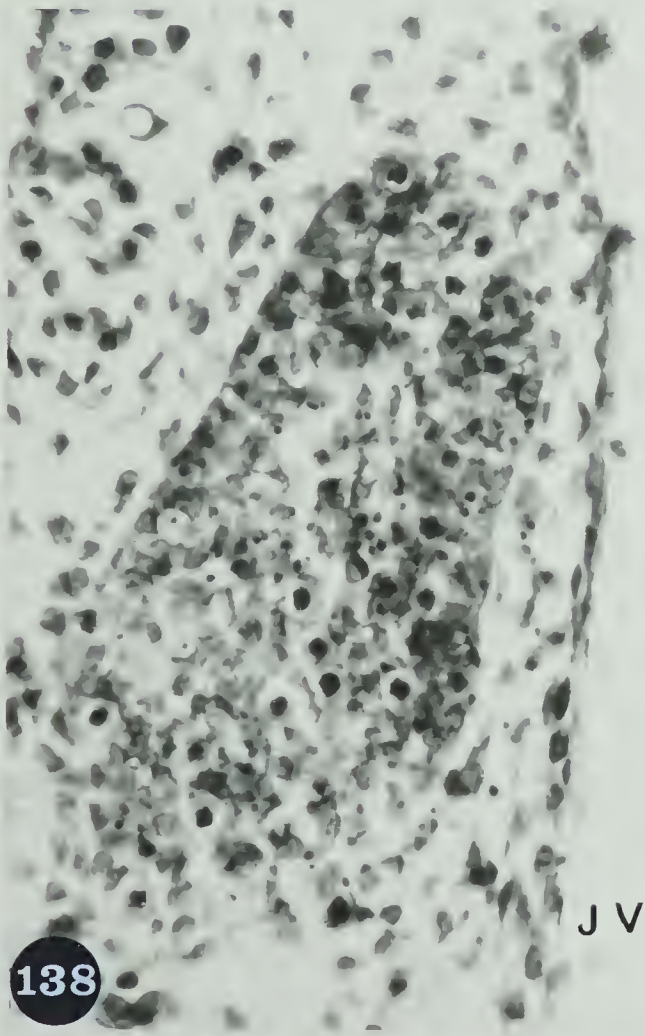
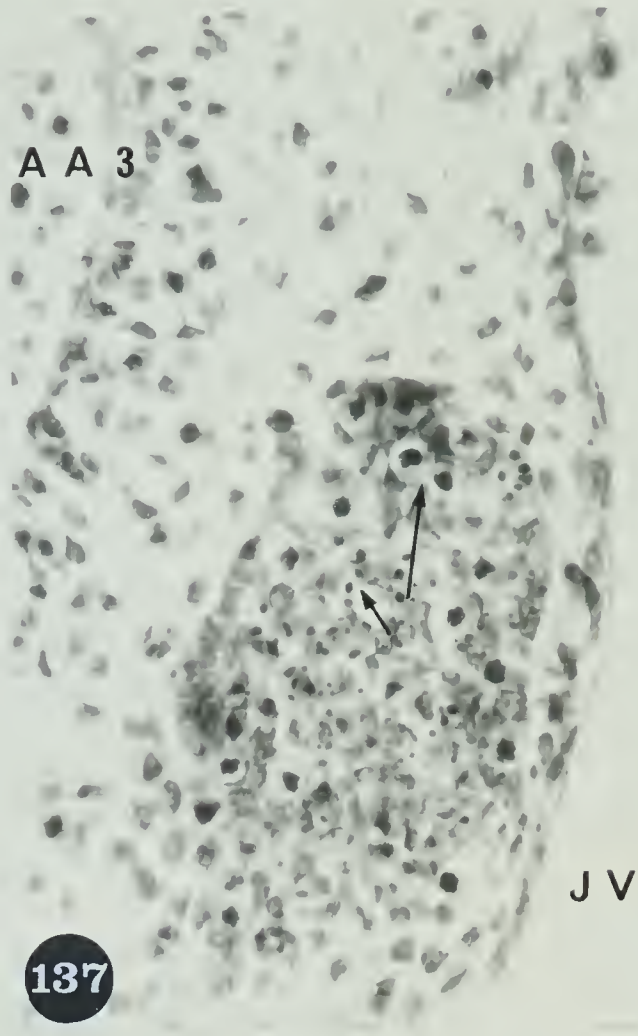
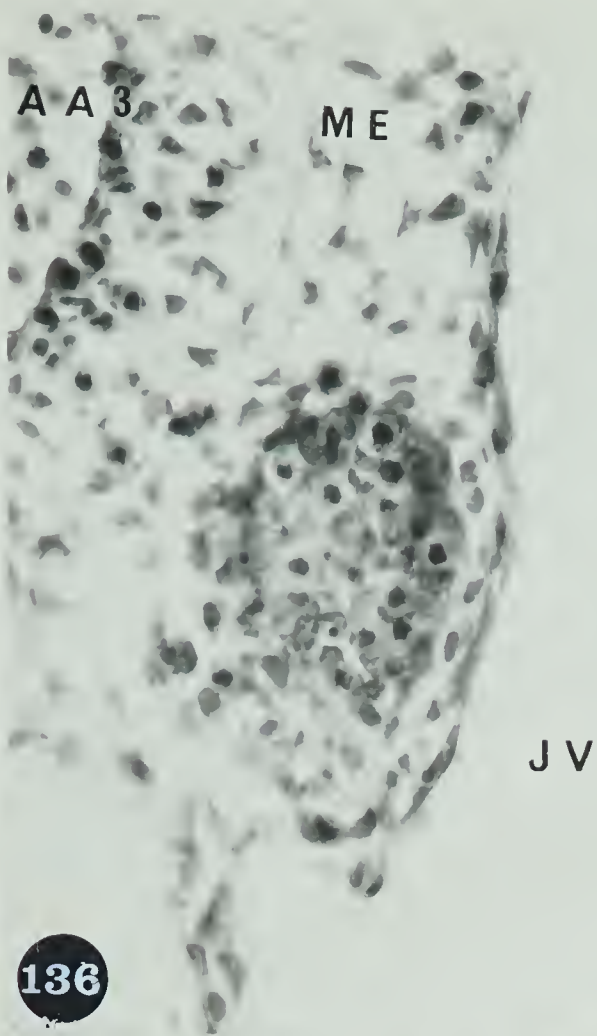
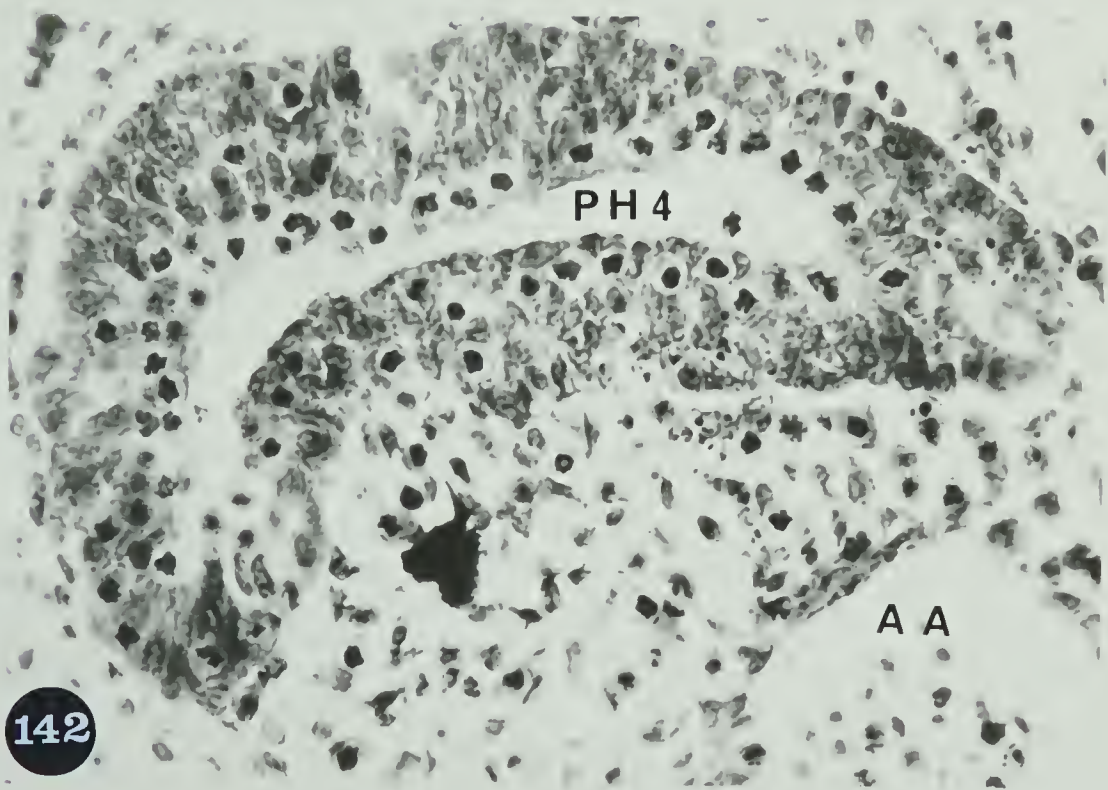
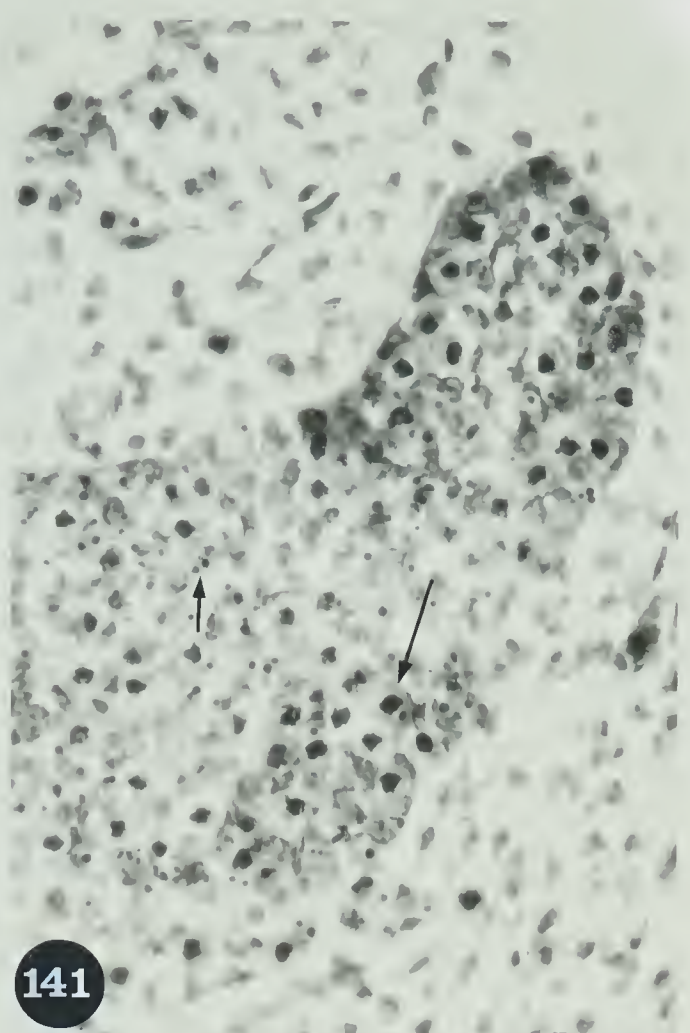
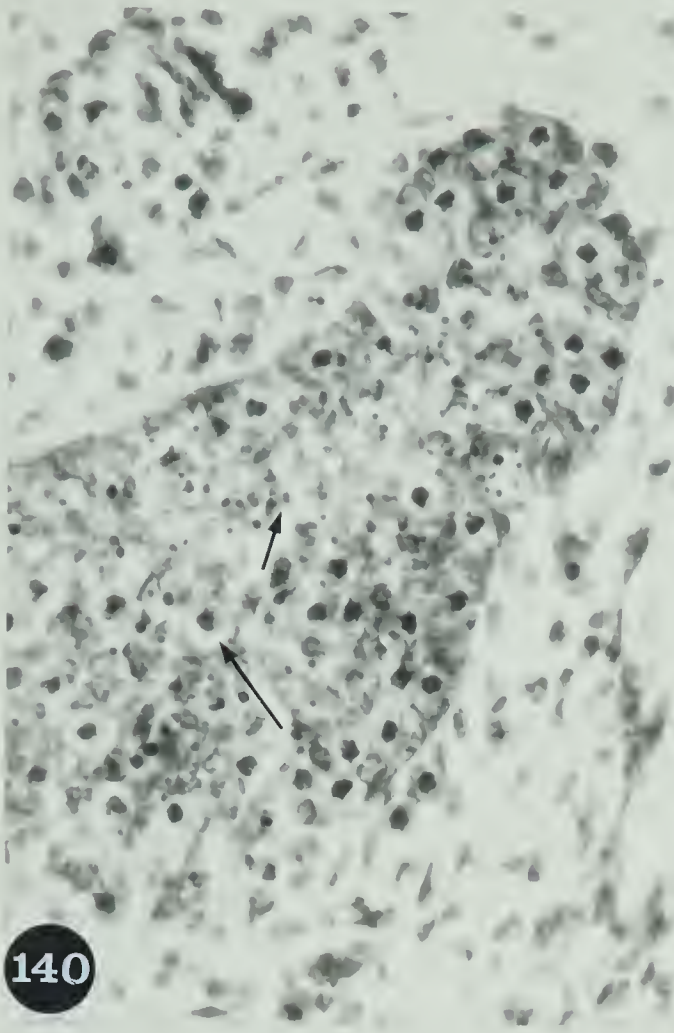


Fig. 142. Pharyngeal Pouch IV (PH4) of a 5-day embryo showing arrested metaphases along the lumen of the pouch after Colcemid treatment. Sections stained with Erhlich haematoxylin. X 580



B29902